The response to chemical stress: Development of preclinical and translational biomarkers of Nrf2 activity

Thesis submitted in accordance with the requirements of the University of Liverpool for the degree of Doctor in Philosophy by

Joanne Henry

September 2012

DECLARATION

This thesis is the result of my own work. The material contained within this thesis has not been presented, nor is currently being presented, either wholly or in part for any other degree or qualification.

Joanne Henry

This research was carried out in the Centre for Drug Safety Science in the Department of Pharmacology and Therapeutics, The University of Liverpool, UK.

Contents **Page**

Abstract

Nrf2 is a transcription factor that plays a vital role in the cytoprotective response to oxidative stress. Under basal conditions Nrf2 is sequestered in the cytosol by Keap1, a molecule which targets Nrf2 for ubiquitination and subsequent proteasomal degradation. Following oxidative insult, Keap1 is no longer able to facilitate the breakdown of Nrf2. Nrf2 accumulates in the cell and is free to translocate to the nucleus where it binds to the antioxidant response element (ARE) in a range of genes resulting in their expression. Nrf2 regulates genes encoding phase II enzymes, proteins important for glutathione synthesis and antioxidants. Nrf2 knockout (KO) mice have been shown to be more susceptible to the toxicity associated with a range of different compounds, in the liver as well as in other organs. Conversely, pharmacological activation of Nrf2 has been shown to be protective in mouse models of hepatotoxicity.

Drug induced liver injury (DILI) is a major concern for the pharmaceutical industry, and there is a clear imperative to improve existing preclinical models of DILI. Oxidative stress is known to result from the administration of a number of model hepatotoxins and has also been associated with cases of idiosyncratic DILI. Biomarkers of Nrf2 activity have potential utility in preclinical models investigating the role of oxidative stress in hepatotoxicity. Furthermore, such biomarkers could also have applications in studies determining the importance and variability of Nrf2 in the human population. Consequently the aim of the work described in this thesis was to characterise the hepatic profiles of mice in which Nrf2 activity had been modulated in order to identify candidate biomarkers of Nrf2 activity.

iTRAQ analysis was employed in order to identify the proteins that were differentially expressed in the livers of wild type (WT) and Nrf2 KO mice. Subsequent pathway analysis identified cytoprotection and lipid metabolism as the processes that were most significantly perturbed in the livers of KO animals, with lipid metabolism found to be negatively regulated by Nrf2. The development of an LC-MS/MS assay for the determination of hepatic GSH and GSSG levels in liver homogenates showed that basal GSH levels were reduced by 21.5% in Nrf2 KO mice when compared to their WT counterparts. GC-FID analysis identified a number of fatty acids with levels that differed in the livers of WT and Nrf2 KO animals, constitutively and following carbohydrate restriction. Preliminary lipidomic analysis also identified differences in the wider hepatic lipid profile of the

animals. iTRAQ was further employed to investigate the hepatic proteomic profile of mice following the administration of a single 3mg/kg dose of the Nrf2 inducer, CDDO-Me. Five proteins were found to be regulated at both the basal and inducible level and so have significant potential to be used in the development of biomarkers indicative of Nrf2 activity.

The work described in this thesis highlights the importance of the roles that Nrf2 plays in the regulation of hepatic homeostasis in terms of both cytoprotection and lipid metabolism. Furthermore, it has identified proteins and pathways that have potential applications in the development of biomarkers of Nrf2 activity. Such biomarkers would have utility in preclinical assays and in investigations into the importance of the transcription factor in the human population.

Acknowledgements

I would like to sincerely thank all the people who have supported me over the course of my PhD studies with their friendship, encouragement and technical advice. I am particularly grateful to my primary supervisor Dr. Neil Kitteringham, for all of his valuable and constructive suggestions as well as his encouragement, advice and sense of humour. The insightful input of my second supervisor, Prof. Kevin Park, is also much appreciated. I would like to express my gratitude to Dr. Chris Goldring, who has always taken the time to help and guide me in my work and to Dr. Helen Powell who has also offered constructive and insightful advice.

Dr. Roz Jenkins made a significant and much appreciated contribution to the iTRAQ studies described in this thesis, and I am also grateful to Dr. Cliff Rowe and Dr. Laura Randle for their assistance with the statistical analysis, and to Jane Hamlett for her technical support.

Dr. Anahi Santoyo Castelazo and Dr. Rowena Sison-Young were both involved in the development of the LC-MS/MS method and I would like to thank them for sharing their time and technical knowledge with me, and for their continued friendship. Thanks are also due to Mike Wong for his CDDO-Me synthesising talents.

I would like to thank Dr. Jules Griffin, Zsuzsi Ament and Emma Lecommandeur at Cambridge University for their hospitality and technical assistance with the lipid analysis. I am also grateful to Prof. Anja Kipar and Val Tilston for their histopathological work.

The expertise and patience of Phil Glaves at AstraZeneca in assisting me with the TLDA experiments was much appreciated and I am grateful for the funding provided by the BBSRC and AstraZeneca.

I would also like to thank Phill Roberts, Pete Metcalfe, Luke Palmer, Jan Lampard and Alison Reid for their technical support and willingness to answer any number of requests for help. My thanks also go to Rhys Sweeney, Sarah Roper and all the staff at the BSU.

I am grateful to all the people who have come and gone in the last four years – especially to Adam, Alvin, Row and Laura who were all there to get me started and to everyone who has kept me going: Ian, Holly, George, Bhav, Jack, Mike, Tom, Pika, James, Ali, Aine, Jon, Sophie, Hayley, Craig, Rachel, Swale, Lewis, Rym, Viv, Rob, Maxine, Awel, Fiazia, Akua, Kay, Dammy, Luke S, Junnat, Jean, Han, Sammy, Mohammad and Karthik.

I would like to say a special thank you to Row E, Lorna, Sam, Hannah, Nicola, Phil and Catherine, who have been a much appreciated support over the last four years and (nearly) always kept me smiling.

My parents have always supported me in everything I have decided to do, even when that involved going back to university to study Pharmacology... and then staying on for another four years. I am very grateful for their love and support and that of Michael, David, Sue, Pat, Eamonn, Joanna, Adam and Em. Finally, I would like to thank my wonderful husband for all his patience, encouragement, computer expertise and love. I would never have got through the PhD without him.

Publications

Papers

Walsh J, Jenkins RE, Olayanju A, Powell H, Goldring CEP, Kitteringham NR, Park BK. Protoemic comparison of basal and inducible Nrf2-regulated protein expression in mouse liver (manuscript in preparation).

Kitteringham NR, Abdullah A, Walsh J, Randle L, Jenkins RE, Sison R*, et al.* (2010). Proteomic analysis of Nrf2 deficient transgenic mice reveals cellular defence and lipid metabolism as primary Nrf2-dependent pathways in the liver. *J Proteomics* **73**(8)**:** 1612-1631.

-This paper forms the basis of chapter 2.

Kratschmar DV, Calabrese D, Walsh J*,* Lister A, Birk J, Appenzeller-Herzog C*, et al.* (2012). Suppression of the Nrf2-dependent antioxidant response by glucocorticoids and 11beta-HSD1-mediated glucocorticoid activation in hepatic cells. *PLoS One* **7**(5)**:** e36774.

Yeang HX, Hamdam JM, Al-Huseini LM, Sethu S, Djouhri L, Walsh J*, et al.* (2012). Loss of transcription factor nuclear factor-erythroid 2 (NF-E2) p45-related factor-2 (Nrf2) leads to dysregulation of immune functions, redox homeostasis, and intracellular signaling in dendritic cells. *J Biol Chem* **287**(13)**:** 10556-10564.

Abstracts

Walsh J, Kitteringham NR, Griffin JL, Goldring CEP, William S, Powell H, Park BK (2011). The role of the transcription factor Nrf2 in lipid metabolism in the liver. BTS Spring meeting, 2011.

Walsh J, Kitteringham NR, Griffin JL, Goldring CEP, Powell H, Park BK (2011). The role of the transcription factor Nrf2 in cytosolic fatty acid metabolism in the liver. Biochemical Society, Hot Topic Event - Nrf2 signalling in health and disease, December, 2011.

Walsh J, Kitteringham NR, Griffin JL, Goldring CEP, Powell H, Park BK (2012). Nrf2 in the adaptive response to chemical stress - development of novel biomarkers of chemically-induced stress. ISSX annual conference, 2012.

Abbreviations

ACC1;	acetyl CoA carboxylase 1
ACL;	ATP-citrate lyase
ACN;	acetonitrile
AIMs;	antioxidant inflammation modulators
AKR;	aldo-keto reductases
ALP;	alkaline phosphatase
ALT;	alanine aminotransferase
AMU;	atomic mass units
AP-1;	activator protein 1
APO;	apolipoprotein
ARE;	antioxidant response element
AST;	alanine aminotransferase
AT;	aminotransferase
ATP;	adenosine triphosphate
BF_3;	boron trifluoride
BH;	Benjamini-Hochberg
BLVRB;	biliverdin reductase B
BPDS;	*batho*-phenanthroline disulphonate
bZip;	basic leucine zipper
cAMP;	cyclic adenosine monophosphate
CBP;	CREB-binding protein
CDDO;	2-cyano-3,12-dioxooleana-1,9,-dien-28-oic acid
CDDO-Im;	CDDO-imidazole
CDDO-Me;	CDDO-methyl ester
CDSS;	Centre for Drug Safety Science
CES-1;	carboxylesterase-1
CHO-R;	carbohydrate-restricted
CKD;	chronic kidney disease
CM-GSH;	S-carboxymethyl-glutathione
CNC;	cap 'n' collar
CO_2;	carbon dioxide
COPD;	chronic obstructive pulmonary disorder
COX-2;	cyclooxygenase-2
CREB;	cAMP-responsive element binding protein
CRM;	chemically reactive metabolite
Cul3;	cullin 3
CV;	coefficient of variation
CYP450;	cytochrome P450
Cys;	cysteine
DAVID;	Database for Annotation, Visualization and Integrated Discovery
dH_2O;	distilled water
DILI;	drug-induced liver injury
DMSO;	dimethyl sulphoxide
DNA;	deoxyribonucleic acid

DTNB;	5,5-dithiobis-1,2-nitrobenzoic acid
ECH;	erythroid cell-derived protein with CNC homology
ECL;	enhanced chemiluminescence
EDTA;	ethylenediaminetetraacetic acid
ENTPD5;	ectonucleoside triphosphate diphosphohydrolase 5
FABP5;	epidermal fatty acid binding protein
FAME;	fatty acid methyl ester
FA;	formic acid
FAS;	fatty acid synthase
FDA;	Food and Drug Administration
FDR;	false discovery rate
FeNTA;	ferric nitrilotriacetate
GC-FID;	gas chromatography/flame-ionisation detector
GCL;	γ-glutamylcysteine ligase
GCLC;	GCL, catalytic subunit
GCLM;	GCL, regulatory subunit
GPX;	glutathione peroxidases
GR;	glutathione reductase
GS;	glutathione synthetase
GSH;	glutathione
GSHee;	glutathione ethyl ester
GSH-IS;	glutathione-(Glycine$^{13}C_2{}^{15}N$).
GSSG;	oxidised glutathione
GST;	glutathione S-transferase
H_2O;	water
H_2O_2;	hydrogen peroxide
HAT;	histone acetyltransferase
HO-1;	haem oxygenase 1
HRP;	horseradish peroxidase
IAA;	iodoacetic acid
ICAT;	isotope-coded affinity tags
IFN-γ;	interferon-gamma
IgG;	immunoglobulin G
IKK-β;	inhibitor of nuclear factor kappa-B kinase subunit beta
iNOS;	inducible nitric oxide synthase
i.p.	intraperitoneal
iTRAQ	isobaric tags for relative and absolute quantification
JAK;	janus kinase
KCl;	potassium chloride
kDa;	kiloDalton
Keap1;	Kelch-like ECH-associated protein 1
Keap1-HKO	Keap1-hepatocyte-specific knockout
KO;	knockout

LLOQ;	lower limit of quantification
MALDI-TOF MS;	matrix-assisted laser desorption ionisation time-of-flight mass spectrometry
MAPK;	mitogen-activated protein kinase
MCD;	methionine- and choline-deficient
MEF;	mouse embryonic fibroblast
mEH;	microsomal epoxide hydrolase
miR;	microRNA
MMTS;	methylmethanethiosulphate
mRNA;	messenger RNA
MS/MS;	tandem mass spectrometry
MUP6;	major urinary protein 6
NaCl;	sodium chloride
NADPH;	nicotinamide adenine dinucleotide phosphate
NAFLD;	non-alcoholic fatty liver disease
NAPQI;	N-acetyl-*p*-benzoquinoneimine
Neh;	Nrf2-ECH homology
NEM;	N-ethylmaleimide
NF-κB;	nuclear factor kappa-light-chain-enhancer of activated B cells
NQO1;	NAD(P)H:quinine oxidoreductase 1
NO;	nitric oxide
Nrf2;	nuclear factor erythroid 2 related factor 2
NSAIDs;	nonsteroidal anti-inflammatory drugs
PBMCs;	peripheral blood mononuclear cell
PBS;	phosphate-buffered saline
PCA;	principal component analysis
PCR;	polymerase chain reaction
PI3K;	phosphatidylinositol 3-kinases
PEITC;	phenethyl isothiocyanate
PLS-DA;	partial least squares discriminant analysis
PKC;	protein kinase C
PPAR-γ;	peroxisome proliferator-activated receptor-gamma
Prx1;	peroxiredoxin 1
RNA;	ribonucleic acid
ROS;	reactive oxygen species
SCD;	stearoyl CoA desaturase
SDS;	sodium dodecyl sulphate
SEM;	standard error of the mean
SILAC;	stable isotope labelling by amino acids in cell culture
SNP;	single nucleotide polymorphisms
SOD;	superoxide dismutase
SREBP1c;	sterol regulatory element-binding protein 1c
SSA;	sulphosalicylic acid
STAT;	signal transducer and activator of transcription

STZ;	streptozotocin
tBHQ;	tert-butylhydroquinone
TBL;	total bilirubin
TBS;	tris-buffered saline
TBST;	TBS-tween
TCEP;	tris(2-carboxyethyl)phosphine
TEAB;	triethyl ammonium bicarbonate
TFA;	trifluoroacetic acid
TLDA;	TaqMan low density array
TNF-α;	tumour necrosis factor-alpha
TrxR;	thioredoxin reductases
Trx;	thioredoxins
UDP;	uridine diphosphate
UGT;	UDP-glucuronosyltransferases
ULN;	upper limit of normal
UMP;	uridine monophosphate
WT;	wild type
w/v;	weight/volume

Designation of significance:

$P < 0.05$ = *
$P < 0.01$ = **
$P < 0.001$ = ***

General Introduction

Contents

1.1 Drug-induced liver injury

1.1.1 Drug-induced damage of the liver

The liver is a vital organ for the maintenance of homeostasis within the body, and has a diverse range of functions in processes including digestion, protein synthesis and immunity. It has key roles in lipid metabolism and glucose regulation and protects organisms from systemic exposure to exogenous toxins through a variety of detoxification pathways. However, as the primary site for the processing of environmental toxins and drugs, the liver is particularly susceptible to drug-related toxicity.

Drug induced liver injury (DILI) encompasses a heterogeneous set of conditions and can result from both acute and chronic exposure to drugs. DILI can be broadly divided into hepatocellular and cholestatic injury. Damage to cells in the liver can lead to hepatic necrosis, the development of fibrosis and hepatitis and in some cases, cancer. In its most serious form, hepatocellular damage can result in fulminant hepatic failure. Cholestatic liver injury occurs when bile flow is perturbed. It is usually reversible, and consequently has less propensity to result in severe liver injury (FDA, 2009).

While drug administration can result in acute liver damage, chronic conditions may also develop as a result of drug toxicity, including non-alcoholic fatty liver disease (NAFLD) and steatosis. In such cases, attributing liver injury to drug administration can be problematic, as both forms of liver disease are closely associated with metabolic syndrome and hyperlipidaemia. 20% of the adult population are estimated to have NAFLD (Chowdhry *et al.*, 2010), consequently it is difficult to monitor the development of drug-induced fatty liver and to distinguish it from lifestyle-related disease. However, in a limited number of cases including that of valproic acid, a link between drug administration and NAFLD has been established (Sato *et al.*, 2005; Verrotti *et al.*, 2009).

1.1.2 The impact of DILI on drug development

Hepatotoxicity is a major concern for the pharmaceutical industry. More than 600 drugs have been linked to cases of liver injury (Park *et al.*, 2005a; Suh *et al.*, 2003) and DILI is the reason most commonly cited for the withdrawal of an approved drug from the market (Lee, 2003). Greater than 50% of cases of acute liver failure in the USA can be attributed to DILI (Antoine *et al.*, 2008) with the majority of patients requiring a liver transplant in order to survive. Given that there is a 60 to 80% mortality rate in patients with acute liver failure

who do not receive a transplant (Bjornsson *et al.*, 2005), together with the contribution of hepatotoxicity to instances of drug withdrawal, it is clear that DILI poses a significant threat to public health.

The problem of DILI is also severe in terms of the cost to the pharmaceutical industry. It is estimated that in the last decade, the cost of developing a drug has risen to in excess of $800 million (DiMasi *et al.*, 2003). This highlights how crucial it is that the potential for toxicity is identified as early in the development process as possible. While the identification of potential hepatotoxins is vital, preclinical assays should also be sufficiently robust to enable the identification of compounds that are safe. If a signal from an assay cannot be definitively interpreted, continued development of the drug may be deemed to be too much of a risk, and potentially beneficial compounds are lost. Consequently there is a clear imperative for the development of improved predictive preclinical models of hepatotoxicity in order to allow the confident identification of compounds that are likely to result in liver damage and crucially, those that are safe.

An understanding of the mechanisms by which liver damage occurs is important for the development of such models. While drug toxicity can have a dose dependent profile and relate to the primary pharmacology of a drug, some of the most severe cases of DILI are idiosyncratic, with the mechanisms by which liver injury occurs poorly understood (Park *et al.*, 2005b). Research investigating the mechanisms by which DILI occurs can be invaluable in informing the drug development process and identifying potentially hepatotoxic compounds, while also contributing to the identification of candidate translational biomarkers of DILI.

1.1.3 Mechanisms of DILI – Reactive metabolite formation and oxidative stress

Although the exact mechanisms of DILI often remain elusive, reactive metabolite formation has been identified as a common step in a significant number of cases of idiosyncratic toxicity (Antoine *et al.*, 2008; Walgren *et al.*, 2005; Zhou *et al.*, 2005). In general, the drug metabolism processes that occur in the liver result in the detoxification and safe excretion of compounds. However, in some instances, metabolism can lead to the generation of species that are more reactive than the parent compound. This is widely documented following cytochrome P450 (CYP450) mediated phase I oxidative metabolism (Antoine *et al.*, 2008; Park *et al.*, 1995) , but can also occur following phase II conjugative metabolism

as has been noted with the formation of protein reactive acyl glucuronide metabolites of some nonsteroidal anti-inflammatory drugs (NSAIDs) including diclofenac (Hargus *et al.*, 1995; Kretz-Rommel *et al.*, 1993).

Reactive metabolite production can result in covalent modification of proteins and damage to mitochondria and DNA. Such pathological processes are closely associated with glutathione depletion and oxidative stress. The toxicity resulting from paracetamol overdose is widely studied as a model of chemically reactive metabolite (CRM)-mediated DILI, and glutathione depletion and oxidative stress are characteristic of paracetamol-induced hepatotoxicity (Hazelton *et al.*, 1986; Lores Arnaiz *et al.*, 1995).

When a therapeutic dose of paracetamol is taken, the majority of the drug undergoes conjugative metabolism via glucuronidation and sulphation pathways, and is safely excreted. Paracetamol toxicity involves the bioactivation of the parent compound to the highly reactive metabolite N-acetyl-*p*-benzoquinone imine (NAPQI) (Dahlin *et al.*, 1984). This occurs via the action of three CYP450 enzymes, CYP2E1, CYP1A2 and CYP3A4 (Dai *et al.*, 1995; Manyike *et al.*, 2000; Nelson, 1995; Tonge *et al.*, 1998). NAPQI is also formed following a therapeutic dose but is readily conjugated to reduced glutathione, either spontaneously or through a glutathione-S-transferase (GST) catalysed mechanism, and is safely excreted.

In cases of paracetamol overdose, the levels of NAPQI that are produced result in glutathione depletion such that cellular defence mechanisms are overwhelmed and oxidative damage to proteins, lipids and DNA can occur. Necrosis can result, although apoptotic cell death has also been shown following paracetamol overdose (Ferret *et al.*, 2001; Ray *et al.*, 2000; Ray *et al.*, 1999; Ray *et al.*, 1996). Significant levels of cell death can lead to severe liver injury, and paracetamol overdose is currently the most frequent cause of acute liver failure in the USA (Larson *et al.*, 2005), and in the UK (Ryder *et al.*, 2001).

In the case of many other compounds, the mechanism by which DILI occurs is less well characterised. While the toxicity of some drugs is known to be associated with CRM formation or the parent compound itself, in other cases, the relative contribution of the metabolite and parent compound to toxicity is not clear. For example, nefazodone, a drug that was withdrawn due to instances of rare but severe hepatitis, has been associated with CRM formation (Kalgutkar *et al.*, 2005), transporter inhibition (Kostrubsky *et al.*, 2006) as

well as oxidative stress and glutathione depletion (Dykens *et al.*, 2008; Xu *et al.*, 2008a), however the mechanism that results in the severe liver damage remains undetermined.

One study using imaging of primary hepatocytes treated with a range of 344 drugs, including many compounds associated with DILI, concluded that the most important contributors to hepatotoxicity are mitochondrial damage, intracellular glutathione depletion and oxidative stress (Xu *et al.*, 2008a). Drugs that are known to cause severe idiosyncratic hepatotoxicity including nefazodone, troglitazone and nimesulide were associated with one or more of the parameters, whereas drugs with superior safety profiles had consistently negative results in the assays. While the role of CRM formation in toxicity associated with the drugs investigated was often unclear, oxidative stress and glutathione depletion were consistently associated with known hepatotoxins.

Other studies evaluating the NSAID nimesulide (Singh *et al.*, 2010) and the anti-epileptic drug, valproic acid (Chang *et al.*, 2006) have also associated hepatotoxicity with oxidative stress. This would suggest that investigations into the role of oxidative stress in DILI could contribute significantly to understanding the mechanisms by which the injury occurs as well as to the identification of potentially hepatotoxic compounds. Characterisation of the pathways associated with the oxidative stress response has the potential to inform the identification of reliable biomarkers of DILI as well as the development of predictive preclinical *in* vitro and *in vivo* models. Biomarkers that are indicative of oxidative stress would have valuable applications in the drug development process and translational value in the clinic, given that the pathologies associated with DILI often reflect natural disease processes (Park *et al.*, 2005a).

1.2 The oxidative stress response

1.2.1 Oxidative and electrophilic stress

Oxidative stress occurs when there is an imbalance in a cell between the pro-oxidant species that can damage key macromolecules, and the anti-oxidative mechanisms that have evolved to protect the body from these potentially harmful species. The redox balance can be perturbed by radicals including reactive oxygen species (ROS), as well as peroxides and electrophiles.

Radical species are constantly produced in the body as a by-product of mitochondrial oxidative phosphorylation and have physiological roles in the immune system and signalling processes. They can also be formed by the actions of enzymes on substrates, including exogenous drugs and toxins. For example, carbon tetrachloride is widely studied as a model compound that is metabolised by the action of CYP450 enzymes to form radical species that result in hepatotoxicity (Weber *et al.*, 2003).

Pathologically, the production of radicals can arise as the result of injury or inflammation, and oxidative stress has been associated with a number of disease processes including neurodegenerative conditions, cancer, and cardiovascular disease (Ames, 1983; Dhalla *et al.*, 2000; Miller, 1970; Valko *et al.*, 2007). Radical species have a single unpaired electron and can cause damage to proteins, lipids and DNA, resulting in reduced function. If the damage is severe, cell death can result.

While some exogenous compounds can be metabolised to form radical species, others have intrinsic electrophilic properties or can be metabolised to form electrophiles thus increasing their reactivity towards nucleophilic centres in macromolecules. Consequently, electrophilic stress can also lead to cellular damage and reduced function.

1.2.2 The cytoprotective response

Cellular defence mechanisms have evolved in a way that allows organisms to manage the basal levels of oxidative stress but also respond robustly to acute oxidative insult. The processes by which cells act to prevent damage to macromolecules by oxidative and electrophilic stress can be broadly categorised into five groups [adapted from (Kensler *et al.*, 2007)]:

- Oxidation and reduction of hydrophobic compounds, whereby functional groups are exposed, often by the action of CYP450 enzymes, facilitating further metabolism.
- Nucelophilic trapping processes, including conjugative metabolism by enzymes such as GSTs and UDP-glucuronosyltransferases (UGTs), as well as inactivation of ROS by catalase, superoxide dismutases (SODs) and glutathione peroxidases (GPXs).
- The export of toxic metabolites via efflux transporters.

- The action of anti-oxidants including vitamin E, vitamin C, β-carotene (the precursor of vitamin A) and bilirubin, which all have the ability to scavenge free radicals.
- The maintenance of reducing capacity by the thiol-containing molecules glutathione and thioredoxin.

A range of cytoprotective proteins are important for mediating this oxidative stress response, these include enzymes that are required for glutathione synthesis as well as Phase I and Phase II metabolism proteins and drug efflux transporters. While these proteins are expressed constitutively, their expression can also be up-regulated following an oxidative insult (Primiano *et al.*, 1997), thereby helping to restore intracellular homeostasis through mechanisms such as glutathione repletion and the direct detoxification of electrophiles. One of the most important mediators of this up-regulation is a transcription factor that belongs to the CNC-bZIP transcription factor family (Jaiswal, 2004) and is termed nuclear factor-erythroid 2–related factor 2 (Nrf2). The role of Nrf2 is described below in section 1.2.3.

The multi-faceted defence response allows cells to successfully prevent damage by oxidative stress and electrophilic species in most instances. However, the ability of a cell to repair damage to macromolecules when it does occur represents an important further tier of the defence response. Repair to proteins is mediated by the thioredoxin and glutaredoxin enzymes, while DNA repair occurs by base or nucleotide excision.

When a toxic insult is severe, cellular defence mechanisms can be overwhelmed. If intracellular damage is of a sufficient magnitude, normal cellular processes including cell division cease, and proteins that are significantly damaged are targeted for proteasomal degradation or autophagic mechanisms. If damage to the cell is irreparable, apoptosis is initiated. The level of damage can be such that the cytoprotective proteins themselves are damaged and can no longer function successfully. Depletion of glutathione following a paracetamol overdose is associated with a reduction in the activity of many of the enzymes that are key in the oxidative stress response, including, glutathione reductase, glutathione peroxidase, γ-glutamylcysteinyl synthase, catalase and superoxide dismutase (Acharya *et al.*, 2010; O'Brien *et al.*, 2000). Such damage has the potential to result in necrotic cell death and severe liver damage.

1.2.3 The role of Nrf2 in the cytoprotective response

The role of Nrf2 in the response to oxidative stress is well established. Following oxidative insult, the transcription factor mediates the regulation of the inducible expression of cytoprotective genes containing a common sequence termed the antioxidant response element (ARE) in their promoter regions (Itoh *et al.*, 1997). Nrf2 is also known to play a significant role in the constitutive regulation of some ARE-containing genes. A list of cytoprotective genes that are constitutively and inducibly regulated by Nrf2 is given in table 1.1.

The Nrf2 gene was first isolated in 1994 (Moi *et al.*, 1994). While the transcription factor is expressed in the majority of tissues, its levels are highest in organs such as the liver and the skin which play the most significant role in detoxification or are most commonly exposed to exogenous compounds.

The level and functional capacity of Nrf2 is regulated at the post-transcriptional level, primarily through its association with an actin-associated protein, kelch-like ECH associated protein 1 (Keap 1). The Nrf2 protein is a high turnover molecule, with a half-life of less than twenty minutes (Itoh *et al.*, 2003; Kobayashi *et al.*, 2004). The rapid turnover rate of the Nrf2 protein means that the transcription factor is difficult to detect under basal conditions. In the absence of oxidative stress, Nrf2 is bound to a Keap1 homodimer, which sequesters Nrf2 in the cytosol. (Itoh *et al.*, 1999). Through interaction with a cullin-dependent E3 ubiquitin ligase complex (cul3), Keap1 targets Nrf2 for ubiquitination (Cullinan *et al.*, 2004; Furukawa *et al.*, 2005), and subsequent proteasomal degradation. However, under conditions of oxidative stress, the interaction of Nrf2 with Keap1 is disrupted. This prevents the turnover of Nrf2, and the transcription factor rapidly accumulates in the cell, thus enabling the transcription of downstream genes. A summary of Nrf2 regulation and activation is shown in figure 1.1.

Table 1.1: Cytoprotective enzymes regulated by Nrf2 (Adapted from Copple *et al.*; 2008).

Full name	Abbreviation	Reference
Aldo-keto reductases	AKR	Lou *et al.*; 2006, Nishinaka *et al.*; 2005
Biliverdin reductase B	BLVRB	Wu *et al.*; 2011
Ferritin		Pietsch *et al.*; 2003
Glutamate cysteine ligase, catalytic subunit	GCLC	Chan *et al.*; 2000, Jeyapaul *et al.*; 2000, Sekhar *et al.*; 2000
Glutamate cysteine ligase, modifier subunit	GCLM	Chan *et al.*; 2000, Moinova *et al.*; 1999, Wild *et al.*; 1999
Glutathione peroxidases	GPX	Wu *et al.*;2011
Glutathione synthetase	GS	Lee *et al.*; 2005
Glutathione S-transferases	GST	Chanas *et al.*; 2002, Hayes *et al.*; 2000, McMahon *et al.*; 2001, Thimmulappa *et al.*; 2002
Haem-oxygenase 1	HO-1	Alam *et al.*; 1999, Ishii *et al.*; 2000
Microsomal epoxide hydrolase	mEH	Ramos-Gomez *et al.*; 2001, Slitt *et al.*; 2006, Thimmulappa *et al.*; 2002
NADPH: quinone oxidoreductases	NQO	Venugopal *et al.*; 1996, Wang *et al.*; 2006
Peroxiredoxin 1	Prx 1	Kim *et al.*; 2007, Wu *et al.*;2011
Superoxide dismutases	SOD	Park *et al.*; 2002
Thioredoxin reductases	TrxR	Sakurai *et al.*; 2005
Thioredoxins	Trx	Kim *et al.*; 2001, Kim *et al.*; 2003
UDP-glucuronosyltransferases	UGT	Shelby *et al.*; 2006, Yueh *et al.*; 2007

1.2.4 The hinge and latch model of Nrf2 activation

As a cysteine-rich molecule, Keap1 is well adapted to act as a sensor for electrophilic and oxidative stress. Human Keap1 contains 27 cysteine residues, while Keap1 in mice and rats contains 25 cysteine residues (Dinkova-Kostova *et al.*, 2002; Itoh *et al.*, 1999). Indeed, a range of compounds including triterpenoids, isothiocynates and dithioethiones that are known to activate Nrf2 have been shown to react with Keap1, modifying different cysteine residues (Dinkova-Kostova *et al.*, 2002; Hong *et al.*, 2005; Luo *et al.*, 2007; Yates *et al.*, 2009).

Oxidative and electrophilic species can modify the sulfhydryl groups of Keap1, altering its conformation (Kobayashi *et al.*, 2006), and this is the basis for the hinge and latch model of Nrf2 activation (Tong *et al.*, 2006). Two motifs in the Nrf2 protein are important for the binding of the transcription factor to Keap1: the high affinity ETGE and the lower affinity DLG. The conformational change that occurs in Keap1 following an oxidative insult results in the detachment of Nrf2 at the DLG domain (the latch), while the association at the ETGE is maintained (the hinge). Keap1 is no longer able to target Nrf2 for ubiquitination and Keap1 molecules quickly become saturated with Nrf2. Aided by a nuclear localisation sequence (Jain *et al.*, 2005), newly synthesised Nrf2 is free to translocate to the nucleus, where the transcription factor mediates the transcription of genes containing the ARE (Itoh *et al.*, 1999).

In order to bind to the ARE, Nrf2 must first form a heterodimer with other bZIP factors, typically small Maf proteins (Itoh *et al.*, 1997). Once bound, Nrf2 recruits coactivator proteins, most notably CREB-binding protein (CBP), and target gene transcription results (Katoh *et al.*, 2001). CBP has intrinsic histone acetyltransferase (HAT) activity, but also interacts with other HAT proteins to facilitate gene transcription.

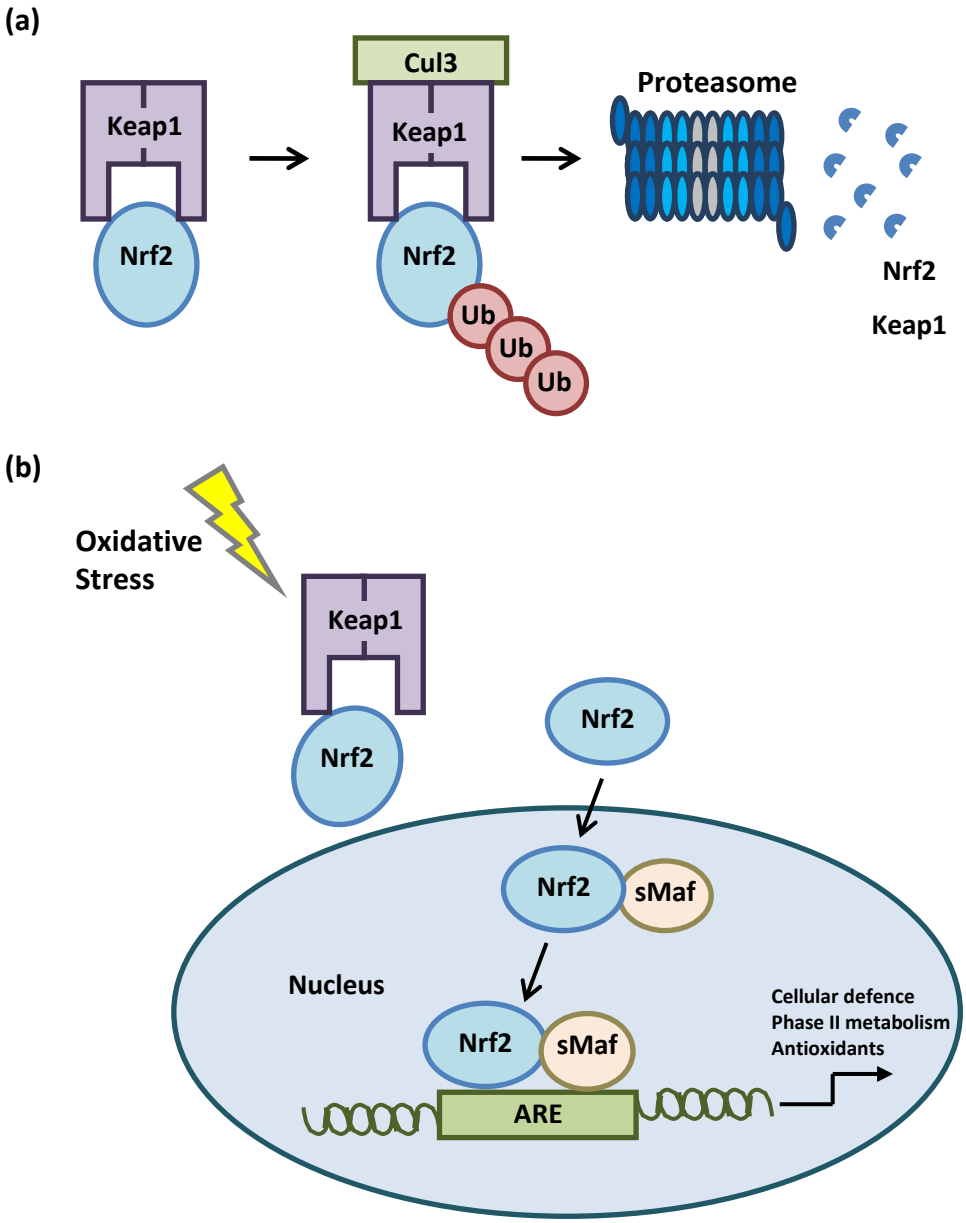

Figure 1.1: The regulation and activation of the transcription factor Nrf2. (a) Under basal conditions, Nrf2 is bound to a Keap1 homodimer, which targets Nrf2 for ubiquitination and subsequent proteosomal degradation. (b) Under conditions of oxidative stress, the interaction between Nrf2 and Keap1 is disrupted and Nrf2 is no longer targeted for degradation. Molecules of Keap1 become saturated and newly synthesised Nrf2 is free to translocate to the nucleus, where it dimerises with partners including small Maf protein (sMaf) and binds to the antioxidant response element (ARE) in a range of cytoprotective genes, mediating their transcription.

1.2.5 The regulation of Nrf2 is complex

There is evidence to suggest that the hinge and latch model is not universally applicable to all instances of Nrf2 activation and that other mechanisms can also play a role in the regulation of the Keap1-Nrf2 interaction. For example, studies have shown that some Nrf2 inducers including the heavy metals result in the complete dissociation of Nrf2 from Keap1 (He *et al.*, 2008; He *et al.*, 2007). Furthermore, other mechanisms may contribute to the modulation of the Keap1-Nrf2 pathway in parallel with those regulating the partial or complete dissociation of Nrf2. Some inducers of Nrf2, including sulphoraphane and tert-butylhydroquinone (tBHQ), have been shown to disrupt the interaction between Keap1 and Cul3 (Zhang *et al.*, 2004), thus inhibiting the ubiquitination and enhancing the stability of the transcription factor.

Evidence from *in vivo* studies suggests that there are further levels of Nrf2 regulation that are not explained by the hinge and latch model of Nrf2 activation. For example, studies in Nrf2 knockout (KO) mice highlight the importance of Nrf2 in the basal as well as inducible expression of target genes (Chanas *et al.*, 2002; McMahon *et al.*, 2001). There is also evidence that Nrf2 inducers increase mRNA levels of the transcription factor (Ramos-Gomez *et al.*, 2001), whereas this increase has not been seen in many *in vitro* studies employing Nrf2 inducers (Itoh *et al.*, 2003; McMahon *et al.*, 2003; Stewart *et al.*, 2003). While such increases in Nrf2 may not be important in the acute response to oxidative stress, they are likely to have more subtle long term implications for regulation of gene expression by the transcription factor. The hypothesis for autoregulation of Nrf2 is supported by the presence of an ARE in the Nrf2 promoter (Kwak *et al.*, 2002).

A range of signalling pathways have been implicated in the regulation of Nrf2, many involving protein kinases and the phosphorylation of the transcription factor. Often, these signalling pathways are hypothesised to be Keap1 independent, but function alongside Keap1 regulation of Nrf2. Protein kinase C (PKC) activation has been shown to induce Nrf2-mediated gene expression, with Ser40 identified as the residue important for Nrf2 phosphorylation by PKC (Bloom *et al.*, 2003; Huang *et al.*, 2002; Huang *et al.*, 2000). Mitogen-activated protein kinase (MAPK) and PI3K pathways have also been implicated in Nrf2 regulation (Alam *et al.*, 2000; Lee *et al.*, 2001; Reddy *et al.*, 2008; Yu *et al.*, 1999). However, Keap1 is fundamental to the regulation of Nrf2 activity *in vivo*, as studies employing organ-specific Keap1 knockdown show that when pharmacological activators of

Nrf2 are used in such models, further Nrf2 activation is limited (Yates *et al.*, 2009). Furthermore when phosphorylation pathways implicated in Nrf2 signalling are inhibited, the effects on Nrf2 activation are modest when compared to Keap1 modulation (Sun *et al.*, 2009).

1.2.6 The role of glutathione in cytoprotection

Glutathione is an essential tripeptide (γ-Glu-Cys-Gly) that has a number of critical functions within cells, including electrophile conjugation and the scavenging of free radicals, and as such is an important molecule for defence against oxidative stress. Glutathione is synthesised sequentially by the action of two enzymes, glutamate cysteine ligase (GCL) and glutathione synthetase (GS). GCL catalyses the formation of a bond between glutamate and cysteine, while GS catalyses the addition of glycine to complete the tripeptide. GCL is composed of two subunits, a catalytic subunit (GCLC) and a modifier subunit (GCLM) and is the rate limiting enzyme in glutathione synthesis.

Glutathione can form covalent bonds with electrophilic species because of its nucleophilic cysteinyl thiol group. Glutathione conjugation increases the solubility of a compound, facilitating excretion and can occur spontaneously or in a reaction catalysed by GST (Leslie *et al.*, 2003). On reaction with electrophiles, glutathione is oxidised non-enzymatically to a disulphide (GSSG), which is in turn reduced back to two molecules of glutathione (GSH) by the enzyme glutathione reductase. This process uses NADPH as an electron donor. Oxidised glutathione is also effluxed from cells, resulting in decreased intracellular glutathione levels. Consequently glutathione homeostasis is maintained by balancing the rate of synthesis of glutathione and reduction of the disulphide against the rate of glutathione conjugation and oxidation together with the transport of the disulphide out of the cell. Glutathione synthesis and redox cycling are summarised in figure 1.2.

While glutathione is present in organelles, including mitochondria and peroxisomes, between 85 and 90% of intracellular glutathione is located in the cytosol. Extracellular concentrations of glutathione are generally low, for example 2-20 μmol/L in plasma (Wu *et al.*, 2004), while levels in the liver are much higher at around 5 mM.

Glutathione deficiency has a role to play in aging as well contributing to oxidative stress in disease pathology. Depletion of glutathione is also associated with the toxicity of a number of drugs and is a hallmark event in paracetamol overdose-induced liver injury (Potter *et al.*,

1974), during which, intracellular glutathione depletion facilitates the covalent modification of macromolecules by NAPQI.

Nrf2 plays an important role in glutathione homeostasis following oxidative insult. Genes encoding enzymes, including GCL and GS, that are key for the synthesis and reduction of glutathione have been identified as Nrf2 targets (Chan *et al.*, 2001; Li *et al.*, 2009; Moinova *et al.*, 1999). While regulation of expression of glutathione synthesis is not exclusively Nrf2-mediated, (for example, the gene encoding GCL has also been shown to contain binding sites for AP-1 and NF-κB (Yang *et al.*, 2001)), evidence from studies showing a significant delay in glutathione recovery in paracetamol treated Nrf2 KO mice (Chan *et al.*, 2001) highlights the importance of the transcription factor in glutathione repletion.

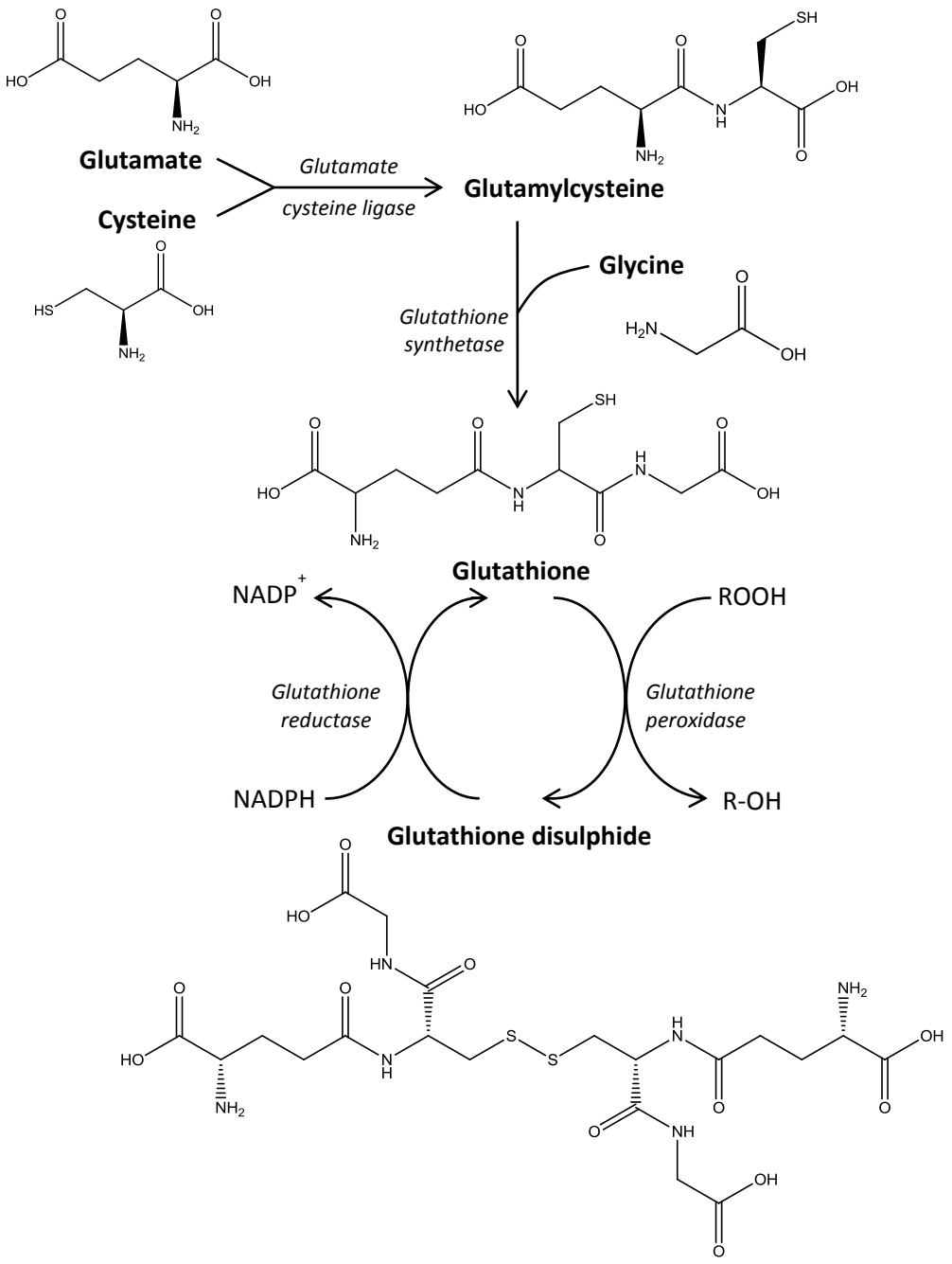

Figure 1.2: Glutathione synthesis and redox cycling. Glutathione is synthesised from glutamate, cysteine and glycine by the action of 2 enzymes, glutamate cysteine ligase and glutathione synthetase. On reaction with electrophiles, glutathione (GSH) is oxidised to the disulphide (GSSG) spontaneously or in a reaction catalysed by glutathione peroxidase. GSSG is reduced back to 2 molecules of GSH in a glutathione reductase catalysed reaction, which requires NADPH as a cofactor.

1.3 *In vivo* models of Nrf2 modulation

1.3.1 The Nrf2 knockout mouse model

In vivo studies have been widely employed to characterise the cytoprotective role of Nrf2, and the Nrf2 KO mouse model has contributed significantly to the current understanding of the transcription factor. The first Nrf2 KO mice were successfully engineered in 1996 (Chan *et al.*, 1996). Mice in which the gene for Nrf2 has been knocked out are viable and survive into adulthood. Young mice show no significant phenotype under basal conditions; however there are reports that aging Nrf2 KO mice develop lupus-like autoimmune disease, a problem that is more common in female mice (Suh *et al.*). Evidence from another study also suggests vacuolar leukoencephalopathy arises in all Nrf2 KO animals by the age of 10 months, a condition characterised by the development of cavities in the brain and the deterioration of myelin sheaths (Hubbs *et al.*, 2007).

Phenotypic differences are in evidence when Nrf2 KO mice, regardless of age, are exposed to oxidative and chemical stress. Nrf2 KO animals are more vulnerable to the toxicity associated with a diverse range of compounds in a variety of organs with examples including hepatotoxicity following paracetamol administration (Chan *et al.*, 2001; Enomoto *et al.*, 2001), hepatic fibrosis on carbon tetrachloride treatment (Xu *et al.*, 2008b), ethanol induced liver injury (Lamle *et al.*, 2008), pulmonary fibrosis resulting from administration of bleomycin (Cho *et al.*, 2004; Sriram *et al.*, 2009), cisplatin-induced renal toxicity (Park *et al.*, 2008), and colitis following dextran sulphate administration (Khor *et al.*, 2006).

Gene array studies have been carried out to compare wild type (Yang *et al.*) and Nrf2 KO mice in terms of mRNA expression both at the constitutive and inducible level following treatment with compounds known to activate Nrf2 including sulphoraphane, the isothiocyanate PEITC and tunicamycin (Hu *et al.*, 2006; Nair *et al.*, 2007; Nair *et al.*, 2006; Thimmulappa *et al.*, 2002). The studies have focussed on gene expression in the liver and small intestine and identified genes important for xenobiotic metabolism, glutathione synthesis, and NADPH generation, as being Nrf2 regulated. Processes such as biosynthesis, metabolism and cell cycle control were also found to be modulated by Nrf2 at some level. Gene arrays provide an unbiased method of identifying mRNA expressional differences, however levels of mRNA do not directly correspond to protein synthesis levels in a cell and so do not always give an accurate representation of protein expression or activity

(Kitteringham *et al.*, 2000). Consequently, the functional relevance of differences in mRNA expression levels is not always clear.

Differences have also been identified in WT and Nrf2 KO mice at the protein level, with studies focussing on a single protein or a small group of proteins. Such studies often investigate the protein expression of enzymes that have been identified as differentially expressed at the mRNA level as a result of Nrf2-modulation or drug administration. However, there is a lack of work investigating the effect of Nrf2 modulation at a proteomic level, looking at global protein expression in a particular organ or system. Such studies would provide insight into pathways in which Nrf2 regulation has a functionally significant role.

1.3.2 Genetic and pharmacological models of Nrf2 induction

Keap1 KO mice have been engineered in order to study the consequences of enhanced Nrf2 activity *in vivo*. However, the mice did not survive beyond 20 days of age (Wakabayashi *et al.*, 2003). The authors suggest that this is the result of hyperkeratosis of the oesophagus and forestomach, a problem that is known to be linked to hyperactivity of Nrf2, with the phenotype being reversed in the offspring of Keap1 KO mice crossbred with Nrf2-null mice.

Organ-specific Keap1 knockdown is however possible and this approach has allowed the development of viable *in vivo* models of Nrf2 hyper-expression. A Keap1-hepatocyte-specific KO (Keap1-HKO) model was developed using the albumin-Cre loxP system, with mice showing resistance to paracetamol-induced hepatotoxicity (Okawa *et al.*, 2006) and to acute inflammatory liver injury (Osburn *et al.*, 2008).

As well as models using genetic manipulation of the Keap1-Nrf2 system, i*n vivo* models using pharmacological modulation of Nrf2 have also been employed. Triterpenoids, isothiocynates and dithioethiones are all known to activate Nrf2 (Dinkova-Kostova *et al.*, 2002; Hong *et al.*, 2005; Luo *et al.*, 2007; Yates *et al.*, 2009). The triterpenoid 2-cyano-3,12-dioxooleana-1,9,-dien-28-oic acid (CDDO) and its derivatives are the most potent inducers of Nrf2 currently identified, and are widely used in studies investigating the effects of differential Nrf2 expression. This group of molecules is described in detail in section 1.4 below.

Understanding how the profiles of pharmacological and genetic modulation of Nrf2 differ is important in the context of drug development and in determining the specificity of a given inducer, but also in giving a clearer picture of the adaptive changes that may occur in the mice that have been modified genetically. A study by Yates *et al.* used the Keap1-HKO model alongside pharmacological activation of Nrf2 using the triterpenoid, CDDO-imidazole (CDDO-Im) in order to compare the role of genetic and pharmacological modulation of Nrf2 (Yates *et al.*, 2009). CDDO-Im increased the expression of the Nrf2-regulated gene, NAD(P)H:quinone oxidoreductase 1 (NQO1) 6.5-fold in livers of WT mice at the level of mRNA expression, while it was increased 24.4-fold in Keap1-HKO mice. Interestingly, in Keap1-HKO mice treated with CDDO-Im, further increases in NQO1 expression were minimal (Yates *et al.*, 2009). While genetic manipulation results in maximal Nrf2 activation, triterpenoid administration is a valuable tool for achieving Nrf2 activation *in vivo*.

Adaptation to genetic manipulation is one of the limitations associated with the use of *in vivo* animal models to study human health and disease, with chronic gene deficiency resulting in alterations in gene and protein expression profiles that differ from those arising from drug administration. However there are other factors associated with the use of experimental animals regardless of whether the model has been genetically modified. Laboratory mouse strains are usually inbred, resulting in a population with little genetic variability. Furthermore, the environment and diet of the animals is closely monitored and controlled, with exposure to pathogens limited. Such conditions are not reflective of a genetically diverse human population experiencing a wide range of environmental influences with highly varied diets and disease profiles. Consequently, these factors need to be taken into account when interpreting results from animal experiments and extrapolating to humans.

1.3.3 NQO1 as a marker of Nrf2 activation

NQO1 is often used as a marker of Nrf2 activation, as was the case in the study of Yates *et al.*, described above. NQO1 was one of the genes that was first identified as an Nrf2 target and the importance of Nrf2 in the regulation of both the basal and inducible expression of NQO1 is now well characterised (Itoh *et al.*, 1997; Kwak *et al.*, 2001; McMahon *et al.*, 2001), with a functional ARE identified in the murine *Nqo1* gene *(Nioi et al., 2003).* NQO1 works as an antioxidant and has a role in the detoxification of quinines, naphthoquinones, quinine imines, nitro and azo compounds, catalysing their two electron reduction and thus

preventing the formation of radical species (Chan *et al.*, 2004; Siegel *et al.*, 1997). Mutations in the NQO1 gene have been associated with an increased risk of developing cancers including breast (Menzel *et al.*, 2004) and colon cancer (Begleiter *et al.*, 2006).

Regulation of NQO1 mRNA expression is not exclusively regulated by Nrf2, with transcription factors including AP-1 and NF-κB also having a role to play in NQO1 up-regulation in response to lead, mercury and oltipraz (Korashy *et al.*, 2008; Park *et al.*, 2004; Yao *et al.*, 1995). However, NQO1 mRNA, protein and activity levels have been widely used as a marker of Nrf2 activation and a measure of cytoprotective enzyme up-regulation.

As a well-defined target of Nrf2, NQO1 is useful as a surrogate marker for the activation of a range of Nrf2-regulated enzymes. It has a wide dynamic range of expression with NQO1 mRNA expression being between 3.5- and 5-fold higher in livers of WT mice when compared with Nrf2 KO animals (Aleksunes *et al.*, 2010b; Tanaka *et al.*, 2008b). Hepatic NQO1 mRNA levels are also significantly increased above those in basal animals by both genetic and pharmacological Nrf2 induction (Yates *et al.*, 2009). Furthermore NQO1 is expressed ubiquitously in tissues in the body, with expression levels in organs such as the liver, lung and kidney well established (Jaiswal, 2000). Consequently, the enzyme provides a useful marker of Nrf2 activation that is applicable in a range of tissues.

1.4 The synthetic triterpenoids

1.4.1 The development of CDDO and its derivatives

The synthetic triterpenoid, CDDO and its derivatives including CDDO-Im and CDDO-methyl ester (CDDO-Me), have been shown to be potent inducers of Nrf2. The structures of the three compounds are shown in figure 1.3. The key role that Nrf2 target genes play in the response to oxidative stress, together with the anti-inflammatory and anti-proliferative properties of the triterpenoids, mean that CDDO-derived compounds have been widely investigated as potential chemotherapeutic as well as chemopreventive agents.

CDDO is an analogue of the naturally occurring oleanolic acid. Oleanolic acid and its isomer, ursolic acid, are two triterpenoids that are known to have weak anti-inflammatory and anti-carcinogenic properties (Huang *et al.*, 1994; Nishino *et al.*, 1988), and CDDO and its derivatives were originally developed as anti-inflammatory agents. However,

subsequent studies have also highlighted their anti-oxidant and anti-proliferative properties (Dinkova-Kostova *et al.*, 2005; Suh *et al.*, 1999).

Initial work showed that the synthetic triterpenoids have anti-cancer properties in a variety of *in vitro* models including human breast cancer, lung cancer and leukaemia cell lines (Ito *et al.*, 2000; Konopleva *et al.*, 2004; Lapillonne *et al.*, 2003; Zou *et al.*, 2004). CDDO-Im has been shown to have anti-proliferative properties and induce differentiation in cell models as well as to decrease tumour burden in a mouse model of melanoma (Place *et al.*, 2003). Furthermore, CDDO and CDDO-Me have been used in Phase I clinical trials for treatment of leukaemia as well as for solid tumours (Vannini *et al.*, 2007). The potential utility of the triterpenoids extends beyond the treatment of cancer, with studies investigating the anti-diabetic effects of CDDO-Me (Saha *et al.*, 2010), as well as the potential benefits of CDDO analogues in the treatment of Huntington's disease and emphysema (Stack *et al.*, 2010; Sussan *et al.*, 2009).

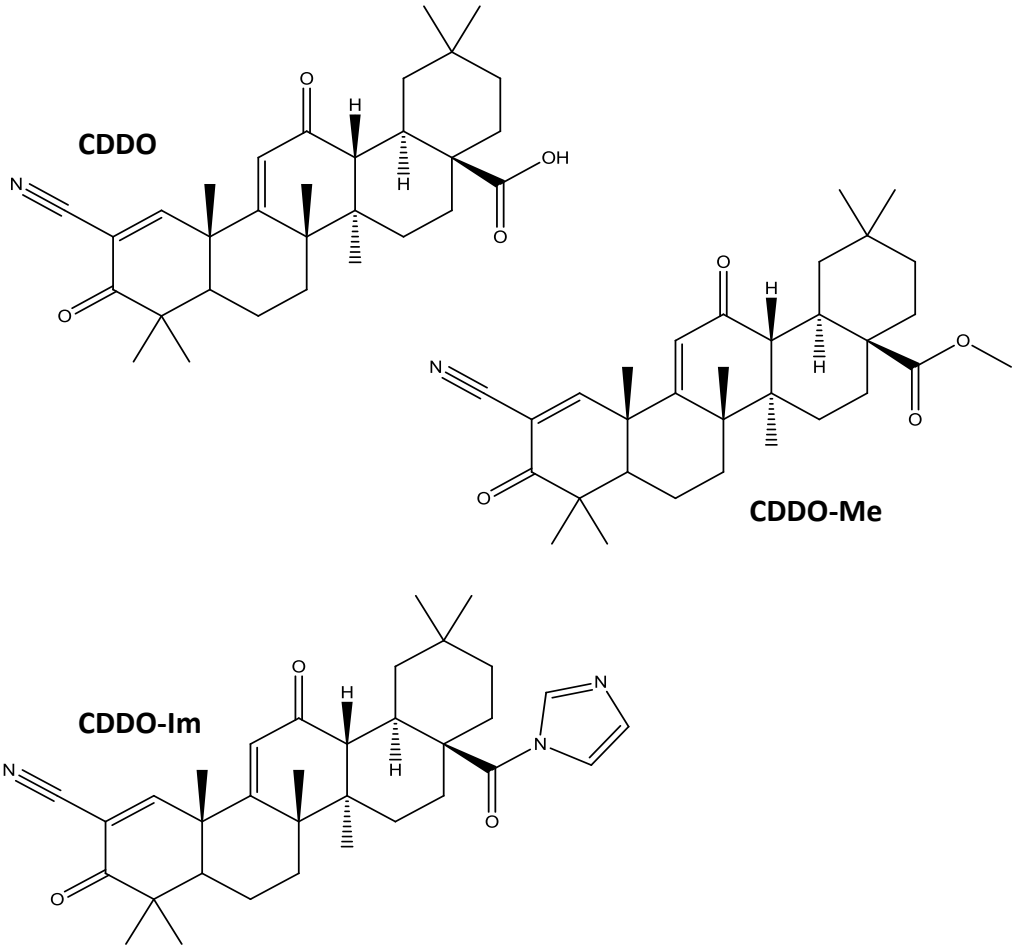

Figure 1.3: The structure of 2-cyano-3,12-dioxooleana-1,9(11)-dien-28-oic acid (CDDO) and its methyl ester (CDDO-Me) and imidazolide (CDDO-Im) derivatives. All three compounds have been shown to be potent inducers of Nrf2.

1.4.2 The synthetic triterpenoids and Nrf2 induction

Initial evidence for triterpenoid activation of Nrf2 came from a study in which CDDO was shown to potently induce the phase II response in embryonic fibroblasts (Dinkova-Kostova *et al.*, 2005), a response that was abolished in cells from the Nrf2 null mouse. Results from the paper also strongly suggest that Keap1 is a molecular sensor for the triterpenoids. In subsequent work, Liby *et al.* demonstrated a time-dependent induction of mRNA levels of the Nrf2-regulated gene, haem oxygenase-1 (HO-1), following treatment of U937 human leukaemia cells with CDDO and CDDO-Im, and also an increase in Nrf2 protein levels (Liby *et al.*, 2005). HO-1 protein induction was also seen *in vivo* via western blot in a variety of organs including the liver, lung and stomach in an experiment using CD-1 mice treated with 2 μmol CDDO-Im.

The parent compound oleanolic acid has also been shown to induce expression of Nrf2 mRNA and the mRNA of Nrf2 target genes when dosed once daily for 4 days to mice and rats (Liu *et al.*, 2008), while other triterpenoid compounds including the avicins, have been associated with induction of the Keap1-Nrf2 pathway (Haridas *et al.*, 2004).

In a 2007 paper by Yates *et al.*, an NQO1-ARE-luciferase reporter gene assay was used in association with *in vivo* bioluminescent imaging to determine NQO1 transcriptional activation in a mouse model following treatment with CDDO derivatives. CDDO-Me was seen to induce *Nqo1* transcripts in the liver, small intestine and lung after a single dose, while CDDO-Me dosed on three consecutive days also maintained or further increased the levels of *Nqo1* expression seen after a single dose, suggesting sustained induction of the Nrf2 pathway using CDDO-Me is possible.

CDDO-Im has been shown to be protective against paracetamol-induced hepatotoxicity in WT but not in Nrf2 KO mice (Reisman *et al.*, 2009). CDDO-Im attenuated the rise in ALTs seen in WT mice 6h after administration of a 500mg/kg dose of paracetamol. A 380% increase was detected in Nrf2 protein levels in nuclear extracts from livers of WT mice treated with CDDO-Im dosed once daily for three days (1mg/kg; *i.p.*). The synthetic triterpenoids have also been shown to offer Nrf2-dependent protection against damage to other organs. For example, CDDO-Im has been shown to induce an Nrf2-mediated protective response in the kidneys of mice treated with ferric nitrilotriacetate (FeNTA), a compound associated with a high incidence of renal adenocarcinomas in rodents (Tanaka

et al., 2008a). Furthermore, CDDO-Im was protective in Nrf2 WT mice against cisplatin-induced renal toxicity (Aleksunes *et al.*, 2010a). Nrf2 has a protective role against neuronal and capillary degeneration in retinal ischemia–reperfusion injury: CDDO-Me is protective in WT but not in Nrf2 KO mice (Wei *et al.*, 2011).

1.4.3 The synthetic triterpenoids also modulate other signalling pathways

A number of other signalling pathways have also been implicated in the documented effects of CDDO and its derivatives. The inflammatory properties are, in part, mediated through modulation of NF-κB signalling and CDDO, CDDO-Im and CDDO-Me have all been shown to inhibit both the constitutive as well as the inducible activation of NF-κB (Shishodia *et al.*, 2006). This may be through inhibition of IKK-β as both CDDO-Me and CDDO-Im have been shown to inhibit IKK-β, an effect that is mediated by oxidation of Cys-179 (Ahmad *et al.*, 2006; Yore *et al.*, 2006). The inhibitory effects of the CDDO analogues on the transcription of TNF-α, INF-γ, inducible COX-2 and iNOS (Honda *et al.*, 1998; Place *et al.*, 2003; Suh *et al.*, 1998; Suh *et al.*, 1999), are also likely to contribute to the potent anti-inflammatory properties of the compounds.

Other intracellular targets for the synthetic triterpenoids have also been identified including the PPAR-γ receptor (Wang *et al.*, 2000) and STAT signalling (Liby *et al.*, 2006), with CDDO-Me shown to inhibit activation of the JAK1/STAT3 pathway (Ahmad *et al.*, 2008). Consequently, while Nrf2 activation may have a role in the therapeutic properties of CDDO and its derivatives, the relative contribution of other pathways remains to be determined.

1.5 Nrf2 in Man

1.5.1 Nrf2 induction as a therapeutic strategy

Given the role of oxidative stress in health and disease, compounds that induce Nrf2 have significant therapeutic potential. The triterpenoid CDDO-Me (also known as bardoxolone methyl) has been used in a Phase I clinical trial for the treatment of advanced solid tumours and lymphomas. In the context of cancer treatment, use of the compound has not advanced further to clinical trials in larger patient populations. The role of Nrf2 in the pathology of cancer is complex, and expression of the transcription factor has been shown to be dysregulated in some cancers (Lister *et al.*, 2011; Shibata *et al.*, 2008; Stacy *et al.*, 2006). Furthermore, induction of Nrf2 in cancer patients may not always be desirable,

given that enhanced resistance to oxidative stress may confer a survival advantage on cancer cells treated with chemotherapeutics. Consequently, while Nrf2 induction has shown promise as a chemopreventive strategy (Kwak *et al.*, 2010; Liby *et al.*, 2007), its potential as a cancer treatment agent may be limited.

However, CDDO-Me was noted in clinical trials to have a beneficial effect on glomerular filtration rate (Hong *et al.*, 2012) and its utility in the treatment of chronic kidney disease (CKD) was subsequently investigated. In fact, CDDO-Me has recently entered phase III trials for the treatment of CKD in patients with type II diabetes. Furthermore, Abbott have invested $400 million in Reata Pharmaceuticals for the development of second generation oral antioxidant inflammation modulators (AIMs), a class in which CDDO-Me is a first generation compound (Crunkhorn, 2012).

1.5.2 Nrf2 in human disease

Given this drive towards the clinical development of compounds known to induce Nrf2, it is becoming more important to understand the role that the transcription factor plays in human health and studies addressing this important issue are currently lacking. There are however, a number of studies that have investigated the importance of the transcription factor in the lung. Studies have shown that Nrf2-regulated gene expression is induced in the lung by cigarette smoke (Hubner *et al.*, 2009), while in patients with chronic obstructive pulmonary disorder (COPD) Nrf2 is down regulated in pulmonary macrophages. This is also the case in lungs of aged smokers, but not in those of younger smokers (Suzuki *et al.*, 2008).

Single nucleotide polymorphisms (SNPs) in the promoter region of the human Nrf2 gene have been identified in a range of ethnic groups (Marzec *et al.*, 2007; Yamamoto *et al.*, 2004) with one SNP at position 617 (C to A), linked to an increase in the risk of acute lung injury after major trauma (Marzec *et al.*, 2007). Oxidative stress is postulated to contribute significantly to acute lung injury.

The role of Nrf2 in children with severe asthma, a condition associated with redox perturbation and glutathione depletion, has also been investigated (Fitzpatrick *et al.*, 2011). Nrf2 mRNA and protein levels were found to be increased in PBMCs taken from children with severe asthma, when compared to those with mild/moderate disease. Expression of downstream genes including GSTs, GCLC and GCLM were not different between groups,

however, glutathione levels were significantly lower in the plasma of children with severe asthma. The authors suggest that this indicates a dysregulation of the Nrf2 pathway, which may contribute to the disease process.

Data from studies investigating the role of Nrf2 in respiratory diseases associated with oxidative stress is important as it shows that the transcription factor has a role to play in the context of human health, however work to determine the role of the transcription factor in other organs, including the liver is currently lacking. Biomarkers of Nrf2 activity in humans would be invaluable in developing our understanding of the Keap1-Nrf2 system in disease and drug-induced toxicity and may serve to validate the use of preclinical *in vivo* models of Nrf2 modulation in toxicity testing.

1.6 Biomarkers

1.6.1 Biomarkers in drug safety

A biomarker can be defined as a characteristic that is objectively measured as an indicator of normal biological processes, pathogenic processes or a pharmacological response to a therapeutic intervention (Biomarkers Definitions Working Group, 2001). In the context of drug safety, biomarkers can be a change at the level of gene, epigenetic, protein or metabolite expression that is indicative of drug-induced injury. Biomarkers have significant utility as tools to assess the safety of a drug, while at the same time having the potential to contribute to the understanding of the mechanisms that result in drug induced-toxicity. They can contribute to each stage of the drug development process: at a preclinical level they can be used to identify potential toxicity at an early stage of development, while further on in the process they can contribute towards the selection of the safest candidate. Biomarkers can be used to inform the dosing regimen that will be used in Phase I clinical trials and beyond, and have subsequent utility during clinical development in order to monitor safety throughout the early and late phases as well as having value in post marketing surveillance (Marrer *et al.*, 2010).

Biomarkers that are reflective of Nrf2 activity would have two important applications. In the case of drug safety assessment they could be used as markers of oxidative stress in *in vitro* and animal models. However, they would also have utility in studies exploring the significance of Nrf2 in the human population and defining the variability that exists in

expression and activity of the transcription factor. As discussed in section 1.5.2, research in this area is currently lacking.

The ideal characteristics of a biomarker depend on the circumstances under which it will be used. In a clinical study, an ideal biomarker would be non-invasive and hence easily accessible in blood or urine. For preclinical assays, biomarker levels in tissues and cells can easily be determined. For a biomarker to be useful as a marker of liver injury in the human population it would ideally be liver specific and reflective of the level of injury sustained, as well as being detectable prior to the occurrence of significant or irreparable liver damage (Antoine *et al.*, 2008). However, in a preclinical *in vivo* model investigating the propensity of a compound to cause liver damage, the need for an early marker of injury is less crucial. Ultimately however, an ideal biomarker would be translational and suitable for use in *in vitro* and *in vivo* models as well as in the clinic. In order to have universal applicability, biomarkers would also need to be cost effective and easy to assess in a standard laboratory.

1.6.2 Current biomarkers of DILI

The functional significance of DILI biomarkers means that many potential candidates have been explored. However, there are only ten DILI biomarkers that are in use or have been validated for use in the USA by the FDA (Shi *et al.*, 2010). The most commonly used markers include serum alanine aminotransferase (ALT), aspartate amino transferase (AST) and alkaline phosphatase as well as total bilirubin (TBL) concentration. Hy's law states the criteria that are widely employed to define DILI and was employed by the FDA to provide the following guidelines to identify drugs in clinical development that are likely to be associated with DILI in the wider population (FDA, 2009):

1. The drug causes hepatocellular injury, generally shown by a higher incidence of 3-fold or greater elevations above the upper limit of normal (ULN) of ALT or AST than the (nonhepatotoxic) control drug or placebo

2. Among trial subjects showing such aminotransferase (AT) elevations, often with ATs much greater than 3xULN, one or more also show elevation of serum TBL to >2xULN, without initial findings of cholestasis (elevated serum ALP)

3. No other reason can be found to explain the combination of increased AT and TBL, such as viral hepatitis A, B, or C; pre-existing or acute liver disease; or another drug capable of causing the observed injury.

ALT is a biomarker that is widely used because it has a number of useful characteristics. It is an enzyme that is abundant in the liver and will leak out of damaged hepatocytes. It is stable in serum with a relatively long half-life of 42 hours (Ozer *et al.*, 2008), and is therefore easily detectable in biological assays. However, it lacks specificity, as ALT levels can also rise following muscle injury, as well as showing evidence of circadian variation (Green *et al.*, 2002). Furthermore, levels only rise once hepatocyte damage has occurred, hence it can be indicative rather than predictive of liver injury. When a rise in ALT does occur, it can be transient and subsequently return to normal levels without significant liver damage, as has been detected in some patients following the administration of aspirin and some statins (FDA, 2009). However, small early rises in ALT can also be caused by drugs that have the potential to cause more severe injury and there is no way to determine which of the two outcomes will follow an early ALT rise.

There is the potential to overcome some of the limitations associated with ALT by using assays that distinguish between the two isoforms of ALT, ALT1 and ALT2. ALT2 has been shown to be more specific for the liver than the ALT1 isoform, while both isoforms increase in the serum in rat models of carbon tetrachloride and paracetamol injury (Yang *et al.*, 2009). Evidence from the study also suggests that ALT2 may be indicative of mitochondrial damage, and consequently assays measuring both isoforms may provide additional information concerning the nature of the liver damage.

Other markers of DILI have been investigated including GST-α, malate dehydrogenase and γ-glutamyl transpeptidase, a marker of cholestasis (Marrer *et al.*, 2010). One of the most promising markers to emerge has been microRNA-122 (miR-122), which has been identified as a biomarker of paracetamol-induced liver injury in both a mouse model and in overdose patients (Starkey Lewis *et al.*, 2011; Wang *et al.*, 2009).

While there is an on-going drive to identify and investigate the potential of a range of biomarkers for DILI, it seems unlikely that a single biomarker will emerge that can be universally applied to determine drug safety. A panel of biomarkers that can be used in combination and have different levels of specificity and sensitivity according to the

mechanism by which damage occurs is likely to have greater utility. Different markers may be employed at different stages of the drug development process, with some providing preclinical information on the mechanism by which damage occurs and the severity of the damage and others used in the clinical phase to predict and identify injury or to determine individuals who may be susceptible to the toxicity associated with a particular compound.

1.6.3 Methods of biomarker discovery

Different 'omic' approaches have been widely employed in the search for biomarkers looking at genetic, epigenetic, protein and metabolic profiles in order to identify drug- or disease-induced changes. One approach that has proved successful in the fields of proteomics and metabolomics is the use of mass spectrometry to perform unbiased profiling of serum, urine and tissue homogenates.

The proteome describes the complete set of proteins produced by an organism or a system and takes into account post-translational modifications to proteins (Wilkins *et al.*, 1996). Proteomic methods involve the large scale analysis of proteins within a given system and often employ mass spectrometric techniques. Quantification by direct mass spectrometry is associated with a high degree of variability and so results are not reproducible, however the use of stable isotope labelling employed by techniques such as stable isotope labelling by amino acids in cell culture (SILAC), isotope-coded affinity tags (ICAT) and isobaric tag for relative and absolute quantitation (iTRAQ) facilitates relative or absolute quantification of proteins in a manner that allows reliable comparisons to be made between samples.

While SILAC is a method for quantifying protein in cultured cells, both ICAT and iTRAQ can be used for the analysis of *in vivo* samples, with iTRAQ having the additional advantage of facilitating the simultaneous quantification of proteins in up to 8 samples. The iTRAQ method was originally developed as a 4-plex procedure (Ross *et al.*, 2004) employing 4 unique reporter tags (m/z 114-117), and was subsequently extended to include 4 further reporters. Each reporter is associated with a balance, such that all tags have a total mass of 145 Da. The tags were designed to include a peptide reactive group which binds covalently to the primary amines at the N-terminus and in peptide side chains. Prior to labelling, the proteins in each sample undergo trypsin digest to yield peptides. Subsequently, each sample is incubated with a different tag, before all samples are combined.

Samples are fractionated by nano liquid chromatorgraphy and analysed by LC-MS/MS. The peptide fragmentation patterns are compared to a database in order to identify the peptides and hence the proteins present. The collision energy also results in the dissociation of the reporter ion and balance in each tag. The peak area of the reporter is used in order to allow the relative quantification of each peptide in one sample compared to another. The labelling and quantification of proteins by iTRAQ is described in figure 1.4.

Mass spectrometric methods are also widely employed in the global profiling of metabolites. Metabolomics can be defined as 'the nonbiased identification and quantification of all metabolites in a biological system' (Ellis *et al.*, 2007). Metabolites can be the products or the intermediates of metabolism, and the term is usually employed to describe a small molecule that falls into one of 3 classes of molecule: carbohydrate, lipid or amino acid. Within the field of metabolomics, metabonomic studies analyse the changes in metabolite profiles that result from the administration of exogenous compounds including drugs or from genetic modification (Robertson, 2005). Lipidomics focuses on the lipid profile of an organism, organ or cell and while it is broadly categorised within metabolomics, it is also considered a discipline in its own right.

While genomic and proteomic approaches have been successfully employed to identify potential biomarkers, there is a consensus that, as the end points of biochemical processes, metabolite expression profiles are more likely to give an accurate representation of disease state because they are more reflective of an organism's phenotype (Ellis *et al.*, 2007). Furthermore, metabolites are highly conserved across species (Coen *et al.*, 2008), and may therefore provide markers that can be directly translated between animal models and into man. Consequently, metabolomic studies have significant potential to contribute to the search for biomarkers. However, if they can be used alongside studies investigating global gene and protein expression profiles then together, the three approaches can contribute significantly to the understanding of a disease process or mechanism of toxicity. Crucially however, in order to be widely adopted in preclinical studies and clinical settings any biomarker needs to be validated as a sensitive, reproducible and quantitative measure indicative of a given condition or toxicity.

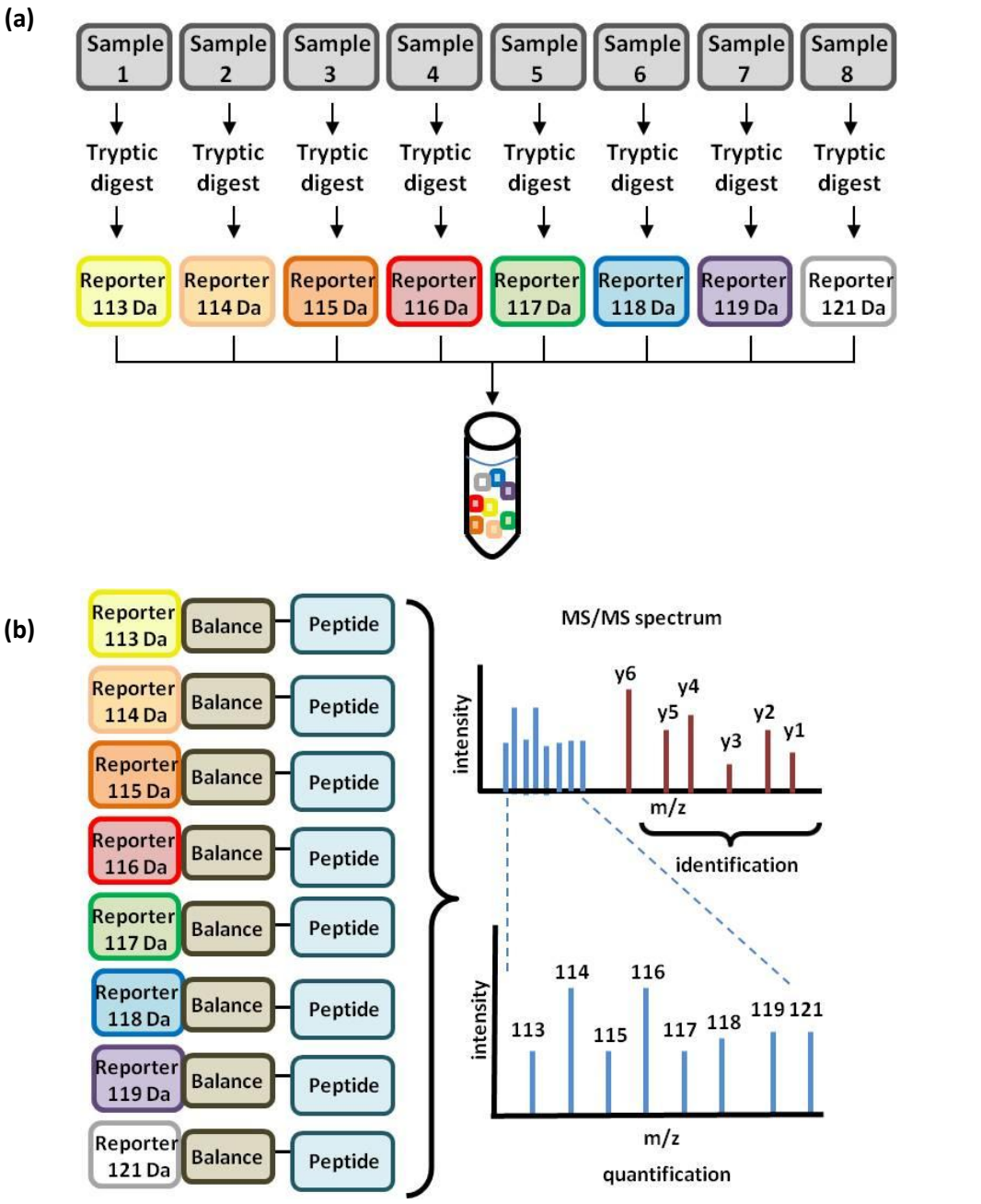

Figure 1.4: Labelling and analysis of iTRAQ samples. iTRAQ analysis allows the simultaneous quantification of peptides in up to eight samples. (a) Proteins in each sample undergo tryptic digest before peptides are labelled with a reporter tag. After labelling all samples are combined into a single sample ready for LC-MS/MS analysis. (b) Each reporter tag is associated with a balance, such that all tags have the same molecular mass. The balance and reporter dissociate during LC-MS/MS analysis permitting the relative quantification of peptides in each sample. The peptide fragmentation pattern facilitates the identification of the peptide and ultimately the protein by way of a database search.

1.6.4 Omic approaches in the identification of drug safety biomarkers

Both metabolomic and proteomic approaches have led to the identification of potential biomarkers, for example a metabolic study identified ophthalmic acid as a potential biomarker for glutathione depletion (Soga *et al.*, 2006). Proteomic methods including iTRAQ have been used to identify potential biomarkers for ovarian cancer (Wang *et al.*, 2012) and metastatic disease in cases of prostate cancer (Rehman *et al.*, 2012). The number of studies employing such methods is growing, and as mass spectrometry and other technologies associated with omic approaches advance, the potential for such approaches to successfully identify biomarkers increases.

Serum and urine are optimal biofluids in which to identify potential biomarkers because both can be collected in a minimally invasive way in preclinical models and in the clinic. Furthermore, it is relatively easy to take repeat samples over the course of hours, days or weeks, as appropriate. However, investigating the proteomic or metabolomic profile of an organ also has the potential to identify biomarkers that are indicative of damage to the organ and can thus be used in preclinical models and may translate to changes in protein or metabolite levels in biofluids, consequently yielding biomarkers that have utility in the clinic. Furthermore, comparing the protein or metabolic profile of a particular organ under different conditions, for example control versus drug treated or gene knockout, can provide important information in the context of drug-induced injury or disease pathology within the organ studied.

Consequently, the use of proteomic and metabolomic approaches in order to profile hepatic Nrf2 modulation, could provide important mechanistic insight into the pathways of oxidative stress while at the same time providing candidate biomarkers of Nrf2 activity with considerable potential for translational applications in characterising the role of Nrf2 in the human population.

1.7 Aims

Nrf2 is a transcription factor that plays a vital role in the cytoprotective response to oxidative stress. Mice in which the Nrf2 gene has been knocked out are more susceptible to the toxicity associated with a range of different compounds, in the liver as well as in other organs. Conversely, pharmacological activation of Nrf2 has been shown to be protective in mouse models of hepatotoxicity.

While a considerable body of research has characterised the role of Nrf2 in mice, work exploring the role of the transcription factor in man is limited. Biomarkers that are indicative of hepatic Nrf2 activity would have significant utility in determining the importance and variability of Nrf2 in the human population. Given that oxidative stress and glutathione depletion have been shown to be associated with the administration of both model hepatotoxins and compounds associated with idiosyncratic hepatotoxicity, biomarkers of Nrf2 activity would also have applications in the development of preclinical models of DILI.

Consequently, the objectives of the work described in this thesis were:

- to characterise the basal hepatic proteomic profile of WT and Nrf2 KO mice in order to construct a list of proteins that are constitutively regulated by Nrf2.
- to identify the protein networks that are constitutively perturbed in the livers of mice in the absence of a functional Nrf2 gene.
- to explore existing methods for the quantification of glutathione and to adapt these methods in order to produce a robust LC-MS/MS assay for the quantification of GSH and GSSG in mouse liver samples.
- to use the LC-MS/MS assay to characterise hepatic glutathione homeostasis in the livers of WT and Nrf2 KO mice.
- to characterise and compare the fatty acid and lipidomic profile of livers of WT and Nrf2 KO mice in order to contribute to the understanding of the role of Nrf2 in lipid homeostasis (a role identified in chapter 2).
- to explore how WT and Nrf2 KO animals respond to the perturbations in hepatic fatty acid metabolism resulting from carbohydrate restriction.
- to characterise the hepatic proteomic profile of Nrf2 induction in order to construct a list of proteins that are inducibly regulated by Nrf2 following the administration of a single dose of CDDO-Me
- To investigate the dynamic range of the expression of proteins that have been identified as Nrf2-regulted

Through the characterisation of the hepatic profiles of mice in which Nrf2 activity has been modulated, the ultimate aim of the work described in this thesis was the identification of candidate biomarkers of Nrf2 activity with potential utility in preclinical models

investigating the role of oxidative stress in DILI and translational value in studies defining the importance of Nrf2 in the human population.

Chapter 2 Proteomic analysis of the livers of WT and Nrf2 KO mice*

***Much of the work described in this chapter has previously been published:** Kitteringham NR, Abdullah A, Walsh J, Randle L, Jenkins RE, Sison R*, et al.* (2010). Proteomic analysis of Nrf2 deficient transgenic mice reveals cellular defence and lipid metabolism as primary Nrf2-dependent pathways in the liver. *J Proteomics* **73**(8)**:** 1612-1631.

Contents

2.1 Introduction

We are constantly exposed to oxidative insult from endogenous and exogenous sources and the ability of a cell to defend itself against oxidative damage is vital for survival. The redox balance within a cell can be perturbed by electrophilic and oxidative stress resulting from drug administration, which can lead to damage to proteins, DNA and lipids. As the primary site for the processing of drugs in the body, the liver is at particular risk of drug-induced toxicity, with DILI being the most common reason for withdrawal of a drug from the market (Lee, 2003). Oxidative stress and glutathione depletion are characteristic of the DILI associated with paracetamol overdose (Hazelton *et al.*, 1986; Lores Arnaiz *et al.*, 1995), and have also been implicated in the hepatotoxicity resulting from administration of a range of drugs including nefazadone and nimesulide (Xu *et al.*, 2008a).

The role of the transcription factor Nrf2 in the cytoprotective response to oxidative stress is well documented. Nrf2 has a key role in regulating the expression of many genes associated with detoxification and defence against oxidative stress, including NQO1, HO-1, GSTs, GCLC and thioredoxin, as detailed in table 1.1 of this thesis. Under basal conditions, Nrf2 is sequestered in the cytosol by Keap1, which targets Nrf2 for ubiquitination and subsequent proteasomal degradation (Cullinan *et al.*, 2004; Furukawa *et al.*, 2005; Itoh *et al.*, 1999). However when the intracellular redox balance is disturbed, modifications to cysteine residues within the Keap1 homodimer result in a conformational change in the molecule (Kobayashi *et al.*, 2006), and while Nrf2 remains bound to Keap1, it is no longer targeted for ubiquitination. The high synthesis rate of Nrf2 means that Keap1 molecules quickly become saturated and newly synthesised Nrf2 is free to translocate to the nucleus, where it binds to the ARE in Nrf2 target genes, thus mediating their transcription (Itoh *et al.*, 1999).

While the transcription factor plays an important protective role in many organs, the vital role of Nrf2 in the hepatic cytoprotective response is highlighted by the fact that transgenic Nrf2 KO mice are more vulnerable to the hepatotoxic effects of a range of compounds. Nrf2 null animals show reduced resistance to liver injury following administration of paracetamol (Chan *et al.*, 2001; Enomoto *et al.*, 2001), ethanol (Lamle *et al.*, 2008), carbon tetrachloride (Xu *et al.*, 2008b) and pyrazole (Lu *et al.*, 2008).

Two key factors may play a role in the enhanced susceptibility of Nrf2 KO mice to drug-induced toxicity. Firstly, loss of Nrf2 may result in a reduction in the ability to mediate an adaptive response to a toxic insult through the up-regulation of cytoprotective gene expression. However, the constitutive expression levels of genes important in the stress response may also impact on the ability of an animal to respond to the chemical stress associated with the administration of some drugs. While the relative importance of these two factors may be a function of the mechanism by which toxicity occurs, and as such differs from compound to compound, the characterisation of constitutive differences in protein expression in the presence and absence of Nrf2 is of fundamental importance in understanding the role that the transcription factor plays in protecting the liver from drug-induced toxicity.

Studies using the Nrf2 KO mouse model together with known inducers of Nrf2 have identified a wide range of genes that are regulated by Nrf2 at an inducible and/or constitutive level. For example, oligonucleotide microarray investigations have suggested a modulatory role for Nrf2 in the expression of more than 200 genes (Hu *et al.*, 2006; Nair *et al.*, 2007; Nair *et al.*, 2006; Thimmulappa *et al.*, 2002). In some cases, the transcription factor regulates both basal and inducible expression of a given gene, while in others, expression of genes that are up-regulated on Nrf2 induction, remains largely unchanged at a constitutive level in the absence of Nrf2.

Changes in gene expression do not always translate to an equivalent change at the protein level (Kitteringham *et al.*, 2000), and consequently the functional significance of changes in gene expression remains to be determined in many cases. A number of the studies looking at gene expression have also investigated the effects of Nrf2 gene deletion and induction on expression levels of proteins, or the level of activity of enzymes important in the cytoprotective response (Chanas *et al.*, 2002; Ramos-Gomez *et al.*, 2001). However, the number of proteins included in the studies is limited, and no global proteomic analysis has been performed to determine how hepatic protein expression profiles differ in WT and Nrf2 KO mice.

Consequently, the aim of the work described in this chapter was to characterise and compare the constitutive proteomic profiles of WT and Nrf2 KO mouse livers using iTRAQ, and to identify the pathways that are differentially regulated in the livers of WT and Nrf2

KO animals. Ultimately, these proteins and pathways may provide candidate preclinical biomarkers of hepatic Nrf2 activation and oxidative stress and give mechanistic insight into the processes by which the cytoprotective response is mediated.

2.2 Materials and methods

2.2.1 Materials

8-plex iTRAQ protein labelling kits were purchased from ABSciex (Warrington, UK). Sequencing grade trypsin, the GoTaq Flexi System and the ImProm-II™ Reverse Transcription System was obtained from Promega UK (Southampton, UK). Nitrocellulose and photographic film were from Amersham/GE Healthcare (Buckinghamshire, UK). Tris glycine, 4x Proto Gel Resolving Buffer, Proto Gel Stacking Buffer, and 30% acrylamide: 0.8% (w/v) Bis-acrylamide stock solution were purchased from Gene Flow (Staffordshire, UK). Protein assay reagent, rainbow molecular weight marker and non-fat dry milk were from BioRad (Hertfordshire, UK). Enhanced Chemiluminescence (ECL) substrate was from Perkin Elmer (Buckinghamshire, UK). ATP citrate lyase (ACL) antibody was obtained from Abcam (Cambridge, UK). GST-P1 antibody was a gift from Lesley McLellan, University of Dundee. RNeasy Mini-kit and DNeasy blood and tissue kit were purchased from Qiagen (Crawley, UK). The RNA 6000 Nano Kit was from Agilent (Berkshire UK). 100 bp ladder was from Invitrogen (Paisley, UK). All other reagents were from Sigma (Poole, UK), unless otherwise specified.

2.2.2 Animal studies

All experiments were undertaken in accordance with criteria outlined in a license granted under the Animals (Scientific Procedures) Act 1986, and approved by the Animal Ethics Committees of the University of Liverpool. Male and female WT and Nrf2 KO C57BL6/SV129 mice were bred in house. Generation of the Nrf2 KO mouse has been described elsewhere (Itoh *et al.*, 1997; McMahon *et al.*, 2001). Mice were given free access to food and water and housed at a temperature of between 19°C - 23°C under 12 h light/dark cycles.

For the ITRAQ study, animals (10-12 weeks) were killed at 10 am by exposure to a rising concentration of carbon dioxide, confirmed by cervical dislocation. Livers were removed, rinsed in 0.9% saline, snap frozen in liquid nitrogen and stored at -80°C.

For Microfluidic analysis, animals (22-24 weeks) were culled between 2 pm and 4 pm by exposure to a rising concentration of carbon dioxide, before cardiac puncture was performed. Livers were removed and stored as above.

2.2.3 Genotyping of mice

PCR was performed in order to confirm the genotype of mice in the Nrf2 colony. DNA was isolated from approximately 25 mg of liver tissue from each mouse using the Qiagen DNeasy blood and tissue kit according to the manufacturer's instructions with samples digested overnight, DNA bound to the spin column before being washed and subsequently eluted. PCR was performed using the Promega GoTaq Flexi system with primers 1 to 3 as detailed in table 2.1. The PCR conditions were 95 °C for 15 minutes followed by 35 cycles of 94 °C for 30 sec; 62 °C for 30 sec; 72 °C for 1 min. The PCR products were run on a 2% agarose gel in 1x TAE buffer (100 V; 30 min), and viewed using a transilluminator.

Table 2.1: Primers used for genotyping

Oligonucleotide	Sequence	Length
Primer 1: Nrf2-5'	TGGACGGGACTATTGAAGGCTG	22
Primer 2: LacZ	GCGGATTGACCGTAATGGGATAGG	24
Primer 3: Nrf2 antisense	GCCGCCTTTTCAGTAGATGGAGG	23

2.2.4 Liver homogenisation – iTRAQ

Sections of liver (50-100 mg) from male WT and Nrf2 KO mice (n=4) were homogenised in iTRAQ buffer [0.5M triethylammonium bicarbonate (TEAB)/0.1% sodium dodecyl sulphate (SDS)] using an eppendorf pestle. Samples were subjected to a freeze thaw cycle (-80°C; overnight), before being sonicated (3 x 10 s at 5 µm amplitude). The homogenate was centrifuged (14 000 g; 10 min), and the supernatant retained. Samples were centrifuged a second time (14 000 g; 5 min), and the supernatant was again retained. Protein concentration was determined using the method described by Bradford (Bradford, 1976).

2.2.5 iTRAQ labelling of liver homogenates

Liver homogenates (75 µg protein) were prepared in iTRAQ buffer. iTRAQ reagent labelling was then carried out according to the ABSciex protocol for an 8plex procedure. Samples were reduced with tris(2-carboxyethyl)phosphine (TCEP) and sulphydryl groups capped

with methylmethanethiosulfate (MMTS), before overnight digestion with trypsin. Samples were then labelled with isobaric tags. In the first three iTRAQ runs, WT samples were labelled with tags 113 to 116 while Nrf2 KO samples received the 117 to 121 tags. In the fourth experiment, the sample labelling was reversed such that the WT animals had the heavier tags and the KO mice the lighter tags, in order to control for labelling bias.

Following labelling, samples were pooled and centrifuged (10 000g; 1 minute). The supernatant was removed to a fresh tube and diluted to a volume of 5 mL using 10 mM potassium dihyrdrogen phosphate/ 25% acetonitrile (ACN: w/v). The pH was adjusted to <3 using phosphoric acid and unbound reagent and trypsin were removed by cation exchange chromatography. Cation exchange was performed on a Polysulphoethyl A strong cation-exchange column (200×4.6 mm, 5 µm, 300 Å; Poly LC, Columbia, MD). A flow rate of 1 mL/min was applied and peptides were eluted by increasing the concentration of potassium chloride (KCl) in the mobile phase to 0.5 M over 60 min. Chromatographic fractions of 2 mL were collected and were dried by centrifugation under vacuum (Eppendorf concentrator 5301). Samples were stored at 4°C prior to LC-MS/MS analysis.

2.2.6 Mass spectrometric analysis of iTRAQ samples

Each cation exchange fraction was resuspended in 120 µL of 5% ACN/0.05% trifluoroacetic acid (TFA) and 60 µL were loaded on to the column. Samples were analysed on a QSTAR® Pulsar i hybrid mass spectrometer (AB Sciex, Warrington, UK) and were delivered into the instrument by automated in-line liquid chromatography (integrated LCPackings System, 5mm C18 nano-precolumn and 75 µm×15 cm C18 PepMap column; Dionex, California, USA) via a nano-electrospray source head and 10 µm inner diameter PicoTip (New Objective, Massachusetts, USA). The precolumn was washed for 30 min at 30 µL/min with 5% ACN/ 0.05% TFA prior to initiation of the solvent gradient in order to reduce the level of salt in the sample. A gradient from 5% ACN/ 0.05% TFA (v/v) to 60% ACN/0.05% TFA (v/v) in 70 min was applied at a flow rate of 300 nL/min. The MS was operated in positive ion mode with survey scans of 1 s, and with an MS/MS accumulation time of 1 s for the three most intense ions. Collision energies were calculated on the fly based on the m/z of the target ion and the formula, collision energy=(slope×m/z)+intercept. The intercepts were increased by 3–5 V compared to standard data acquisition in order to improve the reporter ion intensities/quantitative reproducibility.

2.2.7 iTRAQ data analysis

Data analysis was performed using ProteinPilot software (Version 3, AB Sciex, Warrington, UK). The data were analysed with a fixed modification of MMTS-labelled cysteine, biological modifications were allowed and the confidence was set to 10% to enable the False Discovery Rate to be calculated from screening the reversed SwissProt database. Ratios for each iTRAQ label were obtained, using the "WT mouse 1" sample as the denominator. The detected protein threshold ("unused protscore (conf)") in the software was set to 1.3 to achieve 95% confidence.

2.2.8 iTRAQ statistical analysis

iTRAQ data for proteins within a 1% false discovery rate and for which full quantification data were obtained, were statistically analysed within the R computational environment (R_Development_Core_Team, 2009). R is an open source software environment for statistical computing and graphics (http://www.r-project.org/). Normality of the data and equivalence of variance across the data sets was assessed by Shapiro–Wilk and F-tests, respectively, and also by inspection of histogram plots for all proteins identified. Data were then analysed by unpaired t-test using the module *multtest*, a package designed for re-sampling based multiple hypothesis testing. Benjamini–Hochberg corrections for multiple comparisons were performed on all raw p values generated (Katz, 2003). Protein expression differences between WT and Nrf2 KO mice giving a p value of <0.05 by t-test and a Benjamini–Hochberg value ≤ 0.2 were accepted for further correlative network analysis. The Benjamini–Hochberg cut-off was set at 0.2 to avoid the exclusion of correlated Nrf2-regulated proteins through application of too stringent a correction for multiple testing in accordance with multivariate modelling approaches to account for potential confounders (Katz, 2003).

2.2.9 Network analysis

The accession numbers of the 108 proteins identified as significantly different following Benjamini–Hochberg adjustment for multiple comparisons ($p \leq 0.2$) were converted to Entrez gene IDs using the Database for Annotation, Visualization and Integrated Discovery (DAVID) (http://david.abcc.ncifcrf.gov/conversion.jsp), and analysed for evidence of network wide changes in cellular phenotype using MetaCore from GeneGo Inc., an integrated manually curated knowledge database for pathway analysis of gene lists (http://www.genego.com/metacore.php). The gene list was analysed using the Pathway

Maps tool, which maps the genes listed to defined signalling pathways that have been experimentally validated and are widely accepted. The proteins deemed Nrf2-regulated according to the criteria defined above were compared against a background file containing all of the identified proteins which had similarly been converted to a list of Entrez gene IDs using DAVID. The p values generated by the software were used to determine the statistical significance of the pathways identified. The p value represents the probability that a particular pathway will be represented by chance given the number of genes in the experiment and the number of genes in the pathway.

2.2.10 Liver homogenisation – western immunoblotting

The remaining liver from male WT and Nrf2 KO mice (n=4) was homogenised in phosphate buffered saline (PBS) using 10 passes of a hand held glass-teflon homogeniser. The homogenate was centrifuged (10 000g; 5 min) to pellet unhomogenised tissue and cell debris, and the supernatant retained. Whole livers from female WT and Nrf2 KO mice (n=4) were homogenised in the same way. Protein concentration was determined using the method of Lowry (Lowry *et al.*, 1951).

2.2.11 Western immunoblotting

Whole liver homogenate (25 µg of protein) was separated by denaturing electrophoresis on a 10% polyacrylamide gel using Tris-Glycine-SDS running buffer and transferred to a nitrocellulose membrane. After transfer, a Ponceau Red stain was used to ensure equal loading and the membrane was blocked using 10% milk in TBST [1x tris-buffered saline (TBS)/0.1%Tween] for 30 min at room temperature. After blocking, membranes were incubated (4 °C; overnight) with either a rabbit monoclonal antibody to ACL (1:5000) or a mouse monoclonal antibody to GST-P1 (1: 10 000) in 2% milk in TBST. The membrane was washed with TBST (4x 5 min) and then incubated (1h; room temperature) with the secondary antibody [peroxidise-conjugated goat anti-rabbit immunoglobulin G (IgG), 1:5000 (ACL) or peroxidase-conjugated rabbit anti-mouse IgG 1:10 000 (GST-P1)] in TBST containing 2% milk. The membrane was washed as before. ECL-Plus was used to visualise the level of protein-antibody complex. Band volume was measured by densitometry using Biorad Quantity One 1D Analysis Software (BioRad). Statistical analysis was performed using StatsDirect (version 2.6.8, StatsDirect Ltd, Altrincham, UK). A Shapiro–Wilk test was used to assess the normality of the data. Normal data were analysed to assess statistical

significance using an unpaired t-test, while a Mann Whitney U-test was used for non-normal data.

2.2.12 RNA isolation

RNA isolation was performed using the RNeasy Mini-kit according to the manufacturer's instructions. Approximately 30 mg of liver tissue was weighed out and the weight recorded. 600 µL of buffer RLT was added to the liver sample and tissue was homogenised (2 min: 30 s^{-1}) using the MM400 oscillating mill (Retsch, Haan, Germany). Samples were centrifuged (18 000 g; 3 min), and the supernatant retained. 600 µL of 70% ethanol was added to the homogenate and mixed by pipetting, before the solution was passed through an RNeasy spin column by centrifugation (15 s; 10 000g). The RNA, which had bound to the spin column, was washed in three subsequent centrifugation steps using the buffers provided, before the RNA was eluted in RNase-free dH_2O. The RNA concentration was determined using a NanoDrop ND-1000 (Labtech, East Sussex, UK).

2.2.13 RNA quality determination

The quality of the RNA was determined using the Agilent RNA 6000 Nano Kit according to the manufacturer's instructions. Gel matrix was filtered by centrifugation (1500 g; 10 min), before dye was added (1 µL to 65 µL of gel matrix). The solution was vortexed and centrifuged (13000g; 10 min). The gel-dye mix was added to the RNA 6000 Nano chip before marker (5 µL), ladder (1 µL) and samples (1 µL) were added to the appropriate wells of the chip. The chip was vortexed (2400 rpm; 1 min), before being analysed using the Agilent 2100 bioanalyzer (Agilent, Berkshire, UK).

2.2.14 cDNA synthesis

cDNA synthesis was carried out using the Promega ImProm-II™ Reverse Transcription System according to the manufacturer's instructions, with some minor modifications: 4µL of RNA at a concentration of 0.5 µg/µL was combined with 1 µL of random primer solution, and nuclease-free dH_2O was added to give a final volume of 15 µL. The solution was incubated (70°C; 5 min) and then cooled on ice. A master-mix containing ImProm-II™ reaction buffer, 6mM $MgCl_2$, dNTP mix and ImProm-II™ reverse transcriptase in a final volume of 20 µL was added to the RNA solution. Strands were annealed (25°C; 5 min) and extended (42°C; 1 hour), before the reverse transcriptase was inactivated (70°C; 15 min).

160 µL of nuclease-free dH_2O was added to each tube and cDNA concentration was subsequently determined using the NanoDrop.

2.2.15 Microfluidic cards

Microfluidic cards were designed to include well established Nrf2-regulated genes, genes encoding proteins identified as Nrf2-regulated in iTRAQ analysis and genes encoding proteins that were not identified by iTRAQ but were associated with pathways identified by MetaCore analysis. Cards were custom made by Applied Biosystems (Paisley, UK). 18S was used as a housekeeping gene. The plate layout and represented genes are detailed in figure 2.1 and table 2.2. Samples were run in a randomised order, as determined using random.org (http://www.random.org/), across 5 TaqMan array cards. A pool of cDNA from all samples was run on each card so that data could be compared across plates.

The cDNA that had previously been synthesised was diluted in nuclease-free dH_2O to a concentration of 1ng/µL cDNA. 50 µL of this solution was combined with 50 µL of TaqMan® Gene Expression Master Mix (Life Technologies, Paisley, UK) to give 50 ng of total cDNA. Samples were vortexed and transferred to the appropriate well of the TaqMan array card. Pooled cDNA samples were prepared in the same way. Once loaded, cards were centrifuged at 331g (2x 1 min) and sealed. The wells were removed, and cards were run on the 7900HT Fast Real-Time PCR System (ABSciex) immediately or stored at room temperature for up to 24 hours.

2.2.16 Microfluidic card data analysis

Data was analysed using the comparative C_T method ($\Delta\Delta C_T$). C_T values were determined using the RQ manager 1.2 component of the 7900HT Fast System software. The threshold was manually set to a value of 0.3 for all plates. Gene expression was quantified relative to the sample pool run on the same plate and normalised to 18S gene expression. Statistical analysis was performed to compare relative expression of genes in WT and Nrf2 KO mice where C_T values were available for ≥4 animals in each group. A Shapiro-Wilk test was used to assess the normality of the data with normal data analysed using an unpaired t-test and non-normal data analysed using a Mann-Whitney U test.

Acly	Abcc1	Abcc4	Elovl6	Jun	Nqo1	Ugt1a6a	Ugt2b5	Acaa1b	Acaca	18S	Acsl5	Agxt	Aldh8a1	Bhmt	Ces1g	Cyp1a2	Cyp2c50	Cyp2e1	Cyp7b1	Dbi	Ephx1	Fabp5	Fasn
Glul	Gclc	Gclm	Gsta4	Gstm1	Gstp1	Gstt3	Gsr	Glo1	Keap1	Lipg	Mgst1	Prdx6	Pklr	Sbp1/2	Sds	Slc2a1	Slc22a7	Scd1	Scp2	Srebf1	Usp2	Uox	Nfe2l2
Acly	Abcc1	Abcc4	Elovl6	Jun	Nqo1	Ugt1a6a	Ugt2b5	Acaa1b	Acaca	18S	Acsl5	Agxt	Aldh8a1	Bhmt	Ces1g	Cyp1a2	Cyp2c50	Cyp2e1	Cyp7b1	Dbi	Ephx1	Fabp5	Fasn
Glul	Gclc	Gclm	Gsta4	Gstm1	Gstp1	Gstt3	Gsr	Glo1	Keap1	Lipg	Mgst1	Prdx6	Pklr	Sbp1/2	Sds	Slc2a1	Slc22a7	Scd1	Scp2	Srebf1	Usp2	Uox	Nfe2l2
Acly	Abcc1	Abcc4	Elovl6	Jun	Nqo1	Ugt1a6a	Ugt2b5	Acaa1b	Acaca	18S	Acsl5	Agxt	Aldh8a1	Bhmt	Ces1g	Cyp1a2	Cyp2c50	Cyp2e1	Cyp7b1	Dbi	Ephx1	Fabp5	Fasn
Glul	Gclc	Gclm	Gsta4	Gstm1	Gstp1	Gstt3	Gsr	Glo1	Keap1	Lipg	Mgst1	Prdx6	Pklr	Sbp1/2	Sds	Slc2a1	Slc22a7	Scd1	Scp2	Srebf1	Usp2	Uox	Nfe2l2
Acly	Abcc1	Abcc4	Elovl6	Jun	Nqo1	Ugt1a6a	Ugt2b5	Acaa1b	Acaca	18S	Acsl5	Agxt	Aldh8a1	Bhmt	Ces1g	Cyp1a2	Cyp2c50	Cyp2e1	Cyp7b1	Dbi	Ephx1	Fabp5	Fasn
Glul	Gclc	Gclm	Gsta4	Gstm1	Gstp1	Gstt3	Gsr	Glo1	Keap1	Lipg	Mgst1	Prdx6	Pklr	Sbp1/2	Sds	Slc2a1	Slc22a7	Scd1	Scp2	Srebf1	Usp2	Uox	Nfe2l2
Acly	Abcc1	Abcc4	Elovl6	Jun	Nqo1	Ugt1a6a	Ugt2b5	Acaa1b	Acaca	18S	Acsl5	Agxt	Aldh8a1	Bhmt	Ces1g	Cyp1a2	Cyp2c50	Cyp2e1	Cyp7b1	Dbi	Ephx1	Fabp5	Fasn
Glul	Gclc	Gclm	Gsta4	Gstm1	Gstp1	Gstt3	Gsr	Glo1	Keap1	Lipg	Mgst1	Prdx6	Pklr	Sbp1/2	Sds	Slc2a1	Slc22a7	Scd1	Scp2	Srebf1	Usp2	Uox	Nfe2l2
Acly	Abcc1	Abcc4	Elovl6	Jun	Nqo1	Ugt1a6a	Ugt2b5	Acaa1b	Acaca	18S	Acsl5	Agxt	Aldh8a1	Bhmt	Ces1g	Cyp1a2	Cyp2c50	Cyp2e1	Cyp7b1	Dbi	Ephx1	Fabp5	Fasn
Glul	Gclc	Gclm	Gsta4	Gstm1	Gstp1	Gstt3	Gsr	Glo1	Keap1	Lipg	Mgst1	Prdx6	Pklr	Sbp1/2	Sds	Slc2a1	Slc22a7	Scd1	Scp2	Srebf1	Usp2	Uox	Nfe2l2
Acly	Abcc1	Abcc4	Elovl6	Jun	Nqo1	Ugt1a6a	Ugt2b5	Acaa1b	Acaca	18S	Acsl5	Agxt	Aldh8a1	Bhmt	Ces1g	Cyp1a2	Cyp2c50	Cyp2e1	Cyp7b1	Dbi	Ephx1	Fabp5	Fasn
Glul	Gclc	Gclm	Gsta4	Gstm1	Gstp1	Gstt3	Gsr	Glo1	Keap1	Lipg	Mgst1	Prdx6	Pklr	Sbp1/2	Sds	Slc2a1	Slc22a7	Scd1	Scp2	Srebf1	Usp2	Uox	Nfe2l2
Acly	Abcc1	Abcc4	Elovl6	Jun	Nqo1	Ugt1a6a	Ugt2b5	Acaa1b	Acaca	18S	Acsl5	Agxt	Aldh8a1	Bhmt	Ces1g	Cyp1a2	Cyp2c50	Cyp2e1	Cyp7b1	Dbi	Ephx1	Fabp5	Fasn
Glul	Gclc	Gclm	Gsta4	Gstm1	Gstp1	Gstt3	Gsr	Glo1	Keap1	Lipg	Mgst1	Prdx6	Pklr	SSbp1/2	Sds	Slc2a1	Slc22a7	Scd1	Scp2	Srebf1	Usp2	Uox	Nfe2l2

Figure 2.1: Microfluidic TaqMan low density array card layout. 8 samples were run on each plate. Each loading well corresponds to two adjacent rows of the plate; hence 48 gene targets were amplified per sample. 18S was used as a housekeeping gene. The gene name for each gene code is detailed in table 2.2.

Table 2.2: Each of the genes represented on the Microfluidic TaqMan low density array card.

Gene code	Gene Name	Gene code	Gene Name
Acly	ATP citrate lyase	**Glul**	Glutamate-ammonia ligase/Glutamaine synthetase
Abcc1	ATP binding cassette subfamily C member 1	**Gclc**	Glutamate-cysteine ligase, modifier subunit
Abcc4	ATP binding cassette subfamily C member 4	**Gclm**	Glutamate-cysteine ligase, catalytic subunit
Elovl 6	Elongation of very long chain fatty acids protein 6	**Gsta4**	Glutathione S-transferase alpha 4
Jun	Jun oncogene	**Gstm1**	Glutathione S-transferase mu 1
Nqo1	NAD(P)H dehydrogenase quinone 1	**Gstp1**	Glutathione S-transferase pi 1
Ugt1a6a	UDP glucuronosyltransferase 1 family polypeptide A6	**Gstt3**	Glutathione S-transferase theta 3
Ugt2b5	UDP glucuronosyltransferase 2 family polypeptide B5	**Gsr**	Glutathione reductase
Acaa1b	Acetyl-CoA acyltransferase 1B	**Glo1**	Glyoxalase 1
Acaca	Acetyl-CoA carboxylase alpha	**Keap1**	Kelch-like ECH-associated protein 1
18S	18S ribosomal subunit	**Lipg**	Lipase, endothelial
Acsl5	Acyl-CoA synthetase long-chain family member 5	**Mgst1**	Microsomal glutathione S-transferase 1
Agxt	Alanine-glyoxylate aminotransferase	**Prdx6**	Peroxiredoxin 6
Aldh8a1	Aldehyde dehydrogenase 8 family member A1	**Pklr**	Pyruvate kinase, liver and RBC
Bhmt	Betaine-homocysteine methyltransferase	**Sbp1/2 (Selenbp1; Selenbp2)**	Selenium binding protein 1/Selenium binding protein 2
Ces1g	Carboxylesterase 1G	**Sds**	Serine dehydratase
Cyp1a2	Cytochrome P450 family 1 subfamily A polypeptide 2	**Slc2a1**	Solute carrier family 2 (facilitated glucose transporter) member 1
Cyp2c50	Cytochrome P450 family 2 subfamily C polypeptide 50	**Slc22a7**	Solute carrier family 22 (organic anion transporter) member 7
Cyp2e1	Cytochrome P450 family 2 subfamily E polypeptide 1	**Scd1**	Stearoyl-CoA desaturase 1
Cyp7b1	Cytochrome P450 family 7 subfamily B polypeptide 1	**Scp2**	Stearoyl carrier protein 2
Dbi	Diazepam binding inhibitor/Acyl CoA binding protein	**Srebf1**	Sterol regulatory element binding transcription factor 1
Ephx1	Epoxide hydrolase 1	**Usp2**	Ubiquitin-specific peptidase 2
Fabp5	Fatty acid binding protein 5, epidermal	**Uox**	Urate oxidase/uricase
Fasn	Fatty acid synthase	**Nfe2l2**	Nuclear factor erythroid derivied 2, like 2

2.3 Results

2.3.1 iTRAQ analysis of WT and Nrf2 KO mouse liver proteins

Proteins from the livers of two independent sets of mice were analysed using iTRAQ stable isotope labelling. iTRAQ analysis 1 involved samples from 4 WT and 4 Nrf2 KO mice, which were each analysed on 4 separate occasions using 8-plex iTRAQ reagents. iTRAQ analysis 2 used 6 WT and 6 Nrf2 KO mouse livers, which were each analysed once using 3 sets of 4-plex iTRAQ reagents. Samples from iTRAQ analysis 2 were used in order to validate the reproducibility of the protein changes identified in iTRAQ analysis 1. The number of proteins that were identified and quantified in both iTRAQ analyses is shown in table 2.3.

2.3.2 iTRAQ analysis 1

Within the 4 runs of iTRAQ analysis 1, a total of 1109 unique proteins were identified in at least 1 run within the FDR of 1% (table 2.3). 769 of these proteins were detected in all 8 mice in a single run and were selected for full quantitative analysis. For all samples, protein expression was expressed relative to animal WT1. A mean relative expression value was calculated for each protein for WT and Nrf2 KO mice and this was used to calculate the mean fold change of that protein in Nrf2 KO animals when compared to WTs. When a protein was detected in all 8 mice in more than one run, a mean value for protein expression in a particular mouse across each complete run was calculated and used in subsequent analysis.

While there was considerable variation in the protein coverage between the 4 runs, with run 1 detecting notably fewer proteins than runs 2-4, all runs were used for statistical analysis. This was done in order to maximise the number of proteins included in subsequent network analysis.

Statistical analysis identified 108 proteins that were differentially expressed in the livers of WT and Nrf2 KO mice and these are detailed in table 2.4. 45 proteins were expressed at a lower level in Nrf2 KO mice and 63 expressed at a higher level. Of the 769 proteins analysed, the number of proteins that were expressed at a higher level in Nrf2 KO when compared to WT was approximately equal to the number expressed at a lower level. Figure 2.2 shows a volcano plot of the 769 proteins analysed, with those identified as significantly differentially expressed (t-test – $P \leq 0.05$; Benjamini-Hochberg value ≤ 0.2) represented as

circles. Proteins with relative expression values that differed by at least 20% in WT and Nrf2 KO mice are shown as filled circles.

Table 2.3: Total numbers of proteins identified and quantified with a false discovery rate (FDR) exclusion of 1% in iTRAQ analyses 1 and 2. Numbers are given for proteins identified with a confidence greater than 90% and for those characterized by at least 2 peptides. The number of proteins quantified relates to those proteins determined in all eight mouse liver samples.

iTRAQ analysis	LC-MS analysis	No. of Proteins identified	No. of proteins identified above 1% global FDR	No. of proteins quantified
1	Run 1	486	265	162
	Run 2	1287	911	620
	Run 3	1003	759	593
	Run 4	726	563	426
TOTAL		**1654**	**1109**	**769**
2	Run 1	1068	825	654
	Run 2	1065	780	661
	Run 3	1068	711	637
TOTAL		**1717**	**1070**	**628**

Of the proteins that were expressed at a significantly lower level in Nrf2 KO animals, the majority had roles in cytoprotection, for example the conjugative drug metabolism enzymes GSTP1 and UGT2B5. This is reflective of the findings of previous oligonucleotide assay studies. However, of the proteins up-regulated in the livers of Nrf2 KO mice, most were involved in lipid metabolism. A list of proteins identified as lipid metabolism or lipid transport proteins within the Uniprot database (http://www.uniprot.org/) is given in table 2.5.

Table 2.4: Nrf2-regulated mouse hepatic proteins identified in iTRAQ analysis 1. Relative expression of hepatic proteins in livers of WT and Nrf2 KO mice determined in iTRAQ analysis 1. All values are expressed relative to a WT control mouse (WT1). Proteins listed were significantly different in the null mice compared with WT according to an unpaired t-test followed by Benjamini-Hochberg (BH) correction for multiple testing at a significance level of $p \leq 0.2$. Four replicate iTRAQ analyses were conducted on each sample and the number of runs in which each protein appeared is designated by n in column 3. The values for each mouse thus represent the average of n replicates. The fold change was calculated from the geometric mean values obtained from the 4 individual mice. Variance of the geometric mean for the four animals in each group is expressed as upper and lower 95% confidence intervals (CI). Proteins are listed according to their expression in KO mice relative to WT animals in ascending order of the fold-change value.

					Relative expression compared to WT 1															
					WT							KO							Fold change	
SwissProt Acc. No.	Name	n	Average no. of peptides	Average coverage (%)	mouse WT1	mouse WT2	mouse WT3	mouse WT4	Geometric mean	Lower 95% CI	Upper 95% CI	mouse KO1	mouse KO2	mouse KO3	mouse KO4	Geometric mean	Lower 95% CI	Upper 95% CI	KO / WT	BH *p*
P02762	**Major urinary protein 6**	4	19.8	54.9	1.00	1.35	1.29	1.54	**1.28**	1.07	1.53	0.47	0.28	0.48	0.64	**0.45**	0.32	0.63	**0.35**	0.057
P17427	**AP-2 complex subunit alpha2**	1	1.0	2.5	1.00	1.25	1.93	1.51	**1.38**	1.05	1.82	0.46	0.43	0.71	0.66	**0.55**	0.43	0.71	**0.40**	0.064
P10649	**Glutathione S-transferase Mu 1**	4	13.8	39.2	1.00	1.31	1.00	1.11	**1.10**	0.97	1.24	0.47	0.53	0.44	0.42	**0.46**	0.42	0.51	**0.42**	0.009
Q61656	**Probable ATP-dependent RNA helicase DDX5**	1	2.0	5.4	1.00	1.31	1.19	1.35	**1.20**	1.05	1.38	0.37	0.85	0.51	0.79	**0.59**	0.40	0.87	**0.49**	0.148
Q91WG8	**Bifunctional UDP-N-acetylglucosamine 2-epimerase**	1	2.0	4.0	1.00	0.98	1.13	1.19	**1.07**	0.98	1.17	0.49	0.60	0.68	0.59	**0.59**	0.52	0.67	**0.55**	0.022
P19157	**Glutathione S-transferase P 1**	4	43.0	76.3	1.00	1.21	0.94	1.12	**1.06**	0.95	1.19	0.62	0.56	0.60	0.54	**0.58**	0.55	0.62	**0.55**	0.011
P17717	**UDP-glucuronosyl-transferase 2B5**	4	5.8	15.5	1.00	1.16	0.99	1.08	**1.05**	0.98	1.13	0.59	0.57	0.56	0.61	**0.58**	0.56	0.61	**0.55**	0.004

Q63836	**Selenium-binding protein 2**	4	26.0	47.9	1.00	1.26	0.99	1.48	**1.17**	0.96	1.41	0.61	0.59	0.67	0.72	**0.65**	0.59	0.71	**0.55**	0.051
Q8VCC2	**Liver carboxylesterase 1**	3	2.3	4.6	1.00	1.34	1.06	0.94	**1.08**	0.93	1.25	0.62	0.60	0.58	0.70	**0.62**	0.58	0.68	**0.58**	0.042
Q60991	**Cytochrome P450 7B1**	1	2.0	7.1	1.00	1.43	1.66	1.65	**1.40**	1.11	1.77	0.85	0.82	0.82	0.79	**0.82**	0.80	0.84	**0.58**	0.073
P46425	**Glutathione S-transferase P2**	1	39.0	71.0	1.00	0.70	0.76	0.61	**0.75**	0.61	0.93	0.47	0.45	0.43	0.43	**0.44**	0.43	0.46	**0.59**	0.063
P24472	**Glutathione S-transferase A4**	2	2.5	17.6	1.00	1.01	0.99	0.92	**0.98**	0.94	1.02	0.49	0.62	0.76	0.50	**0.58**	0.48	0.72	**0.60**	0.073
O35660	**Glutathione S-transferase M6**	1	7.0	24.3	1.00	0.68	0.67	0.89	**0.80**	0.66	0.97	0.50	0.69	0.42	0.40	**0.49**	0.38	0.62	**0.61**	0.179
P00186	**Cytochrome P450 1A2**	3	3.0	10.9	1.00	1.14	1.26	1.21	**1.15**	1.04	1.27	0.59	0.61	0.91	0.86	**0.73**	0.58	0.91	**0.63**	0.186
Q9EQU5	**Protein SET**	1	1.0	6.2	1.00	1.22	1.34	0.99	**1.13**	0.97	1.31	1.05	0.63	0.57	0.71	**0.72**	0.56	0.94	**0.64**	0.199
Q91X77	**Cytochrome P450 2C50**	3	6.0	16.5	1.00	1.30	1.29	1.33	**1.22**	1.07	1.40	0.67	0.67	1.03	0.87	**0.80**	0.65	0.98	**0.65**	0.162
Q6XVG2	**Cytochrome P450 2C54**	4	3.5	8.5	1.00	1.00	0.96	1.04	**1.00**	0.97	1.03	0.54	0.70	0.77	0.77	**0.69**	0.58	0.81	**0.69**	0.090
Q91XE8	**Transmembrane protein 205**	2	1.5	11.4	1.00	0.67	0.70	0.60	**0.73**	0.58	0.91	0.49	0.47	0.49	0.57	**0.50**	0.46	0.55	**0.69**	0.153
P15105	**Glutamine synthetase**	4	9.8	25.1	1.00	1.16	1.06	1.29	**1.12**	1.01	1.25	0.70	0.67	0.99	0.83	**0.79**	0.66	0.93	**0.70**	0.182
O55060	**Thiopurine S-methyltransferase**	2	1.0	5.4	1.00	0.85	0.99	0.75	**0.89**	0.78	1.02	0.49	0.71	0.71	0.70	**0.65**	0.54	0.77	**0.72**	0.194
O35490	**Betaine--homocysteine S-methyltransferase 1**	4	18.3	45.2	1.00	0.81	1.11	1.12	**1.00**	0.87	1.16	0.76	0.67	0.78	0.80	**0.75**	0.70	0.81	**0.75**	0.148
P24549	**Retinal dehydrogenase 1**	4	13.8	31.2	1.00	1.07	1.10	1.22	**1.10**	1.01	1.19	0.80	0.76	0.84	0.92	**0.83**	0.77	0.90	**0.76**	0.127

P06801	**NADP-dependent malic enzyme**	3	8.0	20.5	1.00	1.32	1.16	1.22	**1.17**	1.04	1.31	0.75	0.93	1.06	0.84	**0.89**	0.77	1.02	**0.76**	0.201
P62858	**40S ribosomal protein S28**	4	1.0	17.4	1.00	1.03	1.08	1.11	**1.05**	1.01	1.10	0.87	0.76	0.81	0.82	**0.82**	0.77	0.86	**0.77**	0.038
Q91VA0	**Acyl-coenzyme A synthetase ACSM1, mitochondrial**	3	6.3	20.4	1.00	0.95	1.03	0.90	**0.97**	0.91	1.03	0.80	0.71	0.75	0.75	**0.75**	0.72	0.79	**0.78**	0.039
Q9JIF7	**Coatomer subunit beta**	2	3.0	3.9	1.00	0.86	0.92	0.94	**0.93**	0.87	0.99	0.77	0.74	0.65	0.74	**0.72**	0.67	0.77	**0.78**	0.044
O55125	**Protein NipSnap homolog 1**	3	1.0	4.0	1.00	0.76	0.80	0.93	**0.87**	0.77	0.98	0.62	0.68	0.68	0.73	**0.68**	0.64	0.72	**0.78**	0.201
Q99JI4	**26S proteasome non-ATPase regulatory subunit 6**	2	1.0	3.9	1.00	0.76	0.75	0.74	**0.81**	0.70	0.93	0.65	0.67	0.60	0.61	**0.63**	0.60	0.67	**0.78**	0.182
Q99J99	**3-mercaptopyruvate sulfurtransferase**	2	2.0	10.9	1.00	0.99	0.87	0.94	**0.95**	0.89	1.01	0.72	0.71	0.80	0.79	**0.75**	0.71	0.80	**0.79**	0.057
Q76MZ3	**Serine/threonine-protein phosphatase 2A 65 kDa regulatory subunit A alpha**	2	1.0	3.4	1.00	0.76	0.94	0.83	**0.88**	0.78	0.99	0.65	0.73	0.60	0.82	**0.70**	0.61	0.80	**0.80**	0.204
Q9Z0X1	**Apoptosis-inducing factor 1, mitochondrial**	2	1.0	2.1	1.00	0.99	0.89	0.86	**0.93**	0.87	1.00	0.67	0.78	0.76	0.80	**0.75**	0.69	0.81	**0.80**	0.114
O70475	**UDP-glucose 6-dehydrogenase**	3	5.7	19.5	1.00	0.94	0.96	1.06	**0.99**	0.94	1.04	0.77	0.87	0.81	0.75	**0.80**	0.75	0.85	**0.81**	0.061
Q8R1G2	**Carboxymethylene-butenolidase homolog**	2	2.5	12.9	1.00	0.85	0.96	1.06	**0.96**	0.88	1.06	0.71	0.75	0.82	0.86	**0.78**	0.72	0.85	**0.81**	0.178
Q8VCU1	**Liver carboxyl-esterase 31-like**	3	10.0	20.4	1.00	0.95	0.90	0.83	**0.92**	0.85	0.99	0.74	0.69	0.79	0.78	**0.75**	0.70	0.79	**0.81**	0.117

Q8VCA8	**Secernin-2**	1	1.0	4.0	1.00	1.09	1.05	0.92	**1.01**	0.94	1.09	0.87	0.76	0.93	0.78	**0.83**	0.76	0.91	**0.82**	0.156
Q91VS7	**Microsomal glutathione S-transferase 1**	4	5.0	30.2	1.00	0.92	0.95	0.95	**0.95**	0.92	0.99	0.84	0.71	0.73	0.85	**0.78**	0.71	0.86	**0.82**	0.162
Q9D6Y7	**Peptide methionine sulfoxide reductase**	3	3.0	16.7	1.00	1.08	1.04	1.06	**1.04**	1.01	1.08	0.83	0.82	0.93	0.85	**0.86**	0.81	0.91	**0.82**	0.044
P70441	**Na(+)/H(+) exchange regulatory cofactor NHE-RF1**	3	1.7	5.7	1.00	0.82	0.84	0.73	**0.84**	0.74	0.96	0.75	0.68	0.69	0.68	**0.70**	0.67	0.73	**0.83**	0.198
Q8VCW8	**Acyl-CoA synthetase family member 2, mitochondrial**	3	6.3	18.5	1.00	0.98	1.00	0.93	**0.98**	0.94	1.01	0.81	0.77	0.85	0.82	**0.81**	0.78	0.85	**0.83**	0.030
P57776	**Elongation factor 1-delta**	3	3.7	23.5	1.00	0.90	0.87	0.83	**0.90**	0.83	0.97	0.84	0.76	0.78	0.74	**0.78**	0.74	0.82	**0.87**	0.180
P07759	**Serine protease inhibitor A3K**	3	9.0	24.5	1.00	1.03	1.16	1.05	**1.06**	1.00	1.13	0.91	0.91	0.87	0.97	**0.92**	0.88	0.96	**0.87**	0.123
Q91ZJ5	**UTP--glucose-1-phosphate uridylyltransferase**	3	3.0	8.0	1.00	0.99	1.08	1.06	**1.03**	0.99	1.08	0.86	0.89	0.96	0.88	**0.90**	0.85	0.94	**0.87**	0.156
P11352	**Glutathione peroxidase 1**	4	4.5	26.1	1.00	0.96	1.07	1.12	**1.04**	0.97	1.11	0.90	0.88	0.95	0.94	**0.92**	0.89	0.95	**0.89**	0.193
P60867	**40S ribosomal protein S20**	3	2.3	16.2	1.00	0.91	1.01	0.91	**0.96**	0.90	1.01	0.90	0.81	0.86	0.84	**0.85**	0.82	0.89	**0.89**	0.178
Q9JII6	**Alcohol dehydrogenase [NADP+]**	4	5.5	25.0	1.00	0.95	0.97	0.89	**0.95**	0.91	1.00	0.85	0.89	0.86	0.84	**0.86**	0.84	0.88	**0.90**	0.121
Q9DBJ1	**Phosphoglycerate mutase 1**	2	8.0	44.3	1.00	0.98	1.02	1.04	**1.01**	0.98	1.03	1.09	1.06	1.04	1.10	**1.07**	1.05	1.10	**1.07**	0.128
Q8BVI4	**Dihydropteridine reductase**	3	3.0	18.4	1.00	1.09	1.05	1.09	**1.06**	1.02	1.10	1.14	1.12	1.15	1.16	**1.14**	1.12	1.16	**1.08**	0.178

Q8BH00	**Aldehyde dehydrogenase family 8 memberA1**	3	13.3	31.9	1.00	1.07	1.08	1.14	**1.07**	1.02	1.13	1.19	1.19	1.14	1.15	**1.17**	1.14	1.20	**1.09**	0.206
Q8BFR5	**Elongation factor Tu, mitochondrial**	3	2.7	10.4	1.00	0.93	0.97	0.91	**0.95**	0.91	0.99	1.05	0.99	1.07	1.05	**1.04**	1.00	1.08	**1.09**	0.144
Q3UQ44	**Ras GTPase-activating-like protein IQGAP2**	3	3.3	3.4	1.00	1.04	0.99	0.96	**1.00**	0.97	1.03	1.11	1.15	1.09	1.08	**1.10**	1.08	1.13	**1.11**	0.057
P21107	**Tropomyosin alpha-3 chain**	1	1.0	3.5	1.00	1.00	1.03	1.05	**1.02**	1.00	1.04	1.12	1.23	1.04	1.16	**1.14**	1.06	1.22	**1.12**	0.188
Q64374	**Regucalcin**	4	13.8	42.6	1.00	1.07	1.02	1.08	**1.04**	1.01	1.08	1.12	1.22	1.24	1.09	**1.17**	1.10	1.24	**1.12**	0.148
P45952	**Medium-chain specific acyl-CoA dehydrogenase, mitochondrial**	3	4.7	14.2	1.00	1.06	1.11	1.08	**1.06**	1.02	1.11	1.20	1.20	1.24	1.13	**1.19**	1.15	1.23	**1.12**	0.095
P62991	**Ubiquitin**	4	4.8	50.3	1.00	1.08	1.03	1.15	**1.06**	1.00	1.13	1.17	1.27	1.18	1.15	**1.19**	1.14	1.24	**1.12**	0.178
Q8CHT0	**Delta-1-pyrroline-5-carboxylate dehydrogenase, mitochondrial**	3	7.0	18.0	1.00	1.05	1.09	0.97	**1.03**	0.98	1.08	1.17	1.20	1.23	1.05	**1.16**	1.09	1.24	**1.13**	0.193
Q99J08	**SEC14-like protein 2**	3	6.3	25.5	1.00	1.08	1.12	1.21	**1.10**	1.02	1.19	1.27	1.18	1.32	1.23	**1.25**	1.19	1.31	**1.14**	0.186
Q02053	**Ubiquitin-like modifier-activating enzyme 1**	4	3.5	5.6	1.00	1.05	1.00	1.04	**1.02**	1.00	1.05	1.10	1.19	1.24	1.14	**1.16**	1.11	1.22	**1.14**	0.073
O88569	**Heterogeneous nuclear ribo-nucleoproteins A2/B1**	4	4.5	12.5	1.00	0.98	1.03	1.08	**1.02**	0.98	1.07	1.22	1.17	1.10	1.16	**1.16**	1.12	1.21	**1.14**	0.090
Q9QXD6	**Fructose-1,6-bisphosphatase**	4	16.0	46.5	1.00	0.93	0.98	0.92	**0.96**	0.92	0.99	1.16	1.14	1.05	1.01	**1.09**	1.02	1.16	**1.14**	0.144
Q99JI6	**Ras-related protein Rap-1b**	2	1.0	6.5	1.00	1.02	0.99	1.01	**1.00**	1.00	1.01	1.21	1.20	1.08	1.10	**1.14**	1.08	1.21	**1.14**	0.121

P50580	**Proliferation-associated protein 2G4**	2	2.0	6.6	1.00	1.01	1.07	0.98	**1.01**	0.97	1.05	1.10	1.19	1.25	1.10	**1.16**	1.09	1.23	**1.14**	0.127
Q9R0Q7	**Prostaglandin E synthase 3**	2	1.5	13.1	1.00	1.05	1.11	1.10	**1.06**	1.01	1.11	1.17	1.14	1.21	1.36	**1.21**	1.12	1.31	**1.14**	0.199
Q9DCN2	**NADH-cytochrome b5 reductase 3**	3	6.0	27.9	1.00	1.00	0.98	0.98	**0.99**	0.98	1.00	1.18	1.05	1.11	1.21	**1.13**	1.07	1.21	**1.15**	0.072
Q99LP6	**GrpE protein homolog 1, mitochondrial**	2	1.0	6.5	1.00	1.18	1.10	1.09	**1.09**	1.02	1.17	1.31	1.22	1.20	1.31	**1.26**	1.20	1.32	**1.15**	0.142
Q9JI75	**Ribosyldihydronicotinamide dehydrogenase [quinone]**	2	3.0	19.3	1.00	0.88	0.98	0.91	**0.94**	0.88	1.00	1.16	1.12	1.02	1.05	**1.08**	1.02	1.15	**1.15**	0.144
P00329	**Alcohol dehydrogenase 1**	4	13.0	32.8	1.00	1.04	1.10	1.05	**1.05**	1.01	1.09	1.26	1.20	1.18	1.20	**1.21**	1.18	1.24	**1.16**	0.039
P06151	**L-lactate dehydrogenase A chain**	4	12.5	36.1	1.00	0.92	0.96	0.90	**0.94**	0.90	0.99	1.22	1.18	1.00	1.06	**1.11**	1.01	1.22	**1.18**	0.178
Q8CHR6	**Dihydropyrimidine dehydrogenase [NADP+]**	2	2.0	2.6	1.00	0.96	1.00	1.01	**0.99**	0.97	1.01	1.33	1.13	1.16	1.14	**1.18**	1.10	1.28	**1.20**	0.072
P00405	**Cytochrome c oxidase subunit 2**	2	2.5	15.2	1.00	1.16	0.98	0.99	**1.03**	0.95	1.11	1.19	1.26	1.18	1.28	**1.23**	1.18	1.28	**1.20**	0.105
Q9QXE0	**2-hydroxyacyl-CoA lyase 1**	3	2.7	7.5	1.00	1.02	0.89	0.83	**0.93**	0.84	1.02	1.10	1.17	1.13	1.07	**1.12**	1.08	1.16	**1.20**	0.117
Q60932	**Voltage-dependent anion-selective channel protein 1**	2	1.5	6.6	1.00	1.01	0.95	1.05	**1.00**	0.96	1.04	1.24	1.22	1.22	1.16	**1.21**	1.18	1.25	**1.21**	0.022
Q61207	**Sulfated glycoprotein 1**	3	2.0	2.8	1.00	1.08	1.17	1.24	**1.12**	1.02	1.23	1.35	1.50	1.32	1.30	**1.37**	1.28	1.46	**1.22**	0.121

Q8VC12	**Probable urocanate hydratase**	4	8.0	14.9	1.00	1.20	1.12	1.09	**1.10**	1.02	1.18	1.36	1.39	1.30	1.33	**1.35**	1.31	1.39	**1.23**	0.063
P80316	**T-complex protein 1 subunit epsilon**	1	4.0	14.4	1.00	1.22	1.02	1.03	**1.06**	0.97	1.16	1.37	1.30	1.23	1.34	**1.31**	1.25	1.37	**1.23**	0.103
P50172	**Corticosteroid 11-beta-dehydrogenase isozyme 1**	4	2.8	10.2	1.00	1.19	0.98	1.09	**1.06**	0.98	1.16	1.31	1.20	1.41	1.32	**1.31**	1.23	1.39	**1.23**	0.103
Q8VCR7	**Abhydrolase domain-containing protein 14B**	3	3.7	22.1	1.00	1.17	1.01	1.24	**1.10**	0.99	1.22	1.36	1.36	1.31	1.41	**1.36**	1.32	1.40	**1.24**	0.123
Q9DD20	**Methyltransferase-like protein 7B**	3	3.0	15.2	1.00	0.93	0.90	1.05	**0.97**	0.90	1.04	1.19	1.23	1.16	1.21	**1.20**	1.17	1.23	**1.24**	0.044
Q61171	**Peroxiredoxin-2**	3	1.7	10.4	1.00	1.11	0.94	1.21	**1.06**	0.95	1.18	1.26	1.29	1.38	1.35	**1.32**	1.27	1.37	**1.25**	0.142
P24270	**Catalase**	4	12.3	25.9	1.00	1.25	1.02	1.14	**1.10**	0.99	1.21	1.39	1.33	1.41	1.40	**1.38**	1.35	1.42	**1.26**	0.096
P16460	**Argininosuccinate synthase**	4	26.8	47.6	1.00	0.82	1.02	0.89	**0.93**	0.84	1.03	1.26	1.31	1.03	1.11	**1.17**	1.05	1.31	**1.26**	0.162
P31786	**Acyl-CoA-binding protein**	4	4.8	39.1	1.00	0.85	0.92	0.83	**0.90**	0.83	0.97	1.22	1.20	1.05	1.09	**1.14**	1.06	1.22	**1.26**	0.073
Q61425	**Hydroxyacyl-coenzyme A dehydrogenase, mitochondrial**	3	3.3	12.1	1.00	1.04	0.98	1.04	**1.01**	0.99	1.04	1.09	1.25	1.51	1.31	**1.28**	1.12	1.46	**1.26**	0.156
A3KMP2	**Tetratricopeptide repeat protein 38**	3	2.3	6.4	1.00	0.95	0.96	1.16	**1.02**	0.93	1.11	1.21	1.41	1.24	1.33	**1.29**	1.21	1.39	**1.27**	0.117
Q99PG0	**Arylacetamide deacetylase**	3	3.3	12.8	1.00	1.13	1.13	1.12	**1.09**	1.03	1.16	1.44	1.25	1.36	1.54	**1.39**	1.28	1.52	**1.27**	0.072
P12787	**Cytochrome c oxidase subunit 5A, mitochondrial**	2	3.0	36.6	1.00	1.12	0.85	1.12	**1.02**	0.89	1.16	1.18	1.27	1.45	1.33	**1.31**	1.20	1.42	**1.29**	0.148
P32020	**Non-specific lipid-transfer protein**	4	11.8	25.1	1.00	1.34	1.09	1.22	**1.15**	1.02	1.31	1.53	1.41	1.45	1.54	**1.48**	1.42	1.55	**1.29**	0.117

P55096	**ATP-binding cassette sub-family D member 3**	3	2.3	5.8	1.00	1.29	1.08	1.29	**1.16**	1.02	1.32	1.46	1.37	1.53	1.64	**1.50**	1.39	1.61	**1.29**	0.142
P05201	**Aspartate aminotransferase cytoplasmic**	3	5.7	19.4	1.00	0.83	1.02	0.90	**0.94**	0.85	1.03	1.34	1.39	1.04	1.12	**1.22**	1.06	1.39	**1.30**	0.178
P19096	**Fatty acid synthase**	4	30.3	17.7	1.00	1.10	1.03	1.15	**1.07**	1.00	1.13	1.35	1.40	1.44	1.36	**1.39**	1.35	1.43	**1.30**	0.022
Q9R0H0	**Peroxisomal acyl-coenzyme A oxidase 1**	3	12.0	24.2	1.00	1.06	1.01	0.93	**1.00**	0.95	1.05	1.31	1.33	1.29	1.31	**1.31**	1.29	1.33	**1.31**	0.009
P17665	**Cytochrome c oxidase subunit 7C, mitochondrial**	1	2.0	47.6	1.00	0.89	0.87	1.07	**0.95**	0.87	1.05	1.34	1.15	1.34	1.26	**1.27**	1.18	1.36	**1.33**	0.072
Q9QXF8	**Glycine N-methyltransferase**	4	18.0	47.6	1.00	1.27	1.23	1.42	**1.22**	1.06	1.41	1.63	1.66	1.60	1.61	**1.63**	1.60	1.66	**1.34**	0.117
P35492	**Histidine ammonia-lyase**	3	6.7	13.1	1.00	1.08	1.17	1.12	**1.09**	1.02	1.17	1.57	1.54	1.33	1.44	**1.47**	1.36	1.58	**1.34**	0.044
P83940	**Transcription elongation factor B polypeptide 1**	1	1.0	8.0	1.00	1.02	0.87	1.11	**1.00**	0.90	1.10	1.40	1.31	1.33	1.31	**1.34**	1.30	1.38	**1.35**	0.050
P18242	**Cathepsin D**	2	5.0	17.7	1.00	1.20	1.00	1.42	**1.14**	0.97	1.35	1.49	1.86	1.47	1.48	**1.57**	1.40	1.75	**1.37**	0.178
P25688	**Uricase**	4	7.5	27.4	1.00	1.11	0.98	1.04	**1.03**	0.98	1.09	1.39	1.42	1.43	1.50	**1.43**	1.39	1.48	**1.39**	0.009
Q9QXD1	**Peroxisomal acyl-coenzyme A oxidase 2**	1	2.0	3.8	1.00	1.38	1.28	1.32	**1.23**	1.07	1.42	1.68	1.73	1.57	2.01	**1.74**	1.57	1.93	**1.41**	0.117
P62984	**60S ribosomal protein L40**	1	1.0	19.2	1.00	0.96	0.93	1.07	**0.99**	0.93	1.05	1.42	1.52	1.41	1.27	**1.40**	1.31	1.51	**1.42**	0.022
Q99P30	**Peroxisomal coenzyme A diphosphatase NUDT7**	4	4.5	30.3	1.00	1.14	0.90	1.14	**1.04**	0.93	1.16	1.60	1.45	1.40	1.48	**1.48**	1.40	1.57	**1.43**	0.044

Q9DBM2	**Peroxisomal bifunctional enzyme**	4	2.3	4.7	1.00	1.35	1.10	1.20	**1.16**	1.02	1.31	1.52	1.76	1.60	1.73	**1.65**	1.54	1.76	**1.43**	0.057
O35423	**Serine--pyruvate aminotransferase, mitochondrial**	3	1.0	3.1	1.00	0.88	0.86	0.93	**0.92**	0.86	0.98	1.55	1.67	1.15	1.25	**1.39**	1.17	1.65	**1.51**	0.066
Q8VBT2	**L-serine dehydratase**	3	4.3	22.3	1.00	0.72	0.97	0.90	**0.89**	0.77	1.03	1.47	1.58	1.18	1.20	**1.35**	1.17	1.55	**1.51**	0.078
Q8JZR0	**Long-chain-fatty-acid--CoA ligase 5**	2	3.5	7.7	1.00	0.97	0.99	0.88	**0.96**	0.91	1.02	1.58	1.56	1.20	1.59	**1.47**	1.29	1.69	**1.53**	0.044
Q91V92	**ATP-citrate lyase**	3	11.3	14.4	1.00	1.13	1.05	1.09	**1.07**	1.01	1.12	1.97	2.02	1.84	1.79	**1.90**	1.80	2.01	**1.78**	0.003
P62827	**GTP-binding nuclear protein Ran**	1	1.0	8.8	1.00	1.69	1.44	1.61	**1.41**	1.12	1.78	2.37	2.79	3.07	2.11	**2.56**	2.17	3.01	**1.82**	0.101
P13516	**Stearoyl-CoA desaturase 1**	1	2.0	9.0	1.00	1.43	1.09	1.19	**1.17**	1.00	1.36	4.04	2.12	1.53	2.58	**2.41**	1.62	3.59	**2.07**	0.153
Q8VCH0	**3-ketoacyl-CoA thiolase B, peroxisomal**	3	6.7	25.2	1.00	1.89	1.43	1.44	**1.41**	1.09	1.82	2.92	3.61	4.04	2.98	**3.35**	2.88	3.91	**2.39**	0.044
Q05816	**Fatty acid-binding protein, epidermal**	4	1.8	17.0	1.00	1.24	1.01	0.85	**1.02**	0.87	1.18	3.64	3.17	2.74	2.62	**3.02**	2.61	3.50	**2.97**	0.009

Table 2.5: Differentially up-regulated proteins listed in the UniProt database as involved in lipid synthesis or metabolism in ITRAQ analysis 1. The subcellular location for each protein is listed: C = cytosol; ER = endoplastic reticulum; Mi = mitochondria; P = peroxisome.

			Relative expression compared to WT mouse 1					
			WT		KO		fold change	
SwissProt Acc. No.	Name	Subcellular location	Geometric mean	95% CI	Geometric mean	95% CI	KO / WT	*P*
Q05816	Fatty acid-binding protein, epidermal	C	**1.02**	(0.87 - 1.18)	**3.02**	(2.61 - 3.50)	2.97	0.009
Q8VCH0	3-Ketoacyl-CoA thiolase B, peroxisomal	P	**1.41**	(1.09 - 1.82)	**3.35**	(2.88 - 3.91)	2.39	0.044
P13516	Stearoyl-CoA desaturase 1	ER	**1.17**	(1.00 - 1.36)	**2.41**	(1.62 - 3.59)	2.07	0.153
Q91V92	ATP-citrate lyase	C	**1.07**	(1.01 - 1.12)	**1.90**	(1.80 - 2.01)	1.78	0.003
Q8JZR0	Long-chain-fatty-acid--CoA ligase 5	ER, Mi	**0.96**	(0.91 - 1.02)	**1.47**	(1.29 - 1.69)	1.53	0.044
Q9DBM2	Peroxisomal bifunctional enzyme	P	**1.16**	(1.02 - 1.31)	**1.65**	(1.54 - 1.76)	1.43	0.057
Q99P30	Peroxisomal coenzyme A diphosphatase NUDT7	P	**1.04**	(0.93 - 1.16)	**1.48**	(1.40 - 1.57)	1.43	0.044
Q9QXD1	Peroxisomal acyl-coenzyme A oxidase 2	P	**1.23**	(1.07 - 1.42)	**1.74**	(1.57 - 1.93)	1.41	0.117
Q9R0H0	Peroxisomal acyl-coenzyme A oxidase 1	P	**1.00**	(0.95 - 1.05)	**1.31**	(1.29 - 1.33)	1.31	0.009
P19096	Fatty acid synthase	C	**1.07**	(1.00 - 1.13)	**1.39**	(1.35 - 1.43)	1.30	0.022
P32020	Non-specific lipid-transfer protein	C	**1.15**	(1.02 - 1.31)	**1.48**	(1.42 - 1.55)	1.29	0.117
Q61425	Hydroxyacyl-coenzyme A dehydrogenase, mitochondrial	Mi	**1.01**	(0.99 - 1.04)	**1.28**	(1.12 - 1.46)	1.26	0.156
P31786	Acyl-CoA-binding protein	Mi	**0.90**	(0.83 - 0.97)	**1.14**	(1.06 - 1.22)	1.26	0.073
P50172	Corticosteroid 11-beta-dehydrogenase isozyme 1	ER	**1.06**	(0.98 - 1.16)	**1.31**	(1.23 - 1.39)	1.23	0.103
Q9QXE0	2-Hydroxyacyl-CoA lyase 1	P	**0.93**	(0.84 - 1.02)	**1.12**	(1.08 - 1.16)	1.20	0.117

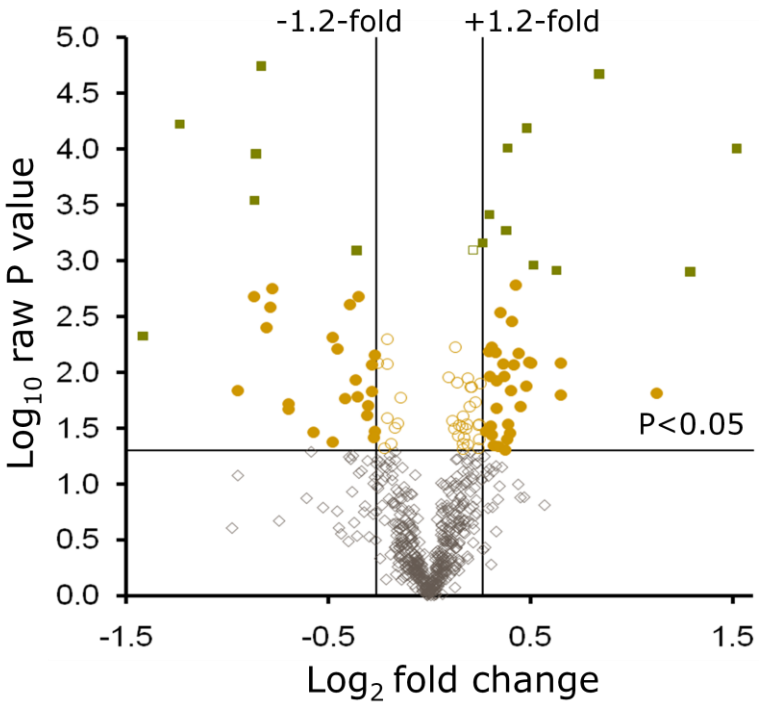

Figure 2.2: Volcano plot of the entire set of proteins quantified during iTRAQ analysis 1. Each point represents the difference in expression (fold-change) between WT and Nrf2 KO mice plotted against the level of statistical significance. Solid filled shapes represent differential expression differences of ±20% and a significance level of P<0.05 (unpaired t-test), with green squares representing proteins with a Benjamini–Hochberg significance value ≤0.2. Proteins represented by diamonds were not differentially expressed.

2.3.3 iTRAQ analysis 2

1070 proteins with a FDR below 1% were identified in iTRAQ run 2, and of these, 628 were identified in all 12 mice (table 2.3). The number of proteins identified in each of the three runs was largely consistent; however the total number of unique proteins that were quantified was slightly lower than in iTRAQ analysis 1. 38 proteins were identified as statistically significantly differentially expressed (t-test - P<0.05; Benjamini-Hochberg value ≤ 0.2) in the livers of WT and Nrf2 KO mice and are shown in table 2.6.

A summary of the overlap between iTRAQ analyses 1 and 2 is given in the Venn diagram in figure 2.3 and in table 2.7.

Table 2.6: Nrf2-regulated mouse hepatic proteins determined in iTRAQ analysis 2 (test set). All values are expressed relative to a WT control mouse (WT1). Proteins listed were significantly different in the Nrf2 KO mice compared with WT controls (Benjamini Hochberg; $p \leq 0.2$).

		Relative expression compared to WT mouse 1							
		WT			KO			fold change KO/WT	
SwissProt Acc. No.	Name	Geometric mean	Lower 95% CI	Upper 95% CI	Geometric mean	Lower 95% CI	Upper 95% CI		*P*
P10649	Glutathione S-transferase Mu 1	**1.00**	0.91	1.10	**0.44**	0.40	0.47	**0.44**	0.001
P17717	UDP-glucuronosyltransferase 2B5	**0.99**	0.93	1.06	**0.55**	0.52	0.57	**0.55**	0.001
Q8VCC2	Liver carboxylesterase 1	**1.06**	0.96	1.17	**0.59**	0.54	0.64	**0.56**	0.001
Q91X77	Cytochrome P450 2C50	**0.97**	0.87	1.08	**0.56**	0.46	0.69	**0.58**	0.001
P19157	Glutathione S-transferase P 1	**0.95**	0.89	1.01	**0.58**	0.54	0.63	**0.62**	0.001
Q9D379	Epoxide hydrolase 1	**0.97**	0.90	1.05	**0.63**	0.59	0.68	**0.65**	0.001
Q64458	Cytochrome P450 2C29	**1.08**	0.90	1.29	**0.75**	0.62	0.90	**0.69**	0.001
P30115	Glutathione S-transferase A3	**1.03**	0.98	1.08	**0.72**	0.66	0.78	**0.70**	0.001
P24549	Retinal dehydrogenase 1	**0.94**	0.86	1.04	**0.68**	0.58	0.80	**0.72**	0.021
O70475	UDP-glucose 6-dehydrogenase	**1.09**	0.97	1.23	**0.79**	0.63	0.99	**0.73**	0.183
Q62452	UDP-glucuronosyltransferase 1-9	**0.99**	0.93	1.06	**0.73**	0.58	0.92	**0.74**	0.183
Q91VA0	Acyl-coenzyme A synthetase ACSM1, mitochondrial	**0.97**	0.91	1.04	**0.79**	0.74	0.84	**0.81**	0.001
Q64442	Sorbitol dehydrogenase	**1.02**	0.92	1.13	**0.84**	0.78	0.91	**0.83**	0.081
P97494	Glutamate--cysteine ligase catalytic subunit	**1.15**	1.06	1.25	**0.95**	0.89	1.02	**0.83**	0.021
Q8CG76	Aflatoxin B1 aldehyde reductase member 2	**1.06**	1.01	1.11	**0.88**	0.81	0.96	**0.83**	0.013
Q9CQX2	Cytochrome b5 type B	**1.01**	0.91	1.13	**0.85**	0.76	0.94	**0.83**	0.197
Q9JII6	Alcohol dehydrogenase [NADP+]	**1.01**	0.98	1.04	**0.86**	0.80	0.92	**0.85**	0.003

Q8VCW8	Acyl-CoA synthetase family member 2, mitochondrial	**1.00**	0.93	1.08	**0.86**	0.79	0.93	**0.86**	0.132
O55022	Membrane-associated progesterone receptor component 1	**1.03**	0.96	1.11	**0.89**	0.81	0.98	**0.86**	0.207
P47738	Aldehyde dehydrogenase, mitochondrial	**1.02**	0.99	1.06	**0.88**	0.85	0.92	**0.86**	0.000
Q8QZS1	3-hydroxyisobutyryl-CoA hydrolase, mitochondrial	**1.07**	1.00	1.13	**0.94**	0.89	1.00	**0.89**	0.084
Q9ET01	Glycogen phosphorylase, liver form	**0.98**	0.96	1.00	**0.87**	0.80	0.94	**0.89**	0.081
O35945	Aldehyde dehydrogenase, cytosolic 1	**0.97**	0.93	1.01	**0.86**	0.83	0.89	**0.89**	0.024
Q8VDJ3	Vigilin	**1.10**	1.05	1.15	**0.99**	0.94	1.04	**0.90**	0.069
Q9EQ20	Methylmalonate-semialdehyde dehydrogenase [acylating], mitochondrial	**1.00**	0.98	1.03	**0.92**	0.87	0.98	**0.92**	0.140
Q9Z2I8	Succinyl-CoA ligase [GDP-forming] subunit beta, mitochondrial	**1.02**	0.99	1.06	**0.96**	0.92	0.99	**0.93**	0.121
Q99P30	Peroxisomal coenzyme A diphosphatase NUDT7	**0.98**	0.93	1.03	**1.10**	1.05	1.17	**1.13**	0.039
Q9CW42	MOSC domain-containing protein 1, mitochondrial	**0.95**	0.90	1.00	**1.09**	1.04	1.15	**1.15**	0.095
Q9QXD6	Fructose-1,6-bisphosphatase 1	**1.02**	0.96	1.09	**1.21**	1.10	1.33	**1.18**	0.117
P31786	Acyl-CoA-binding protein	**1.01**	0.94	1.07	**1.19**	1.06	1.34	**1.18**	0.207
P24369	Peptidyl-prolyl cis-trans isomerase B	**0.95**	0.89	1.01	**1.12**	1.05	1.20	**1.18**	0.017
Q8VDM4	26S proteasome non-ATPase regulatory subunit 2	**0.90**	0.80	1.02	**1.08**	1.00	1.17	**1.20**	0.183
P06151	L-lactate dehydrogenase A chain	**0.97**	0.89	1.05	**1.16**	1.06	1.28	**1.20**	0.086
Q61207	Sulfated glycoprotein 1	**0.94**	0.84	1.05	**1.14**	1.07	1.21	**1.21**	0.057
P16460	Argininosuccinate synthase	**1.02**	0.93	1.13	**1.27**	1.16	1.40	**1.25**	0.038
Q3THE2	Myosin regulatory light chain MRLC2	**1.13**	1.03	1.24	**1.46**	1.25	1.70	**1.29**	0.117
Q8VBT2	L-serine dehydratase	**1.02**	0.91	1.15	**1.37**	1.13	1.67	**1.34**	0.183
Q05816	Fatty acid-binding protein, epidermal	**1.17**	0.96	1.43	**2.10**	1.69	2.60	**1.79**	0.005

Table 2.7: Proteins identified as Nrf2 dependent in two analyses. Each protein was significantly ($p < 0.05$, unpaired t-test) over- or under-expressed in Nrf2 KO mice compared with the WT controls in both of the independent iTRAQ analyses. Fold changes are the ratios of the mean expression changes from 4-6 mice.

		iTRAQ Analysis 1		iTRAQ Analysis 2	
SwissProt Acc. No.	**Protein name**	**Fold-change**	***p***	**Fold-change**	***p***
Q8VCW8	Acyl-CoA synthetase family member 2, mitochondrial	0.83	0.030	0.86	0.132
P31786	Acyl-CoA-binding protein	1.26	0.073	1.18	0.207
Q91VA0	Acyl-coenzyme A synthetase ACSM1, mitochondrial	0.78	0.039	0.81	0.001
Q9JII6	Alcohol dehydrogenase [NADP+]	0.90	0.121	0.85	0.003
P24549	Aldehyde dehydrogenase family 1, subfamily A1	0.76	0.127	0.72	0.021
P16460	Argininosuccinate synthase	1.26	0.162	1.25	0.038
Q91X77	Cytochrome P450 2C50	0.65	0.162	0.58	0.001
Q05816	Fatty acid-binding protein, epidermal	2.97	0.009	1.79	0.005
Q9QXD6	Fructose-1,6-bisphosphatase 1	1.14	0.144	1.18	0.117
P10649	Glutathione S-transferase, mu 1	0.42	0.009	0.44	0.001
P19157	Glutathione S-transferase, pi 1	0.55	0.011	0.62	0.001
Q8VCC2	Liver carboxylesterase 1	0.58	0.042	0.56	0.001
P06151	L-lactate dehydrogenase A chain	1.18	0.178	1.20	0.086
Q8VBT2	L-serine dehydratase	1.51	0.078	1.34	0.183
Q99P30	Peroxisomal coenzyme A diphosphatase NUDT7	1.43	0.044	1.13	0.039
Q61207	Sulfated glycoprotein 1	1.22	0.121	1.21	0.057
O70475	UDP-glucose 6-dehydrogenase	0.81	0.061	0.73	0.183
P17717	UDP-glucuronosyltransferase 2B5	0.55	0.004	0.55	0.001

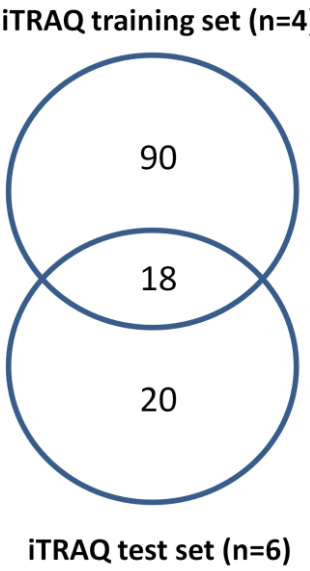

Figure 2.3: Venn diagram indicating the overlap between the proteins identified as Nrf2-regulated across both iTRAQ analyses.

2.3.4 Cellular defence and lipid metabolism are the primary biochemical functions regulated by Nrf2

The functional pathways that were represented by proteins identified as Nrf2-regulated in iTRAQ run 1 were investigated using 2 methods of correlative network analysis: the PANTHER database and MetaCore. Analysis using PANTHER generated a pie chart indicating the specific cellular pathways to which the proteins submitted belonged (figure 2.4). The largest class of proteins were those related to lipid, fatty acid and steroid metabolism (18%). Other metabolism (9.6%), electron transport (9%), carbohydrate metabolism (9%) and immunity and defence (9%) were the pathways that accounted for the next most significant portions of the chart.

The MetaCore software allows the identification of canonical pathways that are over represented by proteins in a data set as compared to a background group of proteins. The 769 proteins used for full quantitative analysis of iTRAQ run 1 were selected as the background file. 752 of the proteins were recognised by the software and 504 had been mapped to pathways. Of the 108 proteins identified as Nrf2-regulated following statistical analysis, 104 were recognised by MetaCore and 68 had been mapped to pathways. Comparison of the Nrf2-regulated pathways against the background data set identified ten pathways that were differentially regulated in the livers of WT and Nrf2 KO mice at a statistically significant level ($P < 0.05$), and these are detailed in table 2.8. The pathway

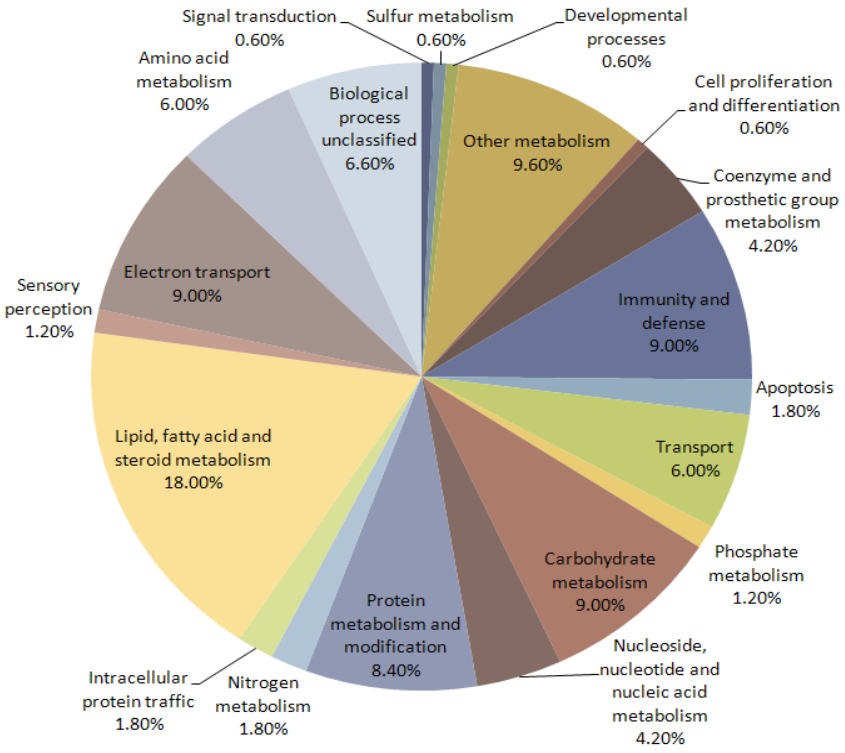

Figure 2.4: Panther functional classification of proteins shown to be differentially regulated in the Nrf2 KO mouse.

diagrams of 4 of the pathways are shown in figure 2.5. 7/10 pathways were linked to fatty acid metabolism or lipid regulation. Only 1, glutathione metabolism, was directly linked to the cytoprotective response, however, 5 of the proteins in this pathway were identified as expressed at a lower level in Nrf2 KO mice in the iTRAQ analysis. Thus both Panther and MetaCore analysis identified lipid metabolism and cytoprotection as key cellular processes regulated by the transcription factor Nrf2.

Table 2.8: MetaCore network analysis of data from iTRAQ analysis 1. Proteins identified in iTRAQ analysis 1 as being differentially expressed (Benjamini-Hochberg $p \leq 0.2$) were interrogated for pathway perturbation using the pathway analysis software MetaCore. The total list of all quantified proteins was applied as a background for the analysis.

	Pathway Name	Negative log *p* value	Number of pathway objects
1	n-6 Polyunsaturated fatty acid biosynthesis	2.52	5
2	n-3 Polyunsaturated fatty acid biosynthesis	2.52	5
3	Regulation of lipid metabolism_Regulation of lipid metabolism via LXR, NF-Y and SREBP	2.44	3
4	Vitamin E (alfa-tocopherol) metabolism	1.98	5
5	Regulation of metabolism_Bile acids regulation of glucose and lipid metabolism via FXR	1.89	4
6	Fatty Acid Omega Oxidation	1.64	4
7	Peroxisomal straight-chain fatty acid beta-oxidation	1.64	4
8	CFTR-dependent regulation of ion channels in Airway Epithelium (norm and CF)	1.62	2
9	Cell cycle_Role of SCF complex in cell cycle regulation	1.62	2
10	Glutathione metabolism / Rodent version	1.3	5

Peroxisomal straight-chain fatty acid beta-oxidation

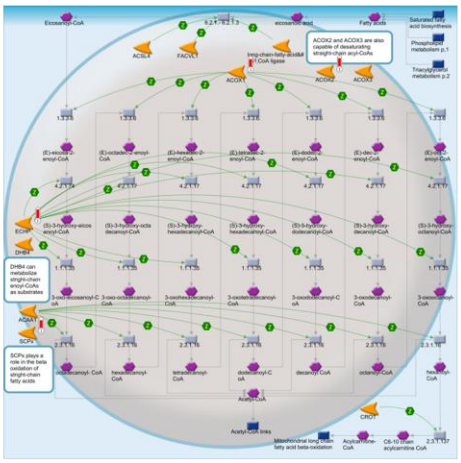

Glutathione metabolism/ Rodent version

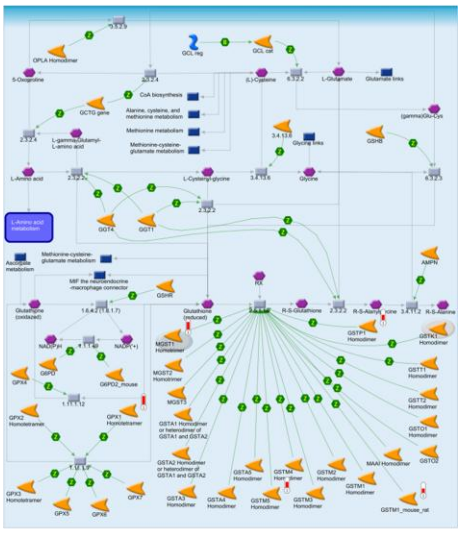

Regulation of lipid metabolism via LXR, NF-Y and SREBP

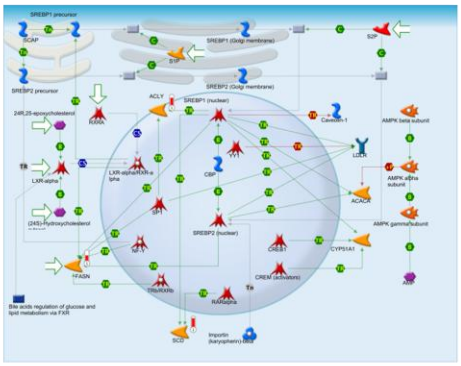

n-6 Polyunsaturated fatty acid biosynthesis

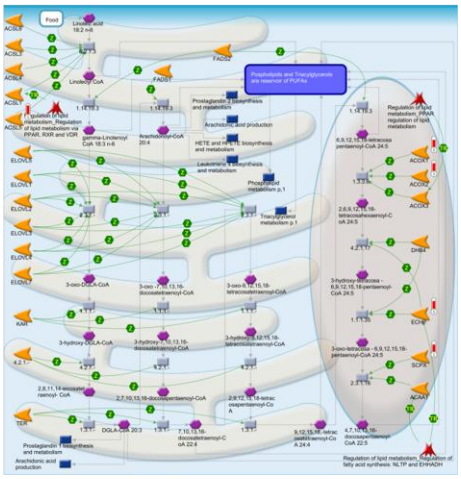

Figure 2.5: Four of the pathways identified as differentially regulated in WT and Nrf2 KO mouse livers by MetaCore analysis.

2.3.5 Western blotting confirmed the changes identified in ACL and GST-pi expression by iTRAQ analysis

In order to validate some of the changes identified in protein expression by iTRAQ analysis, the expression of 2 proteins identified as Nrf2-regulated were selected for western blot analysis. GST-P1 was expressed at a statistically significantly lower level in Nrf2 KO mice in both iTRAQ analysis 1 (0.55-fold change) and iTRAQ analysis 2 (0.62-fold change) and has been confirmed as Nrf2-regulated in previous studies studies (Chanas *et al.*, 2002; Satoh *et al.*, 2002). Conversely, ACL was expressed at a higher level in Nrf2 KO mice in both iTRAQ analysis 1 (1.75-fold change) and iTRAQ analysis 2 (1.2-fold change), however this difference did not reach statistical significance in analysis 2. An increase in ACL at the mRNA level in Nrf2 KO mice has previously been noted (Yates *et al.*, 2009), but a difference in expression at the protein level has not been investigated.

In each case, a Ponceau red stain to show total protein on the membrane was used as a loading control.

Densitometric analysis of the GST-P1 western blot (figure 2.6) showed a 0.63-fold change in the livers of Nrf2 KO mice when compared to WT ($P = 0.01$; unpaired t-test). While densitometry performed on the ACL western blot (figure 2.7) indicated a 3.2-fold change in the protein in the livers of Nrf2 KO mice when compared to WT ($P = 0.0005$; unpaired t-test).

The differences in the magnitude of the fold-change in ACL protein expression as detected by iTRAQ and western blot analyses may reflect a difference in linearity between the 2 methods. However, both techniques provide useful methods for the relative comparison of protein expression and together give confidence that ACL expression is higher in livers of Nrf2 KO animals at a statistically significant level.

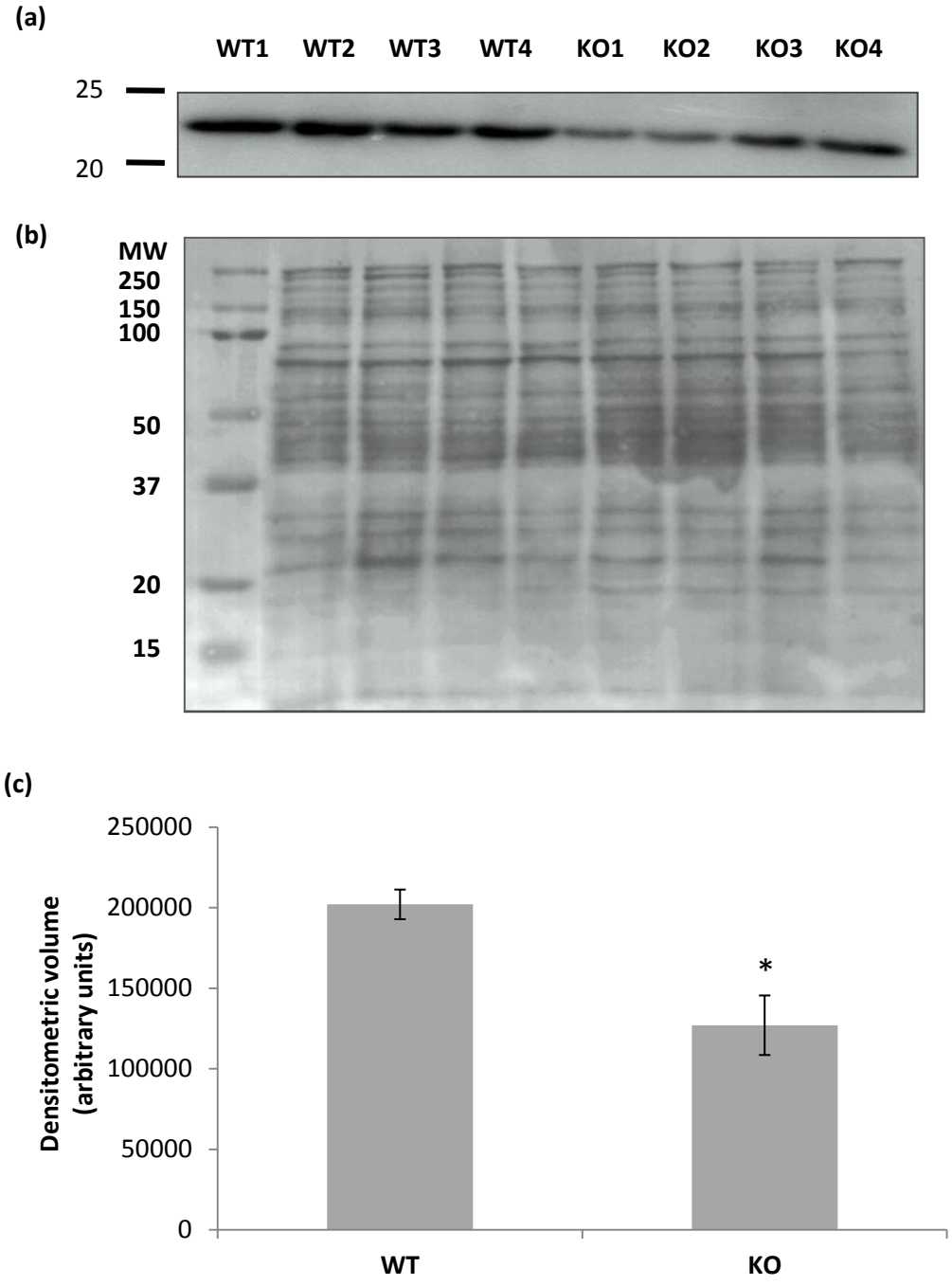

Figure 2.6: Western immunoblot of GST-P1 in liver homogenate from WT and Nrf2 KO mice. (a) Immunoblot for GST-P1. The molecular mass of GST-P1 is approximately 23 kDa. (b) Ponceau protein stain of the transfer membrane shown in (a) indicating approximately equal loading across the gel. (c) Densitometric analysis of immunoblot showing a statistically significant difference in expression of GST-P1 in WT and Nrf2 KO mouse livers (*P<0.05; unpaired t-test).

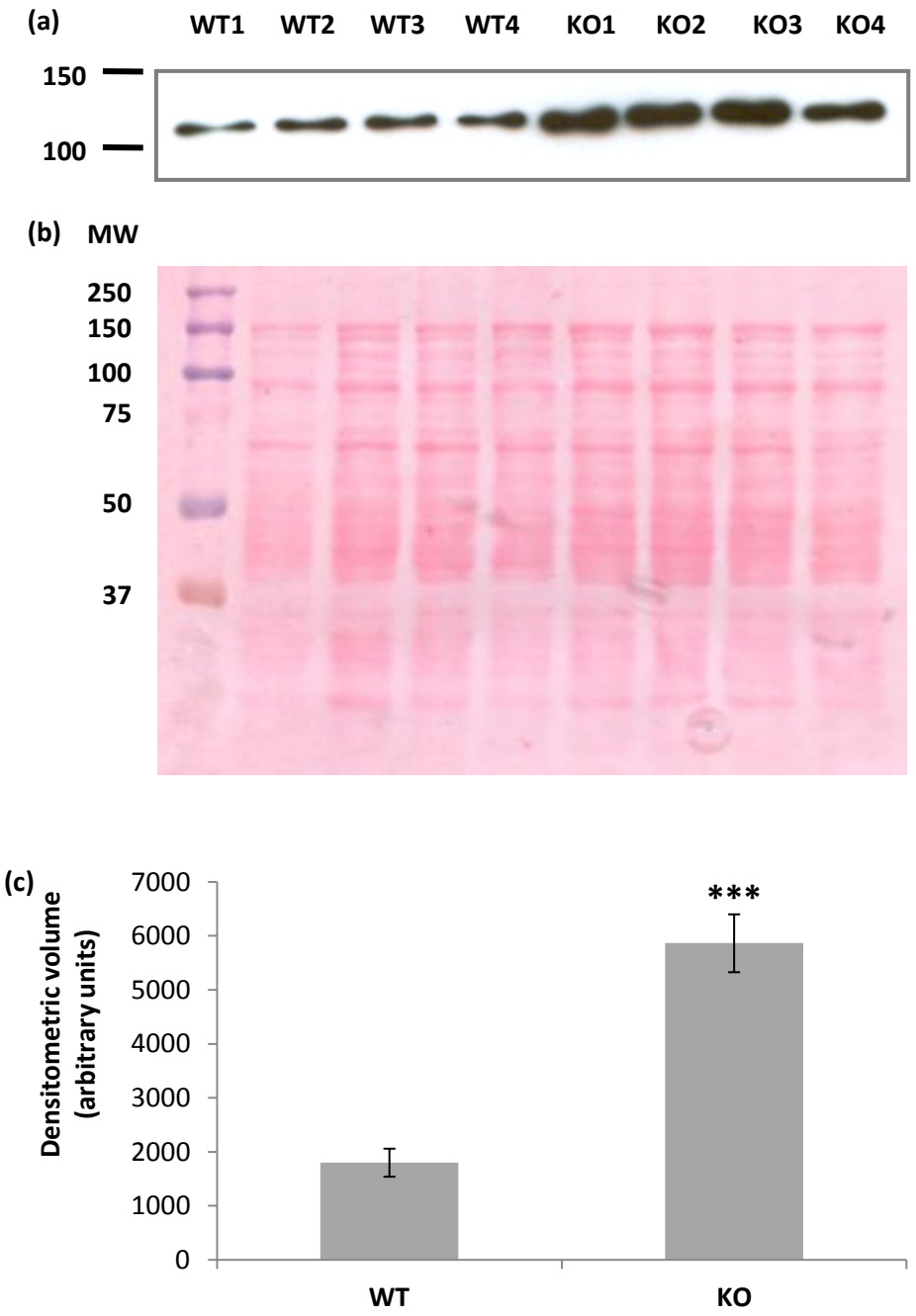

Figure 2.7: Western immunoblot of ATP-citrate lyase (ACL) in liver homogenate from WT and Nrf2 KO mice. (a) Immunoblot for ACL. The molecular mass of ACL is approximately 120 kDa. (b) Ponceau protein stain of the transfer membrane shown in (a) indicating approximately equal loading across the gel. Lane KO1 shows slightly decreased loading which is consistent with the lower level of ACL in the blot above. (c) Densitometric analysis of immunoblot showing a statistically significant difference in expression of ACL in WT and Nrf2 KO mouse livers (***P<0.001; unpaired t-test).

2.3.6 Analysis of livers from female mice confirmed that the increase in ACL protein expression in Nrf2 KO mice was not sex-specific

A potential role for Nrf2 in the negative regulation of lipid metabolism in the liver has only recently been identified. Consequently, in order to confirm whether the differences seen in ACL protein expression were sex-specific, livers from female WT and Nrf2 KO mice were also analysed (n=4; figure 2.8). A 1.8-fold change in ACL expression was also identified by densitometric analysis of western blots from Nrf2 KO female mouse livers (P = 0.0032; unpaired t-test), indicating that the effect was not sex-specific.

2.3.7 Identification of putative antioxidant response elements (ARE) and ARE-related motifs in the promoters of genes encoding the proteins identified as Nrf2-regulated

Nrf2 is known to bind to the ARE in the promoter region of cytoprotective genes, thus initiating their transcription. Consequently, 2000 bp promoter regions of genes encoding each of the proteins that were identified as Nrf2-regulated in iTRAQ analysis 1 were interrogated for ARE or ARE-like enhancer elements. The consensus sequence derived by Nioi et al (Nioi *et al.*, 2003), RTGABNNNTCA, was used as the input term for a string-based search algorithm.

The number of consensus sequences identified in the promoter regions of genes encoding the 9 proteins that were most differentially expressed in WT and Nrf2 KO mice (>0.4-fold difference) are listed in table 2.9. There was little correlation between the fold change in protein expression in WT and Nrf2 KO mice and the number of perfect ARE motifs identified in the genes encoding the proteins. In fact, the mean number of ARE consensus sequences identified in all genes interrogated was 1.21, while in those identified as Nrf2-regulated it was 1.25.

Matrix analysis was also performed, in which the patser algorithm assigns a score for each region within the promoter that matches the position-specific probability matrix. This is based on the degree of similarity to the most frequently observed sequence within a series of known Nrf2 target genes. A reference score was determined by way of searching the promoter regions of all 769 proteins quantified for ARE sequences. For the Nrf2-regulated genes, the mean patser score was 2.03, while for the reference protein set it was 2.50.

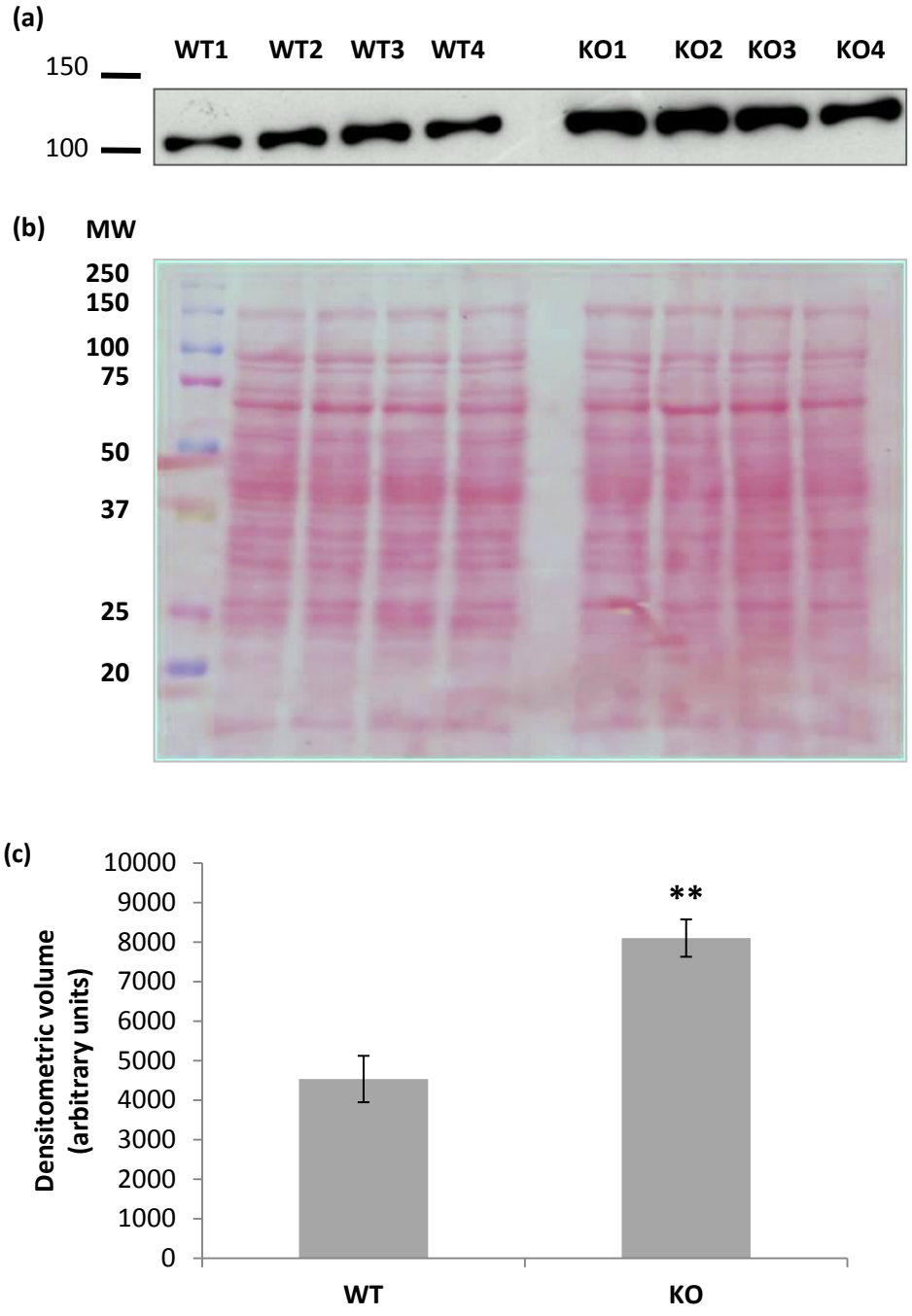

Figure 2.8: Western immunoblot of ATP-citrate lyase (ACL) in liver homogenate from female WT and Nrf2 KO mice. (a) Immunoblot for ACL. The molecular mass of ACL is approximately 120 kDa. (b) Ponceau protein stain of the transfer membrane shown in (a) indicating approximately equal loading across the gel. (c) Densitometric analysis of immunoblot showing a statistically significant difference in expression of ACL in female WT and Nrf2 KO mouse livers (**P<0.01; unpaired t-test).

Table 2.9: Promoter analysis for the mouse genes encoding Nrf2-regulated proteins. Sequences of the genes of Nrf2-regulated proteins were obtained from the ENSMBL mouse genome database and interrogated for ARE and ARE-like consensus sequences using the RSAT analysis software (http://rsat.ulb.ac.be/rsat/). Both string-based (*dna-pattern*) and matrix-based (*patser*) pattern searching strategies were adopted. For the *dna-pattern* analysis, returned sequences were rated against the 'perfect' consensus sequence **RTGAB**NNN**GCA**. For the *patser* analysis, the number of sequences matching the position specific scoring matrix with a score >1 are given, along with the highest score attained. For comparison, equivalent data from the entire set of identified proteins is included at the foot of the table.

			String search (*dna-pattern*)	Matrix analysis (*patser*)				Highest scoring ARE Location		
SwissProt Acc. No.	Protein name	Fold-change	Number of consensus sequences (RTGABNNNGCA)	Number of matching sequences	Highest score	Mean score	SD	from	to	Sequence
P02762	Major urinary protein 6	0.35	0	14	4.89	2.03	1.07	-1935	-1923	ttccCTGTCACTAAGCAtgtt
P10649	Glutathione S-transferase Mu 1	0.41	4	15	4.40	2.42	1.09	-56	-44	gtggGCAGGACAAAACAgcgg
P19157	Glutathione S-transferase P 1	0.54	0	13	4.02	2.11	0.98	-68	-56	aacgTGTTGAGTCAGCAtccg
Q91WG8	Bifunctional UDP-N-acetylglucosamine 2-epimerase/N-acetylmannosamine kinase	0.55	0	12	5.95	2.50	1.70	-387	-375	gcagGGGTGGCAAAGCTtaaa
P17717	UDP-glucuronosyltransferase 2B5	0.55	1	13	5.59	2.40	1.23	-398	-386	cagtCCATGACTGAGTTtgaa
Q99P30	Peroxisomal coenzyme A diphosphatase NUDT7	1.41	1	8	4.68	2.49	1.14	-848	-836	caagGCATTACACAGCCcagg
Q8JZR0	Long-chain-fatty-acid--CoA ligase 5	1.57	1	10	7.66	2.56	1.90	-1234	-1222	cttaGAATGACCCAGCCcttg
Q91V92	ATP-citrate lyase	1.75	1	9	10.02	3.26	2.58	-1899	-1887	agaaAAATGACTAAGCAggta
Q8VCH0	3-ketoacyl-CoA thiolase B, peroxisomal	2.21	2	15	5.84	2.55	1.44	-137	-125	tgggGGAAGACTCAGGAagag
Q05816	Fatty acid-binding protein, epidermal	2.81	0	15	4.37	2.59	0.86	-1728	-1716	agtgGGATGTCGCAGCTcagg
	Mean values for all Nrf2-regulated proteins	**1.26**	**1.25**	**13.69**	**5.62**	**2.50**	**1.33**			
	Mean values for all down-regulated Nrf2-dependent proteins	**0.57**	**1.00**	**15.40**	**5.20**	**2.54**	**1.23**			
	Mean values for all up-regulated Nrf2-dependent proteins	**1.57**	**1.36**	**12.91**	**5.81**	**2.49**	**1.37**			
	Mean values for all proteins identified		**1.21**	**13.20**	**6.48**	**2.03**	**1.62**			

2.3.8 Microfludic TaqMan low density array (TLDA) cards

Following analysis of the iTRAQ data, microfluidic TLDA cards were designed. Each card allows the simultaneous amplification of 48 gene targets in 8 samples. Targets included genes established as Nrf2-regulated, genes encoding a selection of the proteins that were found to be differentially expressed in livers of WT and Nrf2 KO mice by iTRAQ, and genes encoding proteins that were not detected in iTRAQ analysis but were associated with the pathways highlighted by MetaCore analysis. 18S was used as a housekeeping gene.

cDNA reverse transcribed from RNA extracted from the livers of untreated WT and Nrf2 KO mice (n=8) was amplified using real-time PCR, with data analysed using the $\Delta\Delta C_T$ method. As 5 separate plates were required to run the samples, a pool of cDNA from all samples was run in lane 1 on each plate, and expression of all other samples on the plate was expressed relative to the pool and normalised to expression of the house-keeping gene, 18S.

The mean relative expression of each gene was calculated for WT and Nrf2 KO animals and standard error of the mean (SEM) was determined (figure 2.9). Four of the genes, *Abcc1*, *Abcc4*, *Bhmt* and *Fabp5*, were excluded from the analysis because data sets were incomplete for more than 4/8 samples. Of the remaining 43 genes, expression of 9 was statistically significantly higher in WT animals when compared to Nrf2 KO. None of the genes were expressed at a significantly higher level in Nrf2 KO animals. Of the genes differentially expressed, *Ces1* expression differed most between the two groups (KO/WT = 0.11; $P<0.001$).

Expression of the Nrf2 gene was not statistically different in WT and Nrf2 KO animals. However, genotyping of the mice confirmed that exon 5 of the Nrf2 gene was indeed absent in the livers of the KO animals and hence the Nrf2 gene expressed was not functional. Such results have also been noted in previous studies (Lu *et al.*, 2011).

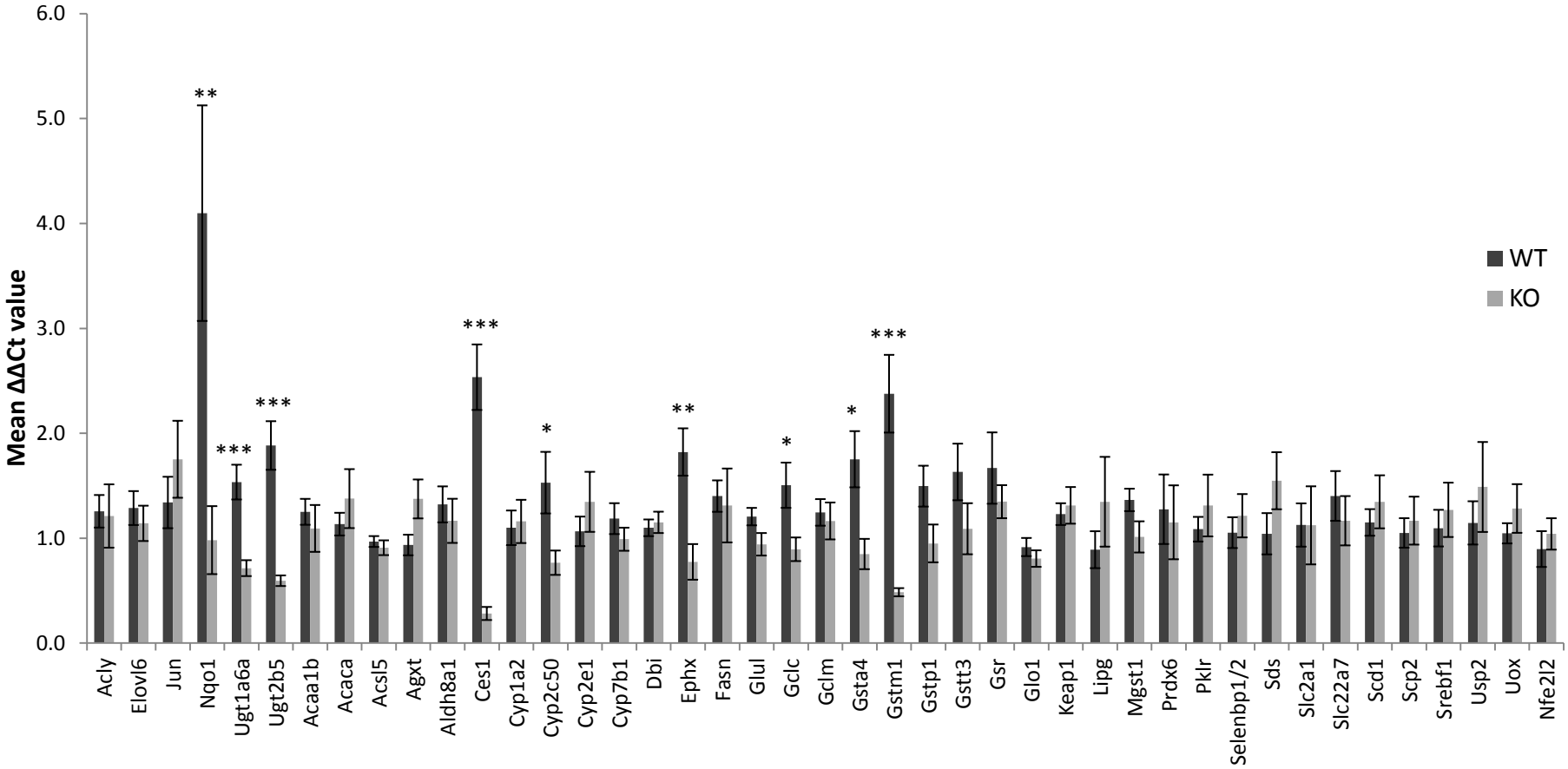

Figure 2.9: Relative level of mRNA expression in livers of WT and Nrf2 KO male mice as detected by Microfluidic TaqMan low density array analysis. Levels of mRNA for NQO1, UGT1a6a, UGT2b5, CES1, CYP2C50, EPHX, GCLC, GSTa4 and GSTm1 were statistically significantly higher in WT animals when compared to Nrf2 KO as determined by unpaired t-test (normal data) or Mann Whitney U-test (non-normal data).

2.4 Discussion

The aim of the work described in this chapter was to identify the protein networks that are constitutively perturbed in the livers of Nrf2 KO mice when compared to WT animals and to construct a list of proteins that are indicative of Nrf2 activity. Such proteins could serve as a pool of biomarkers with applications in preclinical drug safety assessment and have potential translational utility as markers of Nrf2 activity in man.

Results from iTRAQ analysis 1 identified 108 proteins that were differentially expressed in the livers of WT and Nrf2 KO animals. Many were expressed at a higher level in WT mice, although somewhat surprisingly, there was also a group of proteins with hepatic expression that was higher in Nrf2 KO mice. This would suggest that Nrf2 negatively regulates their expression, although it is also possible that the up-regulation of some genes is an adaptation resulting from the permanent disruption of the Nrf2 pathway. The majority of the proteins up-regulated in KO animals were primarily associated with lipid metabolism, and MetaCore analysis was used in order to identify the biochemical pathways that were represented by these proteins. Of the ten pathways that were identified as statistically significantly different in WT and Nrf2 KO animals, seven were related to the biochemistry of lipids, with lipid synthesis being the most prominent functional category. Studies investigating the importance of Nrf2 have largely focussed on the role of the transcription factor in the cytoprotective response, and usually investigate genes that are down-regulated in Nrf2 KO animals. These factors may explain why a role for Nrf2 in the regulation of lipid metabolism has only recently come to light.

A small number of recent studies have noted a relationship between Nrf2 activity and the expression of genes in lipid metabolism pathways. Following the feeding of a high fat diet (HFD) for 4 weeks, expression of genes encoding fatty acid synthesis enzymes and proteins important for cholesterol synthesis and transport were shown to be increased in the livers of Nrf2 KO animals when compared to WT (Tanaka *et al.*, 2008). Treatment with the Nrf2 inducer CDDO-Im dosed for a 3 month period has also been shown to reduce the mRNA levels of fatty acid synthase (FAS) and acetyl CoA carboxylase-1 (ACC1) in WT mice fed a HFD, with no similar reduction in Nrf2 KO animals (Shin *et al.*, 2009). Additionally, lipid metabolism was identified as the functional category that was most significantly altered in the livers of mice treated with CDDO-Im in a study in which mRNA levels of the fatty acid

biosynthesis enzymes including sterol regulatory element-binding protein-1c (SREBP1c), FAS, ACC1, and ACL were also down-regulated on Nrf2 activation (Yates *et al.*, 2009). Together, these studies support the emerging role for Nrf2 in the regulation of lipid metabolism, most notably fatty acid synthesis but also in the storage and transport of lipids and the synthesis of cholesterol. However, further work is required in order to understand the mechanisms by which the transcription factor regulates lipid pathways.

Western immunoblots for ACL were performed on liver homogenate from both male and female WT and Nrf2 KO mice in order to validate the differences in levels of fatty acid synthesis enzymes that had been identified by iTRAQ analysis. Western blotting confirmed that hepatic ACL protein expression was higher in both Nrf2 KO male and female mice when compared to their WT counterparts. ACL plays an important role in providing the cytosolic acetyl CoA required for fatty acid synthesis in hepatocytes as well as other cells. The enzyme has also recently been shown to have a key role in histone acetylation, and thus function to modulate gene transcription (Cousins *et al.*, 2010; Wellen *et al.*, 2009). Given that the loss of Nrf2 results in a significant up-regulation in the levels of ACL, a relatively high-abundance enzyme, regulation of ACL by Nrf2 may have important implications for a range of cellular functions, and this is the subject of further investigation in the department.

A number of proteins, including GSTs and UGTs, that are well characterised as Nrf2-regulated were identified by iTRAQ analysis as having significantly higher expression in WT animals. However, there was little concordance between the proteins identified in the study described in this chapter and the gene expression profiles presented in previous microarray studies. In fact, the number of cytoprotective proteins was surprisingly small, with only one out of ten pathways identified by MetaCore analysis as Nrf2-modulated relating to cellular defence (glutathione metabolism). While iTRAQ is a valuable tool because it enables the simultaneous identification of over one thousand proteins, it is associated with the same limitations as other global proteomic methods in that high abundance species are preferentially detected.

Following analysis of the iTRAQ data, microfluidic TLDA cards were designed to include genes encoding proteins that were identified as Nrf2-regulated in the iTRAQ analysis, genes encoding proteins in associated pathways that were not detected by iTRAQ as well as a

number of well-defined Nrf2 target genes from the literature. Such cards have the potential to be employed as a screen for Nrf2 activity or oxidative stress in preclinical drug safety assessment models. However, in the context of this study they are also a means of investigating the relationship between protein and gene expression changes and can provide preliminary information on the mechanisms of Nrf2 regulation.

While the expression of cytoprotective genes encoding nine enzymes including CES1, NQO1 and a number of GSTs and UGTs were expressed at a statistically significantly higher level in livers of WT mice when compared to Nrf2 KOs, there was no significant difference in expression of any of the lipid metabolism enzymes at the mRNA level. Although no previous study has directly investigated the expression of lipid metabolism genes in basal WT and Nrf2 KO mice, studies exploring the effects of a HFD and diabetes in Nrf2 KO animals have compared the expression of lipid metabolism genes in control animals (Tanaka *et al.*, 2008; Wu *et al.*, 2011). In accordance with our TLDA data, no difference was identified in the basal expression of FAS or ACC1 in livers of WT and Nrf2 KO animals at the mRNA level. However, expression of stearoyl-CoA desaturase-1 (SCD1) was found to be 2-fold higher in Nrf2 KO mice when compared to WT, a differences that was not replicated in our analysis. These data suggest that in the context of Nrf2 regulation at the constitutive level, post translational regulation of fatty acid synthesis enzymes may be more significant than transcriptional regulation.

In summary, the work in this chapter has identified a panel of hepatic proteins with expression that is regulated by Nrf2. In iTRAQ analysis 1, robust statistical analysis showed that 108 proteins were significantly differentially expressed in WT and Nrf2 KO animals, with some of the proteins expressed at a lower level in the Nrf2 KO animals and expression of others enhanced in the absence of the transcription factor. A second independent iTRAQ analysis identified eighteen proteins in common with iTRAQ analysis 1, providing further confidence that these proteins are Nrf2-regulated and have potential utility as candidate biomarkers in preclinical and translational studies. The fact that the majority of proteins that were expressed at a higher level in the livers of Nrf2 KO animals were related to lipid metabolism was an unexpected finding of this study and will be the subject of further investigation.

Chapter 3 The development of an LC-MS/MS method for the quantification of glutathione and glutathione disulphide

Contents

3.1 Introduction

Glutathione is an important antioxidant that functions to protect the cell from oxidative stress. It is involved in the detoxification of reactive species through the scavenging of free radicals and the conjugation of electrophiles. Glutathione is synthesised from glutamate, cysteine and glycine by the action of two enzymes, GCL and GS, with GCL catalysing the rate limiting step in the production of the tripeptide.

Glutathione depletion and the ratio of reduced to oxidised glutathione (GSH/GSSG) are common indicators of oxidative stress. Under physiological conditions, more than 90% of glutathione is in the reduced form; however when the intracellular redox balance is perturbed, levels of the disulphide rise. The administration of a number of drugs that are associated with cases of DILI have also been shown to result in hepatic oxidative stress and glutathione depletion (Xu *et al.*, 2008); Consequently a reliable method for the quantification of GSH and GSSG that can be used in order to identify perturbations in glutathione homeostasis is an important component of any preclinical model used to investigate the role of oxidative stress in drug toxicity.

The results described in chapter 2 of this thesis highlighted the importance of Nrf2 in the regulation of glutathione homeostasis. Pathway analysis identified glutathione metabolism as one of the most significantly differentially regulated pathways between WT and Nrf2 KO mice and proteins including glutathione peroxidase 1, GCLC and a number of GSTs were identified as being expressed at a lower level in Nrf2 KO animals.

Nrf2-mediated regulation of the glutathione pathway is well established, with genes including those encoding the GSTs, GCL and GS all identified as Nrf2 regulated in a range of studies (Chan *et al.*, 2001; Li *et al.*, 2009; Moinova *et al.*, 1999; Thimmulappa *et al.*, 2002). Furthermore, the importance of the transcription factor in glutathione repletion after toxic insult is also widely documented (Chan *et al.*, 2001; Gao *et al.*, 2010; Reisman *et al.*, 2009). While this means that the pathways important in glutathione metabolism have the potential to provide novel candidate biomarkers of Nrf2 activity, it also highlights the importance of the quantification of glutathione levels in gaining a comprehensive insight into the mechanisms by which oxidative stress and Nrf2 activation occur.

A wide variety of methods exist for the quantification of glutathione. Some methods measure total glutathione while others discriminate between GSH and GSSG. The majority

of methods are either spectrophotometric or HPLC-based, although NMR and capillary electrophoresis methods have also been developed (D'Agostino *et al.*, 2011; Reglinski *et al.*, 1992). As the technology associated with LC-MS/MS has advanced, the use of such methods has become increasingly popular as they offer high levels of specificity and sensitivity.

There are a number of important factors to consider when developing a reliable method for the quantification of GSH and GSSG: the thiol group of GSH is particularly susceptible to auto-oxidation resulting in disulphide formation, and this can result in inaccuracy when determining the relative levels of GSH and GSSG. Thiol capping reagents are employed in order to prevent this oxidation, with N-ethylmaleimide (NEM) and iodoacetic acid (IAA) being among the most common. Derivatisation of the thiol group can also improve retention of the highly polar GSH, with HPLC conditions and column selection also having implications for retention time. The choice of protein precipitation reagent and internal standard are also important factors in the development of a sensitive, accurate and reproducible method. The details of a range of validated methods for the measurement of GSH and GSSG are given in table 3.1.

The aim of the work described in this chapter was to explore existing methods for the quantification of glutathione and to adapt these methods in order to produce a robust LC-MS/MS assay that would allow the quantification of GSH and GSSG in mouse liver samples. Appropriate aspects of the FDA guidelines for the validation of bioanalytical methods were employed in order to assess the reproducibility of the method (FDA, 2001). The method developed was subsequently employed to compare the GSH and GSSG levels in livers of WT and Nrf2 KO mice in order to investigate whether the differences in glutathione metabolism previously identified by iTRAQ analysis translate to a statistical difference in levels of reduced and/or oxidised glutathione.

Table 3.1: Validated methods for the quantification of GSH and GSSG in biological samples.

Sample type	LC column type	LC conditions	Detection	Internal Std	Linear range	Thiol trapping/ protein precipitation (PPT)	Reference
PBMCs	Nucleosil 100-7 OH 250x2mm	Acetonitrile (ACN): 1% acetic acid (25:75)	LC-MS	Thiosalicylic acid (TSA)	0.01-20uM GSH, 0.05-20uM GSSG	NEM (100:1 molar ratio); AcN PPT	(Camera *et al.*, 2001)
Hepatocytes	Hamilton PRP-X110S anion exchange 100x2.1mm	0.1% formic acid (FA)/ACN (1:1) and 2% FA/ACN 1/1 Gradient	LC-MS	γ–glutamyl-glutamic acid (γ–Glu-Glu)	0.16-16uM GSH 0.08-81.6uM GSSG	IAA; AcN PPT	(Loughlin *et al.*, 2001)
Blood	Bio-Rad Biosil NH2 column 250x4.6mm,	0-10 min 70 % 80:20 MeOH:H2O, 30% 0.5M acetate buffer pH4.6, linear grad 30-95%B for 35 min	UV	NA	50-1500 uM GSH 2-500uM for GSSG	NEM; TCA PPT	(Giustarini *et al.*, 2003)
Brain, lung, liver, heart, kidneys, erythrocytes and plasma	Adsorbosil C18 250x3.2mm	0-2 min 100% 0.1% Trifluoroacetic acid; 2-13 min linear increase to 60% ACN, held from 13-15 min	LC-MS	Glutathione-ethylester (GSHee)	LOD 0.16 µM for GSH-Ellman and GSSG	Ellman's reagent; SSA PPT	(Guan *et al.*, 2003)
Blood	Stability BSC 17 150mm ×2mm	7.5mM ammonium acetate (pH 2.4): MeOH (50:50)	LC-MS	γ–Glu-Glu	0.01–20 µM GSH 0.05–20 µM GSSG	NEM; SSA PPT	(Steghens *et al.*, 2003)
Liver	Uptisphere C18 100x2mm	0.1%FA and ACN:0.1%FA (20:80) 0-2 min 100% A; 2-4 min linear increase to 100% B; 4-7 min 100% B; 7-15 min 100% A.	LC-MS	GSHee	0.1ug/mL-100ug/mL	IAA; SSA PPT	(Bouligand *et al.*, 2006)
Saliva	Atlantis HILIC 150x2.1mm	0.5mM Ammonium formate (pH4) and ACN 0-20 min 90-70%B	LC-MS	γ–Glu-Glu	0.1-100uM GSH-NEM	NEM (100:1); solid phase extraction	(Iwasaki *et al.*, 2006)
Monocyte/ macrophage cell line	Jupiter 5u 150mmx2mm	0.1% FA and ACN:0.1% FA (80:20) 0-2.5 min 2% B; 2.5-4.5 min 8% B; 4.5-11 min 70-100% B; 11-15 min 100% B; 15.5-24 min 2% B.	LC-MS	$^{13}C_2{}^{15}N_1$-GSH	5-400 nmol/mL GSH 0.5-40 nmol/mL GSSG	4-fluoro-7-sulfamoylbenzofurazan; SSA PPT	(Zhu *et al.*, 2008)

3.2 Materials and methods

3.2.1 Materials

LC-MS grade dH2O and methanol, ethylene diamine-tetracetic acid (EDTA), ammonium bicarbonate and potassium chloride were from Fisher Scientific (Loughborough, UK). Amber eppendorfs for use with light sensitive samples were from Eppendorf UK Ltd (Stevenage, UK). All other reagents were from Sigma (Poole, UK), unless otherwise specified.

3.2.2 Animal Studies

Mice were housed as described previously in this thesis. Livers used for method development were from WT (C57BL/6) animals. For the determination of glutathione levels in WT and Nrf2 KO mice, 8-12 week old males were culled between 10 am and 12 pm. All animals were killed by exposure to a rising concentration of CO_2 followed by cervical dislocation. Livers were removed, snap frozen in liquid nitrogen and stored at -80°C.

The samples used for comparison of the LC-MS/MS and spectrophotometric glutathione methods were from livers of CD1 mice treated with 750mg/Kg paracetamol or vehicle control (0.5% methyl cellulose in 0.1% tween 80; *i.p.*) once daily for up to 4 days (0h, 24h, 48h, 72h) and culled at various time-points after the first dose (2h, 4h, 6h, 24h, 48h, 72h, 96h).

3.2.3 Liver homogenisation

Livers were homogenised using the method of Bouligand *et al* (Bouligand *et al.*, 2006) with minor modifications. 50-100 mg of liver tissue was weighed and homogenised in acidic (pH2) homogenisation buffer (1.15% w/v potassium chloride, 1 mM EDTA and 2 mM *batho*-phenanthroline disulphonate (BPDS) in 0.1% v/v formic acid) using the Retsch oscillating mill (30/s; 3 min). Samples were centrifuged (16 000g; 15 min; 4°C) and the supernatant retained. The pellets were reserved for protein concentration determination by the method of Lowry (Lowry *et al.*, 1951).

3.2.4 Preparation of standard solutions

1mM stock solutions of GSH and GSSG were prepared in dH_2O and aliquots stored at -20°C. As required, a single working solution of 200 µM GSH/GSSG was prepared and serial diluted

in order to achieve solutions of 20x the final desired standard concentration (final concentrations: 10, 7.5, 5, 4, 3, 2, 1, 0.5, 0.1 µM).

During assay optimisation, the use of two different internal standards was explored, glutathione ethyl ester (GSHee) and stable isotope labelled GSH [GSH-Gly($^{13}C_2{}^{15}N$)]. Both were prepared as solutions of 100 µM and stored at -20 °C.

3.2.5 Matrix effects

Given that the biological matrix can impact the quantification of an analyte, matrix effects must be taken into account when producing a standard curve. Consequently, a pooled matrix sample was prepared from livers of six mice homogenised as described above and diluted to give a protein concentration of 5mg/mL. The matrix was used in order to spike standards used for quantification and was stored in aliquots at -80 °C.

3.2.6 Thiol derivatisation

50 µL of internal standard was added to 50 µL of homogenised samples or standards. 50 µL of matrix was also spiked into standards. 100 µL of IAA derivatisation solution [10 mM IAA in 10 mM ammonium bicarbonate with NH_3OH 0.5% (v/v); pH 9.5] was added and the solutions were incubated (1.5 hours; room temperature). Reactions were performed in amber eppendorfs for light sensitive samples.

In order to stop the reaction and precipitate proteins, 50 µL of ice cold sulphosalicylic acid (SSA) solution (10% w/v) was added. Samples and standards were vortexed and centrifuged (16 000g; 15 min; 4 °C) before being filtered (1500 g; 20 min) using a 96 well MultiScreen filter plate (Millipore Ltd, Watford, UK). All solutions were made up to a final volume of 1 mL with 0.1% (v/v) formic acid, and 100 µL transferred to a glass vial for LC-MS/MS analysis.

During assay optimisation, derivatisation with NEM was also tested. The NEM protocol was based on the method of Iwasaki *et al* (Iwasaki *et al.*, 2006). Glutathione standards were incubated with 5mM NEM for 30 minutes at room temperature and centrifuged (10 000g; 3 minutes), before addition of ice cold ACN. Incubation of NEM treated standards for 20 minutes on ice was also tested as described in a paper by Camera *et al (Camera et al., 2001)*. All samples were evaporated to dryness, before re-suspension in 0.1% formic acid.

3.2.7 LC-MS/MS

The Dionex UltiMate 3000 HPLC system with autosampler, bianary pump and column compartment (Thermo Fisher, UK Ltd, Surrey, UK) was used in combination with a Kinetex 2.6µm C18 100 Å 100 x 2.1 mm column (Phenomenex, Macclesfield, UK), in order to achieve separation of analytes. The column oven was held at a temperature of 30 °C. The injection volume was 10 µL, with the syringe washed with 5% methanol prior to each injection. The flow rate was 100 µL/min with mobile phases 0.1% (v/v) formic acid in dH2O (solvent A) and 0.1% (v/v) formic acid in methanol (solvent B). The elution gradient was as follows, with a total run time of 15 minutes:

- 0 minutes: 0% B
- 0-5 minutes: 0-20% B
- 5-10 minutes: 20% B
- 10.01-15 minutes: 0% B

An ABSciex Q Trap mass spectrometer (ABSciex UK Ltd, Warrington, UK) was used for analyte detection using a multiple reaction monitoring (MRM) method. The parameters used for each analyte are detailed in table 3.2.

Table 3.2: Parameters used for MS/MS analyte detection. DP = declustering potential; CE = collision energy; CXP = collision cell exit potential.

Analyte	Q1 mass	Q3 mass	DP (volts)	CE (volts)	CXP (volts)
CM-GSH	366.3	237.0	65.0	16.0	10.0
GSSG	613.4	355.2	83.0	32.0	10.0
CM-GSH-IS	369.1	84.0	71.0	53.0	2.0

3.2.8 Assay validation

Appropriate aspects of the FDA industry guidelines for bioanalytical method validation (FDA, 2001) were employed in order to validate the assay. Accuracy and precision were determined using matrix-spiked solutions of known GSH and GSSG concentration (n=6) at a high (7.5 µM), medium (4 µM) and low (0.5 µM) concentration. The same solutions were used to determine percentage recovery, with recovery calculations based on comparison to unspiked standards.

3.2.9 Spectrophotometric enzymatic recycling method for determination of total glutathione levels

Approximately 50 mg of liver tissue was homogenised in 800 µL sodium phosphate buffer (0.1M NaH_2PO_4 with 0.5M EDTA; pH 7.4) with 200 µL 6.5% (w/v) SSA using the Retsch oscillating mill (30/s; 3 min). Samples were centrifuged (16 000g; 5 min) and the supernatant removed to a fresh tube and stored at -80°C. The pellets were reserved for protein concentration determination by the method of Lowry (Lowry *et al.*, 1951).

A 1 mM GSH stock solution was prepared in sodium phosphate buffer and used in order to prepare standards (0 – 80 nmol/mL). Samples were diluted in sodium phosphate buffer and 20 µL of samples and standards were added to wells of a 96 well plate. A further 20 µL of sodium phosphate buffer was added to each well before 200 µL of daily assay reagent (1 mM 5,5-dithiobis-1,2-nitrobenzoic acid (DTNB) with 0.28 mg/mL NADPH in sodium phosphate buffer) was added and the plate incubated (room temperature; 5 min). 50 µL of GSH reductase (6.96 units/mL) was added to each well and the plate read immediately at 405 nm using the MRE^e plate reader (Dynex Technologies Limited, Worthing, West Sussex) in order to determine total glutathione levels.

3.3 Results

3.3.1 Assay development

In order to develop a robust LC-MS/MS method for the quantification of GSH and GSSG in liver tissue, previously validated methods were identified in the literature (table 3.1). These methods had been optimised for a range of different tissues and biofluids and employed different methods of sample preparation, thiol capping, protein precipitation, internal standard normalisation and analyte detection.

3.3.2 Liver Homogenisation

Given that the method of Bouligand *et al* had been optimised for the quantification of GSH and GSSG in liver samples, the protocol described in the paper was used for sample homogenisation (Bouligand *et al.*, 2006). The acidity of the homogenisation buffer (pH2) inhibits the oxidation of GSH to the disulphide, while EDTA and BPDS function as metal ion chelators.

3.3.3 Thiol derivatisation

The most commonly employed reagents for thiol derivatisation in methods identified were IAA and NEM. NEM has been shown to react with thiols at a faster rate, but its use is associated with the presence of artifacts in the spectra (Gilbert, 1995; Giustarini *et al.*, 2003; Santori *et al.*, 1997). Treatment of GSH with NEM results in a GSH-NEM derivative, while treatment with IAA results in a carboxymethyl-GSH (CM-GSH) derivative (figure 3.1). Incubation of liver homogenates with NEM at room temperature and on ice both resulted in the presence of a double peak in the chromatogram generated by MS analysis (figure 3.2). IAA gave a single peak that was also more intense and was therefore selected as the derivatisation agent for use in the assay.

An IAA concentration of 10 mM was selected for thiol derivatisation as this concentration had been employed in a number of the methods identified (Bouligand *et al.*, 2006; Loughlin *et al.*, 2001). A relatively long incubation time of 1.5 hours was required in order to achieve complete derivatisation of the GSH, with underivatised GSH detected after incubation times of 1 and 1.25 hours. The reaction was carried out in amber eppendorfs designed for light sensitive samples as it has been suggested that exposure to light can facilitate GSH oxidation (Rahman *et al.*, 2006).

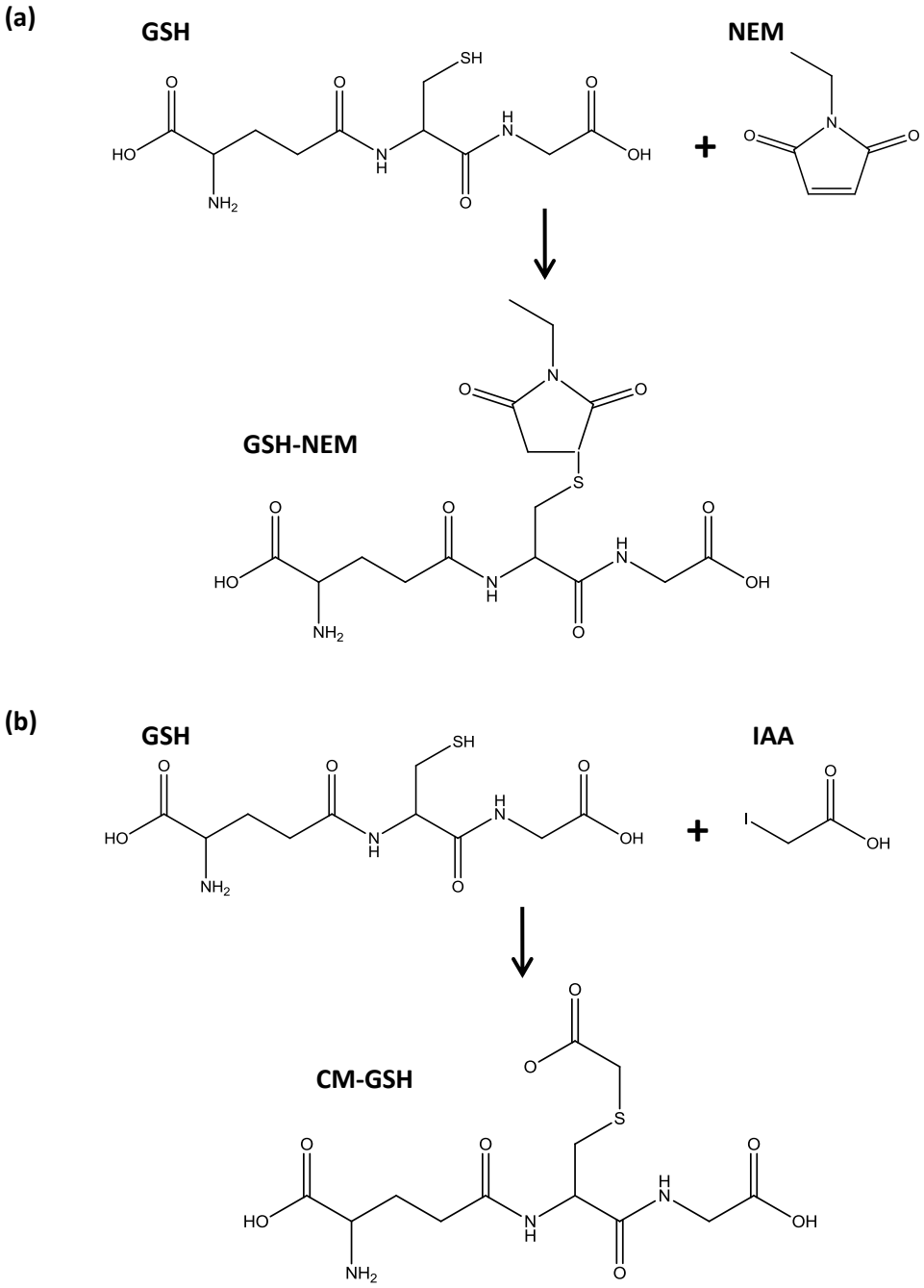

Figure 3.1: The derivatisation of GSH with N-ethylmaleimide (NEM) and iodoacetic acid (IAA). (a) Thiol capping of GSH with NEM results in formation of the GSH-NEM derivative. (b) Thiol capping of GSH with IAA results in the formation of S-carboxymethyl-glutathione (CM-GSH).

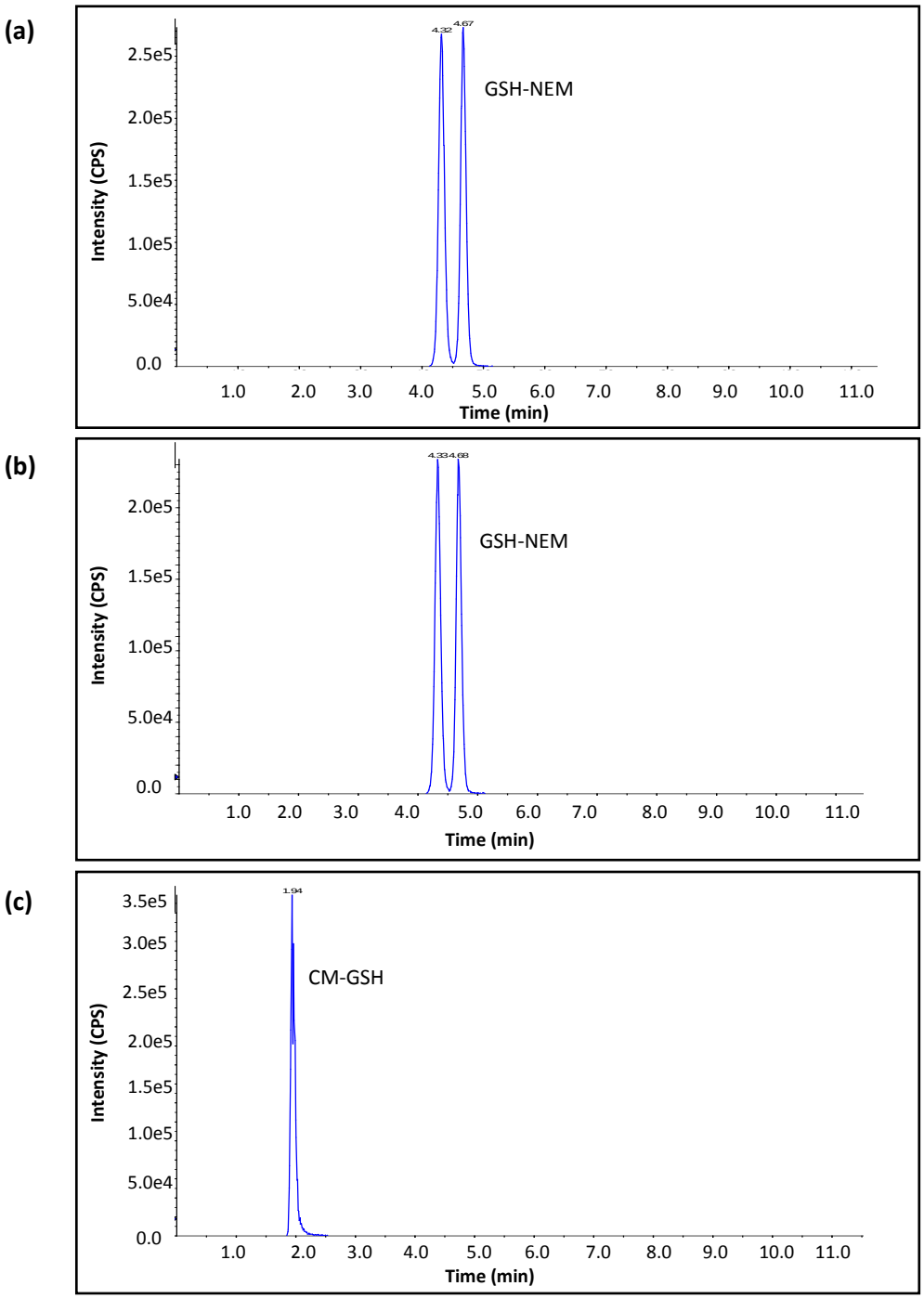

Figure 3.2: Chromatograms for derivatised GSH. GSH was derivatised using (a) N-ethylmaleimide (NEM) at room temperature, (b) NEM on ice and (c) iodoacetic acid (IAA) at room temperature. Samples were analysed by LC-MS/MS.

3.3.4 Internal standard selection

The suitability of GSHee and glutathione-(*glycine*-$^{13}C_2$,^{15}N) were investigated for use as an internal standard. The structure of both molecules is given in figure 3.3. GSHee was employed as an internal standard in two of the methods identified in the literature [Bouligand and also Guan]. However, when a solution of GSHee was treated with the IAA derivatisation solution and analysed by LC-MS/MS, CM-GSH was also identified (figure 3.4). This suggests that a degree of GSHee hydrolysis had occurred, something that has also been noted in the literature (Iwasaki *et al.*, 2006). Consequently glutathione-(*glycine*-$^{13}C_2$,^{15}N) was selected for use as the internal standard (GSH-IS). The optimised spectra for CM-GSH, GSSG and CM-GSH-IS are given in figure 3.5.

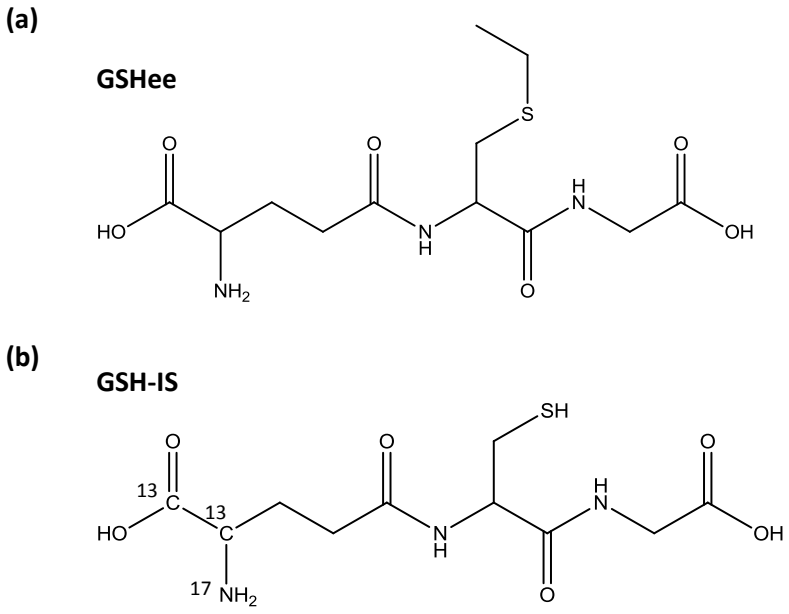

Figure 3.3: Structure of (a) glutathione ethyl ester (GSHee) and (b) Glutathione-(*glycine*-$^{13}C_2$,^{15}N) (GSH-IS).

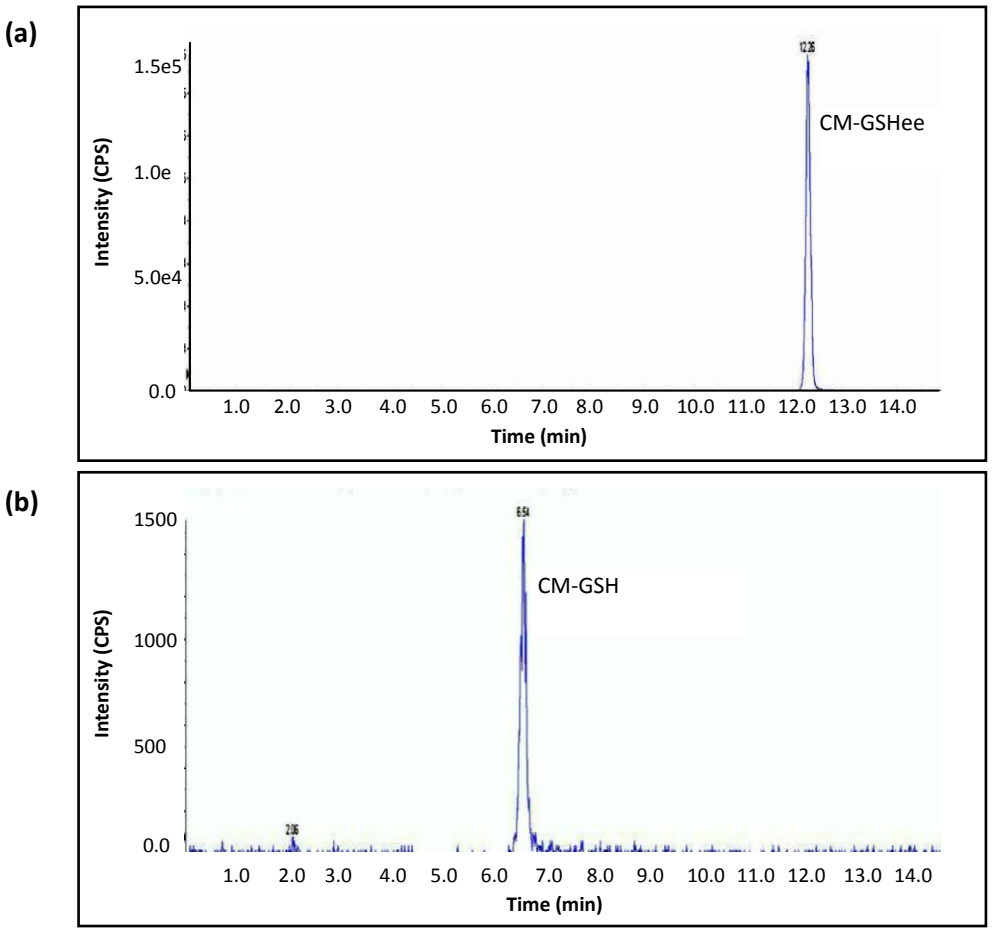

Figure 3.4: GSHee can be hydrolysed to GSH (a) A solution of 0.5 µM GSHee was treated with IAA to yield CM-GSHee. (b) CM-GSH was also detected when the sample was analysed by LC-MS/MS.

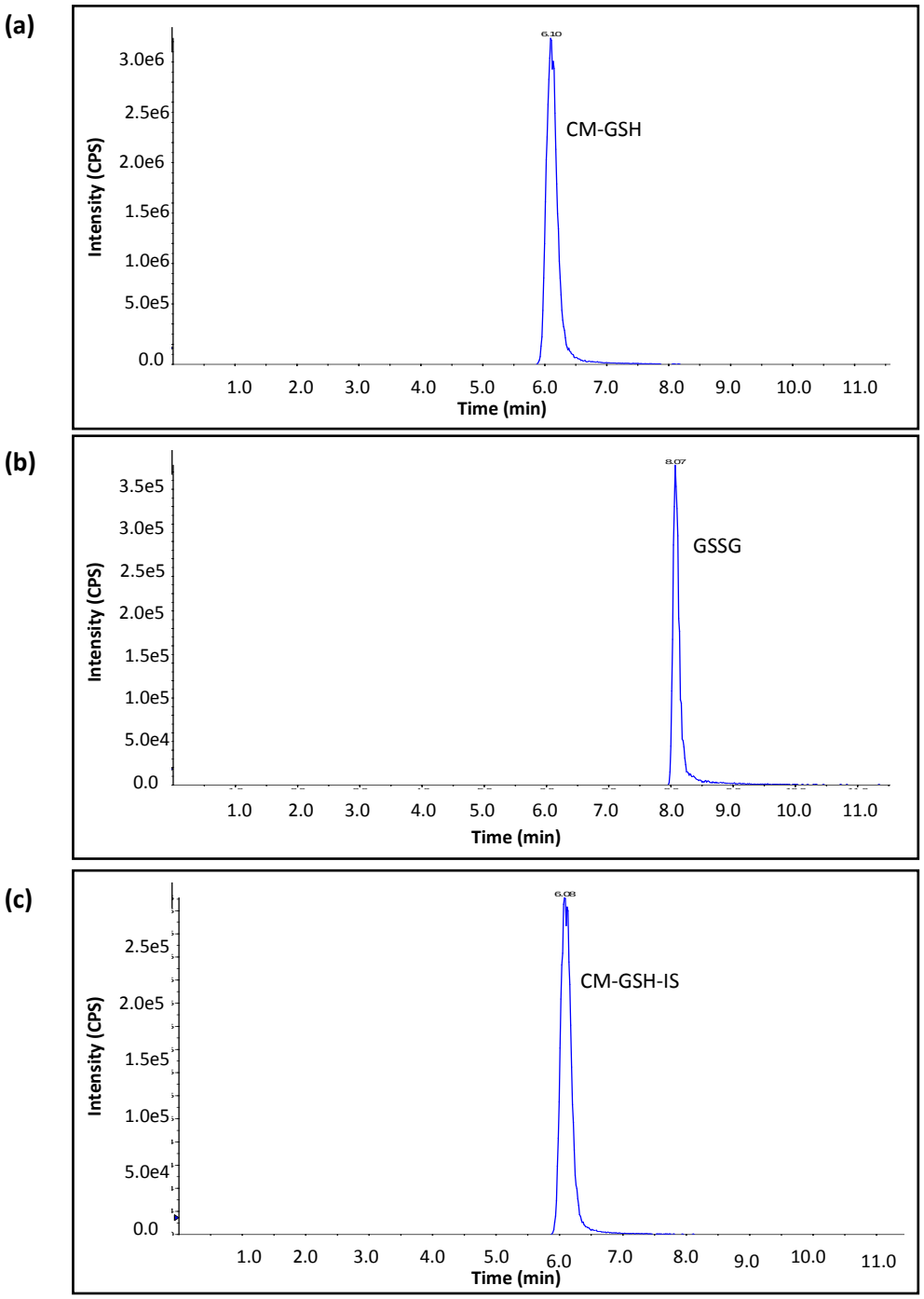

Figure 3.5: Representative chromatograms for CM-GSH (a), GSSG (b) and CM-GSH-IS (c). The concentration of all analytes is 5 µM.

3.3.5 Matrix effects

The biological matrix can have a significant impact on the quantification of an analyte within a sample. Consequently, it is necessary to take the matrix effect into account when generating a standard curve. Example standard curves constructed from standards that have been spiked with matrix are compared to curves from unspiked standards in figure 3.6. The addition of the matrix to GSSG standards was found to have a notable effect on the gradient of the standard curve.

3.3.6 Method validation

Assay validation was performed using three different concentrations of matrix-spiked standards (n=6). The three selected values were all within the range of the standard curve, with low (0.5 µM), medium (4 µM) and high (7.5µM) concentrations used. The accuracy and precision of the assay were determined, as well as the percentage recovery of analytes. Recovery values were calculated by comparing values obtained from matrix-spiked and un-spiked standards, with unspiked standard values designated as 100% recovery.

FDA guidelines for assay validation state that in order to be considered accurate, mean concentration values as determined by a given method should be within 15% of actual values, except at the lower limit of quantification (LLOQ) where a deviation of 20% is acceptable. In terms of precision, the range of values for a given concentration should not exceed 15% of the coefficient of variation (CV), or 20% at the LLOQ (FDA, 2001). Accuracy for CM-GSH determination was ≥90% for the medium and high values, and so fell within the FDA guidelines, while accuracy at the lowest concentration was 80%, and thus represents the LLOQ (table 3.3). The values calculated for all three concentrations of CM-GSH were found to be precise.

Precision for GSSG in standards that were treated with IAA was also within the acceptable range, however accuracy was low and recovery values showed that levels of GSSG were being underestimated by 70-80%. There is evidence to suggest that when thiol derivatisation reagents are used, the equilibrium of the system is affected such that derivatisation of GSH promotes the reduction of GSSG, thus resulting in GSSG levels being underestimated (Rossi *et al.*, 2002).

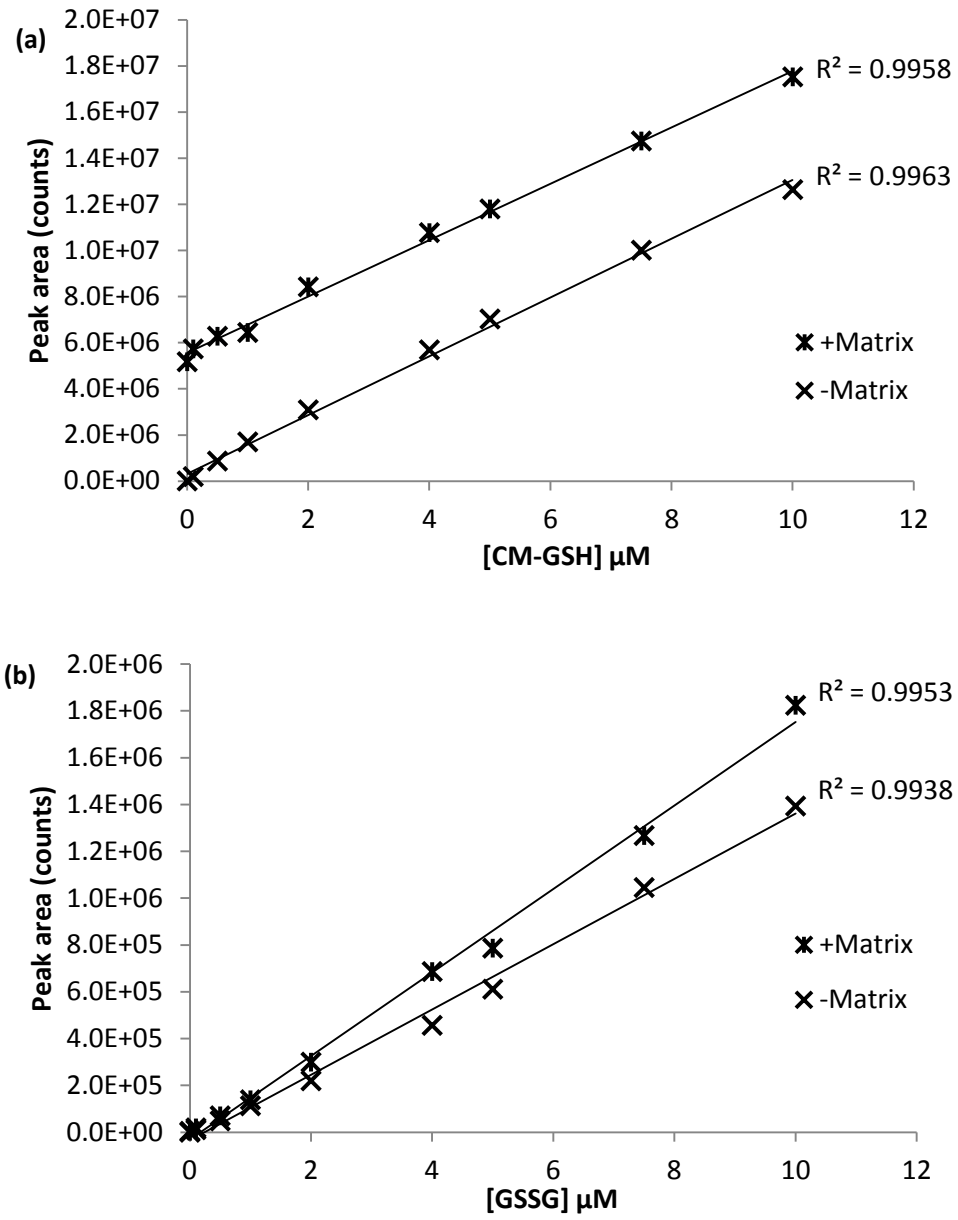

Figure 3.6: The effect of liver homogenate matrix on glutathione quantification. Standard curves were produced for (a) S-carboxymethyl-glutathione (CM-GSH) and (b) oxidised glutathione (GSSG) standards in the presence and absence of mouse liver homogenate (matrix).

Table 3.3: Accuracy, precision and recovery values for the determination of CM-GSH and GSSG levels by LC-MS/MS. Matrix-spiked standards at three concentrations (low: 0.5µM; medium: 4 µM and high: 7.5 µM) were used in order to validate the assay (n=6). GSSG validation was performed in the presence and absence of iodoacetic acid (IAA). CV = coefficient of variation.

		Accuracy (%)	Precision (%CV)	Recovery (%)
CM-GSH	Low	80.0	10.3	115.2
	Medium	91.7	4.9	103.8
	High	90.0	3.9	86.3
GSSG + IAA	Low	44.0	8.0	21.3
	Medium	53.0	6.4	25.9
	High	53.7	10.0	26.2
GSSG - IAA	Low	58.0	14.8	73.5
	Medium	68.7	12.0	76.4
	High	60.7	12.1	66.8

In order to investigate the effect of IAA derivatisation on the recovery and accurate quantification of analytes, standards were also prepared without the addition of IAA. Precision was reduced when compared to IAA treated GSSG standards, but values were still within FDA guidelines. Accuracy did improve, but was still below 85%. Recovery levels were approximately 3-fold higher in the absence of IAA at 65-80%, thus suggesting that treatment of samples with IAA did impact the GSH/GSSG equilibrium.

3.3.7 LC-MS/MS and spectrophotometric method comparison

The spectrophotometric enzymatic recycling assay is commonly used in order to determine the concentration of glutathione in tissues, biofluids and cell extracts (Rahman *et al.*, 2006; Tietze, 1969). Consequently the spectrophotometric assay and the LC-MS/MS assay were both used to analyse the same samples in order to investigate whether the two methods were comparable. Homogenates of livers from mice treated with a 750mg/kg dose of paracetamol daily for up to 4 days and culled at different time points after the first dose were analysed for total glutathione content (figure 3.7). The concentrations of glutathione detected by LC-MS/MS in the samples were slightly higher at 6/8 time points but the values were not statistically different between the two methods. SEM values were also comparable.

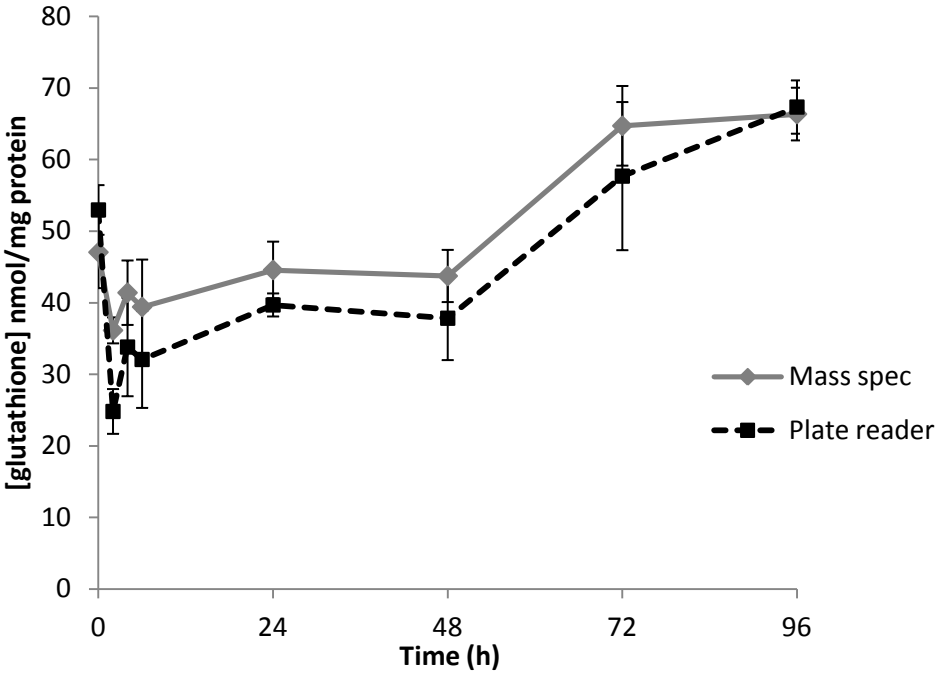

Figure 3.7: Comparison of LC-MS/MS and plate reader methods for the determination of glutathione concentration. Samples are from livers of mice treated with repeat doses of paracetamol and culled at various time-points after the initial dose (750 mg/kg; n=4). Total glutathione was determined using the plate reader assay, while GSH and GSSG were determined independently by LC-MS/MS and the values combined to give total glutathione. Values are normalised to protein concentration (mg/mL). Error bars represent SEM.

3.3.8 Determination of GSH and GSSG levels in livers of WT and Nrf2 KO mice by LC-MS/MS

Following validation, the LC-MS/MS assay was used in order to determine the level of GSH and GSSG in the livers of WT and Nrf2 KO animals, with GSSG levels corrected for recovery values as determined during the validation process. Hepatic GSH levels in Nrf2 KO animals were 78.5% of those in WT animals ($P<0.001$; figure 3.8). GSSG levels were not statistically different between the genotypes. The GSH/GSSG ratio was also calculated and did not differ in WT and Nrf2 KO livers, yielding values of 13.5 and 13.4 respectively.

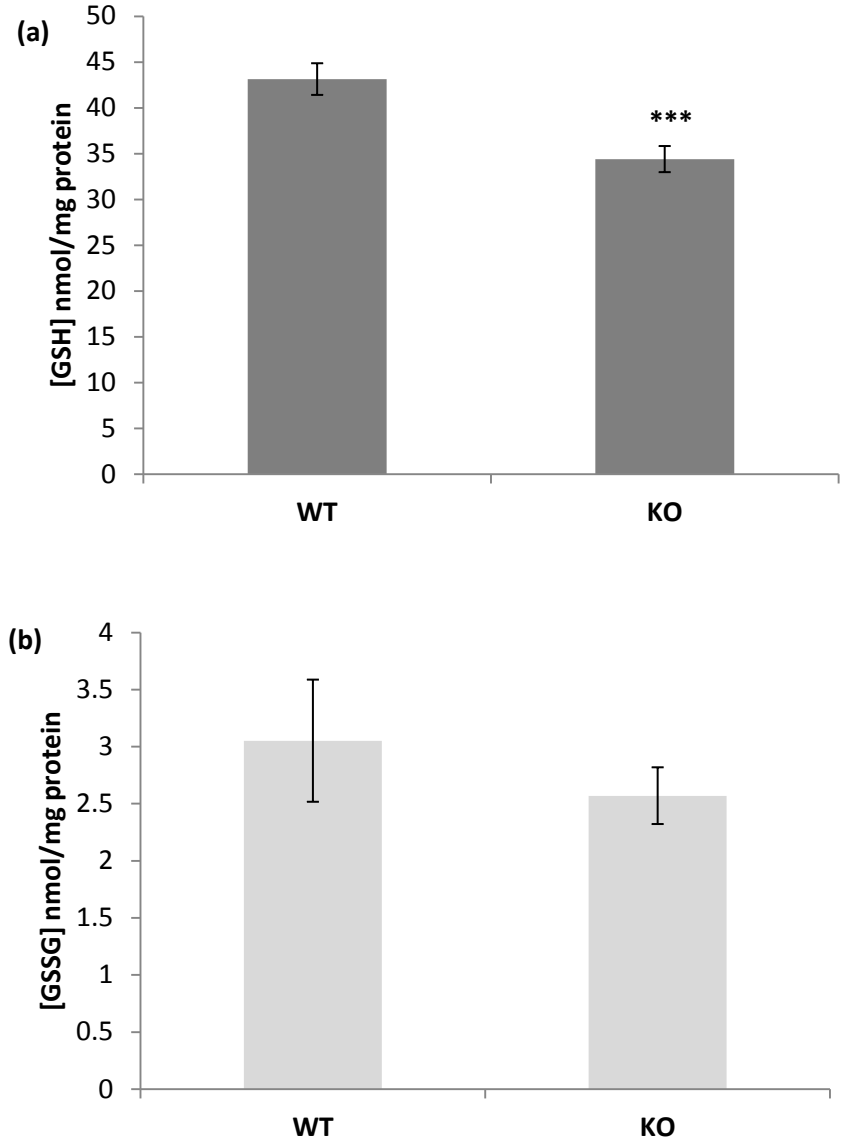

Figure 3.8: Concentrations of reduced (GSH) and oxidised (GSSG) glutathione in homogenates from the livers of WT and Nrf2 KO mice as determined by LC-MS/MS. Values are normalised to protein concentration (mg/mL). Error bars represent SEM (n=8). Statistical significance was determined using an unpaired t=test (***P<0.001). There was no difference in the GSSG levels detected in WT and Nrf2 KO animals.

3.4 Discussion

The aim of the work described in this chapter was to investigate validated LC-MS/MS methods for the determination of GSH and GSSG in biological samples and to develop a robust assay that would allow quantification of the two analytes in mouse liver homogenates.

GSH can undergo auto-oxidation to the disulphide and so one of the major challenges in accurately quantifying GSH and GSSG is to minimise the oxidation of GSH during sample preparation. Given that the oxidation of GSH has been shown to occur rapidly in solutions of pH>7 (Anderson, 1985; Camera *et al.*, 2002; Rossi *et al.*, 2002) this was achieved by use of an acidic buffer for sample homogenisation, and subsequent treatment of homogenised samples with the thiol derivatising agent, IAA.

Experiments designed to validate the method showed that GSH could be accurately and precisely quantified within the range of the standard curve (0.5-10µM). However, while GSSG could be precisely measured, the accuracy was well below the value recommended by the FDA for assay validation (FDA, 2001) and recovery of the analyte was determined to be only 20-30%. Evidence suggests that while GSH oxidation can occur during sample preparation, conversely, derivatisation of the GSH thiol can result in perturbation of the GSH/GSSG equilibrium, with the system acting to restore GSH levels by reduction of GSSG (Rossi *et al.*, 2002).

In order to investigate whether IAA treatment was contributing to the underestimation of GSSG levels, samples were prepared for LC-MS/MS analysis without IAA treatment. The percentage recovery of GSSG in these samples was increased to values of 65-80%. This suggests that the method employed for derivatisation of GSH did have a significant impact on the concentration of the disulphide, although accuracy was still below 85% and so other factors may also have a role to play.

One strategy that could be investigated for improving GSSG quantification is the inhibition of glutathione reductase (GR), the enzyme that catalyses the reduction of GSSG to GSH. For example, the use of the GR inhibitor, 1,3-bis(2-chloroethyl)-1-nitrosourea, has been shown to significantly reduce the loss of GSSG in blood samples treated with IAA (Rossi *et al.*, 2002). It should also be noted however, that the incubation time of 1.5 hours for IAA

derivatisation is relatively long, for example, in the paper of Bouligand *et al* the incubation time was only 15 minutes (Bouligand *et al.*, 2006). During the process of method development, shorter IAA incubation times were investigated but were found to be insufficient for complete derivatisation of GSH. The concentration of IAA in the derivatisation solution could be increased to facilitate a shorter incubation time, for example other methods have employed concentrations up to 100 mM IAA (Santori *et al.*, 1997).

The method described in this chapter is largely based on that of Bouligand *et al (Bouligand et al., 2006)*. However the notable difference between the two methods is the use of the stable isotope labelled glutathione-(*glycine*-$^{13}C_2{}^{15}N$) internal standard as opposed to GSHee. Hydrolysis of GSHee to yield GSH was detected during validation, and while the levels of GSH detected as a result of hydrolysis were low compared to GSH levels in liver homogenates, further investigation found that levels of hydrolysis was variable across samples and so difficult to control for. Furthermore, if the assay were to be adapted for use in cell extracts or other samples in which levels of glutathione were considerably lower than those in mouse liver, the relative contribution of GSH from GSHee hydrolysis would be greater.

The LC-MS/MS method described in this chapter was compared to the spectrophotometric enzymatic recycling method (Rahman *et al.*, 2006; Tietze, 1969), which is an assay widely used in the department and elsewhere for the determination of total glutathione levels in biological samples. There was no significant difference between glutathione levels as determined by the two assays, suggesting that both are valuable for the determination of total glutathione concentrations in liver homogenates.

However, there are advantages to the LC-MS/MS assay: While the determination of GSSG levels is possible if a second assay employing GSH-derivatising agents such as 2-vinylpridine is used alongside the enzymatic recycling method (Griffith, 1980), the LC-MS/MS method can quantifying GSH and GSSG in a single assay. Furthermore, the LC-MS/MS method could also be adapted to investigate levels of protein-bound GSH and may be optimised to include other thiols and disulphides which are important in the synthesis of glutathione (Bouligand *et al.*, 2006). Such methods could be used to provide valuable insight into the impact of oxidative stress on the wider glutathione metabolism pathway.

While there were limitations associated with the quantification of GSSG, the LC-MS/MS method was used in order to determine the levels of the analytes in the livers of WT and Nrf2 KO mice, with GSSG levels corrected according to the calculated recovery values determined during method validation. Work described in chapter 2 of this thesis highlighted the important role that Nrf2 plays in regulating glutathione metabolism. Previous investigations suggest that genetic modulation of the Keap1:Nrf2 pathway has implications for hepatic glutathione concentration, with lower levels reported in Nrf2 KO mice when compared to WT animals and an increase in hepatic glutathione levels in a Keap1 heaptocyte specific model (Wu *et al.*, 2011). However, it is important to establish the baseline glutathione levels in mice from the Nrf2 colony at the University of Liverpool as basal glutathione status may have important implications for future studies.

Nrf2-regulation of glutathione metabolism was shown to have functional implications in terms of basal levels of hepatic glutathione, as levels of GSH in livers of Nrf2 KO animals were 78.5% of those in WT animals ($P<0.001$). This result is comparable to the differences in total glutathione levels identified in previous studies (Wu *et al.*, 2011). Furthermore, the absolute concentrations of both GSH and GSSG in livers of WT mice in the study were within the range of those previously determined in livers of C57BL/6 mice (Bouligand *et al.*, 2006), thus giving confidence in the calculation correcting for GSSG levels based on percentage recovery values.

In summary, the LC-MS/MS method described in this chapter allows precise and accurate determination of GSH levels in mouse liver homogenates. While improvements are necessary in order to allow the accurate quantification of GSSG, a preliminary calculation of GSSG levels in livers of WT and Nrf2 KO mice was possible based on the percentage recovery values determined during method validation.

Chapter 4 Nrf2 in the regulation of hepatic lipid metabolism

Contents

4.1 Introduction

Nrf2 is a transcription factor that plays a vital and well documented role in the cytoprotective response to chemical stress. Work described in chapter 2 of this thesis characterising the constitutive hepatic proteomic profile of WT and Nrf2 KO mice, highlighted the importance of Nrf2 in the regulation of the expression of proteins important for cytoprotection. However, the study also identified lipid metabolism as a process that was significantly differentially regulated in the WT and Nrf2 KO animals. A number of proteins involved in lipid metabolism were expressed at a higher level in the absence of a functional Nrf2 gene, thus suggesting that the transcription factor negatively regulates hepatic lipid metabolism.

There is a growing body of evidence pointing to a functionally significant role for Nrf2 in the regulation of lipid synthesis. When mice are fed a HFD, the expression of genes encoding enzymes key for fatty acid synthesis has been shown to be increased at a significantly higher level in Nrf2 KO mice when compared with WT animals (Tanaka *et al.*, 2008). While administration of the Nrf2-inducer CDDO-Im prevented the weight gain and increase in serum triglycerides associated with a HFD in an Nrf2-dependent manner (Shin *et al.*, 2009). Furthermore, Yates *et al* identified lipid metabolism as the functional category most significantly modulated at the mRNA level following both genetic and pharmacological activation of Nrf2 (Yates *et al.*, 2009).

Although the relationship between the roles of cytoprotection and lipid regulation is not currently well defined, Nrf2 is emerging as a multifunctional transcription factor with a pivotal role in two processes that are both vital for the maintenance of homeostasis in the liver. While a wealth of studies have been carried out on the role of Nrf2 in cell defence, the emerging role for Nrf2 in the regulation of hepatic lipid metabolism has yet to be fully elucidated.

Of the fifteen lipid metabolism-related proteins that were significantly up-regulated in Nrf2 KO animals in the iTRAQ study, SCD1, ACL and FAS, are key enzymes in the cytosolic fatty acid synthesis pathway. In the pathway, fatty acids are synthesised from the precursors, acetyl-CoA and malonyl-CoA, with the primary product of the FAS enzyme being the saturated fatty acid, palmitic acid. Longer chain and desaturated fatty acids are

subsequently synthesised by the action of elongases and desaturases respectively. These fatty acids go on to be incorporated into triglycerides, cholesterols and phospholipids. Consequently, the modulation of fatty acid synthesis by Nrf2 could have important implications for the homeostasis of the hepatic lipid profile. The fatty acid synthesis pathway is summarised in figure 4.1.

While there is evidence pointing to a role for Nrf2 in the regulation of a number of enzymes in this pathway at the mRNA level following Nrf2 induction (Shin *et al.*, 2009; Yates *et al.*, 2009), the iTRAQ data in this thesis was the first showing how basal Nrf2 expression affects protein levels of the enzymes. Furthermore, although lipid profile changes have been identified following the modulation of Nrf2 expression in mouse models (Shin *et al.*, 2009; Tanaka *et al.*, 2008), the effect of Nrf2 deletion on levels of hepatic fatty acids has not been investigated. Consequently, the functional outcome of changes in fatty acid synthesis enzymes at the mRNA and protein level has yet to be elucidated.

Dietary modulation provides a method by which the effects of perturbations in lipid metabolism pathways can be investigated. A number of the studies noted above have explored the effects of a HFD on Nrf2 expression and lipid profiles (Shin *et al.*, 2009; Tanaka *et al.*, 2008). However, no study has investigated the effects of altering dietary carbohydrate content in the context of Nrf2 signalling and lipid metabolism. Carbohydrate restriction has been shown to result in perturbations in hepatic fatty acid levels in the triglyceride, sphingomyelin and phosphatidylcholine lipid classes, as well as altering the ratio of unsaturated to saturated fatty acids in the liver (Bruss *et al.*, 2010; Forsythe *et al.*, 2008; Rojas *et al.*, 1993).

Given the pivotal role that the hepatic fatty acid pathway plays in lipid homeostasis, and the emerging role for Nrf2 in the regulation of lipid metabolism, the aim of the work described in this chapter was to characterise and compare the fatty acid profile of livers of WT and Nrf2 KO mice, both basally and following feeding of a carbohydrate-restricted (CHO-R) diet. Carbohydrate restriction was employed as a tool to explore how WT and Nrf2 KO animals respond to perturbations in hepatic fatty acid metabolism. Preliminary investigations characterised the effects of the CHO-R diet on the Nrf2 pathway, before work was carried out in order to determine whether hepatic lipid profiles of WT and Nrf2 KO animals were altered by carbohydrate restriction. The characterisation of the hepatic lipid

profile of mice in which Nrf2 expression has been modulated may provide valuable insight into the role of Nrf2 in the regulation of lipid metabolism as well as identifying potential preclinical biomarkers of Nrf2 activity.

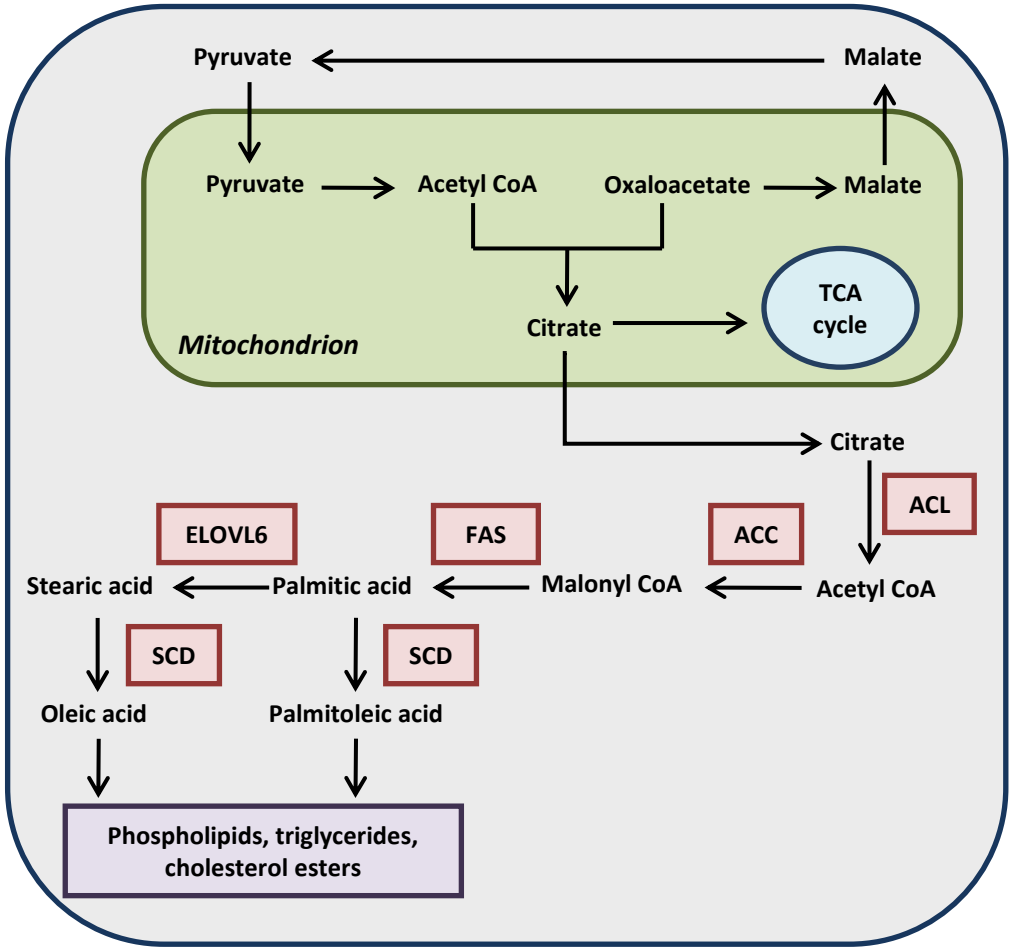

Figure 4.1: The synthesis of fatty acids. Fatty acid synthesis occurs in the cytosol, however the precursor acetyl CoA is synthesised in the mitochondria from pyruvate. It must be converted into citrate in order to be transported to the cytosol where ATP citrate lyase (ACL) converts it back to acetyl CoA. Acetyl CoA carboxylase (ACC1) catalyses the synthesis of malonyl CoA from 2 molecules of acetyl CoA. Malonyl CoA is used in order to synthesise the 16 carbon chain fatty acid, palmitic acid, in a reaction catalysed by fatty acid synthase (FAS). Subsequent elongation and desaturation reactions are catalysed by enzymes including fatty acid elongase 6 (ELOVL6) and stearoyl CoA desaturase (SCD), producing monounsaturated and very long chain fatty acids, which are used in the synthesis of phospholipids, triglycerides and cholesterol esters.

4.2 Materials and Methods

4.2.1 Materials

NQO1 goat monoclonal antibody, GCLC rabbit monoclonal antibody and glycogen assay kit were from Abcam, (Cambridge, UK). Peroxidise-conjugated rabbit anti-goat Immunoglobulins was from Dako, (Denmark). All other reagents were from Sigma (Poole, UK), unless otherwise specified.

4.2.2 Animal Studies

All mice were housed as described previously in this thesis. For the work investigating the effects of carbohydrate-restriction, a preliminary study (study 1; n=3) and a follow-up study (study 2; n=4) were carried out. Animals in study 1 were 8-10 weeks old at the outset, while animals in study 2 were 12-14 weeks old.

All mice had their body weight recorded before being fed a control diet for 1 week and were subsequently fed either a control or a CHO-R diet for 4 weeks, with their body weight and weight of food consumed recorded each day. Food for both diets was from Special Diet Services (Essex, UK). For the CHO-R diet, carbohydrate was reduced by 40% but all other dietary components were comparable to the control diet. At the end of the 4 week period, animals were culled between 10 am and 12 pm by exposure to a rising concentration of CO_2 followed by cardiac puncture. Livers were removed, and in study 2 were also weighed, before being snap frozen in liquid nitrogen and stored at -80°C.

4.2.3 Glutathione concentration determination

GSH and GSSG concentration in the livers of all mice was determined using the LC-MS/MS method that is detailed in chapter 3 of this thesis.

4.2.4 Liver homogenisation for western immunoblotting

Sections from livers (≈ 100 mg) were homogenised in 1 mL of PBS (30 s^{-1}; 2 min) using a Retsch oscillating mill. Samples were centrifuged (10 000 g; 5 min) and the supernatant retained. Protein concentration was determined using the method described by Lowry (Lowry *et al.*, 1951).

4.2.5 Western immunoblotting

Western immunoblotting for the ACL protein and subsequent analysis was performed on mouse liver homogenate as described in chapter 2. Western blots for NQO1 and GCLC were performed using the same protocol with the primary antibody for NQO1 a goat polyclonal antibody (1:5000) and for GCLC a rabbit polyclonal antibody (1:10000). The secondary antibodies were a peroxidase-conjugated rabbit anti-goat immunoglobulins/HRP (1:5000; NQO1) and a peroxidase-conjugated goat anti-rabbit IgG (1:10000; GCLC).

Actin was tested as a potential loading control. Actin western blots were performed using the same protocol with minor modifications, in that membranes were blocked overnight in 10% milk and primary antibody incubation was for 20 minutes (mouse monoclonal antibody; 1:20000). The secondary antibody was a peroxidase-conjugated rabbit anti-mouse IgG (1:20000).

4.2.6 Methanol-chloroform-water metabolite extraction

Liver samples from all mice were extracted using a method adapted from Le Belle *et* al (Le Belle *et al.*, 2002). Approximately 50 mg of tissue were pulverised in 600 µL methanol:chloroform (2:1 v/v) for 10 min at a frequency of 1/17 s^{-1} using the Qiagen TissueLyser (Qiagen, Crawley, UK). Samples were sonicated for 15 minutes and 200 µL of chloroform and 200 µL dH_2O added to form an emulsion. The samples were centrifuged (18 000 g; 5 min) in order to generate distinct aqueous and organic fractions, which were subsequently separated. The organic layer was dried overnight in a fume hood, while the aqueous layer was dried overnight in an evacuated centrifuge.

4.2.7 GC-FID

Once dried, the organic layer was resuspended in 600 µL of chloroform:methanol (1:1 v/v). 150 µL were transferred to a glass vial, before again being evaporated to dryness in the fume hood. The samples were resuspended in 750 µL of chloroform:methanol (1:1 v/v), and 250 µL of D-25 tridecanoic acid (200 µM in chloroform) was added as an internal standard. 125 µL 10% boron trifluoride (BF_3) in methanol was added as a derivatisation agent and the solution incubated (80°C; 90 minutes). Vials were cooled, before the addition of 500 µL of dH_2O and 1 mL of hexane. After vortexing, the solution separated into two distinct layers, the majority of the upper organic layer was transferred to a glass vial and evaporated to dryness in the fume hood overnight, before being reconstituted in 200 µL of hexane prior to

gas chromatography/flame-ionisation detector (GC/FID) analysis. A fatty acid methyl ester (FAME) standard (Supelco 37 component FAME mix 10 000 µg/mL in CH_2Cl_2) was also prepared using the same method.

Samples were separated by GC using a ZB-WAX column (Phenomenex, Macclesfield, UK; 30 m × 0.25 mm ID × 0.25 µm; 100% polyethylene glycol). The temperature was held at 60 °C for 2 minutes and was then increased by 15 °C/minute to 150 °C. It was subsequently increased by 3 °C/minute to reach a temperature of 230 °C. The column was held at this temperature for 10 minutes. The eluent was passed to a FID (Thermo Electron Corporation, Herts, UK). Chromatograms obtained were analysed using Xcalibur (Version 2.0; Thermo Fisher) and peak area normalised to that of D-25 tridecanoic acid in the corresponding sample.

4.2.8 LC-MS/MS lipidomic analysis

The lipid fraction of samples from study 1 that had previously been dried and stored at -80°C were reconstituted in 300 µL methanol:chloroform (2:1 v/v). 10 µL of sample were added to a glass vial together with 190 µL of the methanol:chloroform mixture. A pooled sample constituting 10 µL of each individual sample was also made.

Samples were run in duplicate and in a randomised order using an ACQUITY UPLC® system (Waters Ltd, Hertfordshire) equipped with an ACQUITY UPLC 1.7 µm bridged ethyl hybrid C8 column (2.1×100 mm) which was kept at 65 °C and coupled to a Micromass QToF-Ultima™ API with a Z-spray™ electrospray source (Waters Ltd, Hertfordshire), with the electrospray used in positive ion mode.

Solvent A was 10 mM ammonium acetate with 0.1% FA, while solvent B was 10 mM ammonium acetate in ACN:ICN (5:2) with 0.1% FA. The flow rate was set to 0.6 mL/min and the gradient used was as follows:

- 0 minutes : 60% B
- 0.5 minutes: 60% B
- 8 minutes: 100% B
- 10.10 minutes: 60% B
- 12 minutes: 60% B

Reserpine (0.5 µM in 0.2% FA) was used as a lock spray reference compound to compensate for any drift. Data were processed using Micromass MarkerLynx Applications Manager (Waters Ltd, Hertfordshire).

4.2.9 Multivariate analysis

Principal component analysis (PCA) and partial least squares discriminant analysis (PLS-DA) were performed in order to analyse the LC-MS/MS data using SIMCA-P 11.0 (Umetrics, Umea, Sweden).

4.2.10 Glycogen assay

A glycogen assay kit was used in order to determine relative glycogen levels in the livers of WT and Nrf2 KO animals from study 2 according to the manufacturer's instructions. Briefly, 10 mg of liver tissue was homogenised in dH_2O and heated at 100 °C for 5 minutes. Samples were centrifuged (13000 rpm; 5 min) and the supernatant retained. Samples and glycogen standards were diluted as desired with hydrolysis buffer and samples were incubated at room temperature for 30 minutes. Reaction mix containing development buffer, development enzyme mix and OxiRed probe was added to each sample before they were incubated in the dark for 30 minutes at room temperature. Intensity was measured at 570 nm using the MRE^e plate reader (Dynex Technologies Limited, Worthing, West Sussex).

4.3 Results

4.3.1 The effect of CHO-R on body weight and liver weight

Body weight was recorded on each of the 28 days during both study 1 and 2 (figure 4.2). The weight of the control diet mice rose by a mean value of 1.4 g during study 1, while the weight increased by a mean value of only 0.2g in study 2. This reflects the fact that the animals used in study 2 were approximately 4 weeks older than those in study 1. Although the mean weight of the Nrf2 KO animals was slightly lower than the WT animals in both studies, the difference was not statistically significant. The CHO-R animals of both genotypes steadily lost weight for the first 7 days in both studies and then the weight remained constant until the end of the study. Weight was not statistically different between the WT and Nrf2 KO mice in the CHO-R groups.

At the end of study 2, liver weight was also recorded (figure 4.3). Liver weight and liver weight as a percentage of body weight was statistically significantly lower in the CHO-R Nrf2 KO animals when compared to control. Both were also lower in CHO-R WT animals when compared to control, however this did not reach significance. The weight of the liver of one of the WT control animals (WT ctrl 3) was only 64% of that of the other livers in the same group (0.73 g when compared to 1.21 ± 0.04 g). The spleen of this animal was noted to be enlarged, so an underlying condition may have contributed to the lower liver weight in this animal.

4.3.2 Histopathology

A summary of the histological analysis of livers from WT and Nrf2 KO fed a control or CHO-R diet in study 2 is detailed in tables 4.1 and 4.2 respectively. There were no consistent signs of liver injury in all animals within any one group, although some individual animals did show signs of liver damage. WT ctrl 3, the animal that was noted to have a reduced liver weight, was identified as having the most severe liver damage of all the mice thus providing further evidence of underlying disease. KO CHO-R 4 also showed signs of liver damage that was more severe than other animals within the group.

Glycogen was present in the livers of control diet mice but was largely absent from livers of mice fed a CHO-R diet. Within the control diet animal groups, two KO mice showed signs of glycogen depletion, while the three healthy WT control animals did not. The Oil-Red Orange stain did not provide any evidence of significant differences in hepatocellular fat content between mice based on diet or genotype.

Other organs including the lung, pancreas, kidney, adrenal gland and a cross section of the heart were also examined, with none of the organs exhibiting any significant histological differences.

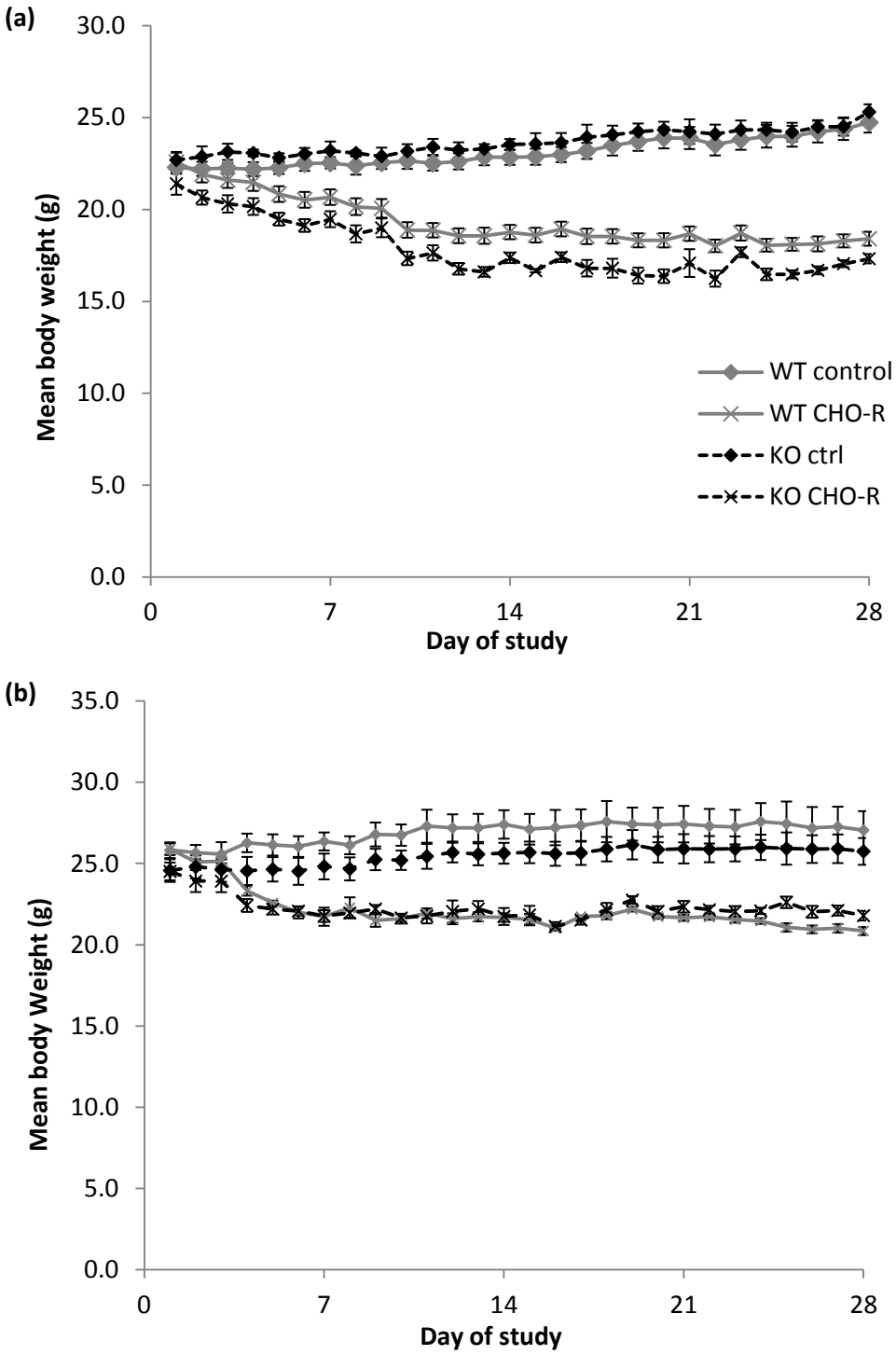

Figure 4.2: **Mean body weights of WT and Nrf2 mice fed a control or CHO-R diet for 4 weeks** (a) represents the weight of mice in study 1, while (b) represents the weight of mice in study 2. Error bars represent standard error of the mean.

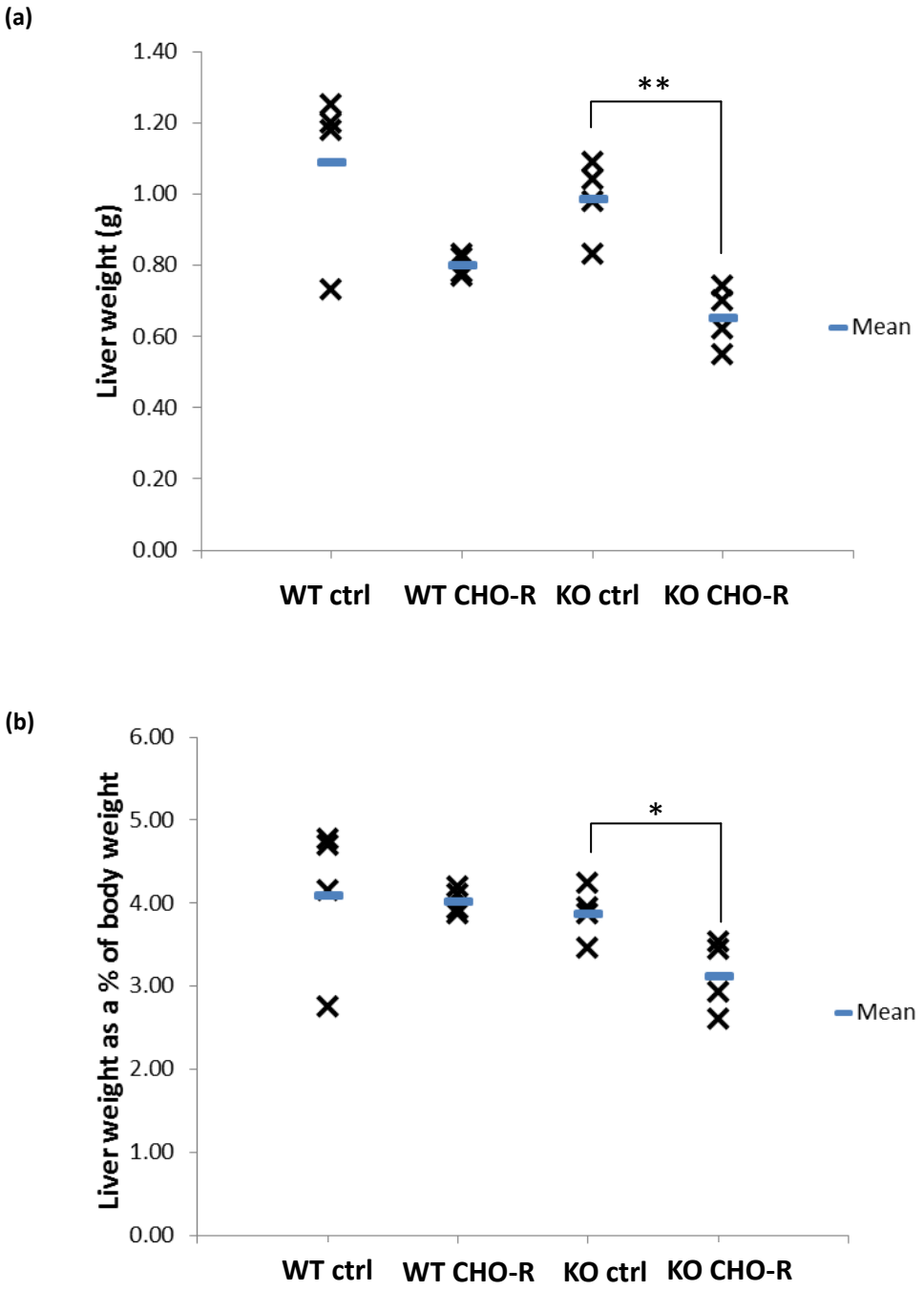

Figure 4.3: (a) Liver weight and (b) liver weight expressed as a percentage of body weight of WT and Nrf2 KO mice fed a control or carbohydrate restricted (CHO-R) diet for 4 weeks in study 2. An unpaired t-test was performed to determine statistical significance (*P < 0.05; **P < 0.01).

Table 4.1: A summary of the results from histopathological analysis of liver samples from WT and Nrf2 KO mice fed a control diet in study 2.

Mouse	Findings	PAS reaction	Fat stain	Comments
WT ctrl 1	Diffuse glycogen; no histological abnormality is recognised (NHAIR)	Diffuse glycogen	One to a few small fat droplets within hepatocytes (approx 30%).	
WT ctrl 2	Diffuse glycogen; NHAIR	Diffuse glycogen	Negative	
WT ctrl 3	Marked anisokaryosis; centrolobular hydropic swelling and most intense megalocytosis, bile duct hyperplasia; individual hepatocyte necrosis, small NL aggregates, dilated central veins (CV) with activated endothelial cells (EC) and focal adjacent LC aggregates	Patchy glycogen (mainly centrolobular); mitotic hepatocytes neg. [RVG: No fibrosis]	Negative	Cause for liver changes cannot be identified
WT ctrl 4	Diffuse glycogen; multiple small leukocyte aggregates (extramedullary haematopoiesis (EMH)?)	Diffuse glycogen	Hepatocytes negative, Ito (stellate) cells positive	
KO ctrl 1	Diffuse glycogen; moderate random mixed cellular (with EMH?) focal aggregates with occasional dying hepatocytes	Diffuse glycogen	Hepatocytes negative, scattered Ito (stellate) cells positive.	
KO ctrl 2	Diffuse glycogen; scattered leukocyte aggregates with necrotic hepatocytes	Diffuse glycogen (but in wide areas relatively low amount)	Negative	
KO ctrl 3	No glycogen; random small mixed cellular aggregates (EMH?)	Patchy glycogen, mainly individual cells	Most hepatocytes negative, scattered with several small cytoplasmic fat droplets	
KO ctrl 4	Diffuse glycogen; NHAIR	Diffuse glycogen	Some hepatocytes with small fat droplets, Ito (stellate) cells often positive	

Table 4.2: A summary of the results from histopathological analysis of liver samples from WT and Nrf2 KO mice fed a CHO-R diet in study 2.

Mouse	Findings	PAS reaction	Fat stain	Comments
WT CHO-R 1	No glycogen; hepatocytes reduced in size?; bile duct hyperplasia (+)?	No glycogen	Negative [small tissue fragment]	
WT CHO-R 2	No glycogen; hepatocytes reduced in size?; bile duct hyperplasia (+)?	Very low level of glycogen, mainly in zone 2 hepatocytes	Negative	
WT CHO-R 3	No glycogen; hepatocytes reduced in size?; multiple small leukocyte aggregates (EMH)	No glycogen	Negative	
WT CHO-R 4	No glycogen; hepatocytes reduced in size?; bile duct hyperplasia (+)?	Very low level of glycogen, mainly in zone 2 hepatocytes	Hepatocytes negative, Ito (stellate) cells positive	
KO CHO-R 1	No glycogen; hepatocytes reduced in size?; multiple small leukocyte aggregates (EMH?)	No glycogen	Negative	
KO CHO-R 2	No glycogen; hepatocytes reduced in size?; moderate multifocal random, relatively small aggregates of mixed cellular (LC, NL, macrophages) infiltration; bile duct hyperplasia (+)?	No glycogen	Hepatocytes negative, Ito (stellate) cells positive	
KO CHO-R 3	No glycogen; random small mixed cellular aggregates (EMH?)	Patchy areas of cells with glycogen, majority negative	Hepatocytes negative, some Ito (stellate) cells positive?	
KO CHO-R 4	No glycogen; NL between hepatic cords; small aggregates, disseminated, moderate; individual hepatocyte death (apoptosis?), also (predominantly) centrolobular (?); bile duct hyperplasia (+)?; increased anisokaryosis	No glycogen (some positive macrophages) [RVG: No fibrosis]	Most hepatocytes with variable amounts of small fat droplets	Cause for liver changes cannot be identified

4.3.3 The effect of CHO-R on hepatic glutathione levels in WT and Nrf2 KO mice

In order to investigate the hepatic glutathione status of animals fed a CHO-R diet, GSH and GSSG levels were measured by LC-MS/MS in the livers of mice from both study 1 and 2. CHO-R resulted in GSH-depletion in both genotypes at a statistically significant level ($P < 0.001$) with 30% depletion in WT and 50% depletion in Nrf2 KO animals (figure 4.4). Mean GSH levels in the livers of Nrf2 KO mice were 14% lower than that in WT animals, but this difference was not statistically significant. There were no differences in GSSG levels between any of the groups, and the mean GSH/GSSG was >10 for all treatment groups.

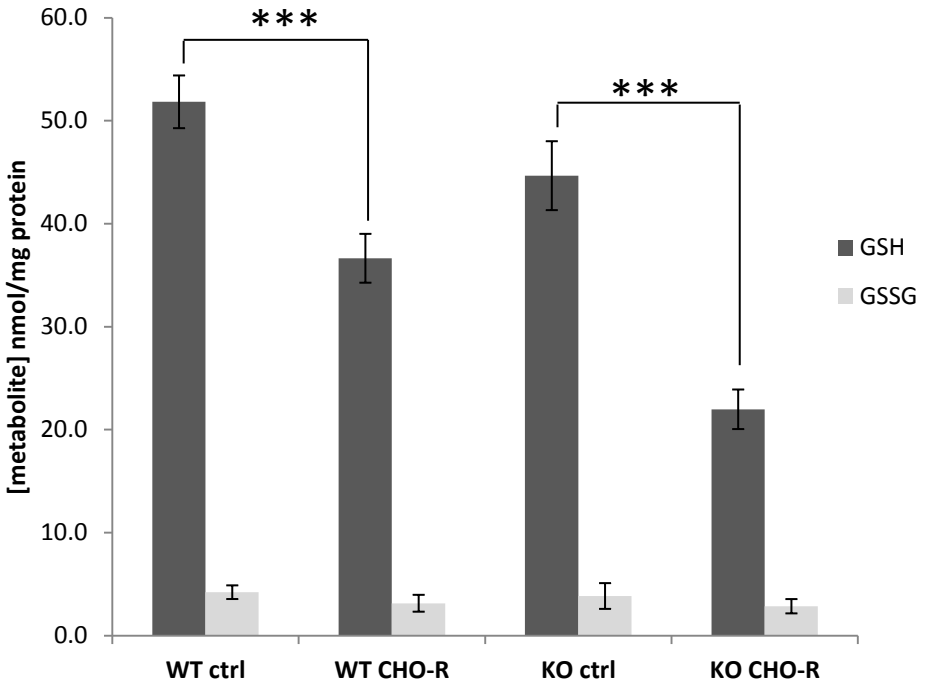

Figure 4.4: The effect of carbohydrate restriction (CHO-R) on levels of reduced (GSH) and oxidised (GSSG) glutathione in livers of WT and Nrf2 KO male mice (n=7). Glutathione levels were determined by LC-MS/MS and normalised to protein concentration. Statistical analysis was performed with normal data analysed by an unpaired t-test and non-normal data analysed by a Mann Whitney U-test (***$P < 0.001$).

4.3.4 Relative actin expression in mice fed a control or CHO-R diet

Actin was tested as a protein loading control for immunoblotting, however relative actin expression was statistically significantly lower in WT animals fed a CHO-R diet when compared to those fed a control diet. A Ponceau stain showed that total protein loading was equal across the samples (figure 4.5). Consequently the Ponceau total protein stain was used in subsequent experiments in the study to show consistent protein loading.

4.3.5 CHO-R results in Nrf2 activation

Given that a CHO-R diet resulted in glutathione depletion in the livers of mice, the effect of CHO-R on Nrf2 activation was also investigated., Western immunoblotting for NQO1 was performed on liver homogenates from mice in both study 1 (figure 4.6) and 2 (figure 4.7). WT control mouse 3 in study 2 showed high expression of NQO1 when compared to all other WT control animals. This is likely to be reflective of the underlying disease identified by histological analysis, and consequently the animal was excluded from statistical analysis performed on the combined data from both studies. NQO1 protein expression was found to be induced 2.6-fold in CHO-R animals when compared to those fed a control diet ($P < 0.01$; figure 4.8) indicating that CHO-R induces Nrf2 expression in the livers of mice. NQO1 expression was not induced in the livers of Nrf2 KO mice fed a CHO-R diet.

4.3.6 GCLC protein expression is not statistically altered by CHO-R

GCLC is the catalytic subunit of the enzyme that catalyses the rate limiting step in glutathione synthesis. Expression of the GCLC is also known to be regulated, in part, by Nrf2. Consequently, the expression levels of GCLC was also investigated in samples from study 1 (figure 4.6) and study 2 (figure 4.7). Statistical analysis of GCLC protein levels in livers of mice from both studies combined showed that while CHO-R reduced the mean level of GCLC expression in both WT and Nrf2 KO animals, the difference was not significant (figure 4.8).

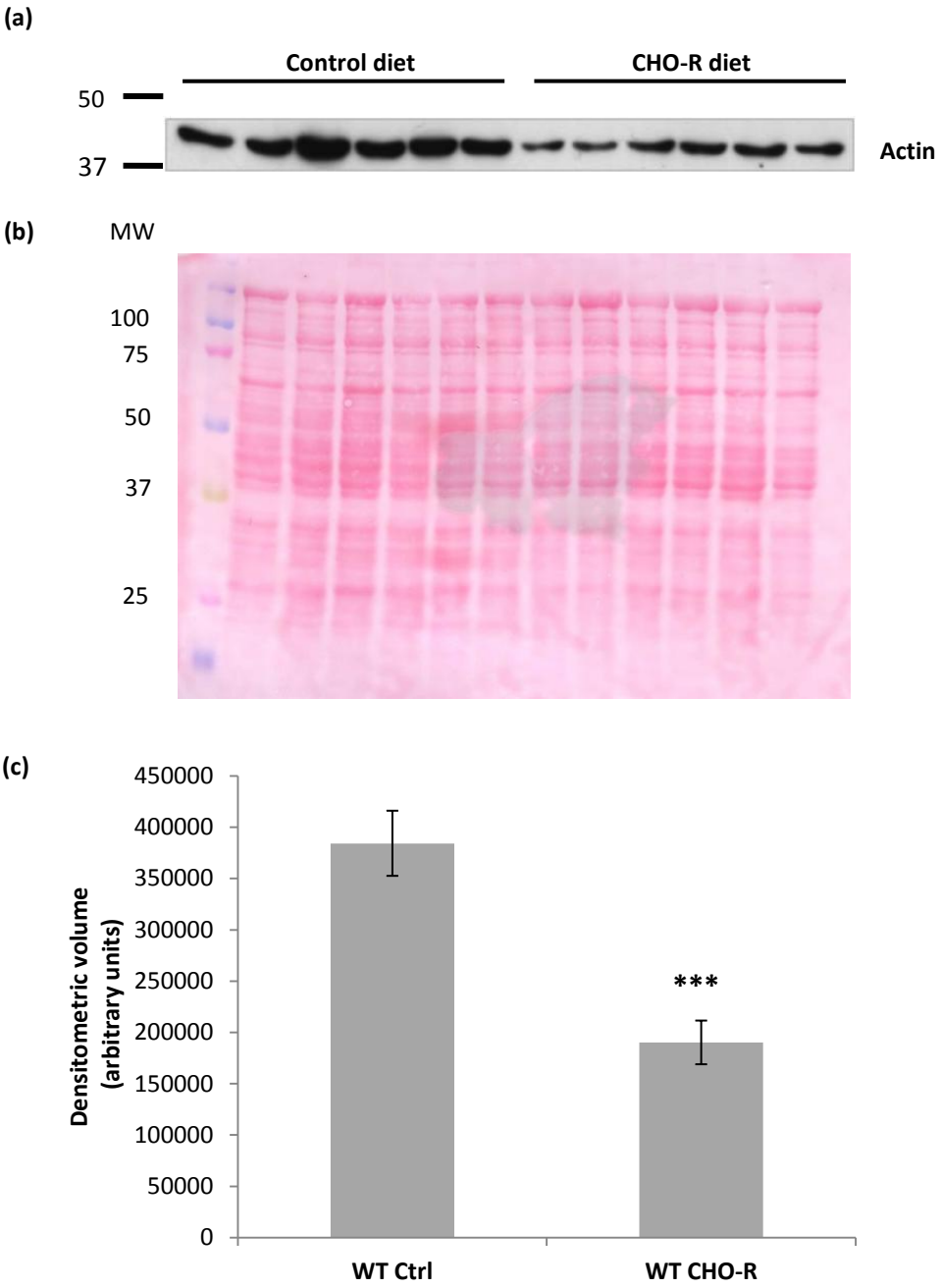

Figure 4.5: Western immunoblot of actin in livers from WT mice fed a control or carbohydrate restricted (CHO-R) diet. (a) Immunoblot for actin (n=6). The molecular mass of actin is approximately 42 kDa. (b) Ponceau protein stain of the transfer membrane. (c) Densitometric analysis of the immunoblots. An unpaired t-test was performed in order to determine statistical significance (***P < 0.001).

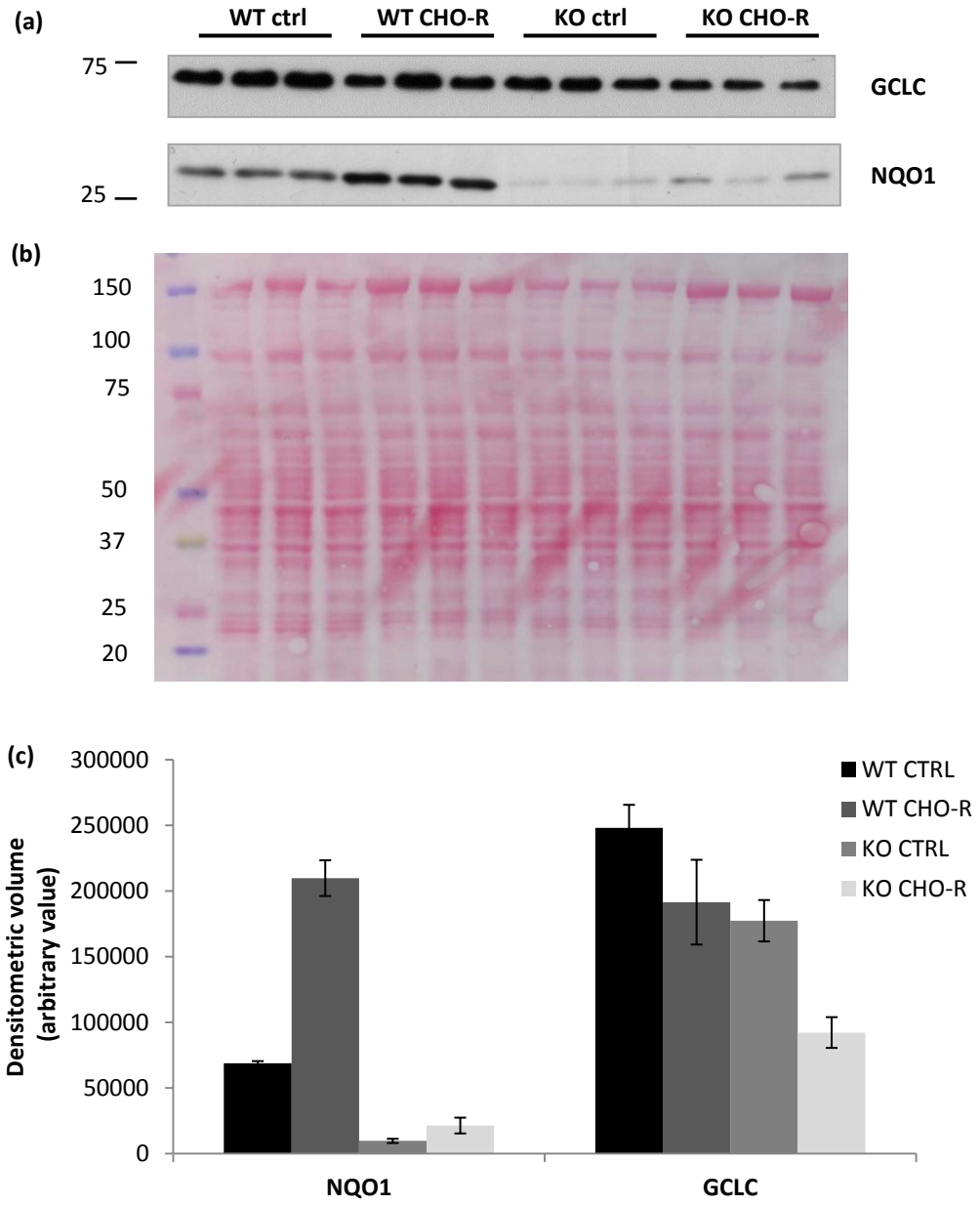

Figure 4.6: Western immunoblots of NQO1 and GCLC in livers from WT and Nrf2 KO mice fed a control or carbohydrate restricted (CHO-R) diet in study 1. (a) Immunoblots for NQO1 and GCLC in livers of the mice (n=3). The molecular mass of NQO1 is approximately 31 kDa, while the molecular mass of GCLC is approximately 73 kDa. (b) Ponceau protein stain of the transfer membrane, both proteins were run on the same membrane. (c) Densitometric analysis of the immunoblots.

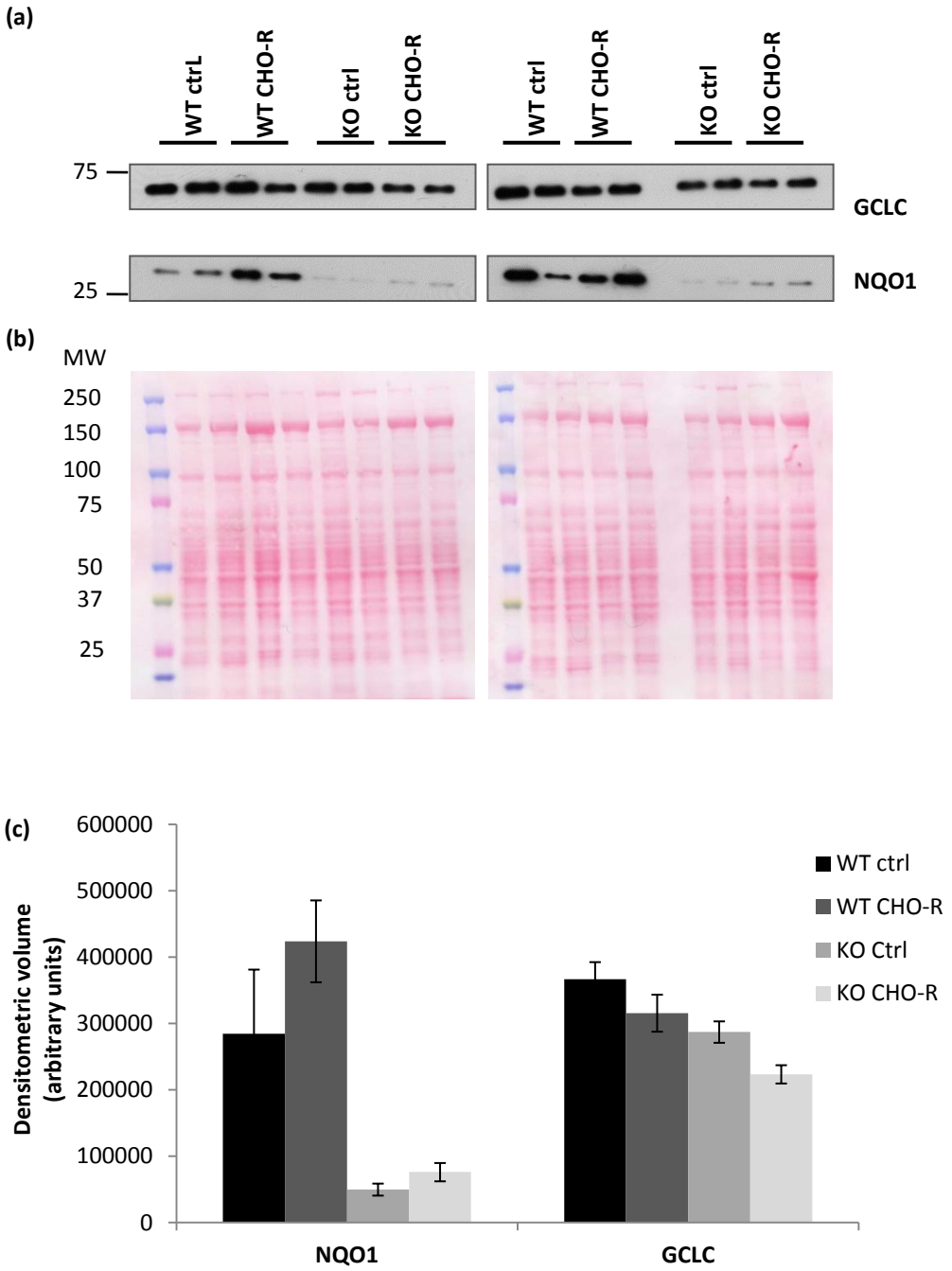

Figure 4.7: Western immunoblots of NQO1 and GCLC in livers from WT and Nrf2 KO mice fed a control or carbohydrate restricted (CHO-R) diet in study 2. (a) Immunoblots for NQO1 and GCLC in livers of the mice (n=4). The molecular mass of NQO1 is approximately 31 kDa, while the molecular mass of GCLC is approximately 73 kDa. (b) Ponceau protein stains of the transfer membranes, both proteins were run on the same membrane. (c) Densitometric analysis of the immunoblots

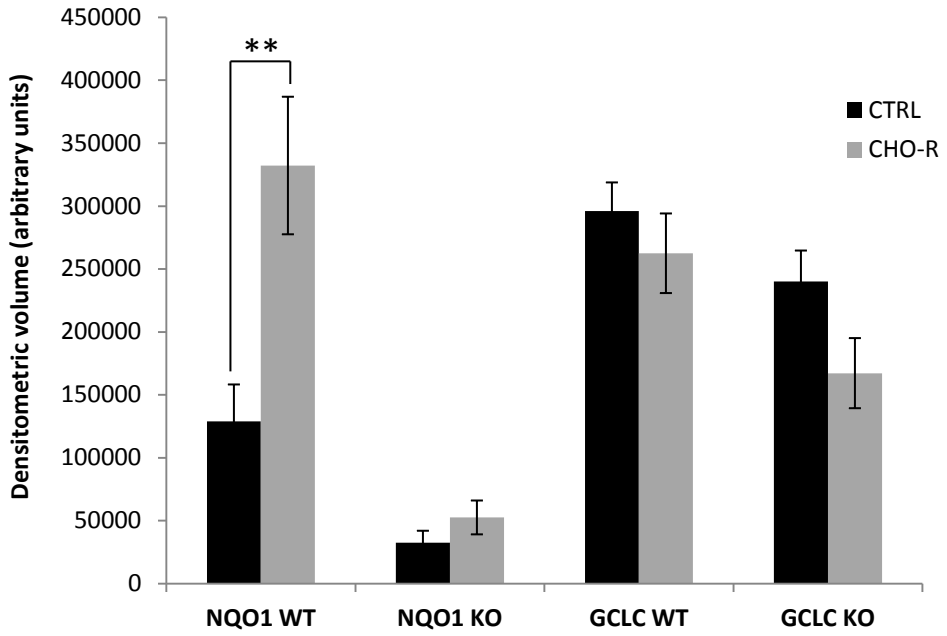

Figure 4.8: Combined statistical analysis of densitometric data from western immunoblots of NQO1 and GCLC in livers from WT and Nrf2 KO mice fed a control or carbohydrate restricted (CHO-R) diet in study 1 and 2 (n=7). WT control 3 from study 2 was excluded from the analysis because of an underlying liver condition as identified by histopathology, therefore n=6 for the WT control group. Normal data were analysed by an unpaired t-test, while non-normal data were analysed by a Mann Whitney U-test (**P < 0.01).

4.3.7 ACL protein expression in CHO-R mice

The effect of CHO-R restriction on hepatic ACL expression was determined by western immunoblotting in order to investigate the impact of the diet on protein expression of enzymes in the fatty acid synthesis pathway. Immunoblotting was performed on samples from livers of WT and Nrf2 KO mice fed a control or CHO-R diet in study 1 (figure 4.9) and study 2 (figure 4.10). Analysis of the combined data (figure 4.11) showed that carbohydrate restriction reduced ACL expression in Nrf2 KO animals by 36.4% at a statistically significant level ($P < 0.001$). Levels of ACL were also reduced by 17.8% in livers of WT animals but the difference was not statistically significant. In line with data from chapter 2 of this thesis, ACL was also found to be expressed at a level that was 49.0% higher in Nrf2 KO animals when compared to WT ($P < 0.001$).

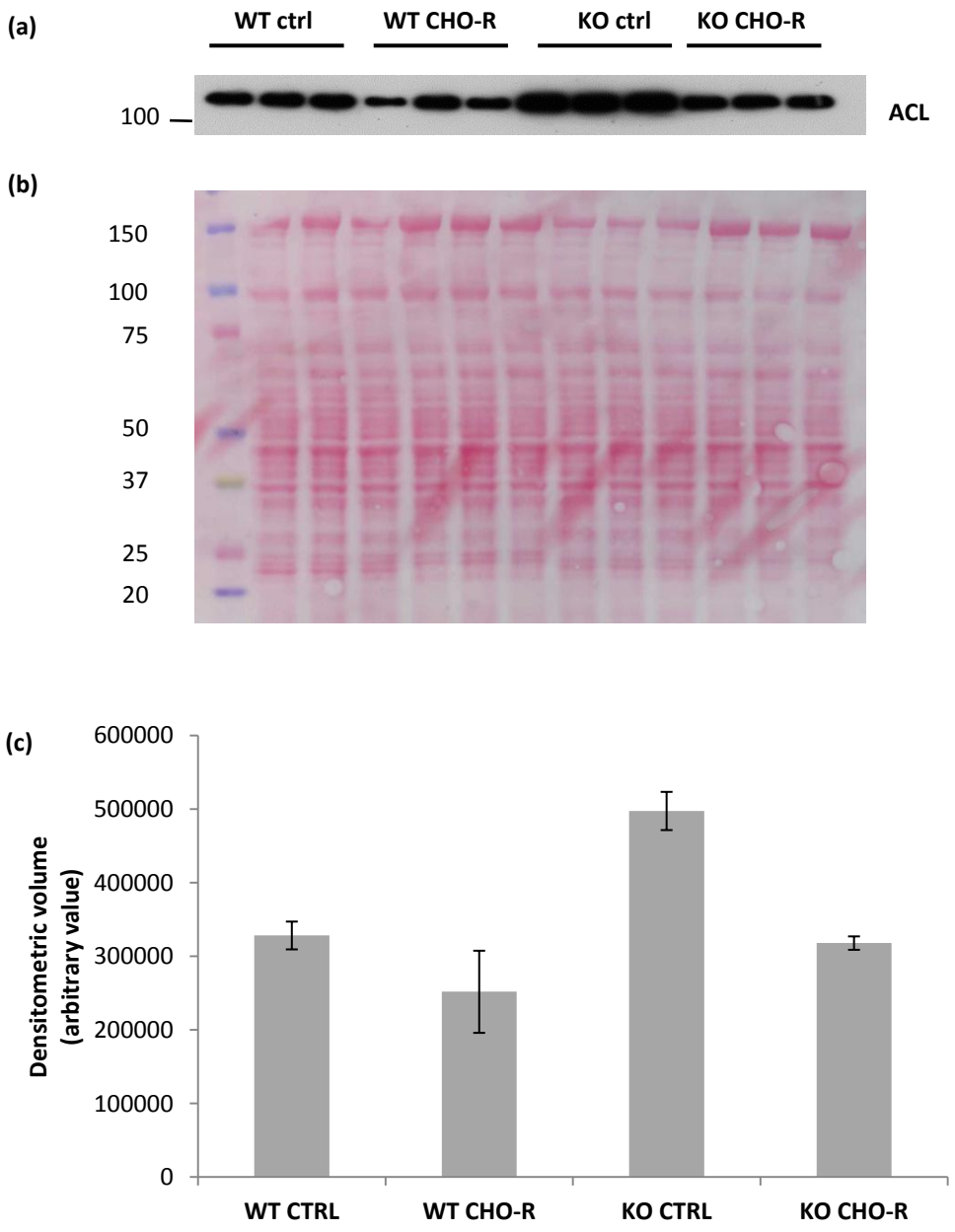

Figure 4.9: Western immunoblot of ACL in livers from WT and Nrf2 KO mice fed a control or carbohydrate restricted (CHO-R) diet in study 1. (a) Immunoblot for ACL in livers of the mice (n=3). The molecular mass of ACL is approximately 120 kDa. (b) Ponceau protein stain of the transfer membrane. (c) Densitometric analysis of the immunoblot.

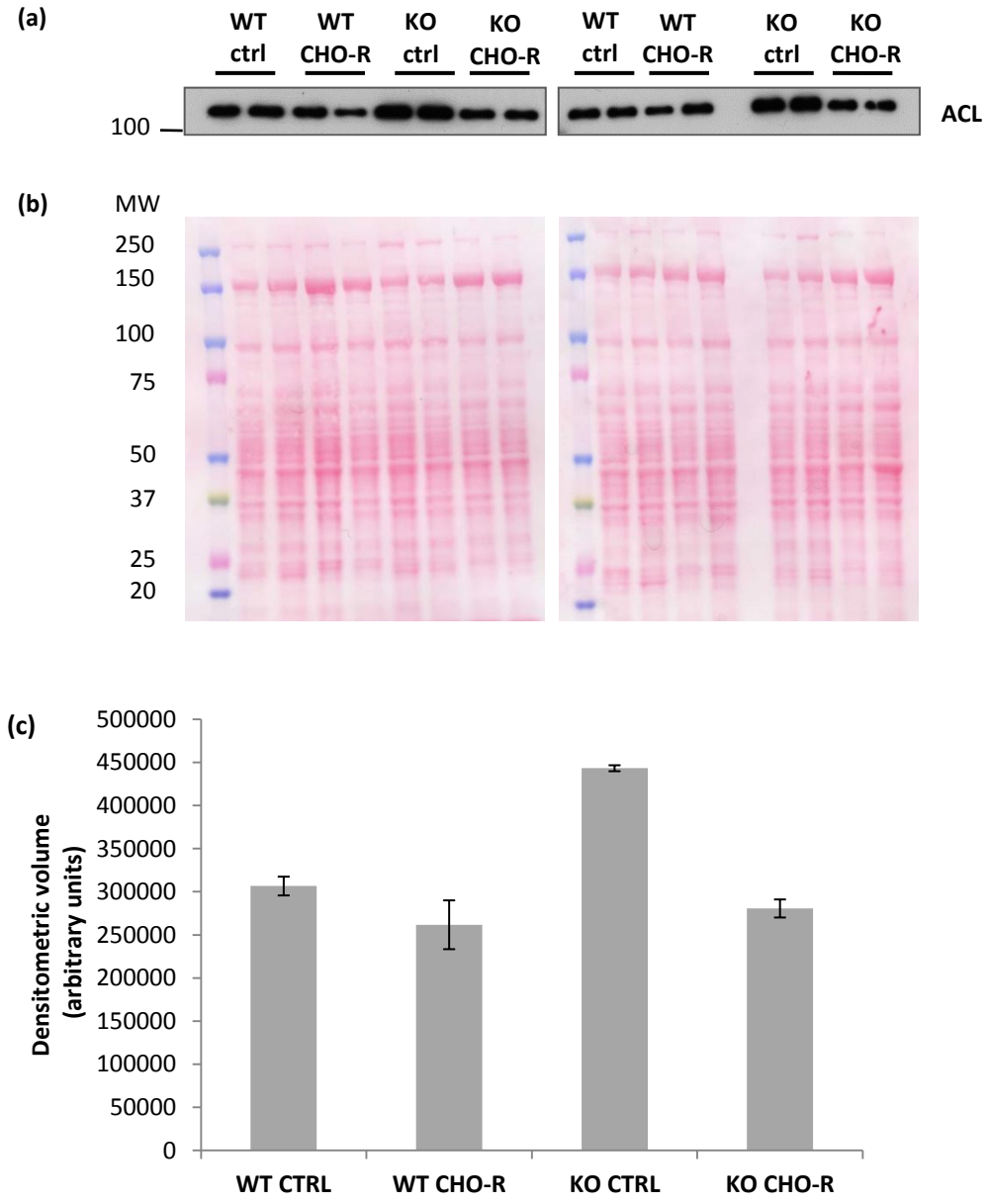

Figure 4.10: Western immunoblot of ACL in livers from WT and Nrf2 KO mice fed a control or carbohydrate restricted (CHO-R) diet in study 2. (a) Immunoblot for ACL in livers of the mice (n=4). The molecular mass of ACL is approximately 120 kDa. (b) Ponceau protein stains of the transfer membranes. (c) Densitometric analysis of the immunoblot.

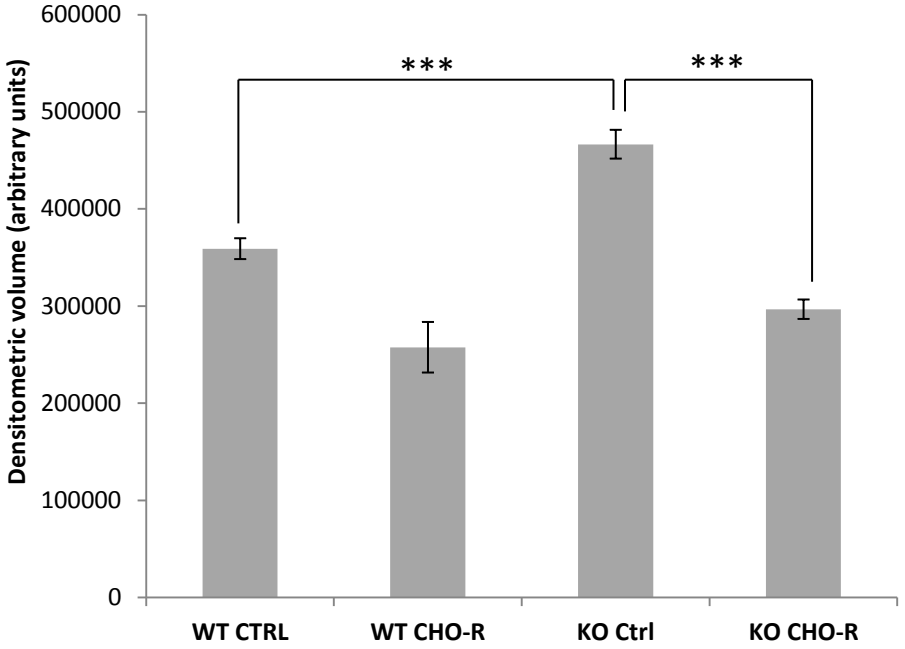

Figure 4.11: Combined statistical analysis of densitometric data from western immunoblots of ACL in livers from WT and Nrf2 KO mice fed a control or carbohydrate restricted (CHO-R) diet in study 1 and 2 (n=7). WT control 3 from study 2 was excluded from the analysis because of an underlying liver condition as identified by histopathology, therefore n=6 for the WT control group. Normal data were analysed by an unpaired t-test, while non-normal data were analysed by a Mann Whitney U-test (***P < 0.001).

4.3.8 GC-FID analysis of fatty acids

GC-FID analysis was performed in order to determine the relative levels of fatty acids in WT and Nrf2 KO mice fed a control or CHO-R diet. Prior to being run on the GC-FID, fatty acids were derivatised to yield fatty acid methyl esters (FAMEs). The peaks generated from the analysis were integrated and normalised to an internal standard, D-25 tridecanoic acid, and levels of each fatty acid detected were expressed as a percentage of total fatty acids within that sample. Peaks were assigned based on retention time and relative concentration using a FAME standard spectra, an example of which is given in figure 4.12.

A list of the 20 (study 1) and 19 (study 2) most abundant fatty acids that were detected are summarised in table 4.3. 16 fatty acids were assigned based on the FAME standard spectra, however 7 peaks could not be identified. 3 cholesterol esters were also detected in study 1. Figures 4.13 and 4.14 show the relative levels of fatty acids detected in livers of mice in study 1 and study 2 respectively.

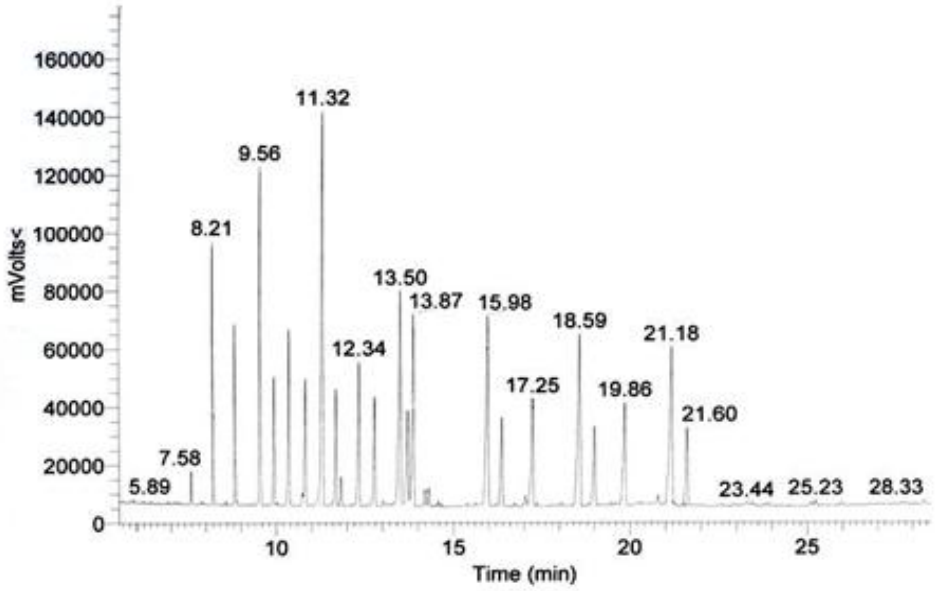

Figure 4.12: A typical FAME standard spectra. Each peak represents a different fatty acid. The retention time of known peaks in the FAME standard spectra was used to identify fatty acids within the samples.

14 of the fatty acids were detected in both study 1 and 2 and differences in these fatty acids were analysed for statistical significance. In the control diet group (figure 4.15), 8/14 fatty acids had mean levels that were higher in Nrf2 KO animals when compared to their WT counterparts, however levels of only one of the fatty acids, pentadecanoic acid (C15:1), was statistically significantly different ($P<0.05$). 5/14 fatty acids were detected at lower levels in Nrf2 KO animals and this difference was significant ($P<0.05$) for stearic acid (C18:0) and lignoceric acid (C24:0). It should be noted that the statistical analysis for C18:0 is based on results of study 2 as it was not detected in Nrf2 KO livers of either diet group in study 1.

In CHO-R animals, mean levels of 8/14 fatty acids were also detected as being higher in Nrf2 KO animals (figure 4.16), with oleic acid (C18:1; $P<0.05$), linoleic acid (C18:2; $P<0.05$) and α-linoleic acid (C18:3; $P<0.01$) significantly different. 6/14 fatty acids had levels that were, on average, lower in Nrf2 KO animals, but only C18:0 was statistically significant ($P<0.01$).

Table 4.3: Fatty acids detected by GC-FID analysis. Peaks were assigned based on retention time and comparison to previously assigned FAME standard peaks.

Peak number (run 1)	Peak number (run 2)	Fatty acid	Name
1		C11:0	Undecylic acid
2	1		Internal standard
	2		not identified
3		C14:0	Myristic acid
	3		not identified
4		C15:1	Pentadecenoic acid
5	4	C16:0	Palmitic acid
6	5	C17:0	Margaric acid
7	6	C18:0	Stearic acid
8	7	C18:1	Oleic acid
	8		not identified
9	9	C18:2	Linoleic acid
	10		not identified
10	11	C18:3	α-linoleic acid
11	12	C20:0	Arachidic acid
	13		not identified
12	14	C20:2	Eicosadienoic acid
13	15	C20:3	Eicosatrienoic acid
14	16	C20:4	Arachidonic acid
15	17	C23:0	Tricosylic acid
	18		not identified
16	19	C24:0	Lignoceric acid
17	20	C24:1	Nervonic acid
18			not identified
19			Cholesterol ester
20			Cholesterol ester
21			Cholesterol ester

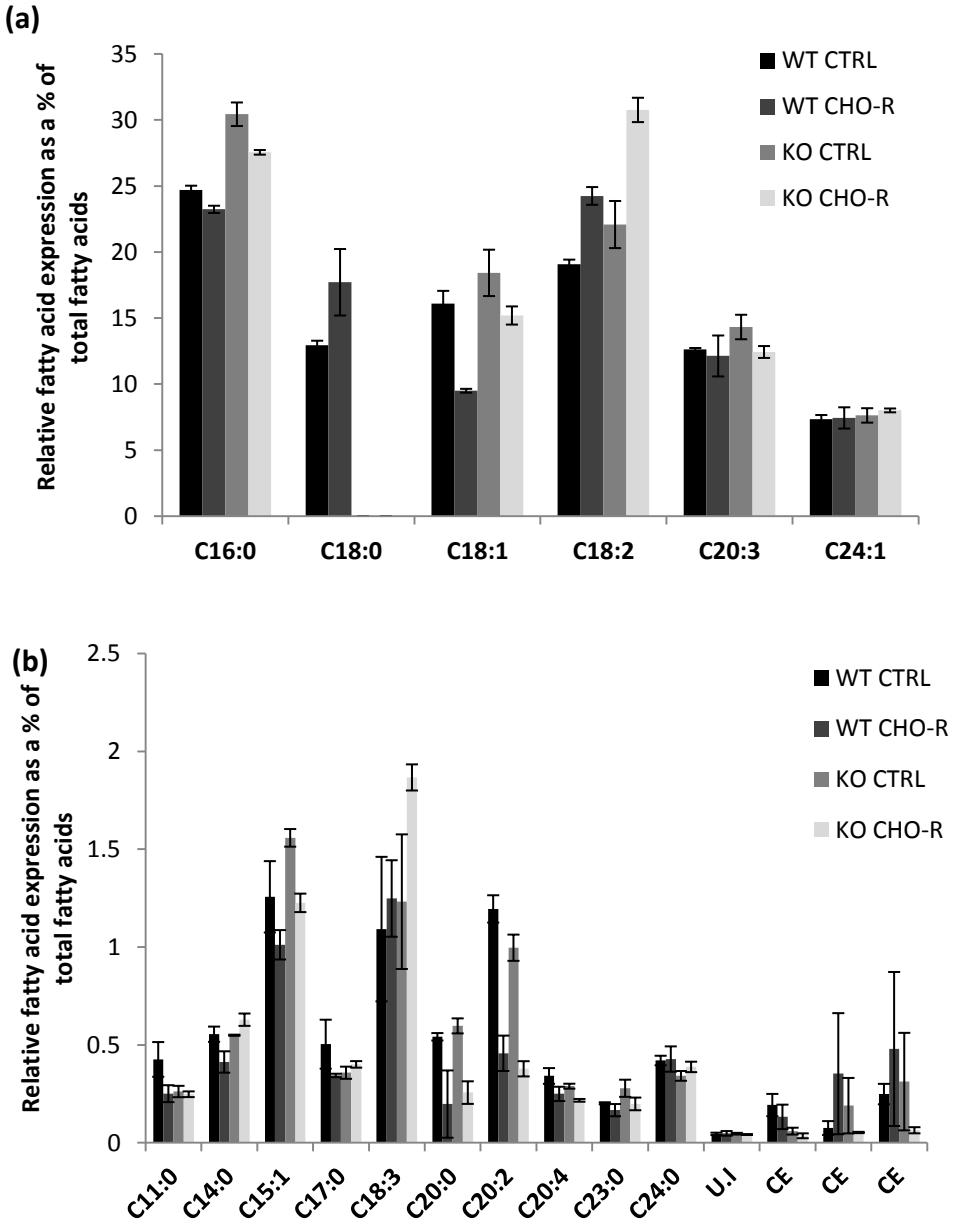

Figure 4.13: Relative levels of fatty acids detected by GC-FID analysis of livers from WT and Nrf2 KO mice fed a control or carbohydrate-restricted (CHO-R) diet in study 1. The relative peak areas were normalised to an internal standard (D-25 tridecanoic acid) and expressed as a % of total fatty acids. (a) shows the 6 fatty acids that each make up more than 5% of the total fatty acids detected while (b) shows the 14 less abundant fatty acids. Error bars show standard error of the mean (n=3). U.I. = unidentified; CE = cholesterol ester.

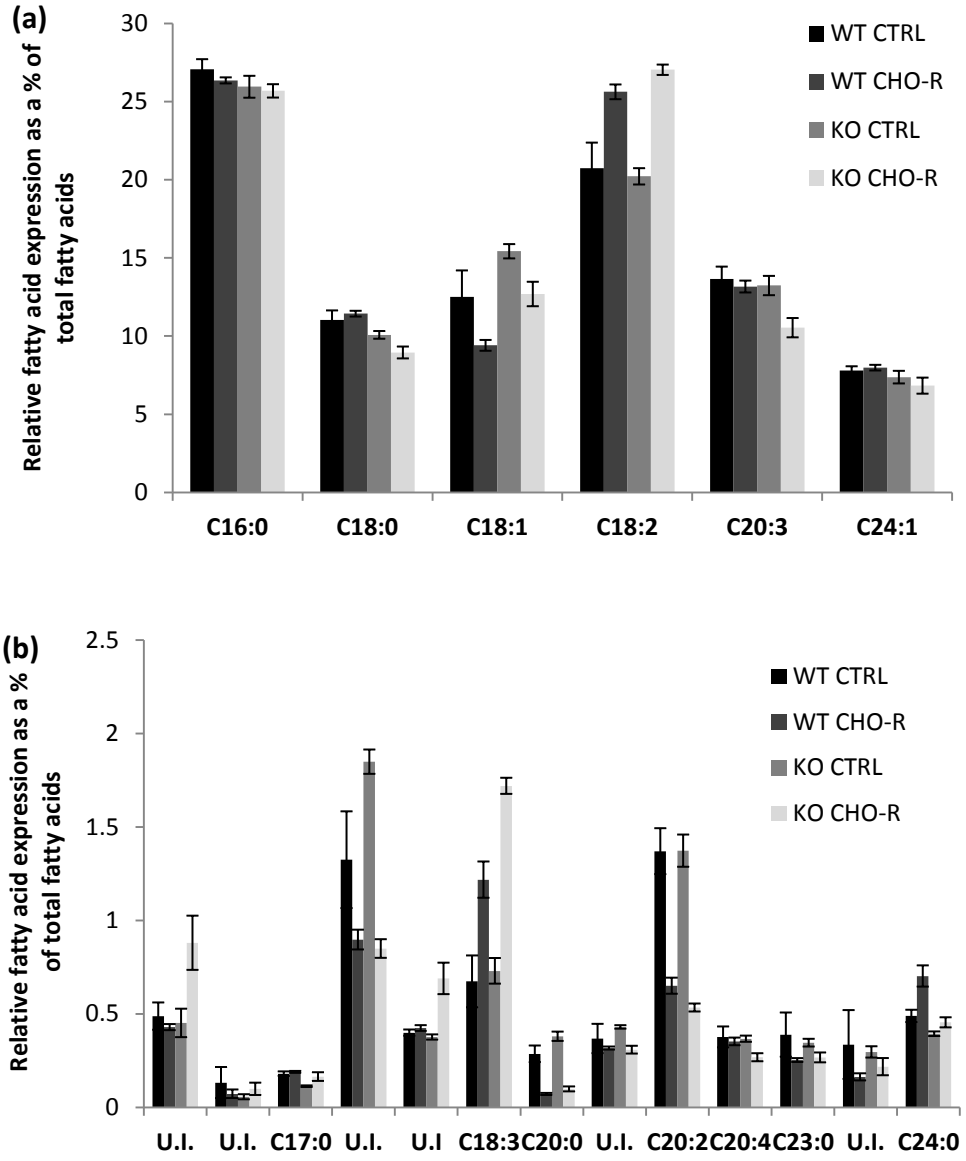

Figure 4.14: Relative levels of fatty acids detected by GC-FID analysis of livers from WT and Nrf2 KO mice fed a control or carbohydrate-restricted (CHO-R) diet in study 2.The relative peak areas were normalised to an internal standard (D-25 tridecanoic acid) and expressed as a % of total fatty acids. (a) shows the 6 fatty acids that each make up more than 5% of the total fatty acids detected while (b) shows the 13 less abundant fatty acids. Error bars show standard error of the mean (n=3). U.I. = unidentified.

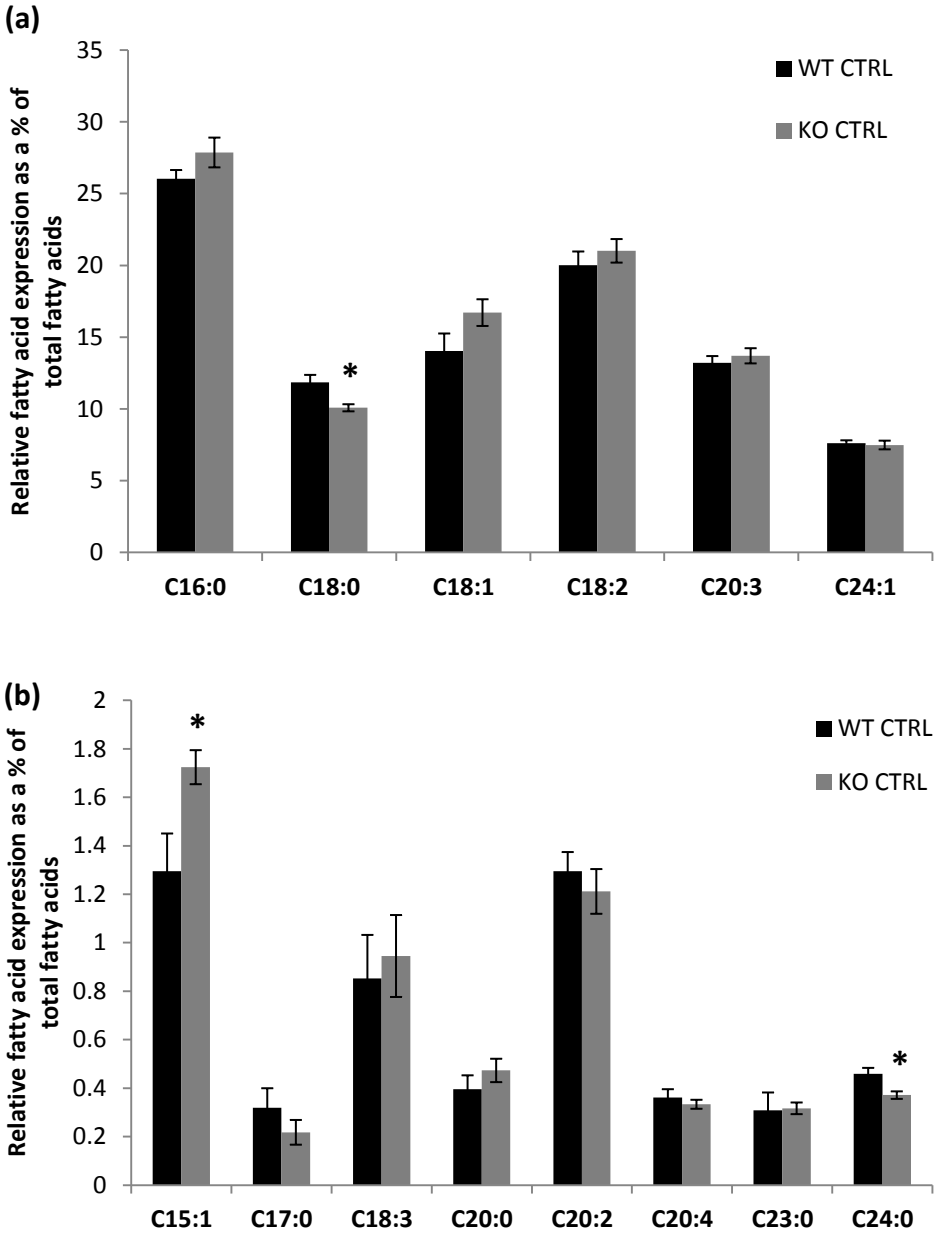

Figure 4.15: Relative levels of fatty acids in livers of WT and Nrf2 KO mice fed a control diet detected in both study 1 and 2. The relative peak areas were normalised to an internal standard (D-25 tridecanoic acid) and expressed as a % of total fatty acids. (a) Shows the six most abundant fatty acids detected, while (b) shows the eight less abundant fatty acids. Error bars show standard error of the mean (n=7). Statistical analysis was performed with normal data analysed by an unpaired t-test and non-normal data analysed by a Mann Whitney U test. *P<0.05.

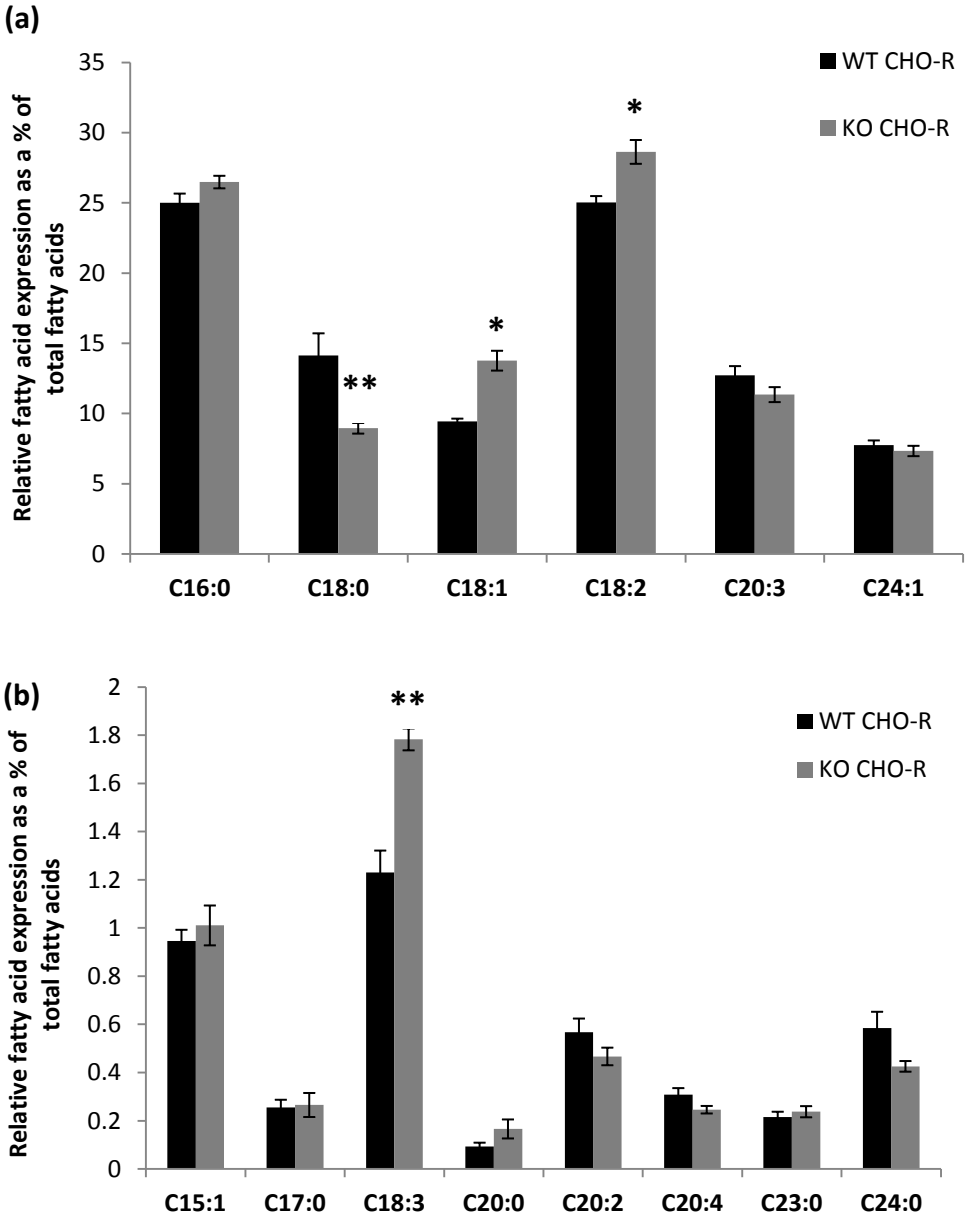

Figure 4.16: Relative levels of fatty acids in livers of WT and Nrf2 KO mice fed a CHO-R diet detected in both study 1 and 2. The relative peak areas were normalised to an internal standard (D-25 tridecanoic acid) and expressed as a % of total fatty acids. (a) Shows the six most abundant fatty acids detected, while (b) shows the eight less abundant fatty acids. Error bars show standard error of the mean (n=7). Statistical analysis was performed with normal data analysed by an unpaired t-test and non-normal data analysed by a Mann Whitney U test (*P<0.05; **P<0.01).

4.3.9 LC-MS/MS lipidomic analysis

LC-MS/MS analysis was also performed on extracts from livers of mice in study 1 in order to give a more comprehensive picture of the hepatic lipid profile of the animals. PCA was used to analyse the data. PLS-DA is a method by which components from PCA can be rotated in order to achieve maximum separation between classes, and to identify the components that account for the separation. Q2 and R2 are used in order to assess the validity of the model. A high Q2 value indicates a good predictive model, while a low R2 value is indicative of high noise. In general for analysis of biological samples, Umetrics guidelines state that a good model would have R2 ≥ 0.5 and Q2 ≥ 0.4 (http://www.umetrics.com/simca).

PLS-DA of all data showed separation between animals fed a control and CHO-R diet in study 1 (Q2: 0.461; R2: 0.803) suggesting that the components of the model accounting for the most variation differ as a result of diet. Within the CHO-R group there was separation between WT and Nrf2 KO mice, while the genotypes were not separated in the control diet group (figure 4.17).

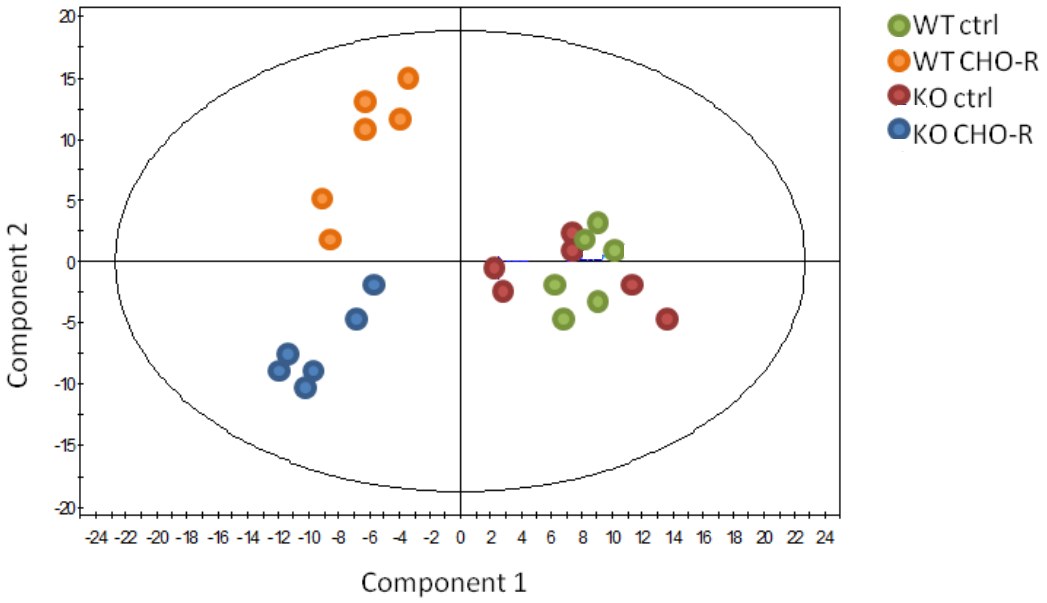

Figure 4.17: Partial least square discriminant analysis (PLS-DA) scores plots following LC-MS/MS analysis of livers from WT and Nrf2 KO mice fed a control or CHO-R diet for 4 weeks in study 1 (Q2: 0.461; R2: 0.803). All samples were run in duplicate (n=3).

PLS-DA focussing on selected groups of data (figure 4.18) showed separation between control diet WT and Nrf2 KO animals (Q2: 0.629; R2: 0.273), WT and Nrf2 KO animals fed a CHO-R diet (Q2: 0.791; R2: 0.341), WT animals fed a control or CHO-R diet (Q2: 0.89; R2: 0.319) and Nrf2 KO animals fed a control or CHO-R diet (Q2: 0.8741; R2: 0.342) in study 1. The Q2 and R2 values in each case suggest that while the analysis is valid as a predictive model, the data contains a high level of irrelevant information that does not contribute to the model.

Multivariate analysis of LC-MS/MS data suggests that there are differences in the lipid profiles of WT and Nrf2 KO animals both in control and CHO-R diet groups. However, the lipids that are responsible for the separation have yet to be identified as while PLS-DA lists the peaks that account for the variation between groups in a given model these peaks have not been assigned thus far.

4.3.10 Glycogen

Although histopathology results showed no consistent differences in WT and Nrf2 KO animals with respect to hepatic glycogen levels, there was some evidence of glycogen depletion in 2/4 Nrf2 KO control animals. Glucose can be stored intracellularly as glycogen or converted to pyruvate via glycolysis. Pyruvate is a precursor to acetyl CoA and is therefore important for the synthesis of fatty acids, as well as energy production via the tricarboxylic acid cycle. Consequently, there may be a link between the increase in fatty acid synthesis in Nrf2 KO animals and glycogen depletion.

A quantitative glycogen assay was used in order to determine whether there were any difference in glycogen levels in WT and Nrf2 KO mouse livers. The assay employs the enzyme glucoamylase, which hydrolyses the glycogen yielding glucose. Oxidation of the glucose and subsequent reaction with the OxiRed probe results in a proportional change in colour. A measurement of background glucose allows the relative concentration of glycogen across the samples to be determined.

Hepatic glycogen was depleted to levels that were not detectable in CHO-R animals regardless of genotype (data not shown). In animals fed a control diet, mean glycogen levels were lower in Nrf2 KO animals when compared to their WT counterparts; however this difference was not statistically significant (figure 4.19).

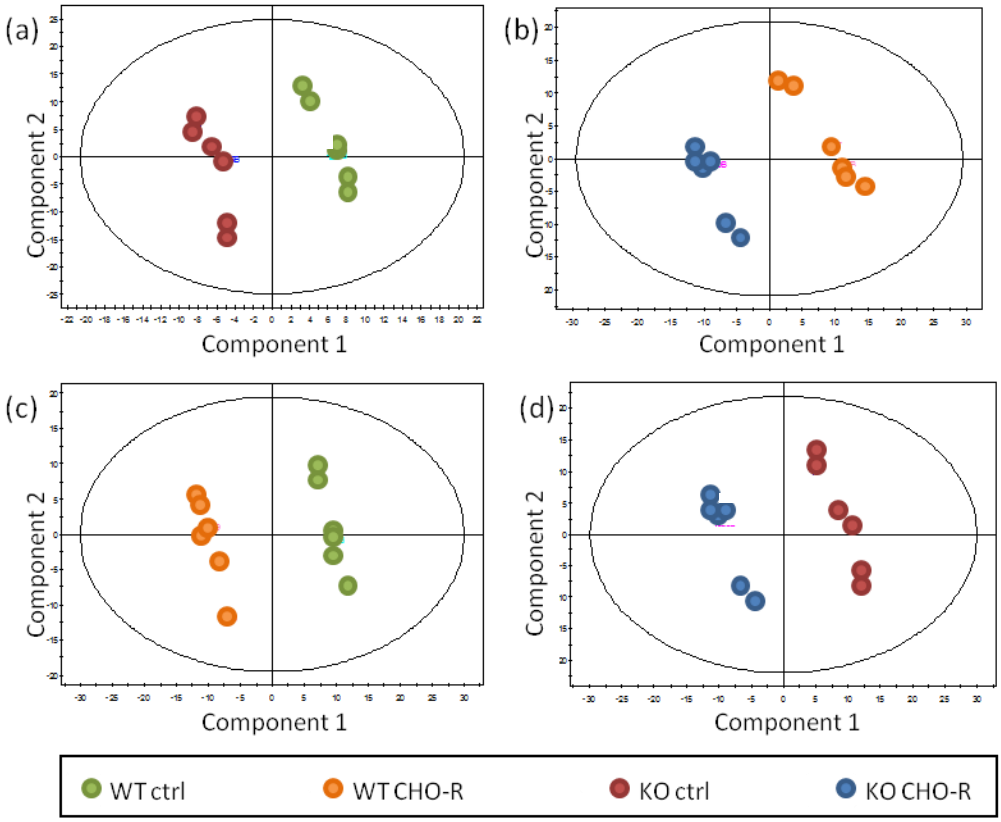

Figure 4.18: Partial least square discriminant analysis (PLS-DA) scores plots following LC-MS/MS analysis of livers from WT and Nrf2 KO mice fed a control or CHO-R diet for 4 weeks. (a) Plots WT v KO mice on the control diet (Q2: 0.629; R2: 0.273). (b) Plots WT v KO mice on the carbohydrate-restricted diet (Q2: 0.791; R2: 0.341). (c) Plots control diet v carbohydrate-restricted diet WT mice (Q2: 0.89; R2: 0.319). (d) Plots control diet v carbohydrate-restricted diet KO mice (Q2: 0.8741; R2: 0.342). All samples were run in duplicate (n=3).

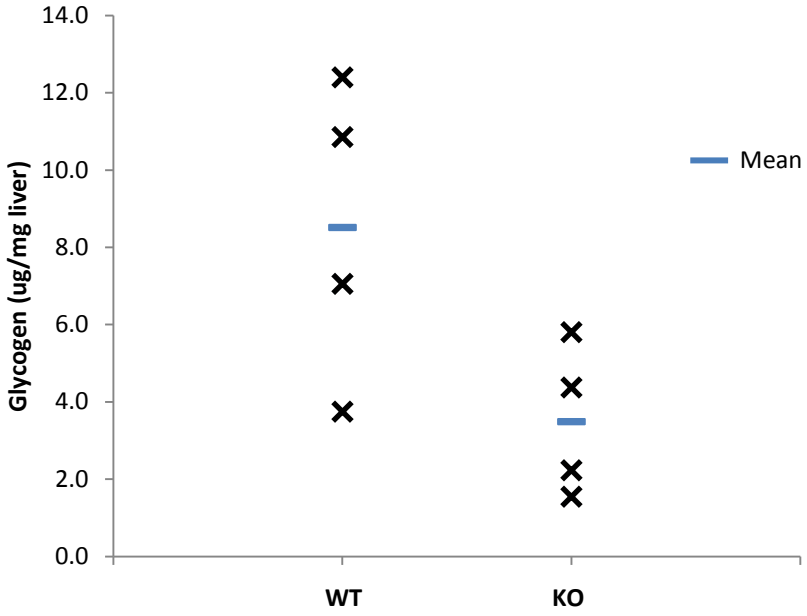

Figure 4.19: Glycogen levels in livers from WT and Nrf2 KO mice fed a control diet in study 2 (n=4). Values were determined by a colorimetric assay. Statistical analysis was performed using an unpaired t-test, with no statistical difference identified.

4.4 Discussion

Work described in chapter 2 of this thesis identified lipid metabolism as a process that is regulated by Nrf2. A number of proteins associated with lipid pathways, including enzymes important for fatty acid biosynthesis, were expressed at a higher level in the livers of Nrf2 KO mice when compared to WT animals suggesting that Nrf2 negatively regulates their expression. The function of Nrf2 in the regulation of lipid metabolism has only recently emerged and has yet to be comprehensively defined. The aim of this chapter was to contribute to the understanding of the role of Nrf2 in lipid homeostasis by characterising the hepatic lipid profile of WT and Nrf2 KO mice.

A CHO-R diet was also used as a tool in order to investigate how mice with differing Nrf2 genotypes responded to perturbations in lipid metabolism. Carbohydrate restriction has previously been shown to have an impact on the hepatic fatty acid profile (Bruss *et al.*, 2010; Forsythe *et al.*, 2008; Rojas *et al.*, 1993). Levels of ACL, an important enzyme for cytosolic fatty acid synthesis, were determined by western immunoblotting performed on samples from livers of WT and NRF2 KO mice. Analysis of the blots showed that CHO-R resulted in a decrease in the expression of the protein, thus confirming that carbohydrate restriction resulted in perturbations in fatty acid metabolism.

Preliminary results from experiments characterising the carbohydrate restricted mice showed that body weight and liver weight was reduced when compared to their control diet counterparts. The diet also resulted in hepatic glutathione depletion in both WT and Nrf2 KO animals. Nrf2 did offer protection against glutathione depletion as levels were depleted by 50% in Nrf2 KO animals but by only 30% in WT animals. However, the transcription factor could not completely prevent perturbations in glutathione homeostasis. NQO1 western blotting demonstrated that Nrf2 was activated by a CHO-R diet as NQO1 was induced in the livers of WT animals.

Given that iTRAQ analysis identified a significant role for Nrf2 in the regulation of the expression of fatty acid synthesis enzymes, fatty acid levels were the primary focus of the investigations into the hepatic lipid profiles of WT and Nrf2 KO mice. GC-FID served as a powerful tool for the targeted analysis of fatty acids by way of a method optimised for the detection of fatty acid methyl esters. Extracts from livers from WT and Nrf2 KO animals fed

a control or CHO-R diet were analysed by GC-FID, with 14 fatty acids detected in samples from both study 1 and study 2.

While there were small differences in levels of fatty acids in the livers of WT and Nrf2 KO mice, with a majority of fatty acids increased in Nrf2 KO animals, in most cases the differences were not statistically significant. The biological significance of small changes in relative fatty acid levels however, remains unclear. Interestingly, a number of the fatty acids that were differentially expressed were those with chains of 18 carbon atoms. C18:0 was expressed at a statistically higher level in WT animals fed either a control or CHO-R diet when compared to their Nrf2 KO counterparts, and was not detected at all in livers of Nrf2 KO animals in study 1 regardless of diet group. Conversely, in CHO-R Nrf2 KO mouse livers, C18:1, C18:2 and C18:3 were all detected at a statistically higher level when compared to those in WT animals.

C18:1 is synthesised from C18:0 in a reaction catalysed by the Δ9 desaturase enzyme, SCD, an enzyme that was shown by iTRAQ analysis to be up-regulated in the livers of Nrf2 KO mice. However, while C18:2 (linoleic acid) and C18:3 (linolenic acid) are also fatty acids with chains of 18 carbon atoms, they are essential fatty acids that cannot be synthesised by mammals, so levels of fatty acid synthesis enzymes cannot account for differences in levels of C18:2 or C18:3. Both fatty acids are precursors for the synthesis of longer chain fatty acids, including C20:4 (arachidonic acid) which is formed by the action of Δ5 and Δ6 desaturases as well as elongase enzymes. It may be that the synthesis of one of the desaturases required for modification of C18:2 and C18:3 is reduced as levels of SCD are increased, thus resulting in an increase in levels of the two fatty acids, however further work is required in order to investigate this hypothesis.

In order to give a more comprehensive view of lipid profiles of the livers of WT and Nrf2 KO mice, samples from study 1 were also analysed by LC-MS/MS. Although the small number of samples analysed was a limiting factor, PLS-DA revealed that while diet accounted for the most significant differences between mice in the study, there was also separation based on genotype. To date, the peaks that were identified as contributing most to the model have yet to be assigned and consequently the lipids with expression levels that differ in WT and Nrf2 KO have not been determined. However, the data do provide further evidence of a role for Nrf2 in the regulation of lipid metabolism and the lipids represented

by these peaks have the potential to provide further insight into the nature of this emerging relationship.

The work in this chapter has shown that there are differences in the hepatic lipid profiles of WT and Nrf2 KO mice, although the link between the up-regulation of fatty acid synthesis enzymes in Nrf2 KO animals and differences in fatty acid levels has yet to be defined. When animals are fed a CHO-R diet, a number of the differences in fatty acid levels between WT and Nrf2 KO mice are exacerbated. These results suggest that Nrf2 plays a role in regulating the response to the changes in lipid metabolism imposed by CHO-R, thus providing further evidence of a role for Nrf2 in the regulation of lipid homeostasis. Together, the studies emphasise the potential that lipids and other metabolites associated with lipid synthesis may have to serve as preclinical biomarkers of Nrf2 activity and suggest that a comprehensive lipidomic analysis of WT and Nrf2 KO mice could provide valuable insight.

Chapter 5 Investigating the proteomic profile of Nrf2 induction using the synthetic triterpenoid CDDO-Me

Contents

5.1 Introduction

The role of Nrf2 in the cytoprotective response is widely documented and has been highlighted by work previously described in this thesis. The identification of Nrf2 as a 'master regulator' of cell defence has generated considerable interest in its potential as a therapeutic target, with inducers undergoing clinical evaluation for cancer and chronic kidney disease (Pergola *et al.*, 2011; Speranza *et al.*, 2012; Tsao *et al.*, 2010). Pre-clinically, Nrf2 induction has also been investigated as a means of protection in *in vivo* models of inflammatory liver injury (Osburn *et al.*, 2008) and paracetamol-induced hepatotoxicity (Reisman *et al.*, 2009), and has shown promise as a chemopreventive strategy (Kwak *et al.*, 2010; Liby *et al.*, 2007).

The synthetic triterpenoid, 2-cyano-3,12-dioxooleana-1,9-dien-28-oic acid (CDDO) and its derivatives have been shown to be particularly potent inducers of Nrf2, resulting *in vitro* Nrf2 activation at nanomolar concentrations (Liby *et al.*, 2005). CDDO was originally synthesised for its anti-inflammatory properties through the modification of the A and C rings of oleanolic acid and was found to potently inhibit nitric oxide production (Honda *et al.*, 1998). Analogues including the methyl ester (CDDO-Me) and imidazole (CDDO-Im) derivatives were subsequently synthesised with the aim of further optimising potency and bioavailability (Honda *et al.*, 1999; Place *et al.*, 2003).

A link between Nrf2 induction and CDDO treatment was first identified in a study in which the compound was shown to potently induce the phase II response in mouse embryonic fibroblasts (Dinkova-Kostova *et al.*, 2005), a response that was abolished in Nrf2-null cells. Further *in vitro* work showed that CDDO and its derivatives induced Nrf2 protein levels as well as mRNA levels of the Nrf2 target gene haem oxygenase 1 (HO-1) (Liby *et al.*, 2005). Evidence of *in vivo* Nrf2 induction came from a study showing that the Nrf2-regulated gene, NQO1 was transcriptionally activated in the liver, lung and small intestine of CDDO-Im and CDDO-Me-treated mice after a single oral dose (Yates *et al.*, 2007).

As well as activation of the Nrf2 pathway, CDDO and its derivatives have been shown to modulate signalling associated with the PPAR-γ receptor (Wang *et al.*, 2000) and JAK-STAT pathway (Ahmad *et al.*, 2008; Liby *et al.*, 2006) and to inhibit both the constitutive and inducible activation of NF-κB (Ahmad *et al.*, 2006; Shishodia *et al.*, 2006; Yore *et al.*, 2006),

with some of these effects noted *in vitro* following triterpenoid treatment in the nanomolar range.

CDDO-Me, which is also known as bardoxolone methyl, is currently in Phase III clinical trials as an Nrf2 inducer for the treatment of chronic kidney disease (CKD) in patients with type II diabetes. However, the precise mechanism of action of CDDO-Me in CKD and the beneficial effects of Nrf2 inducers in other conditions remains to be defined. Given that activation of alternative pathways has also been postulated to account for the therapeutic properties of compounds known to activate Nrf2, it is important to define the precise effects of Nrf2 inducers at the protein level and to ascribe these effects as Nrf2 dependent or independent actions. Furthermore, in order to directly assess the efficacy of drugs such as CDDO-Me, biomarkers that specifically reflect Nrf2 activity at both the constitutive and induced level would be invaluable to define the level of human Nrf2 variability and its activation in response to chronic drug exposure.

There is consequently a clear imperative to generate a definitive list of Nrf2-regulated genes, since this may yield proteins or protein products that are potential biomarkers for such translational research. The Nrf2 KO mouse model provides a useful tool to define which of the changes in protein expression following CDDO-Me administration are Nrf2-dependent.

Differences in the basal hepatic profiles of WT and Nrf2 KO mice have been compared in chapter 2 of this thesis using iTRAQ-based proteomic analysis. Other studies have employed gene microarrays and targeted protein analysis in order to investigate constitutive differences and the effects of compounds identified as inducers of Nrf2, such as the isothiocynates, in the small intestine and liver (Hu *et al.*, 2006a; Hu *et al.*, 2006b; Thimmulappa *et al.*, 2002). However, to date no comprehensive comparative proteomic characterisation of liver tissue from WT and Nrf2 KO mice following administration of an Nrf2 inducer has been conducted.

The aim of the work described in this chapter was to treat WT and Nrf2 KO mice with the potent Nrf2 activator, CDDO-Me, in order to define the Nrf2-inducible hepatic proteome. The two methods employed alongside each other allows the full range of Nrf2 activity to be defined, from zero in the Nrf2 KO mouse model through to the maximum activation

following an acute dose of CDDO-Me. By the characterisation of protein profiles resulting from Nrf2 activation, it is hoped that biomarkers will be identified that have translational potential as tools to assess the importance of Nrf2 variability and activation in the human population.

5.2 Materials and Methods

5.2.1 Materials

The ectonucleoside triphosphate diphosphohydrolase 5 (ENTPD5) antibody was from Abcam (Cambridge, UK). The CYP2A5 antibody was kindly provided by Risto Juvonen (University of Eastern Finland, Kuopio, Finland). CDDO-Me was synthesised by Michael Wong (Department of Chemistry, University of Liverpool, UK). All other reagents were of analytical grade and quality and purchased from Sigma (Poole, Dorset, UK).

5.2.2 Animal studies

All mice were housed as described previously in this thesis. Male mice of 10-12 weeks of age were used for both the pilot study and subsequent proteomic study.

In order to determine a dose of CDDO-Me that would result in Nrf2 activation and subsequent protein expression after 24 hours, WT mice were given a single *i.p*. injection of CDDO-Me (0, 0.1, 0.3, 1, 3, or 10 mg/kg; n=2) in DMSO vehicle control (total volume 100 uL) at 10 am. At 24 h after dosing, the animals were culled by exposure to a rising concentration of CO_2 followed by cardiac puncture. Livers were removed, snap-frozen in liquid nitrogen and stored at -80°C.

For the proteomic study, livers were harvested from WT and Nrf2 KO mice dosed with 3mg/kg CDDO-Me or DMSO vehicle control (n=6), using the same protocol as described for the pilot study.

5.2.3 iTRAQ labelling and mass spectrometric analysis of liver homogenates

Liver samples (≈100 mg wet weight) were homogenised, labelled with iTRAQ isobaric tags and subjected to cation exchange as described in chapter 2 of this thesis. Fractions were desalted using a macroporous C_{18} column (Agilent, Santa Clara, California) on a Vision workstation and dried by centrifugation under vacuum (SpeedVac, Eppendorf). Samples were analysed on a Triple TOF 5600 mass spectrometer (AB Sciex) and were delivered into

the instrument by automated in-line liquid chromatography Eksigent NanoUltra cHiPLC System mounted with microfluidic trap and analytical column (15 cm × 75 µm) packed with ChromXP C_{18}-CL 3µm via a nano-electrospray source head and 10 µm inner diameter PicoTip (New Objective, Massachusetts, USA). The precolumn was washed for 10 min at 2 µL/min with 2%ACN/0.1% FA. A gradient from 2%ACN/0.1% FA (v/v) to 50% ACN/0.1% FA (v/v) in 90 min was applied at a flow rate of 300 nL/min.

The MS was operated in positive ion mode with survey scans of 250 ms, and with an MS/MS accumulation time of 100 ms for the 25 most intense ions (total cycle time 2.5 s). A threshold for triggering of MS/MS of 100 counts per second was used, together with dynamic exclusion for 12 seconds and rolling collision energy, adjusted for the use of iTRAQ reagent in the Analyst method. Information-dependent acquisition was powered by Analyst TF 1.5.1. software, using mass ranges of 400-1600 atomic mass units (amu) in MS and 100-1400 amu in MS/MS . The instrument was automatically calibrated after every fifth sample using a beta-galactosidase digest.

5.2.4 iTRAQ Protein Identification and Statistical Analyses

Liver samples from WT and Nrf2 KO mice treated with CDDO-Me or DMSO vehicle control (n=6), were analysed across four iTRAQ runs with a comparator pooled sample incorporated in each run for normalisation between iTRAQ experiments. Samples were randomised across the four runs to minimise label bias. Ratios for each iTRAQ label were obtained, using the common pool as the denominator (iTRAQ label 113). Data analysis was performed using ProteinPilot software (Version 3, Applied Biosystems, Warrington, UK). The data were analysed with MMTS as a fixed modification of cysteine and biological modifications. The SwissProt database was searched with a confidence interval of 95% and also screened in reverse to facilitate false discovery rate (FDR) analysis. Proteins identified from peptides with more than 95% confidence and a global FDR of less than 1% were included in the statistical analysis.

The *limma* package within the R programming environment (Team, 2005) allowed simultaneous comparisons between multiple treatments using design and contrast matrices. This open source software generates a linear regression model (lm) to facilitate the analysis of differential protein expression. Mean fold changes were calculated and

analysis conducted on the logged fold-change values. Unadjusted (raw) P values and P values following Benjamini-Hochberg (BH) correction for multiple testing were determined.

Nrf2- and CDDO-Me-dependent protein expression was defined by comparing Nrf2 KO control with WT control (group A), WT control with WT CDDO-Me (group B) and Nrf2 KO control with Nrf2 KO CDDO-Me mice (group C). The resulting protein lists for genetic disruption and pharmacological pathway activation were compared to identify changes that were both *common* and *unique* to Nrf2 and CDDO in a similar manner to the gene expression studies performed in Keap1 hepatocyte-specific KO and triterpenoid-treated mice reported by Yates et al. (2009).

5.2.5 Network analysis

Pathway analysis was performed as in chapter 2 of this thesis using MetaCore from GeneGo Inc. The software was used in order to identify the pathways most significantly differentially regulated in livers of WT and Nrf2 KO mice as well as in WT vehicle control and WT CDDO-Me-treated animals.

5.2.6 Immunoblotting for Nrf2 target proteins

Western immunoblotting for NQO1 and ACL was performed as described in chapter 4. In order to validate the iTRAQ-identified expression changes in key Nrf2- and CDDO-driven gene targets, immunoblotting was also undertaken for CYP2A5 and ENTPD5. The same protocol was employed with minor modifications, in that membranes were blocked overnight in 10% milk and primary antibody incubation was for 1 hour (monoclonal chicken anti-CYP2A5 antibody: 1:10000; monoclonal rabbit anti-ENTPD5 antibody: 1:10000). The secondary antibodies used were a peroxidase-conjugated rabbit anti-chicken IgG (CYP2A5; 1:10000) and a peroxidase-conjugated goat anti-rabbit IgG (ENTPD5; 1:10000).

5.3 Results

5.3.1 CDDO-Me pilot study for dose determination

A pilot study was performed in order to determine a suitable dose of CDDO-Me that would result in Nrf2 induction and downstream protein expression 24 hours after a single dose. The dose range used in the study was based on data from an investigation in which CDDO-Me was dosed to ICR mice resulting in an increase in NQO1 activity 24h after administration of the compound (Yates *et al.*, 2007). Nrf2 induction was determined by NQO1 western immunoblotting (figure 5.1). A dose of 3mg/kg CDDO-Me was found to produce the highest NQO1 signal, with the response appearing to diminish at higher doses. Consequently 3mg/kg was selected for use in the subsequent proteomic study.

5.3.2 Induction of Nrf2 by CDDO-Me in the proteomic study

WT and Nrf2 KO mice were administered a dose of 3mg/kg CDDO-Me (i.p) and culled 24 hours later. In order to confirm that a dose of 3mg/kg had indeed resulted in hepatic Nrf2 induction in WT mice, the expression of NQO1 was assessed by immunoblotting. Figure 5.1c shows a representative blot of NQO1 levels in each treatment group (n=3), while figure 5.1d shows densitometric analysis of expression of NQO1 in all animals in the study (n=6). Administration of CDDO-Me resulted in a two-fold increase in NQO1 in WT animals at 24h but no statistically significant change in the Nrf2 KO mice. NQO1 was expressed at a level that was 8-fold lower in Nrf2 KO control animals when compared to their WT counterparts.

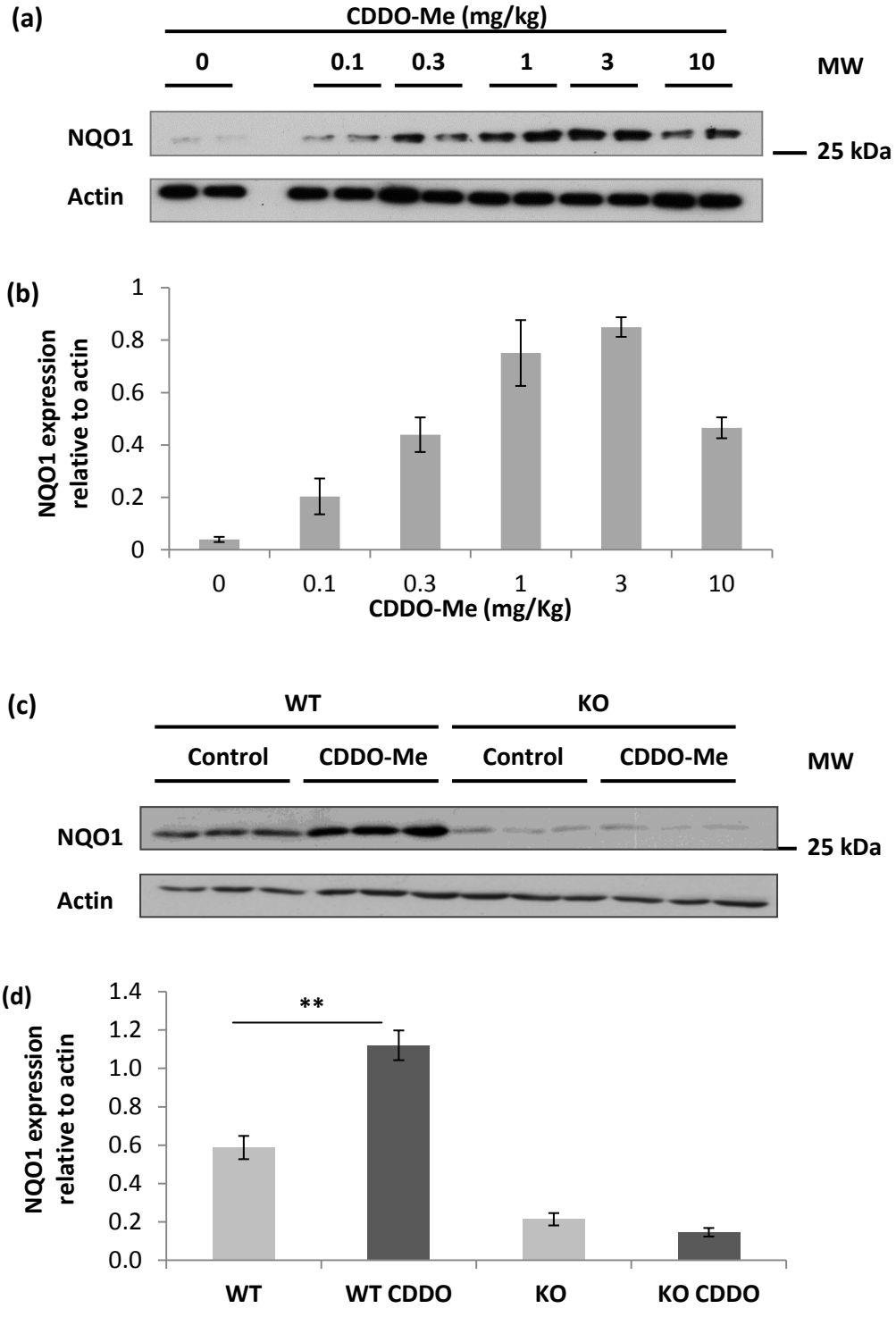

Figure 5.1: Immunoblots of liver homogenates from mice treated with CDDO-Me in DMSO (i.p) and culled 24 hours later. Immunoblots for NQO1 and actin from (a) the pilot study to determine the dose of CDDO-Me that results in maximum NQO1 induction and (c) the iTRAQ study employing a dose of 3mg/kg CDDO-Me. (b) and (d) show densitometric analysis of the immunoblots in (a) and (c) respectively with NQO1 expressed relative to actin. Error bars represent SEM (n=2, pilot study; n=6, iTRAQ study). Statistical analysis was performed using an unpaired t-test (**P< 0.01).

5.3.3 Characterization of the constitutive Nrf2-responsive hepatic proteome

A comparative iTRAQ-based proteomic analysis of livers from WT and Nrf2 KO mice was conducted. In order to define Nrf2-dependent expression of proteins at both the basal and inducible (24h post dosing) levels, proteins were extracted from both DMSO vehicle treated mouse livers and those treated with CDDO-Me (3 mg/kg). Proteome profiling of all mouse liver samples yielded 3655 unique identifications at a FDR of <1%. From this total, 1521 were shown to be quantifiable in at least four mice belonging to each of the four treatment groups, and these proteins were incorporated in the full statistical analysis.

Table 5.1 shows the list of proteins that were up- or down-regulated by at least 30% (unpaired t-test, $P<0.05$) in Nrf2 KO mice when compared to WT animals at the basal level. By applying a relatively non-stringent statistical analysis (without correction for multiple testing), a total of 165 liver proteins were deemed statistically different between WT and Nrf2-null mice. Whilst this level of statistical analysis is insufficient for unequivocal designation of Nrf2-driven proteins, it provides a sufficient number of nominally Nrf2-regulated proteins to provide candidates for biomarker assessment and to allow meaningful ontology and pathway analysis. As noted by Subramanian et al. (Subramanian *et al.*, 2005), the application of stringent multiple testing correction algorithms (such as Bonferroni or Benjamini Hochberg analyses) to large scale global analysis data can preclude the identification of modest expression changes that can collectively modulate a specific pathway.

Of the 165 Nrf2-regulated proteins identified, 99 were expressed at a lower level in the null mice and 66 were up-regulated. This is in line with work in chapter 2 of this thesis, and with genomic studies, which show both positive and negative regulation through the Nrf2 transcription pathway. Protein expression differences between WT and Nrf2 KO animals were evaluated to identify the primary biological functions and pathways associated with these genes. Analysis using MetaCore identified 48 pathways that were significantly differentially regulated in the livers of WT and Nrf2 KO mice (table 5.2; $P<0.05$). The network diagrams for the four most significantly different pathways are shown in figure 5.2.

Table 5.1: Constitutively regulated Nrf2-dependent proteins. iTRAQ-based proteomic comparison of liver proteins in WT and Nrf2 KO mice. Proteins with expression that was down- or up-regulated by at least 30% (unpaired t-test $P < 0.05$) in Nrf2 KO relative to WT mice are listed. Mean expression values relative to a common pool are given for n = 4-6 animals. Proteins are ordered according to the ratio between WT and Nrf2-null mice (WT/Nrf2 KO; highest to lowest) such that proteins with expression that is most markedly reduced in Nrf2 deficient animals appear at the top of the list.

Protein Accession	Name	WT/ Nrf2 KO ratio	P-value
Proteins down-regulated in Nrf2$^{(-/-)}$ mouse liver			
P17717	UDP-glucuronosyltransferase 2B17	4.28	0.001
P10649	Glutathione S-transferase Mu 1	4.11	0.001
P19639	Glutathione S-transferase Mu 3	4.04	0.001
P02762	Major urinary protein 6	3.62	0.005
Q8VCC2	Liver carboxylesterase 1	2.64	0.010
O70475	UDP-glucose 6-dehydrogenase	2.64	0.003
P97493	Thioredoxin, mitochondrial	2.52	0.033
P30115	Glutathione S-transferase A3	2.42	0.005
Q9WUZ9	Ectonucleoside triphosphate diphosphohydrolase 5	2.22	0.001
P24549	Retinal dehydrogenase 1	2.17	0.001
O08709	Peroxiredoxin-6	2.16	0.003
P20852	Cytochrome P450 2A5	2.12	0.045
P19157	Glutathione S-transferase P 1	2.12	0.025
Q60991	25-hydroxycholesterol 7-alpha-hydroxylase	2.09	0.027
P15626	Glutathione S-transferase Mu 2	2.09	0.001
P22907	Porphobilinogen deaminase	2.04	0.001
Q9D379	Epoxide hydrolase 1	2.00	0.001
P06801	NADP-dependent malic enzyme	1.91	0.001
Q6XVG2	Cytochrome P450 2C54	1.88	0.006
Q91X77	Cytochrome P450 2C50	1.79	0.002
Q8R0Y6	Cytosolic 10-formyltetrahydrofolate dehydrogenase	1.70	0.003
Q9CXN7	Phenazine biosynthesis-like domain-containing protein 2	1.70	0.008
Q9D1L0	Coiled-coil-helix-coiled-coil-helix domain-containing protein 2	1.69	0.020
Q9DCY0	Glycine N-acyltransferase-like protein Keg1	1.65	0.002

Q91VA0	Acyl-coenzyme A synthetase ACSM1, mitochondrial	1.64	0.001
Q9QZX7	Serine racemase	1.62	0.029
Q64442	Sorbitol dehydrogenase	1.58	0.002
P24472	Glutathione S-transferase A4	1.58	0.003
Q64458	Cytochrome P450 2C29	1.56	0.042
Q9EQK5	Major vault protein	1.55	0.001
O70570	Polymeric immunoglobulin receptor	1.55	0.003
P52760	Ribonuclease UK114	1.55	0.001
Q922Q8	Leucine-rich repeat-containing protein 59	1.52	0.023
Q8CG76	Aflatoxin B1 aldehyde reductase member 2	1.51	0.001
O55022	Membrane-associated progesterone receptor component 1	1.50	0.002
Q80W22	Threonine synthase-like 2	1.49	0.007
Q7TNG8	Probable D-lactate dehydrogenase, mitochondrial	1.49	0.028
Q91V76	Ester hydrolase C11orf54 homolog	1.48	0.003
Q9DCM0	Protein ETHE1, mitochondrial	1.48	0.013
O88844	Isocitrate dehydrogenase [NADP] cytoplasmic	1.46	0.004
P15105	Glutamine synthetase	1.46	0.034
Q9R0P3	S-formylglutathione hydrolase	1.45	0.003
Q6ZWV3	60S ribosomal protein L10	1.43	0.015
O08966	Solute carrier family 22 member 1	1.42	0.035
P11589	Major urinary protein 2	1.39	0.032
Q8K1N1	Calcium-independent phospholipase A2-gamma	1.39	0.016
Q9JII6	Alcohol dehydrogenase [NADP+]	1.39	0.018
P47738	Aldehyde dehydrogenase, mitochondrial	1.38	0.040
Q64514	Tripeptidyl-peptidase 2	1.37	0.028
P97494	Glutamate--cysteine ligase catalytic subunit	1.37	0.014
Q9DBG5	Perilipin-3	1.37	0.050
Q9Z1Z2	Serine-threonine kinase receptor-associated protein	1.37	0.015
Q61425	Hydroxyacyl-coenzyme A dehydrogenase, mitochondrial	1.36	0.022
Q3UJU9	Regulator of microtubule dynamics protein 3	1.35	0.001
P28474	Alcohol dehydrogenase class-3	1.35	0.011
Q8K157	Aldose 1-epimerase	1.33	0.024

O35945	Aldehyde dehydrogenase, cytosolic 1	1.32	0.011
Q9Z2W0	Aspartyl aminopeptidase	1.32	0.015
Q99KQ4	Nicotinamide phosphoribosyltransferase	1.31	0.013
Q9JMH6	Thioredoxin reductase 1, cytoplasmic	1.30	0.033
Q9DCQ2	Putative L-aspartate dehydrogenase	1.30	0.049
Q9ET01	Glycogen phosphorylase, liver form	1.30	0.027
Proteins up-regulated in Nrf2$^{(-/-)}$ mouse liver			
Q91V92	ATP-citrate lyase	0.69	0.023
P48678	Prelamin-A/C	0.68	0.005
P21981	Protein-glutamine gamma-glutamyltransferase 2	0.66	0.008
P08032	Spectrin alpha chain, erythrocyte	0.66	0.021
Q9WU19	Hydroxyacid oxidase 1	0.65	0.001
O08917	Flotillin-1	0.63	0.015
Q99P30	Peroxisomal coenzyme A diphosphatase NUDT7	0.62	0.044
P32020	Non-specific lipid-transfer protein	0.62	0.014
Q9CQC9	GTP-binding protein SAR1b	0.60	0.035
P11714	Cytochrome P450 2D9	0.58	0.004
P42225	Signal transducer and activator of transcription 1	0.51	0.043
Q8BVA5	UPF0554 protein C2orf43 homolog	0.46	0.032
Q05816	Fatty acid-binding protein, epidermal	0.40	0.009

Table 5.2: Pathway analysis of Nrf2-regulated gene products at the basal level. GeneGo MetaCore was used to identify pathways enriched in the WT animals compared with the Nrf2 KO mice. All significant ($P < 0.05$) pathways are listed along with the number of objects within the protein set associated with that pathway. The total number of objects in the entire pathway is shown in parentheses.

	Pathway	P Value	Objects
1	Pyruvate metabolism/ Rodent version	0.0000040	7 (66)
2	NRF2 regulation of oxidative stress response	0.000016	6 (54)
3	Naphthalene metabolism	0.000032	6 (61)
4	Glutathione metabolism / Rodent version	0.000075	6 (71)
5	Glutathione metabolism	0.00048	5 (65)
6	Glutathione metabolism / Human version	0.00051	5 (66)
7	Tryptophan metabolism/ Rodent version	0.00055	6 (102)
8	CAR-mediated direct regulation of xenobiotic metabolizing enzymes / Rodent version	0.00074	4 (41)
9	CAR-mediated direct regulation of xenobiotic metabolizing enzymes / Human version	0.00074	4 (41)
10	Pyruvate metabolism	0.0015	4 (49)
11	Lysine metabolism/ Rodent version	0.0018	5 (87)
12	Transcription_Transcription regulation of aminoacid metabolism	0.0019	3 (25)
13	Folic acid metabolism	0.0019	4 (53)
14	Triacylglycerol metabolism p.1	0.0031	4 (60)
15	Tryptophan metabolism	0.0035	5 (101)
16	Ascorbate metabolism / Rodent version	0.0036	3 (31)
17	Butanoate metabolism	0.0037	4 (63)
18	Development_EPO-induced Jak-STAT pathway	0.0051	3 (35)
19	Retinol metabolism / Rodent version	0.0053	4 (70)
20	Transcription_Role of AP-1 in regulation of cellular metabolism	0.0065	3 (38)
21	Retinol metabolism	0.0065	4 (74)
22	Propionate metabolism p.1	0.0070	3 (39)
23	Histidine-glutamate-glutamine and proline metabolism/ Rodent version	0.0072	5 (120)
24	Leucine, isoleucine and valine metabolism/ Rodent version	0.0085	4 (80)
25	Benzo[a]pyrene metabolism	0.0086	3 (42)

26	Immune response_IL-7 signaling in B lymphocytes	0.0092	3 (43)
27	Immune response_IL-5 signalling	0.0098	3 (44)
28	Lysine metabolism	0.011	4 (85)
29	Mechanisms of CFTR activation by S-nitrosoglutathione (normal and CF)	0.011	3 (46)
30	Androstenedione and testosterone biosynthesis and metabolism p.1	0.016	3 (53)
31	Immune response_Fc epsilon RI pathway	0.018	3 (55)
32	Androstenedione and testosterone biosynthesis and metabolism p.1/ Rodent version	0.020	3 (57)
33	Immune response_CCR5 signaling in macrophages and T lymphocytes	0.021	3 (58)
34	Propionate metabolism p.2	0.029	3 (66)
35	Polyamine metabolism	0.031	3 (68)
36	Acetaminophen metabolism	0.034	2 (29)
37	Histamine metabolism	0.034	2 (29)
38	Immune response_Signaling pathway mediated by IL-6 and IL-1	0.036	2 (30)
39	Cholesterol and Sphingolipids transport / Distribution to the intracellular membrane compartments (normal and CF)	0.039	2 (31)
40	Beta-alanine metabolism/ Rodent version	0.041	2 (32)
41	Signal transduction_ERK1/2 signaling pathway	0.041	2 (32)
42	(L)-Arginine metabolism	0.041	3 (76)
43	Leucine, isoleucine and valine metabolism.p.2	0.044	3 (78)
44	Development_CNTF receptor signalling	0.046	2 (34)
45	Fatty Acid Omega Oxidation	0.046	2 (34)
46	Immune response_Role of the Membrane attack complex in cell survival	0.046	2 (34)
47	Immune response_Oncostatin M signaling via MAPK in mouse cells	0.048	2 (35)
48	Estrone metabolism	0.048	2 (35)

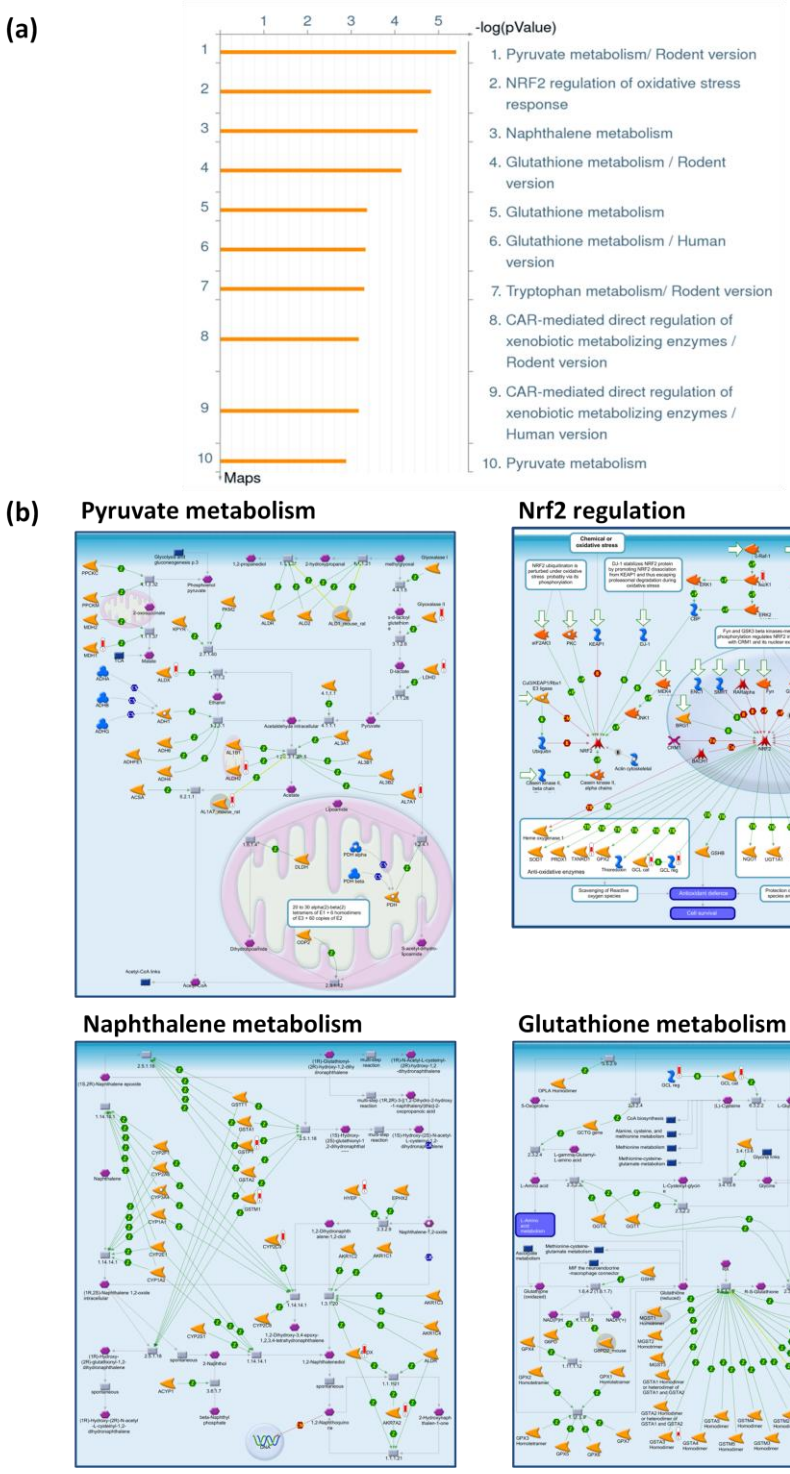

Figure 5.2: Pathway analysis of Nrf2-regulated gene products at the basal level. GeneGo MetaCore was used to identify pathways enriched in the WT animals compared with the Nrf2 KO mice. (a) Shows the 10 most significant pathways along with the –log(P value). (b) Shows the pathway diagrams for the 4 most significant pathways as detailed by the software.

5.3.4 Characterization of the CDDO-Me inducible Nrf2-dependent hepatic proteome

Following administration of CDDO-Me, 59 proteins were either up- or down-regulated in WT mice. Of these, only 2 were similarly altered in Nrf2 KO mice. These data are displayed graphically in Figure 5.3, which presents the fold difference for each individual protein identified in at least 4 mice (1521 in total) plotted against the unpaired t-test derived P value; figure 5.3a represents the comparison between WT and Nrf2 KO mice at the basal level, whilst the effect of CDDO-Me treatment in WT animals is shown in figure 5.3b.

Inspection of these plots suggests that the influence of Nrf2 upon the basal proteome may be generally more profound than the effect of induction. Overall, more proteins lie above the statistical cut-off of $P<0.05$ with the comparison at the basal level than are statistically induced by CDDO-Me. Moreover, with the exception of CYP2A5 (labelled in fig 5.3b), the fold differences between WT and Nrf2 KO mice at the constitutive level comprised a far greater range than those following CDDO-Me treatment.

It is also notable that a sizable proportion of proteins were expressed at a lower level in WT animals than in Nrf2 KO animals, indicating a level of negative regulation by Nrf2. In contrast, the majority of the changes observed following CDDO-Me treatment were up-regulations. A summary of proteins uniquely up- or down-regulated by at least 30% in WT mice, but not in Nrf2-deficient animals, is given in Table 5.3. Sixteen proteins were induced compared with just four with expression that was decreased after CDDO-Me.

As with the constitutively regulated proteins (table 5.1), proteins induced by CDDO-Me were heavily dominated by drug metabolizing enzymes and proteins involved in lipid synthesis/metabolism. However, there was no indication that CDDO-Me resulted in a reduced expression of proteins involved in fatty acid synthesis. A negative regulation of such proteins, including ACL, FAS and SCD, at the *constitutive* level was observed both in the current iTRAQ analysis and in the work described in chapter 2 of this thesis. Several of the key lipid metabolic enzymes showed a numerically reduced expression following CDDO-Me administration, with ACL for example reduced by 25% following induction. However, these values were not statistically significant.

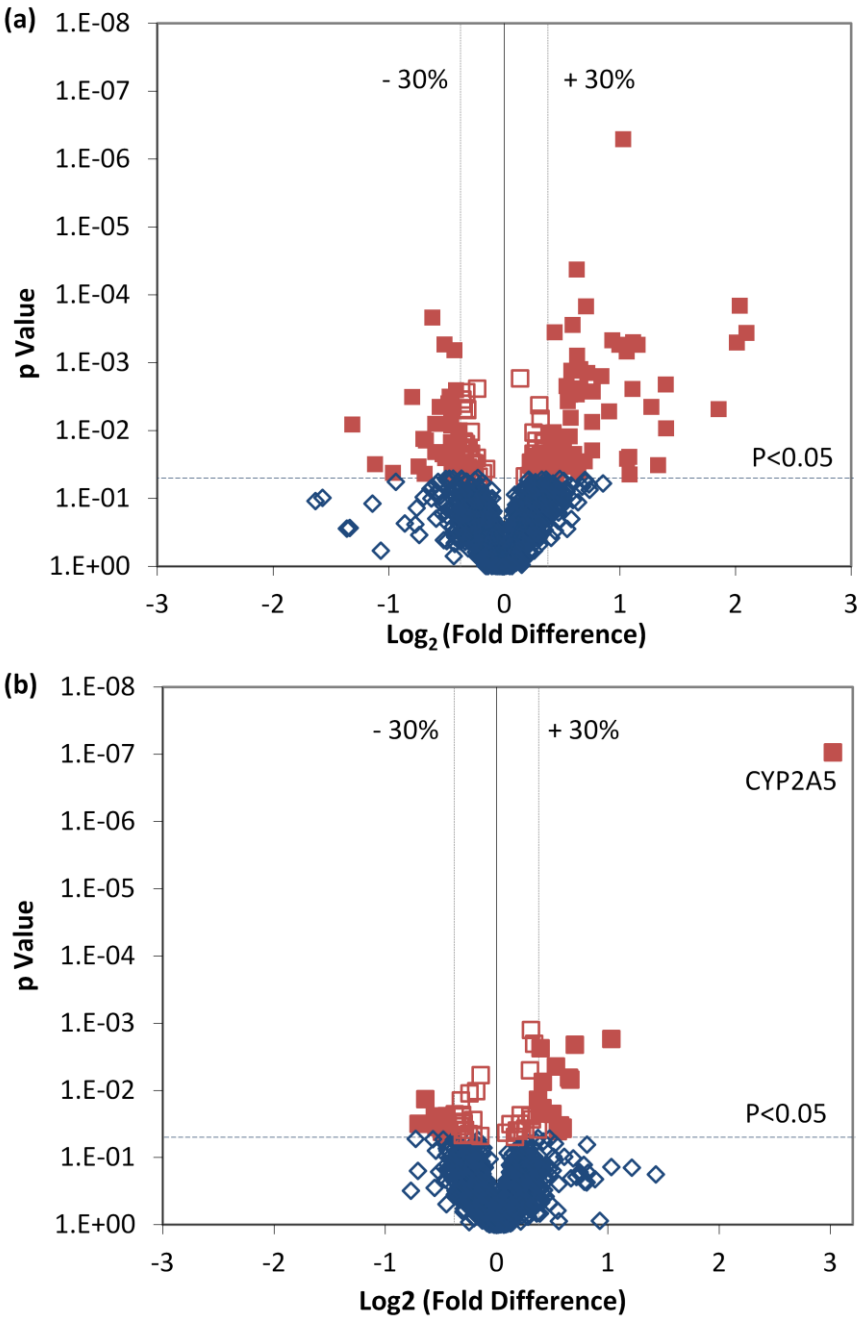

Figure 5.3: Volcano plots of the proteins quantified during iTRAQ analysis comparing (a) WT ctrl and Nrf2 KO ctrl and (b) WT CDDO and WT ctrl mice. Each point represents the difference in expression (fold-change) between the two groups of mice compared plotted against the level of statistical significance. Dotted vertical lines represent differential expression differences of ±30%, while the dotted horizontal line represents a significance level of p<0.05 (unpaired t-test). Proteins represented by a filled square are those with expression that differs by at least 30% at a statistically significant level.

T**able 5.3: CDDO-Me inducible Nrf2-dependent proteins.** iTRAQ-based proteomic comparison of liver proteins in DMSO vehicle control treated and CDDO-Me treated WT mice. Proteins with expression that was up- or down-regulated in WT mice (but not in Nrf2 KO mice) by at least 30% (unpaired t-test $P < 0.05$) following CDDO-Me administration are listed. Mean expression values relative to a common pool are given for n = 4-6 animals. Proteins are ordered according to the ratio between CDDO-Me treated WT mice and vehicle control treated WT mice (WT CDDO/WT ctrl) highest to lowest such that proteins with expression that is most markedly induced by CDDO-Me appear at the top of the list.

Uniprot Accession	Name	WT CDDO/ WT ctrl	P-value
Proteins up-regulated by CDDO-Me			
P20852	Cytochrome P450 2A5	8.12	0.001
Q9WUZ9	Ectonucleoside triphosphate diphosphohydrolase 5	2.04	0.002
P48758	Carbonyl reductase [NADPH] 1	1.63	0.003
P19639	Glutathione S-transferase Mu 3	1.58	0.007
O70475	UDP-glucose 6-dehydrogenase	1.57	0.007
O35386	Phytanoyl-CoA dioxygenase, peroxisomal	1.51	0.036
P24456	Cytochrome P450 2D10	1.51	0.038
Q9D379	Epoxide hydrolase 1	1.48	0.034
O88455	7-dehydrocholesterol reductase	1.46	0.041
P50285	Dimethylaniline monooxygenase [N-oxide-forming] 1	1.45	0.005
Q07076	Annexin A7	1.42	0.006
Q9R1J0	Sterol-4-alpha-carboxylate 3-dehydrogenase, decarboxylating	1.42	0.023
Q923D2	Flavin reductase (NADPH)	1.33	0.008
Q9DD20	Methyltransferase-like protein 7B	1.33	0.019
P29341	Polyadenylate-binding protein 1	1.32	0.003
P37040	NADPH--cytochrome P450 reductase	1.31	0.022
Proteins down-regulated by CDDO-Me			
Q91Y97	Fructose-bisphosphate aldolase B	0.69	0.036
Q9QXD6	Fructose-1,6-bisphosphatase 1	0.68	0.025
P70398	Probable ubiquitin carboxyl-terminal hydrolase FAF-X	0.64	0.014
P70255	Nuclear factor 1 C-type	0.61	0.032

Analysis using MetaCore identified 8 pathways that were significantly altered in the livers of WT mice treated with CDDO-Me, when compared to vehicle control-treated mice (table 5.4; P<0.05). The network diagrams for four of the pathways are shown in figure 5.4.

Table 5.4: Pathway analysis of Nrf2-regulated gene products induced by CDDO-Me. GeneGo MetaCore was used to identify pathways enriched in the WT animals treated with CDDO-Me (3 mg/kg) for 24h compared with the vehicle control-treated WT mice. All significant (P < 0.05) pathways are listed along with the number of objects within the protein set associated with that pathway. The total number of objects in the entire pathway is shown in parentheses.

	Pathway	P Value	Objects
1	Glycolysis and gluconeogenesis (short map)	0.0015	3 (66)
2	Cholesterol Biosynthesis	0.0034	3 (88)
3	Glycogen metabolism	0.0076	2 (38)
4	SCAP/SREBP Transcriptional Control of Cholesterol and FA Biosynthesis	0.0084	2 (40)
5	Galactose metabolism	0.018	2 (59)
6	Fructose metabolism	0.027	2 (74)
7	Peroxisomal branched chain fatty acid oxidation	0.033	2 (83)
8	Fructose metabolism/ Rodent version	0.034	2 (84)

5.3.5 Characterisation of proteins regulated by Nrf2 at both basal and CDDO-Me-inducible level

Five proteins were basally expressed at a significantly lower level in Nrf2 KO when compared to WT and were also significantly up-regulated following CDDO-Me treatment in WT mice, with expression differences in each case of >30%. A summary of the function of the proteins is given in table 5.5. Of the proteins identified as most significantly regulated by Nrf2, Glutathione S-transferase Mu 3 and Epoxide hydrolase 1 are well characterised as an Nrf2-regulated proteins. The regulation of CYP2A5 and UDP-glucose 6-dehydrogenase by Nrf2 has also been noted previously (Abu-Bakar *et al.*, 2007; Thimmulappa *et al.*, 2002). However, as far as I am aware, Nrf2-regulation of ENTPD5 is a novel finding of this study.

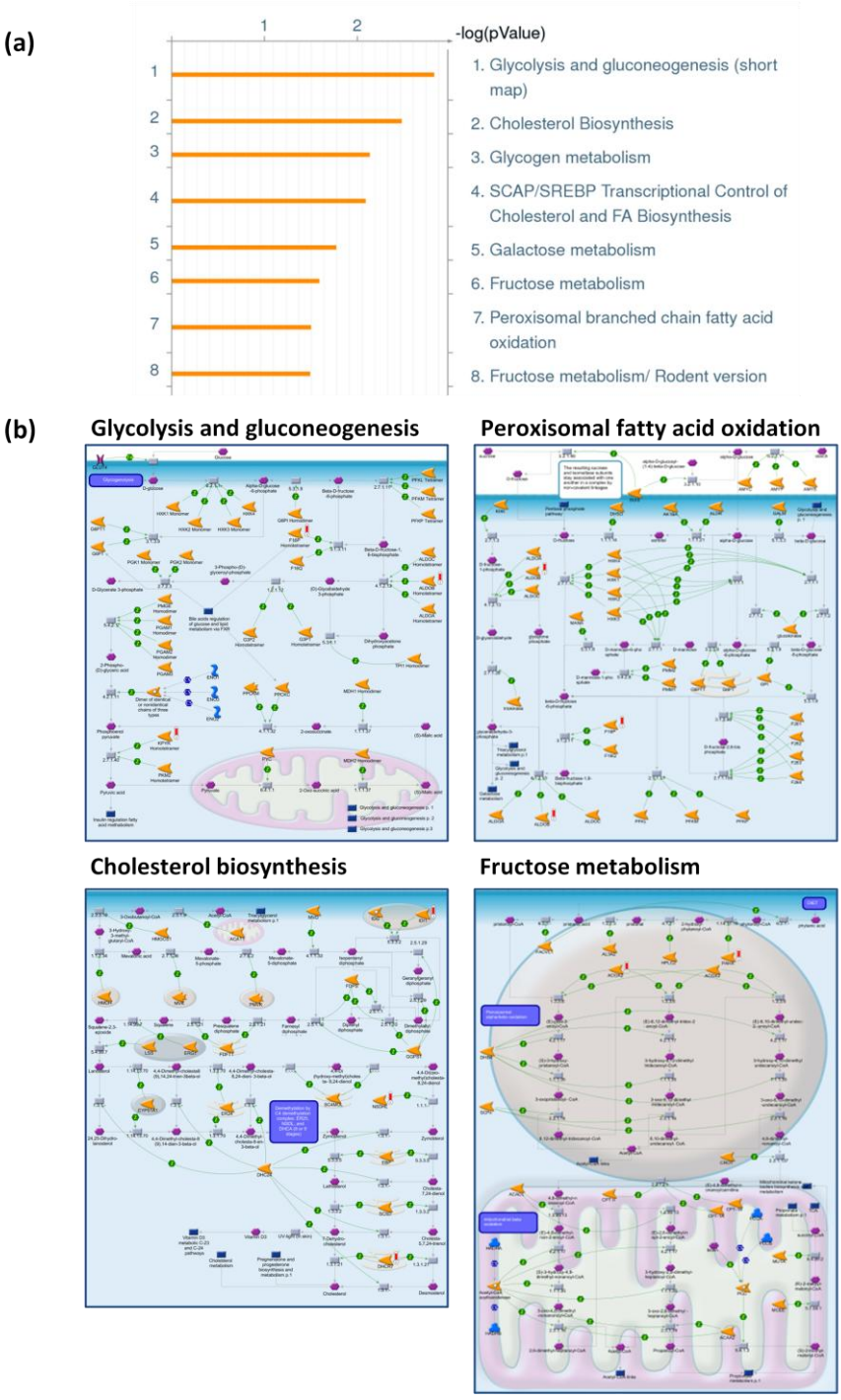

Figure 5.4: Pathway analysis of Nrf2-regulated gene products induced by CDDO-Me. GeneGo MetaCore was used to identify pathways enriched in the WT animals treated with CDDO-Me (3 mg/kg) for 24h compared with the vehicle treated WT mice. (a) Shows the 8 most significant pathways along with the –log(P value). (b) Shows the pathway diagrams for 4 of the most significant pathways that have not previously been represented in figure 5.2.

Table 5.5: ***Proteins regulated by Nrf2 at both basal and CDDO-Me-inducible level.*** iTRAQ-based proteomic comparison of liver proteins in DMSO vehicle control treated WT and Nrf2 KO mice and CDDO-Me treated WT mice. Proteins with expression that was up-regulated by at least 30% in both WT/KO and WT-CDDO/WT comparisons are listed. Mean expression values relative to a common pool are given for n = 4-6 animals. Proteins are ordered according to the ratio between CDDO-Me treated WT and Nrf2 KO mice, such that proteins showing the widest range of Nrf2 regulation appear at the top of the list. [a]Protein function based on the UniProt database annotation (http://www.uniprot.org/).

Uniprot Accession	Name	Mean expression level relative to pool			Expression ratios			[a]Protein function
		KO	WT	WT-CDDO	WT / KO	WT-CDDO / WT	WT-CDDO / KO	
P20852	Cytochrome P450 2A5	0.19	0.40	3.26	**2.12**	**8.12**	**17.24**	Cytochrome P450 exhibiting high coumarin 7-hydroxylase activity
P19639	Glutathione S-transferase Mu 3	0.33	1.33	2.11	**4.04**	**1.58**	**6.39**	Mediates the conjugation of GSH to a wide number of exogenous and endogenous electrophiles
Q9WUZ9	Ectonucleoside triphosphate diphosphohydrolase 5	0.47	1.05	2.15	**2.22**	**2.04**	**4.55**	Uridine diphosphatase that promotes protein N-glycosylation and ATP regulation. With CMPK1 and AK1, constitutes an ATP hydrolysis cycle converting ATP to AMP resulting in a compensatory increase in aerobic glycolysis. Plays a key role AKT1-PTEN pathway by promoting glycolysis in proliferating cells in response to PI3K signalling.
O70475	UDP-glucose 6-dehydrogenase	0.45	1.19	1.87	**2.64**	**1.57**	**4.14**	Involved in the biosynthesis of UDPGA, glycosaminoglycans, hyaluronan, chondroitin sulfate, and heparan sulphate
Q9D379	Epoxide hydrolase 1	0.63	1.25	1.86	**2.00**	**1.48**	**2.96**	Enzyme that catalyzes the hydrolysis of arene and aliphatic epoxides to less reactive and more water soluble dihydrodiols by the trans addition of water.

5.3.6 Western immunoblotting validation of regulation of CYP2A5 and ENTPD5 by Nrf2

Western immunoblotting was performed in order to validate the differences noted in expression of CYP2A5 and ENTPD5 (figure 5.5). Densitometric analysis of immunoblots identified a 2.4-fold induction in CYP2A5 levels in WT mice treated with CDDO-Me when compared to vehicle control mice, while no induction was identified in Nrf2 KO mice treated with the triterpenoid. Expression of the CYP2A5 was 7.4-fold lower in vehicle control Nrf2 KO animals when compared to their WT counterparts. ENTPD5 expression was induced 2.3-fold in CDDO-Me treated WT animals, with no induction in Nrf2 KO mice. Furthermore, comparison of the vehicle control groups showed that ENTPD5 expression was reduced by 4.6-fold in Nrf2 KO animals.

5.3.7 ACL in CDDO-Me treated mice

In order to further investigate potential differences in fatty acid metabolism enzymes in control- and CDDO-Me-treated WT mice, a western immunoblot for ACL was performed (figure 5.6). The results confirmed the iTRAQ analysis showing that there was no statistical difference in expression of the protein between WT animals in the vehicle control and those treated with CDDO-Me.

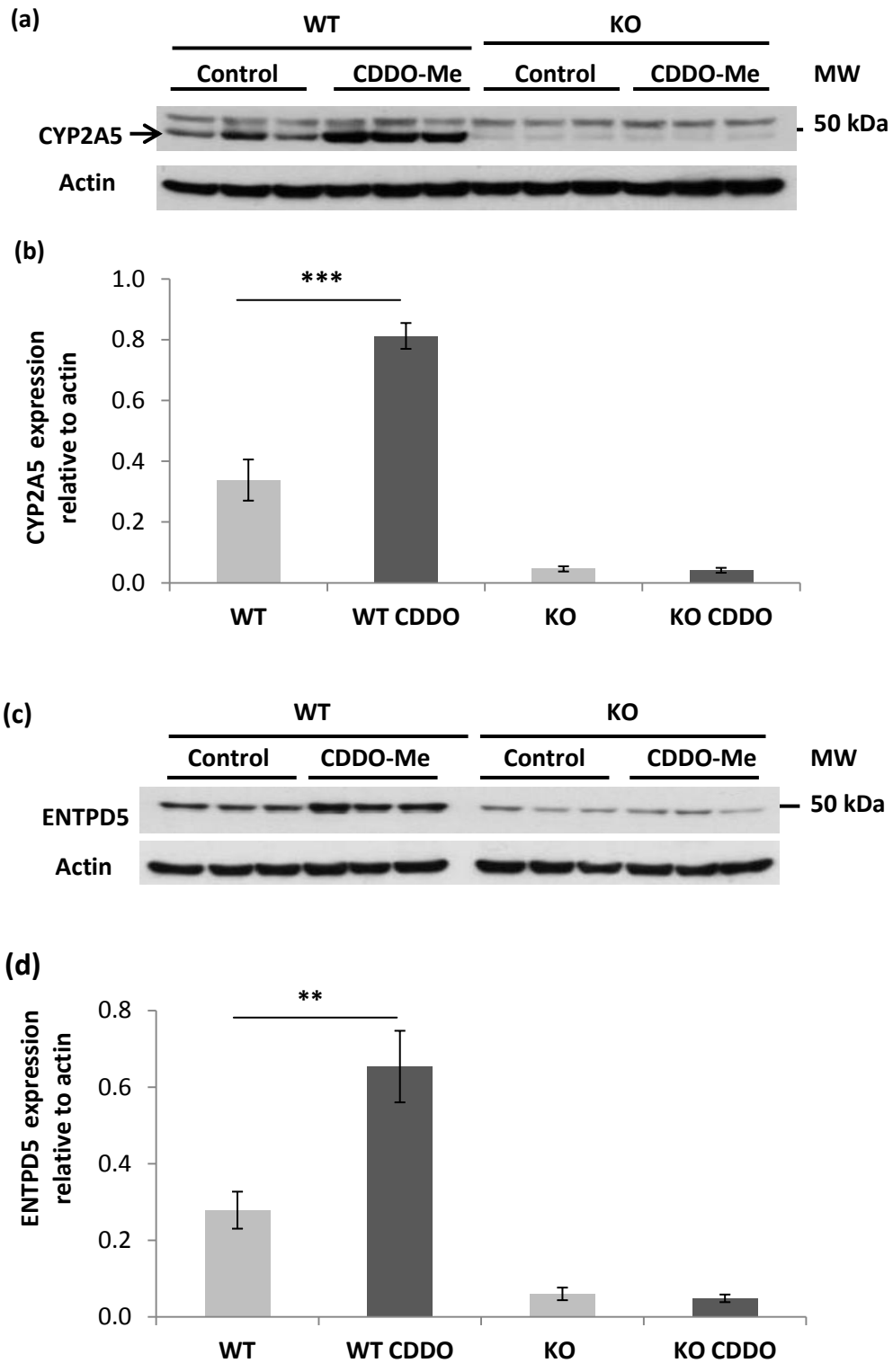

Figure 5.5: Immunoblots of liver homogenates from WT and Nrf2 KO mice treated with CDDO-Me or DMSO vehicle control (i.p) and culled 24 hours later. (a) and (c) show representative immunoblots for CYP2A5 and ENTPD5 respectively, together with the corresponding actin immunoblot. (b) and (d) show densitometric analysis of immunoblots for all animals in each group (n=6), with CYP2A5 and ENTPD5 expressed relative to actin. Error bars represent SEM. Statistical analysis was performed using an unpaired t-test (**P< 0.01; ***P<0.001).

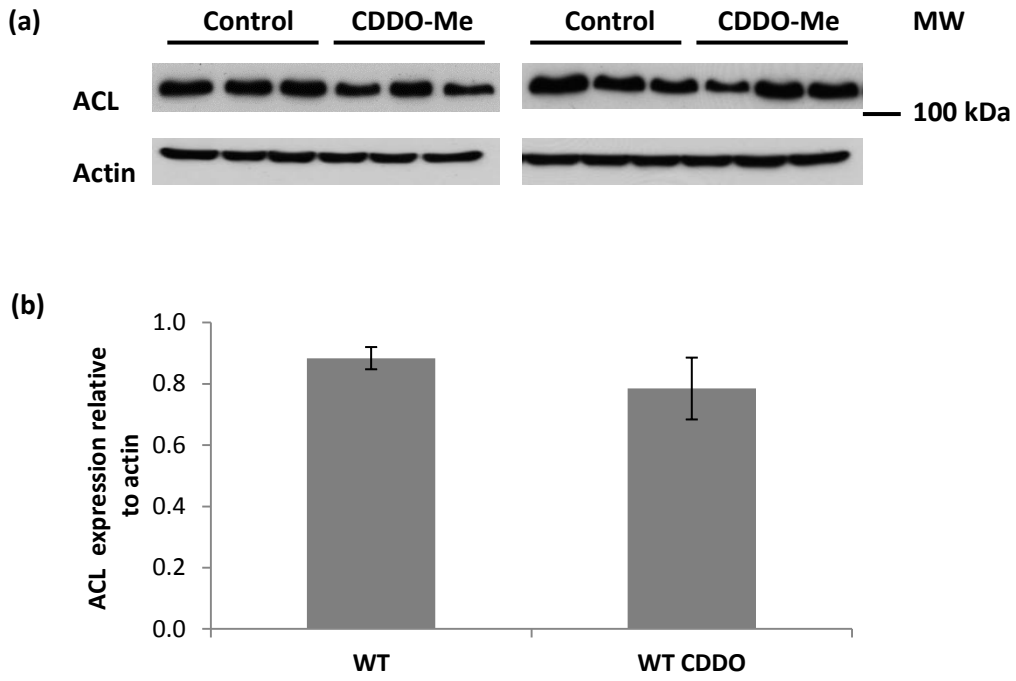

Figure 5.6: Immunoblots of liver homogenates from WT mice treated with CDDO-Me or DMSO vehicle control (i.p) and culled 24 hours later. (a) Immunoblots for ACL and actin. (b) Densitometric analysis of immunoblots for all animals in each group (n=6). ACL is expressed relative to actin. Error bars represent SEM. There was no statistical difference between groups.

5.4 Discussion

The aim of the work described in this chapter was to define the hepatic proteomic profile of Nrf2 activation. A dose of 3mg/kg (*i.p*) CDDO-Me was shown to result in optimal Nrf2 activation 24 hours after dosing, as determined by NQO1 immunoblotting, and was subsequently used in order to dose WT and Nrf2 KO mice for iTRAQ-based hepatic protein analysis. The use of the Nrf2 knockout mouse model was a particular strength of this study because it facilitated comparison of CDDO-Me induced protein expression changes in Nrf2 competent and deficient mice, thus allowing any changes observed to be assigned as Nrf2 dependent or independent effects.

CDDO and its derivatives have been shown to affect several different intracellular signalling pathways, including NF-κB (Ahmad *et al.*, 2006; Shishodia *et al.*, 2006; Yore *et al.*, 2006), JAK-STAT (Ahmad *et al.*, 2008; Liby *et al.*, 2006) and PPAR-γ receptor signalling (Wang *et al.*, 2000). However, somewhat surprisingly very few of the proteins induced by CDDO-Me in WT mice were similarly changed in the Nrf2 KO animals, indicating that at the relatively low dose of CDDO-Me administered, nearly all the changes in protein expression were mediated via the Keap1:Nrf2 signalling pathway.

The iTRAQ analysis identified more proteins that were differentially expressed at the basal level in WT versus Nrf2 KO mice than at the inducible level in WT control versus WT CDDO-Me treated mice. The Nrf2 KO mouse is a model of chronic Nrf2 deficiency and is therefore likely to have a more profound influence on protein homeostasis than a single dose of an Nrf2 inducer. However, the study emphasises the important role that Nrf2 plays in the basal regulation of protein expression, and suggests that the influence of Nrf2 may be more notable in the constitutive regulation of proteins than it is following acute induction.

In work described in chapter 2 of this thesis investigating the proteomic hepatic profile of Nrf2-null mice, lipid metabolism featured strongly in the differentially regulated proteins, confirming a key role for Nrf2 in the modulation of fatty acid synthesis. In other studies, both pharmacological and genetic methods of Nrf2 induction have been shown to result in the down-regulation of pivotal enzymes in the fatty acid synthesis pathway at the mRNA level (Shin *et al.*, 2009; Yates *et al.*, 2009), with Yates *et al* identifying a reduction in ACL and FAS mRNA after a single dose of CDDO-Im. Interestingly, results from the current study show that whilst WT mice clearly under-expressed these proteins when compared with

Nrf2-deficient mice, treatment of WT animals with CDDO-Me did not result in a further decrease in expression. Thus the effects observed by Yates *et al* at the mRNA level may not translate into altered expression at the protein level at least within the time-course of this study.

It should be noted that in a second study by the same group, FAS mRNA levels were not affected by the administration of CDDO-Im to HFD-fed WT mice 3 times per week for a 21 day period, however a significant reduction was noted after a 95 day dosing period, along with a reduction in triglyceride levels when compared to control animals (Shin *et al.*, 2009). These results suggest that chronic administration of CDDO derivatives is required to achieve functional modulation of lipid metabolism pathways.

It is clear that Nrf2 has an important role for maintenance of lipid homeostasis in the liver; however, the work described in this chapter suggests that Nrf2 has a more significant role in modulating lipid metabolism at the basal level than it does following acute induction. However, it remains to be determined whether Nrf2 has a greater influence on expression of proteins important for lipid metabolism in models of chronic induction.

Of the proteins that were up-regulated in CDDO-Me treated WT mice, CYP2A5 was most significantly increased. Nrf2-regulation of CYP2A5 has previously been documented (Abu-Bakar *et al.*, 2007; Lamsa *et al.*, 2010), while studies employing human hepatocytes have also identified CYP2A6, the human analogue, as Nrf2 regulated (Yokota *et al.*, 2011). Interestingly, CYP2A5/6 is important for the metabolism of compounds including coumarin, nicotine and caffeine, with products of coumarin and caffeine metabolism being employed as markers of enzyme activity (Hakooz *et al.*, 2007; Satarug *et al.*, 2004). Consequently, there may be the potential to utilize CYP2A5/6 activity as a biomarker for Nrf2 activation through the administration of a non-toxic exogenous CYP2A5/6 substrate. However, CYP2A6 has been shown to be polymorphic in a range of ethnic populations, with some polymorphisms resulting in functional differences in enzyme activity (Han *et al.*, 2012; Nurfadhlina *et al.*, 2006; Shimada *et al.*, 1996). This would therefore have to be taken into account were CYP2A6 activity to be used as a biomarker for Nrf2 activity in the human population.

ENTPD5 was another protein that was expressed at a significantly higher level in WT mice treated with CDDO-Me, as well as at a constitutively lower level in Nrf2 KO animals.

ENTPD5 is a uridine diphosphatase that hydrolyzes uridine diphosphate (UDP) to uridine monophosphate (UMP). It is important in the glycosylation and folding of proteins, as well as in ATP regulation. It has been shown to play a role in regulation of the PI3K-PTEN-AKT signalling loop (Fang *et al.*, 2010). Interestingly, the PI3K/AKT signalling pathway has been implicated in Nrf2 signalling, notably in the triterpenoid-mediated activation of Nrf2 (Liby *et al.*, 2005), and this is currently the subject of further investigation within the department.

The work described in this chapter has defined a list of proteins with expression that was induced following Nrf2 activation resulting from the administration of a single 3mg/kg dose of CDDO-Me. Furthermore, it has shown that the majority of changes in protein expression that result from such a dose are attributable to Keap1:Nrf2 pathway modulation. By determining the proteins that are induced on Nrf2 activation, a number of candidate proteins have been identified that may have utility as biomarkers for investigating Nrf2 activity and variability in preclinical and translational models. Those proteins that were identified as down-regulated in Nrf2 KO when compared to WT mice, as well as up-regulated in WT mice on CDDO-Me treatment, have significant potential because of their dynamic range of Nrf2-regulated expression.

Chapter 6 Concluding Discussion

Contents

6.1 Summary of thesis aims and major findings

The Keap1:Nrf2 pathway plays an important and well characterised role in the cytoprotective response. Under conditions of oxidative stress, Keap1 is no longer able to target Nrf2 for degradation and the transcription factor accumulates in the nucleus, where it binds to the ARE in a range of genes thus mediating their expression. Nrf2 has a role in regulating the expression of genes encoding phase II proteins, enzymes important for glutathione synthesis, and antioxidants.

Hepatotoxicity resulting from drug administration is a significant problem for the pharmaceutical industry. Often the mechanisms by which DILI occurs are poorly understood and there is a clear imperative to improve preclinical models of hepatotoxicity. Oxidative stress and glutathione depletion have been implicated in the toxicity associated with model hepatotoxins, as well as in cases of idiosyncratic DILI. Nrf2 KO mice have also been shown to be more susceptible to the toxicity resulting from the administration of compounds including paracetamol, carbon tetrachloride and cisplatin (Chan *et al.*, 2001; Enomoto *et al.*, 2001; Park *et al.*, 2008; Xu *et al.*, 2008). Consequently, the Keap1:Nrf2 system provides a potential focus for the development of novel therapeutic strategies for the management of DILI. Biomarkers that are indicative of Nrf2 activity may reflect oxidative stress levels, thus having applicability in preclinical models of hepatotoxicity.

Biomarkers of Nrf2 activity would also have utility in studies investigating the importance and variability of Nrf2 levels in the human population. While Nrf2 has been widely studied in mouse models, the role of the transcription factor in man has received limited attention. However, Nrf2 induction has been investigated for its therapeutic potential, with CDDO-Me recently entering Phase III clinical trials for the treatment of CKD in patients with type II diabetes. Consequently, there is a pressing need to characterise the variability of Nrf2 expression in the human population and explore the functional roles of the transcription factor in man.

The overall aim of the work described in this thesis was to investigate the hepatic profile of mice in which Nrf2 signalling had been modulated in order to identify potential biomarkers of Nrf2 activity. Work detailed in chapter 2 set out to characterise the basal hepatic proteomic profile of WT and Nrf2 KO mice. Analysis of iTRAQ data identified lipid and glutathione metabolism as the processes that were most significantly differentially

regulated in Nrf2 KO animals. Glutathione synthesis was found to be positively regulated by Nrf2 and lipid metabolism was identified as a process that is negatively regulated by the transcription factor.

Given the importance of Nrf2 in glutathione regulation and the association between glutathione depletion and drug toxicity noted in chapter 1 of this thesis, the aim of the work described in chapter 3 was to develop and validate an LC-MS/MS assay for the quantification of GSH and GSSG. The assay was employed to determine the basal levels of GSH and GSSG in the livers of WT and Nf2 KO mice, with levels of GSH found to be reduced by 21.5% in Nrf2 KO animals.

Evidence of a role for Nrf2 in the regulation of lipid metabolism has only recently emerged and has yet to be definitively characterised. Lipids and other metabolites associated with lipid synthesis may have the potential to serve as biomarkers of Nrf2 activation. Therefore, the aim of the work set out in chapter 4 of this thesis was to investigate the hepatic lipid profiles of WT and Nrf2 KO mice. The fatty acid synthesis pathway was the major focus of the work described, as this process was noted as significantly regulated by Nrf2 in the proteomic analysis set out in chapter 2. Carbohydrate restriction was employed as a tool to investigate how the animals responded to perturbations in the fatty acid synthesis pathway. The level of a number of fatty acids differed in the livers of WT and Nrf2 KO animals at a statistically significant level, with some of the differences exacerbated by a CHO-R diet. Preliminary lipidomic analysis provided further evidence for the importance of Nrf2 in lipid regulation.

The synthetic triterpenoid, CDDO-Me has been shown to be a particularly potent inducer of Nrf2 and was used in the studies detailed in chapter 5 in order to investigate the hepatic proteomic profile of Nrf2 activation in mice. The use of both WT and Nrf2 KO animals allowed any changes resulting from CDDO-Me administration to be identified as Nrf2-depndent or –independent. iTRAQ results and subsequent MetaCore analysis highlighted the important role of Nrf2 in the constitutive regulation of protein expression, with significantly more proteins and pathways differentially regulated in WT and Nrf2 KO control animals when compared to the differences identified in WT control and CDDO-Me treated mice. Five proteins were identified as being constitutively expressed at a lower level in Nrf2 KO animals when compared to their WT counterparts and also up-regulated in the

livers of WT animals treated with CDDO-Me. The dynamic range of Nrf2-inducible expression means that these proteins have significant potential as candidate biomarkers of Nrf2 activity.

6.2 The importance of Nrf2 in constitutive regulation

In the context of drug toxicity it is often the function of the Keap1:Nrf2 pathway in the adaptive response to chemical stress that is the focus, whereby the interaction between Keap1 and Nrf2 is disrupted following oxidative insult and Nrf2 mediates the up-regulation of the expression of cytoprotective genes and thus synthesis of enzymes key for detoxification. However, Nrf2 is also known to have a role in controlling the basal expression of many defence genes and work described in this thesis further highlights the importance of Nrf2 in the regulation of the constitutive hepatic profile. The iTRAQ studies detailed in chapter 2 identified 127 proteins that were differentially expressed in the livers of WT and Nrf2 KO mice at a basal level, including many proteins with a role in cytoprotection. Analysis of hepatic glutathione levels in WT and Nrf2 KO animals detailed in chapter 3 also showed that levels of reduced glutathione were statistically significantly lower in Nrf2 KO animals when compared to their WT counterparts. Furthermore, work set out in chapter 5 investigating the hepatic proteomic profile of acute Nrf2 induction, showed that a greater proportion of proteins were regulated at the basal level by Nrf2 than were induced following a single dose of the synthetic triterpenoid CDDO-Me.

The function of Nrf2 in regulating the basal expression of proteins is likely to be of particular significance in the initial phase of the response to acute toxic insult. It is probable that the Nrf2-mediated constitutive expression of proteins including the GSTs and UGTs is vital in mounting a successful response to such stress. For example, a functional Keap1:Nrf2 system has been shown to confer protection against drug-induced hepatotoxicity including damage associated with paracetamol overdose (Chan *et al.*, 2001). Paracetamol toxicity is associated with hepatocellular damage in Nrf2 KO animals within 2 hours of drug administration at doses that do not result in detectable damage in WT animals at the same time point (Enomoto *et al.*, 2001). The timeframe for up-regulation of mRNA expression and subsequent protein synthesis cannot account for the protection conferred by Nrf2 in WT animals (Kitteringham *et al.*, 2000). While the up-regulation of gene expression by Nrf2 may be important for the longer term response to stress and contribute to the effective recovery of an animal following chemical insult, it seems unlikely

that this process is able to influence the crucial primary response to stress within a relevant time-frame.

Given that Nrf2 has an important role in regulating the basal expression of cytoprotective proteins and basal glutathione levels, as highlighted by work described in this thesis, it is important that the constitutive variability of Nrf2 in the human population is established. Individuals in whom Nrf2 expression is constitutively low may be predisposed to the toxicity associated with oxidative stress-inducing compounds and this may be relevant for some cases of idiosyncratic DILI.

6.3 A role for Nrf2 in the regulation of lipid metabolism

While the importance of Nrf2 in the oxidative stress response is well documented, the study described in chapter 2 of this thesis was one of the first to identify a role for Nrf2 in the modulation of lipid metabolism. In a paper published in 2008, Tanaka *et al.* reported that genes encoding enzymes key for fatty acid synthesis, including FAS and ACC1, were increased in livers of Nrf2 KO mice fed a HFD for 4 weeks when compared to WT animals (Tanaka *et al.*, 2008). Interestingly, the feeding of a HFD also led to a 56% reduction in Nrf2 mRNA expression in WT animals. These findings suggest a negative role for Nrf2 in the regulation of hepatic fatty acid metabolism and are therefore in accordance with the results detailed in chapter 2.

While one subsequent study has suggested that levels of fatty acid synthesis enzymes are in fact higher in livers of WT mice fed a HFD when compared to Nrf2 KO animals (Huang *et al.*, 2010), the majority of studies in the literature support the hypothesis that Nrf2 negatively regulates hepatic lipid metabolism. For example, in a study investigating the effect of CDDO-Im administration in a HFD model, mRNA levels of FAS and ACC1 were reduced in animals treated with CDDO-Im 3 times weekly for a 95 day period in WT HFD fed and WT control diet groups. This was not the case in Nrf2 KO groups (Shin *et al.*, 2009). Furthermore, in a comprehensive study by Yates *et al.* (Yates *et al.*, 2009), lipid metabolism was the functional category that was most significantly altered by both genetic and pharmacological Nrf2 induction, with a majority of lipid metabolism-related genes down-regulated with increasing Nrf2 activation. Within the lipid metabolism class, genes linked with fatty acid biosynthesis were most notably affected and included FAS, ACC1, SREBP1c and ACL.

Such studies, together with the results from iTRAQ analysis set out in chapter 2 of this thesis, have provided significant evidence that the regulation of hepatic lipid metabolism is an important function of Nrf2. Yates *et al.* suggest that Nrf2 may function to sense lipids or the intermediates of lipid metabolism (Yates *et al.*, 2009), however, further studies investigating the role of Nrf2 in lipid regulation are required before conclusions can be drawn.

The mechanism of negative regulation of lipid metabolism by Nrf2 may be the result of a direct or an indirect interaction. Given that the evidence for a role for microRNAs (miRNAs) in the regulation of lipid metabolism is growing, these small non coding RNA species may be hypothesised to contribute to the mechanisms by which Nrf2 regulates lipid pathways at a transcriptional and post-transcriptional level. miRNAs including miR122 and miR370 have been shown to have a role in the regulation of lipid and cholesterol homeostasis (Esau *et al.*, 2006; Iliopoulos *et al.*, 2010), while Nrf2 has been shown to have a role in the regulation of levels of miR29B (Chorley *et al.*, 2012). A comprehensive study that identifies miRNAs that are regulated by Nrf2 and subsequently investigates the effect of modulation of levels of such miRNAs on lipid metabolism may provide valuable insight into Nrf2-mediated regulation of lipid pathways.

Given the evidence for a role for Nrf2 in the regulation of enzymes important for cytosolic fatty acid synthesis, the work described in chapter 4 of this thesis set out to explore the functional significance of the changes in enzyme expression by investigating the hepatic fatty acid profile of WT and Nrf2 KO animals. While many of the differences in fatty acid levels that were detected were subtle, results suggest that the differences in the expression of enzymes including SCD may have functional consequences in terms of fatty acid homeostasis.

The lipidomic analysis of livers from WT and Nrf2 KO mice also detailed in chapter 4 of this thesis provided preliminary evidence that the modulation of Nrf2 expression results in changes in the levels of some lipids, thus highlighting the potential for lipids to serve as biomarkers of Nrf2 activity. A comprehensive lipidomic analysis employing methods to identify the lipids that are altered in the absence of a functional Nrf2 gene could provide considerable insight. Furthermore, the analysis of serum alongside liver homogenate could

result in the identification of lipids or lipid metabolites with potential as preclinical and translational biomarkers of Nrf2 activity.

A number of the studies noted above employed CDDO derivatives in order to investigate the effect of Nrf2 induction on lipid pathways. These studies have shown that the compounds reduce mRNA levels of lipid synthesis enzymes in an Nrf2-dependent manner. In the iTRAQ analysis of livers from mice treated with a single dose of CDDO-Me detailed in chapter 5 of this thesis, no statistical difference was noted in the protein level of fatty acid synthesis enzymes when WT control and WT CDDO-Me-treated mice were compared. While the HFD studies using CDDO-Im treatment involved the chronic administration of the compound, the study by Yates *et al.* identified an Nrf2-dependent reduction in mRNA levels of FAS and ACL after a single dose (Yates *et al.*, 2009). This apparent discrepancy between the effects at the mRNA and protein level may reflect the different time-frames of expression of these biomolecules: a change in mRNA that occurs within the 24 hour period may not translate to the protein level within this same period. Furthermore, to see a decrease in protein level following reduced mRNA production is a function of protein degradation, and it is likely that proteins involved in fundamental cellular metabolism would be long-lived with long half-lives. Conversely, the turnover of proteins important for cytoprotection is likely to occur more quickly and hence an increase in these enzymes was detected in the study.

Future studies are needed in order to investigate the hepatic proteomic profile of mice following chronic CDDO-Me treatment. However, it may be necessary to investigate the use of an alternative vehicle control for the administration of the compound as evidence suggests that DMSO is associated with neurotoxicity (Hanslick *et al.*, 2009) and natural killer T cell infiltration of the liver (Masson *et al.*, 2008). These factors may be limiting in a chronic dosing study. However, such a study would also be better suited to oral drug administration and consequently this leaves scope for the compound, which is insoluble in aqueous conditions, to be administered as a suspension.

The characterisation of the hepatic effects of repeat CDDO-Me dosing is important for further defining the role of Nrf2 in the regulation of lipid metabolism, but also in the wider context of investigating pathways that are modulated by chronic Nrf2 activation, as this may provide evidence of other potential therapeutic targets for Nrf2 activation.

Conversely, such a study would also have utility in identifying potential toxicity risks. Furthermore, It is yet to be determined whether the Nrf2 cytoprotective response is down-regulated upon chronic stimulation of the pathway, and this would also be important were Nrf2 activation to be used for wider therapeutic applications or as a chemoprevention strategy.

While fatty acid synthesis was the lipid metabolism-associated process that emerged as most notably regulated by Nrf2 following the study described in chapter 2, other aspects of lipid metabolism were also highlighted in the proteomic analysis. Peroxisomal proteins were significantly represented amongst the proteins that were expressed at a constitutively higher level in Nrf2 KO mice (table 2.5) with peroxisomal straight-chain fatty acid beta-oxidation one of the pathways that was identified by MetaCore analysis as differentially regulated in WT and Nrf2 KO animals. Peroxisomes have a major role in fatty acid β-oxidation, a process involving the breakdown of fatty acids into 2 carbon chain units, which are subsequently converted into acetyl CoA. The acetyl CoA produced in the peroxisomes is transported back to the cytosol. Consequently, enzymes important in both the synthesis and breakdown of fatty acids were up-regulated in the livers of Nrf2 KO animals, further highlighting the complexity of the role of Nrf2 in the regulation of lipid metabolism.

When statistically significant fold-changes in protein expression identified by iTRAQ analysis in chapter 2 were considered, the protein that was expressed at the lowest level in Nrf2 KO mice when compared to WT was major urinary protein 6 (MUP6; 0.35 KO/WT), while the protein most induced in KO animals was epidermal fatty acid binding protein (FABP5; 2.97 KO/WT). The major urinary proteins (MUPs) are lipid binding proteins that function to transport pheromones. While the expression profile of MUPs is species and sex specific, most mammals have genes encoding MUPs, although there is no functional human MUP gene. In male mice MUPs are employed in territorial marking, mate attraction and other behavioural functions. The fatty acid binding proteins (FABPs) are involved in the transport, uptake and metabolism of fatty acids and are highly conserved across species.

Interestingly, as well as functioning as lipid transport proteins, both the MUPs and FABPs belong to the lipocalin class of proteins. The fact that the two proteins that were most disparately expressed in the presence and absence of Nrf2 have similar functions, serves to further emphasise the complex role that the transcription factor plays in the regulation of

lipid metabolism. It may be the case that the increase in FABP5 expression was at the expense of MUP6 synthesis, however further work is required in order to establish the relationship between the two proteins and the role that Nrf2 is playing.

6.4 Nrf2 and lipid regulation in health and disease

The mounting evidence that Nrf2 negatively regulates hepatic lipid metabolism, together with the fact that chronic triterpenoid administration has been shown to attenuate the fatty liver associated with the feeding of a HFD to mice, means that Nrf2 induction is an attractive strategy for the treatment of diseases associated with fatty liver. NAFLD and steatosis are conditions characterised by the accumulation of lipids in cytosolic vesicles. The feeding of a methionine- and choline-deficient (MCD) diet to mice is a model employed to stimulate the development of steatosis. Two studies have reported that the development of the condition is significantly accelerated in Nrf2 KO mice fed an MCD diet when compared to their WT counterparts (Chowdhry *et al.*, 2010; Sugimoto *et al.*, 2010). A third study also reporting an exacerbation in steatosis in Nrf2 KO mice, further employed a Keap1 knockdown (K1-kd) model to investigate the effect of Nrf2 activation in the MCD diet model (Zhang *et al.*, 2010). In the study, K1-kd was protective, with animals showing reduced steatosis when compared to WT mice.

However, while the evidence for the beneficial effects of Nrf2 activation in the treatment of lipid-associated hepatic diseases is growing, the role of the transcription factor in modulating lipid pathways in other tissues remains unclear. There is evidence for Nrf2 regulation of lipid metabolism in adipose tissue, although there is a lack of consensus as to whether Nrf2 promotes or inhibits lipid synthesis. *In vitro,* Nrf2-dependent inhibition of lipid droplet accumulation has been shown in a mouse embryonic fibroblast (MEF) model of adipocyte differentiation (Shin *et al.*, 2007), while *in vivo* evidence suggests that loss of Nrf2 expression promotes a low adipose tissue mass and the formation of small adipocytes, suggesting Nrf2 positively regulates lipid accumulation in adipose tissue (Pi *et al.*, 2010).

In the context of diseases associated with the perturbation of lipid homeostasis, the role of Nrf2 also remains unclear. In a streptozotocin (STZ)-induced mouse model of type I diabetes, hyperglycaemia was more marked in Nrf2 KO mice when compared to WT, while glucose tolerance was also found to be significantly reduced in basal Nrf2 KO animals (Aleksunes *et al.*, 2010), suggesting Nrf2 is protective in diabetes. However, in a study

using an apolipoprotein (apo) E-null background to investigate atherosclerosis, Nrf2 deficiency was suggested to be protective against the formation of atherosclerotic lesions. Nrf2 KO animals were reported to have lower levels of total plasma cholesterol and reduced expression of genes important for lipogenesis (Barajas *et al.*, 2011).

Results from these studies show that there is still considerable work to be done in order to understand the role that Nrf2 plays in the pathology of diseases in which lipid pathways are dysregulated, and to determine the potentially tissue-specific effects of the transcription factor in modulating lipid metabolism. Such work is becoming increasingly important as Nrf2 inducers move closer to the market.

6.5 Mass spectrometric techniques in biomarker discovery

iTRAQ analysis has proved to be a useful technique for hepatic proteomic profiling in the studies detailed in chapter 2 and chapter 5 of this thesis. The method also has great utility in terms of hypothesis generation, with the work described in chapter 2 resulting in the design of subsequent experiments to investigate the role of Nrf2 in hepatic lipid metabolism. However, iTRAQ is associated with a number of limitations. For example, there can be significant variation in the number of proteins detected in different runs, as was the case in the four runs of iTRAQ analysis 1 in chapter 2 (table 2.3). This variation can be the result of a range of factors associated with the preparation and storage of samples and sensitivity of the mass spectrometer. Such factors may also account for the differences in the proteins identified as Nrf2-regulated in iTRAQ analyses 1 and 2 in that chapter.

The high level of variability means that fold changes of less than 30% are unlikely to be validated as statistically significant, even though a small reduction in protein expression may have important biological consequences, particularly in the context of the threshold for toxicity. The value of iTRAQ is however enhanced when it is employed alongside methods that allow the functional grouping of proteins identified as differentially regulated between treatment groups. This type of systems analysis can be used to integrate small changes in a number of proteins to reveal novel biologically relevant pathways that are regulated by the target of interest.

The development of the LC-MS/MS method for the quantification of glutathione that was described in chapter 3 of this thesis was associated with a number of problems in the

accurate determination of GSSG levels. Calculations for GSSG concentrations were ultimately corrected based on the recovery values determined from solutions of known GSSG concentration. Such a method was valid in this instance because the recovery samples were run in the same assay as the WT and Nrf2 KO mouse livers that were analysed. However, in order for the method to be applicable to a wide range of studies it is important that the intra-assay precision levels are also determined. The running of quality control samples could also contribute to the validation of concentrations calculated in different runs.

Validation of the assay showed that it was considerably more accurate and precise in terms of GSH quantification. This suggests that there is scope to develop the assay to include other glutathione precursors including glycine, glutamate and the thiol containing amino acid, cysteine. Such a method could be used in order to further investigate the impact of Nrf2 modulation on the glutathione synthesis. Given the importance of Nrf2 in the regulation of glutathione, the pathway has the potential to provide biomarkers of Nrf2 activity as is highlighted by a paper detailing the use of the GSH analogue, ophthalmic acid as an oxidative stress biomarker (Soga *et al.*, 2006).

6.6 The identification of potential biomarkers

While biomarkers that are reflective of Nrf2 activity remain to be definitively characterised, some of the Nrf2 regulated proteins and processes that have been identified by work described in this thesis have the potential to fulfil the criteria defining an ideal biomarker that were set out in chapter 1 of this thesis. One of the key characteristics of a biomarker that can be used in the human population is that it can be assessed in a non-invasive manner. While the levels of proteins and lipids have been determined in liver homogenates in all of the investigations detailed in this thesis, there is the potential for the knowledge of Nrf2 hepatic protein regulation to translate into an assay that can be carried out in urine or serum samples. For example, the regulation of CYP2A5 by Nrf2 means that non-toxic substrates of the enzyme such as caffeine could be administered and the production of a metabolite assessed in urine in order to determine Nrf2 activity. Such assays can be implemented in both preclinical and clinical settings and are relatively cost effective.

The fact that the expression of proteins including CYP2A5 and ENTPD5 is regulated by Nrf2 at a constitutive and inducible level is particularly important in the context of biomarker discovery because it means that their levels of expression cover a wide dynamic range and so changes in their expression, or alterations in metabolites produced from a reaction catalysed by the enzyme, are likely to be easily detected.

The specificity and selectivity of a given biomarker is also an important factor to consider. While expression of proteins such as CYP2A5 is not liver specific, the relative contribution of the enzyme in different tissues to the metabolism of particular substrate could be characterised and the information used to validate the use of the biomarker. Given the important role of the liver in lipid homeostasis, lipid metabolites may have a greater propensity towards hepatic specificity however, this remains to be determined.

The work described in this thesis has investigated a range of Nrf2-regulated targets including proteins important for cytoprotection, glutathione levels and lipid metabolism pathways. Each of the processes that are regulated by Nrf2 has the potential to yield further markers of Nrf2 activity that can be used in preclinical models of oxidative stress and have potential applications in defining the importance of variability of Nrf2 in the human population.

6.7 Concluding remarks

In summary, the work described in this thesis has sought to identify potential candidate biomarkers of Nrf2 activity through the characterisation of the hepatic profile of mice in which the Keap1:Nrf2 pathway has been modulated. This aim has been achieved by addressing a series of key questions:

How do the constitutive hepatic proteomic profiles of WT and Nrf2 KO mice differ?
Can GSH and GSSG be reliable quantified in the livers of WT and Nrf2 KO animals, and given the differences noted in glutathione metabolism pathways in proteomic analysis, do levels of glutathione also differ in the livers of WT and Nrf2 KO animals?
Do the differences identified in levels of proteins related to lipid metabolism in chapter 2 translate to a functional difference in the hepatic lipid profile of WT and Nrf2 KO animals?
How does acute Nrf2 activation affect the hepatic proteomic profile of mice?

In seeking to answer each of these questions, the work detailed in this thesis has highlighted the important role that Nrf2 plays in regulating the constitutive hepatic phenotype and contributed to the growing evidence of a role for Nrf2 in the regulation of lipid metabolism. Ultimately, the most promising candidates for biomarker development that have emerged are those proteins that have been shown to be down-regulated in Nrf2 KO mouse livers, while also being up-regulated following acute Nrf2 activation because they have the greatest dynamic range of expression and are therefore likely to result in differences that are quantifiable. The need to define the importance of Nrf2 in the human population is becoming more pressing as Nrf2 inducers move closer to the market and research into the functions of Nrf2 identify further potential therapeutic applications for the modulation of Nrf2. It is hoped that the biomarkers of Nrf2 activity and the pathways identified as Nrf2-regulated in this thesis can contribute to understanding the role of Nrf2 in man and the importance of oxidative stress in drug safety.

Bibliography

Abu-Bakar A, Lamsa V, Arpiainen S, Moore MR, Lang MA, Hakkola J (2007). Regulation of CYP2A5 gene by the transcription factor nuclear factor (erythroid-derived 2)-like 2. *Drug Metab Dispos* **35**(5)**:** 787-794.

Acharya M, Lau-Cam CA (2010). Comparison of the protective actions of N-acetylcysteine, hypotaurine and taurine against acetaminophen-induced hepatotoxicity in the rat. *J Biomed Sci* **17 Suppl 1:** S35.

Ahmad R, Raina D, Meyer C, Kharbanda S, Kufe D (2006). Triterpenoid CDDO-Me blocks the NF-kappaB pathway by direct inhibition of IKKbeta on Cys-179. *J Biol Chem* **281**(47)**:** 35764-35769.

Ahmad R, Raina D, Meyer C, Kufe D (2008). Triterpenoid CDDO-methyl ester inhibits the Janus-activated kinase-1 (JAK1)-->signal transducer and activator of transcription-3 (STAT3) pathway by direct inhibition of JAK1 and STAT3. *Cancer Res* **68**(8)**:** 2920-2926.

Alam J, Wicks C, Stewart D, Gong P, Touchard C, Otterbein S*, et al.* (2000). Mechanism of heme oxygenase-1 gene activation by cadmium in MCF-7 mammary epithelial cells. Role of p38 kinase and Nrf2 transcription factor. *J Biol Chem* **275**(36)**:** 27694-27702.

Aleksunes LM, Goedken MJ, Rockwell CE, Thomale J, Manautou JE, Klaassen CD (2010a). Transcriptional regulation of renal cytoprotective genes by Nrf2 and its potential use as a therapeutic target to mitigate cisplatin-induced nephrotoxicity. *J Pharmacol Exp Ther* **335**(1)**:** 2-12.

Aleksunes LM, Reisman SA, Yeager RL, Goedken MJ, Klaassen CD (2010b). Nuclear factor erythroid 2-related factor 2 deletion impairs glucose tolerance and exacerbates hyperglycemia in type 1 diabetic mice. *J Pharmacol Exp Ther* **333**(1)**:** 140-151.

Ames BN (1983). Dietary carcinogens and anticarcinogens. Oxygen radicals and degenerative diseases. *Science* **221**(4617)**:** 1256-1264.

Anderson ME (1985). Determination of glutathione and glutathione disulfide in biological samples. *Methods Enzymol* **113:** 548-555.

Antoine DJ, Williams DP, Park BK (2008). Understanding the role of reactive metabolites in drug-induced hepatotoxicity: state of the science. *Expert Opin Drug Met* **4**(11)**:** 1415-1427.

Barajas B, Che N, Yin F, Rowshanrad A, Orozco LD, Gong KW*, et al.* (2011). NF-E2-related factor 2 promotes atherosclerosis by effects on plasma lipoproteins and cholesterol transport that overshadow antioxidant protection. *Arteriosclerosis, thrombosis, and vascular biology* **31**(1)**:** 58-66.

Begleiter A, Hewitt D, Maksymiuk AW, Ross DA, Bird RP (2006). A NAD(P)H:quinone oxidoreductase 1 polymorphism is a risk factor for human colon cancer. *Cancer Epidemiol Biomarkers Prev* **15**(12)**:** 2422-2426.

Bessems JG, Vermeulen NP (2001). Paracetamol (acetaminophen)-induced toxicity: molecular and biochemical mechanisms, analogues and protective approaches. *Crit Rev Toxicol* **31**(1)**:** 55-138.

Biomarkers Definitions Working Group B (2001). Biomarkers and surrogate endpoints: preferred definitions and conceptual framework. *Clin Pharmacol Ther* **69**(3)**:** 89-95.

Bjornsson E, Olsson R (2005). Outcome and prognostic markers in severe drug-induced liver disease. *Hepatology* **42**(2)**:** 481-489.

Bloom DA, Jaiswal AK (2003). Phosphorylation of Nrf2 at Ser40 by protein kinase C in response to antioxidants leads to the release of Nrf2 from INrf2, but is not required for Nrf2 stabilization/accumulation in the nucleus and transcriptional activation of antioxidant response element-mediated NAD(P)H:quinone oxidoreductase-1 gene expression. *J Biol Chem* **278**(45)**:** 44675-44682.

Bouligand J, Deroussent A, Paci A, Morizet J, Vassal G (2006). Liquid chromatography-tandem mass spectrometry assay of reduced and oxidized glutathione and main precursors in mice liver. *Journal of chromatography. B, Analytical technologies in the biomedical and life sciences* **832**(1)**:** 67-74.

Bradford MM (1976). A rapid and sensitive method for the quantitation of microgram quantities of protein utilizing the principle of protein-dye binding. *Analytical biochemistry* **72:** 248-254.

Bruss MD, Khambatta CF, Ruby MA, Aggarwal I, Hellerstein MK (2010). Calorie restriction increases fatty acid synthesis and whole body fat oxidation rates. *American journal of physiology. Endocrinology and metabolism* **298**(1)**:** E108-116.

Camera E, Picardo M (2002). Analytical methods to investigate glutathione and related compounds in biological and pathological processes. *Journal of chromatography. B, Analytical technologies in the biomedical and life sciences* **781**(1-2)**:** 181-206.

Camera E, Rinaldi M, Briganti S, Picardo M, Fanali S (2001). Simultaneous determination of reduced and oxidized glutathione in peripheral blood mononuclear cells by liquid chromatography-electrospray mass spectrometry. *Journal of chromatography. B, Biomedical sciences and applications* **757**(1)**:** 69-78.

Chan K, Han XD, Kan YW (2001). An important function of Nrf2 in combating oxidative stress: detoxification of acetaminophen. *Proc Natl Acad Sci U S A* **98**(8)**:** 4611-4616.

Chan K, Lu R, Chang JC, Kan YW (1996). NRF2, a member of the NFE2 family of transcription factors, is not essential for murine erythropoiesis, growth, and development. *Proc Natl Acad Sci U S A* **93**(24)**:** 13943-13948.

Chan TS, Wilson JX, O'Brien PJ (2004). Coenzyme Q cytoprotective mechanisms. *Methods Enzymol* **382:** 89-104.

Chanas SA, Jiang Q, McMahon M, McWalter GK, McLellan LI, Elcombe CR*, et al.* (2002). Loss of the Nrf2 transcription factor causes a marked reduction in constitutive and inducible

expression of the glutathione S-transferase Gsta1, Gsta2, Gstm1, Gstm2, Gstm3 and Gstm4 genes in the livers of male and female mice. *Biochem J* **365**(Pt 2)**:** 405-416.

Chang TK, Abbott FS (2006). Oxidative stress as a mechanism of valproic acid-associated hepatotoxicity. *Drug Metab Rev* **38**(4)**:** 627-639.

Cho HY, Reddy SP, Yamamoto M, Kleeberger SR (2004). The transcription factor NRF2 protects against pulmonary fibrosis. *FASEB J* **18**(11)**:** 1258-1260.

Chorley BN, Campbell MR, Wang X, Karaca M, Sambandan D, Bangura F*, et al.* (2012). Identification of novel NRF2-regulated genes by ChIP-Seq: influence on retinoid X receptor alpha. *Nucleic Acids Res* **40**(15)**:** 7416-7429.

Chowdhry S, Nazmy MH, Meakin PJ, Dinkova-Kostova AT, Walsh SV, Tsujita T*, et al.* (2010). Loss of Nrf2 markedly exacerbates nonalcoholic steatohepatitis. *Free Radic Biol Med* **48**(2)**:** 357-371.

Coen M, Holmes E, Lindon JC, Nicholson JK (2008). NMR-based metabolic profiling and metabonomic approaches to problems in molecular toxicology. *Chem Res Toxicol* **21**(1)**:** 9-27.

Cousins RJ, Aydemir TB, Lichten LA (2010). Plenary Lecture 2: Transcription factors, regulatory elements and nutrient-gene communication. *The Proceedings of the Nutrition Society* **69**(1)**:** 91-94.

Crunkhorn S (2012). Deal watch: Abbott boosts investment in NRF2 activators for reducing oxidative stress. *Nat Rev Drug Discov* **11**(2)**:** 96.

Cullinan SB, Gordan JD, Jin J, Harper JW, Diehl JA (2004). The Keap1-BTB protein is an adaptor that bridges Nrf2 to a Cul3-based E3 ligase: oxidative stress sensing by a Cul3-Keap1 ligase. *Mol Cell Biol* **24**(19)**:** 8477-8486.

D'Agostino LA, Lam KP, Lee R, Britz-McKibbin P (2011). Comprehensive plasma thiol redox status determination for metabolomics. *Journal of proteome research* **10**(2)**:** 592-603.

Dahlin DC, Miwa GT, Lu AY, Nelson SD (1984). N-acetyl-p-benzoquinone imine: a cytochrome P-450-mediated oxidation product of acetaminophen. *Proc Natl Acad Sci U S A* **81**(5)**:** 1327-1331.

Dai Y, Cederbaum AI (1995). Cytotoxicity of acetaminophen in human cytochrome P4502E1-transfected HepG2 cells. *J Pharmacol Exp Ther* **273**(3)**:** 1497-1505.

Dhalla NS, Temsah RM, Netticadan T (2000). Role of oxidative stress in cardiovascular diseases. *J Hypertens* **18**(6)**:** 655-673.

DiMasi JA, Hansen RW, Grabowski HG (2003). The price of innovation: new estimates of drug development costs. *Journal of health economics* **22**(2)**:** 151-185.

Dinkova-Kostova AT, Holtzclaw WD, Cole RN, Itoh K, Wakabayashi N, Katoh Y*, et al.* (2002). Direct evidence that sulfhydryl groups of Keap1 are the sensors regulating induction of

phase 2 enzymes that protect against carcinogens and oxidants. *Proc Natl Acad Sci U S A* **99**(18)**:** 11908-11913.

Dinkova-Kostova AT, Liby KT, Stephenson KK, Holtzclaw WD, Gao X, Suh N*, et al.* (2005). Extremely potent triterpenoid inducers of the phase 2 response: correlations of protection against oxidant and inflammatory stress. *Proc Natl Acad Sci U S A* **102**(12)**:** 4584-4589.

Dykens JA, Jamieson JD, Marroquin LD, Nadanaciva S, Xu JJ, Dunn MC*, et al.* (2008). In vitro assessment of mitochondrial dysfunction and cytotoxicity of nefazodone, trazodone, and buspirone. *Toxicol Sci* **103**(2)**:** 335-345.

Ellis DI, Dunn WB, Griffin JL, Allwood JW, Goodacre R (2007). Metabolic fingerprinting as a diagnostic tool. *Pharmacogenomics* **8**(9)**:** 1243-1266.

Enomoto A, Itoh K, Nagayoshi E, Haruta J, Kimura T, O'Connor T*, et al.* (2001). High sensitivity of Nrf2 knockout mice to acetaminophen hepatotoxicity associated with decreased expression of ARE-regulated drug metabolizing enzymes and antioxidant genes. *Toxicol Sci* **59**(1)**:** 169-177.

Esau C, Davis S, Murray SF, Yu XX, Pandey SK, Pear M*, et al.* (2006). miR-122 regulation of lipid metabolism revealed by in vivo antisense targeting. *Cell Metab* **3**(2)**:** 87-98.

Fang M, Shen Z, Huang S, Zhao L, Chen S, Mak TW*, et al.* (2010). The ER UDPase ENTPD5 promotes protein N-glycosylation, the Warburg effect, and proliferation in the PTEN pathway. *Cell* **143**(5)**:** 711-724.

FDA - Food and Drug Adminsitration (2001). Guidance for Industry Bioanalytical Method Validation.

FDA - Food and Drud Administration (2009). Guidance for Industry Drug-Induced Liver Injury: Premarketing Clinical Evaluation: U.S. Department of Health and Human Services, Food and Drug Administration.

Ferret PJ, Hammoud R, Tulliez M, Tran A, Trebeden H, Jaffray P*, et al.* (2001). Detoxification of reactive oxygen species by a nonpeptidyl mimic of superoxide dismutase cures acetaminophen-induced acute liver failure in the mouse. *Hepatology* **33**(5)**:** 1173-1180.

Fitzpatrick AM, Stephenson ST, Hadley GR, Burwell L, Penugonda M, Simon DM*, et al.* (2011). Thiol redox disturbances in children with severe asthma are associated with posttranslational modification of the transcription factor nuclear factor (erythroid-derived 2)-like 2. *The Journal of allergy and clinical immunology* **127**(6)**:** 1604-1611.

Forsythe CE, Phinney SD, Fernandez ML, Quann EE, Wood RJ, Bibus DM*, et al.* (2008). Comparison of low fat and low carbohydrate diets on circulating fatty acid composition and markers of inflammation. *Lipids* **43**(1)**:** 65-77.

Franklin CC, Backos DS, Mohar I, White CC, Forman HJ, Kavanagh TJ (2009). Structure, function, and post-translational regulation of the catalytic and modifier subunits of glutamate cysteine ligase. *Molecular aspects of medicine* **30**(1-2)**:** 86-98.

Furukawa M, Xiong Y (2005). BTB protein Keap1 targets antioxidant transcription factor Nrf2 for ubiquitination by the Cullin 3-Roc1 ligase. *Mol Cell Biol* **25**(1)**:** 162-171.

Gao SS, Choi BM, Chen XY, Zhu RZ, Kim Y, So H*, et al.* (2010). Kaempferol suppresses cisplatin-induced apoptosis via inductions of heme oxygenase-1 and glutamate-cysteine ligase catalytic subunit in HEI-OC1 cell. *Pharm Res* **27**(2)**:** 235-245.

Gilbert HF (1995). Thiol/disulfide exchange equilibria and disulfide bond stability. *Methods Enzymol* **251:** 8-28.

Giustarini D, Dalle-Donne I, Colombo R, Milzani A, Rossi R (2003). An improved HPLC measurement for GSH and GSSG in human blood. *Free Radic Biol Med* **35**(11)**:** 1365-1372.

Green RM, Flamm S (2002). AGA technical review on the evaluation of liver chemistry tests. *Gastroenterology* **123**(4)**:** 1367-1384.

Griffith OW (1980). Determination of glutathione and glutathione disulfide using glutathione reductase and 2-vinylpyridine. *Analytical biochemistry* **106**(1)**:** 207-212.

Guan X, Hoffman B, Dwivedi C, Matthees DP (2003). A simultaneous liquid chromatography/mass spectrometric assay of glutathione, cysteine, homocysteine and their disulfides in biological samples. *Journal of pharmaceutical and biomedical analysis* **31**(2)**:** 251-261.

Hakooz N, Hamdan I (2007). Effects of dietary broccoli on human in vivo caffeine metabolism: a pilot study on a group of Jordanian volunteers. *Current drug metabolism* **8**(1)**:** 9-15.

Han S, Choi S, Chun YJ, Yun CH, Lee CH, Shin HJ*, et al.* (2012). Functional characterization of allelic variants of polymorphic human cytochrome P450 2A6 (CYP2A6*5, *7, *8, *18, *19, and *35). *Biol Pharm Bull* **35**(3)**:** 394-399.

Hanslick JL, Lau K, Noguchi KK, Olney JW, Zorumski CF, Mennerick S*, et al.* (2009). Dimethyl sulfoxide (DMSO) produces widespread apoptosis in the developing central nervous system. *Neurobiology of disease* **34**(1)**:** 1-10

Hargus SJ, Martin BM, George JW, Pohl LR (1995). Covalent modification of rat liver dipeptidyl peptidase IV (CD26) by the nonsteroidal anti-inflammatory drug diclofenac. *Chem Res Toxicol* **8**(8)**:** 993-996.

Haridas V, Hanausek M, Nishimura G, Soehnge H, Gaikwad A, Narog M*, et al.* (2004). Triterpenoid electrophiles (avicins) activate the innate stress response by redox regulation of a gene battery. *The Journal of clinical investigation* **113**(1)**:** 65-73.

Hazelton GA, Hjelle JJ, Klaassen CD (1986). Effects of cysteine pro-drugs on acetaminophen-induced hepatotoxicity. *J Pharmacol Exp Ther* **237**(1)**:** 341-349.

He X, Chen MG, Ma Q (2008). Activation of Nrf2 in defense against cadmium-induced oxidative stress. *Chem Res Toxicol* **21**(7)**:** 1375-1383.

He X, Lin GX, Chen MG, Zhang JX, Ma Q (2007). Protection against chromium (VI)-induced oxidative stress and apoptosis by Nrf2. Recruiting Nrf2 into the nucleus and disrupting the nuclear Nrf2/Keap1 association. *Toxicol Sci* **98**(1)**:** 298-309.

Honda T, Rounds BV, Bore L, Favaloro FG, Jr., Gribble GW, Suh N*, et al.* (1999). Novel synthetic oleanane triterpenoids: a series of highly active inhibitors of nitric oxide production in mouse macrophages. *Bioorg Med Chem Lett* **9**(24)**:** 3429-3434.

Honda T, Rounds BV, Gribble GW, Suh N, Wang Y, Sporn MB (1998). Design and synthesis of 2-cyano-3,12-dioxoolean-1,9-dien-28-oic acid, a novel and highly active inhibitor of nitric oxide production in mouse macrophages. *Bioorg Med Chem Lett* **8**(19)**:** 2711-2714.

Hong DS, Kurzrock R, Supko JG, He X, Naing A, Wheler J*, et al.* (2012). A Phase I First-in-Human Trial of Bardoxolone Methyl in Patients with Advanced Solid Tumors and Lymphomas. *Clin Cancer Res* **18**(12)**:** 3396-3406.

Hong F, Sekhar KR, Freeman ML, Liebler DC (2005). Specific patterns of electrophile adduction trigger Keap1 ubiquitination and Nrf2 activation. *J Biol Chem* **280**(36)**:** 31768-31775.

Hu R, Xu C, Shen G, Jain MR, Khor TO, Gopalkrishnan A*, et al.* (2006a). Gene expression profiles induced by cancer chemopreventive isothiocyanate sulforaphane in the liver of C57BL/6J mice and C57BL/6J/Nrf2 (-/-) mice. *Cancer Lett* **243**(2)**:** 170-192.

Hu R, Xu C, Shen G, Jain MR, Khor TO, Gopalkrishnan A*, et al.* (2006b). Identification of Nrf2-regulated genes induced by chemopreventive isothiocyanate PEITC by oligonucleotide microarray. *Life Sci* **79**(20)**:** 1944-1955.

Huang HC, Nguyen T, Pickett CB (2002). Phosphorylation of Nrf2 at Ser-40 by protein kinase C regulates antioxidant response element-mediated transcription. *J Biol Chem* **277**(45)**:** 42769-42774.

Huang HC, Nguyen T, Pickett CB (2000). Regulation of the antioxidant response element by protein kinase C-mediated phosphorylation of NF-E2-related factor 2. *Proc Natl Acad Sci U S A* **97**(23)**:** 12475-12480.

Huang MT, Ho CT, Wang ZY, Ferraro T, Lou YR, Stauber K*, et al.* (1994). Inhibition of skin tumorigenesis by rosemary and its constituents carnosol and ursolic acid. *Cancer research* **54**(3)**:** 701-708.

Huang J, Tabbi-Anneni I, Gunda V, Wang L (2010). Transcription factor Nrf2 regulates SHP and lipogenic gene expression in hepatic lipid metabolism. *American journal of physiology. Gastrointestinal and liver physiology* **299**(6)**:** G1211-1221.

Hubbs AF, Benkovic SA, Miller DB, O'Callaghan JP, Battelli L, Schwegler-Berry D*, et al.* (2007). Vacuolar leukoencephalopathy with widespread astrogliosis in mice lacking transcription factor Nrf2. *The American journal of pathology* **170**(6)**:** 2068-2076.

Hubner RH, Schwartz JD, De Bishnu P, Ferris B, Omberg L, Mezey JG*, et al.* (2009). Coordinate control of expression of Nrf2-modulated genes in the human small airway epithelium is highly responsive to cigarette smoking. *Mol Med* **15**(7-8)**:** 203-219.

Iliopoulos D, Drosatos K, Hiyama Y, Goldberg IJ, Zannis VI (2010). MicroRNA-370 controls the expression of microRNA-122 and Cpt1alpha and affects lipid metabolism. *Journal of lipid research* **51**(6)**:** 1513-1523.

Ito Y, Pandey P, Place A, Sporn MB, Gribble GW, Honda T*, et al.* (2000). The novel triterpenoid 2-cyano-3,12-dioxoolean-1,9-dien-28-oic acid induces apoptosis of human myeloid leukemia cells by a caspase-8-dependent mechanism. *Cell Growth Differ* **11**(5)**:** 261-267.

Itoh K, Chiba T, Takahashi S, Ishii T, Igarashi K, Katoh Y*, et al.* (1997). An Nrf2/small Maf heterodimer mediates the induction of phase II detoxifying enzyme genes through antioxidant response elements. *Biochem Biophys Res Commun* **236**(2)**:** 313-322.

Itoh K, Wakabayashi N, Katoh Y, Ishii T, Igarashi K, Engel JD*, et al.* (1999). Keap1 represses nuclear activation of antioxidant responsive elements by Nrf2 through binding to the amino-terminal Neh2 domain. *Genes & development* **13**(1)**:** 76-86.

Itoh K, Wakabayashi N, Katoh Y, Ishii T, O'Connor T, Yamamoto M (2003). Keap1 regulates both cytoplasmic-nuclear shuttling and degradation of Nrf2 in response to electrophiles. *Genes Cells* **8**(4)**:** 379-391.

Iwasaki Y, Hoshi M, Ito R, Saito K, Nakazawa H (2006). Analysis of glutathione and glutathione disulfide in human saliva using hydrophilic interaction chromatography with mass spectrometry. *Journal of chromatography. B, Analytical technologies in the biomedical and life sciences* **839**(1-2)**:** 74-79.

Jackson SJ, Singletary KW, Venema RC (2007). Sulforaphane suppresses angiogenesis and disrupts endothelial mitotic progression and microtubule polymerization. *Vascul Pharmacol* **46**(2)**:** 77-84.

Jain AK, Bloom DA, Jaiswal AK (2005). Nuclear import and export signals in control of Nrf2. *J Biol Chem* **280**(32)**:** 29158-29168.

Jaiswal AK (2004). Nrf2 signaling in coordinated activation of antioxidant gene expression. *Free Radic Biol Med* **36**(10)**:** 1199-1207.

Jaiswal AK (2000). Regulation of genes encoding NAD(P)H:quinone oxidoreductases. *Free Radic Biol Med* **29**(3-4)**:** 254-262.

Kalgutkar AS, Vaz AD, Lame ME, Henne KR, Soglia J, Zhao SX*, et al.* (2005). Bioactivation of the nontricyclic antidepressant nefazodone to a reactive quinone-imine species in human liver microsomes and recombinant cytochrome P450 3A4. *Drug Metab Dispos* **33**(2)**:** 243-253.

Katoh Y, Itoh K, Yoshida E, Miyagishi M, Fukamizu A, Yamamoto M (2001). Two domains of Nrf2 cooperatively bind CBP, a CREB binding protein, and synergistically activate transcription. *Genes Cells* **6**(10)**:** 857-868.

Katz MH (2003). Multivariable analysis: a primer for readers of medical research. *Ann Intern Med* **138**(8)**:** 644-650.

Kensler TW, Wakabayashi N, Biswal S (2007). Cell survival responses to environmental stresses via the Keap1-Nrf2-ARE pathway. *Annu Rev Pharmacol Toxicol* **47:** 89-116.

Khor TO, Huang MT, Kwon KH, Chan JY, Reddy BS, Kong AN (2006). Nrf2-deficient mice have an increased susceptibility to dextran sulfate sodium-induced colitis. *Cancer Res* **66**(24)**:** 11580-11584.

Kitteringham NR, Abdullah A, Walsh J, Randle L, Jenkins RE, Sison R*, et al.* (2010). Proteomic analysis of Nrf2 deficient transgenic mice reveals cellular defence and lipid metabolism as primary Nrf2-dependent pathways in the liver. *J Proteomics* **73**(8)**:** 1612-1631.

Kitteringham NR, Powell H, Clement YN, Dodd CC, Tettey JNA, Pirmohamed M*, et al.* (2000). Hepatocellular response to chemical stress in CD-1 mice: Induction of early genes and gamma-glutamylcysteine synthetase. *Hepatology* **32**(2)**:** 321-333.

Kobayashi A, Kang MI, Okawa H, Ohtsuji M, Zenke Y, Chiba T*, et al.* (2004). Oxidative stress sensor Keap1 functions as an adaptor for Cul3-based E3 ligase to regulate proteasomal degradation of Nrf2. *Mol Cell Biol* **24**(16)**:** 7130-7139.

Kobayashi M, Yamamoto M (2006). Nrf2-Keap1 regulation of cellular defense mechanisms against electrophiles and reactive oxygen species. *Adv Enzyme Regul* **46:** 113-140.

Konopleva M, Tsao T, Estrov Z, Lee RM, Wang RY, Jackson CE*, et al.* (2004). The synthetic triterpenoid 2-cyano-3,12-dioxooleana-1,9-dien-28-oic acid induces caspase-dependent and -independent apoptosis in acute myelogenous leukemia. *Cancer Res* **64**(21)**:** 7927-7935.

Korashy HM, El-Kadi AO (2008). NF-kappaB and AP-1 are key signaling pathways in the modulation of NAD(P)H:quinone oxidoreductase 1 gene by mercury, lead, and copper. *J Biochem Mol Toxicol* **22**(4)**:** 274-283.

Kostrubsky SE, Strom SC, Kalgutkar AS, Kulkarni S, Atherton J, Mireles R*, et al.* (2006). Inhibition of hepatobiliary transport as a predictive method for clinical hepatotoxicity of nefazodone. *Toxicol Sci* **90**(2)**:** 451-459.

Kretz-Rommel A, Boelsterli UA (1993). Diclofenac covalent protein binding is dependent on acyl glucuronide formation and is inversely related to P450-mediated acute cell injury in cultured rat hepatocytes. *Toxicol Appl Pharmacol* **120**(1)**:** 155-161.

Kwak MK, Itoh K, Yamamoto M, Kensler TW (2002). Enhanced expression of the transcription factor Nrf2 by cancer chemopreventive agents: role of antioxidant response element-like sequences in the nrf2 promoter. *Mol Cell Biol* **22**(9)**:** 2883-2892.

Kwak MK, Itoh K, Yamamoto M, Sutter TR, Kensler TW (2001). Role of transcription factor Nrf2 in the induction of hepatic phase 2 and antioxidative enzymes in vivo by the cancer chemoprotective agent, 3H-1, 2-dimethiole-3-thione. *Mol Med* **7**(2)**:** 135-145.

Kwak MK, Kensler TW (2010). Targeting NRF2 signaling for cancer chemoprevention. *Toxicol Appl Pharmacol* **244**(1)**:** 66-76.

Lamle J, Marhenke S, Borlak J, von Wasielewski R, Eriksson CJ, Geffers R*, et al.* (2008). Nuclear factor-eythroid 2-related factor 2 prevents alcohol-induced fulminant liver injury. *Gastroenterology* **134**(4)**:** 1159-1168.

Lamsa V, Levonen AL, Leinonen H, Yla-Herttuala S, Yamamoto M, Hakkola J (2010). Cytochrome P450 2A5 constitutive expression and induction by heavy metals is dependent on redox-sensitive transcription factor Nrf2 in liver. *Chem Res Toxicol* **23**(5)**:** 977-985.

Lapillonne H, Konopleva M, Tsao T, Gold D, McQueen T, Sutherland RL*, et al.* (2003). Activation of peroxisome proliferator-activated receptor gamma by a novel synthetic triterpenoid 2-cyano-3,12-dioxooleana-1,9-dien-28-oic acid induces growth arrest and apoptosis in breast cancer cells. *Cancer Res* **63**(18)**:** 5926-5939.

Larson AM, Polson J, Fontana RJ, Davern TJ, Lalani E, Hynan LS*, et al.* (2005). Acetaminophen-induced acute liver failure: results of a United States multicenter, prospective study. *Hepatology* **42**(6)**:** 1364-1372.

Le Belle JE, Harris NG, Williams SR, Bhakoo KK (2002). A comparison of cell and tissue extraction techniques using high-resolution 1H-NMR spectroscopy. *NMR in biomedicine* **15**(1)**:** 37-44.

Lee WM (2003). Drug-induced hepatotoxicity. *N Engl J Med* **349**(5)**:** 474-485

Lee JM, Hanson JM, Chu WA, Johnson JA (2001). Phosphatidylinositol 3-kinase, not extracellular signal-regulated kinase, regulates activation of the antioxidant-responsive element in IMR-32 human neuroblastoma cells. *J Biol Chem* **276**(23)**:** 20011-20016.

Lee JI, Kang J, Stipanuk MH (2006). Differential regulation of glutamate-cysteine ligase subunit expression and increased holoenzyme formation in response to cysteine deprivation. *Biochem J* **393**(Pt 1)**:** 181-190.

Leslie EM, Bowers RJ, Deeley RG, Cole SP (2003). Structural requirements for functional interaction of glutathione tripeptide analogs with the human multidrug resistance protein 1 (MRP1) (vol 304, pg 643, 2003). *J Pharmacol Exp Ther* **305**(2)**:** 798-798.

Li M, Chiu JF, Kelsen A, Lu SC, Fukagawa NK (2009). Identification and characterization of an Nrf2-mediated ARE upstream of the rat glutamate cysteine ligase catalytic subunit gene (GCLC). *J Cell Biochem* **107**(5)**:** 944-954.

Liby K, Hock T, Yore MM, Suh N, Place AE, Risingsong R*, et al.* (2005). The synthetic triterpenoids, CDDO and CDDO-imidazolide, are potent inducers of heme oxygenase-1 and Nrf2/ARE signaling. *Cancer Res* **65**(11)**:** 4789-4798.

Liby K, Royce DB, Williams CR, Risingsong R, Yore MM, Honda T*, et al.* (2007). The synthetic triterpenoids CDDO-methyl ester and CDDO-ethyl amide prevent lung cancer induced by vinyl carbamate in A/J mice. *Cancer Res* **67**(6)**:** 2414-2419.

Liby K, Voong N, Williams CR, Risingsong R, Royce DB, Honda T*, et al.* (2006). The synthetic triterpenoid CDDO-Imidazolide suppresses STAT phosphorylation and induces apoptosis in myeloma and lung cancer cells. *Clin Cancer Res* **12**(14 Pt 1)**:** 4288-4293.

Lister A, Nedjadi T, Kitteringham NR, Campbell F, Costello E, Lloyd B*, et al.* (2011). Nrf2 is overexpressed in pancreatic cancer: implications for cell proliferation and therapy. *Mol Cancer* **10:** 37.

Liu J, Wu Q, Lu YF, Pi J (2008). New insights into generalized hepatoprotective effects of oleanolic acid: key roles of metallothionein and Nrf2 induction. *Biochemical pharmacology* **76**(7)**:** 922-928.

Lores Arnaiz S, Llesuy S, Cutrin JC, Boveris A (1995). Oxidative stress by acute acetaminophen administration in mouse liver. *Free Radic Biol Med* **19**(3)**:** 303-310.

Loughlin AF, Skiles GL, Alberts DW, Schaefer WH (2001). An ion exchange liquid chromatography/mass spectrometry method for the determination of reduced and oxidized glutathione and glutathione conjugates in hepatocytes. *Journal of pharmaceutical and biomedical analysis* **26**(1)**:** 131-142.

Lowry OH, Rosebrough NJ, Farr AL, Randall RJ (1951). Protein measurement with the Folin phenol reagent. *J Biol Chem* **193**(1)**:** 265-275.

Lu H, Cui W, Klaassen CD (2011). Nrf2 protects against 2,3,7,8-tetrachlorodibenzo-p-dioxin (TCDD)-induced oxidative injury and steatohepatitis. *Toxicol Appl Pharmacol* **256**(2)**:** 122-135.

Lu Y, Gong P, Cederbaum AI (2008). Pyrazole induced oxidative liver injury independent of CYP2E1/2A5 induction due to Nrf2 deficiency. *Toxicology* **252**(1-3)**:** 9-16.

Luo Y, Eggler AL, Liu D, Liu G, Mesecar AD, van Breemen RB (2007). Sites of alkylation of human Keap1 by natural chemoprevention agents. *J Am Soc Mass Spectrom* **18**(12)**:** 2226-2232.

Manyike PT, Kharasch ED, Kalhorn TF, Slattery JT (2000). Contribution of CYP2E1 and CYP3A to acetaminophen reactive metabolite formation. *Clin Pharmacol Ther* **67**(3)**:** 275-282.

Marrer E, Dieterle F (2010). Impact of biomarker development on drug safety assessment. *Toxicol Appl Pharmacol* **243**(2)**:** 167-179.

Masson MJ, Carpenter LD, Graf ML, Pohl LR (2008). Pathogenic role of natural killer T and natural killer cells in acetaminophen-induced liver injury in mice is dependent on the presence of dimethyl sulfoxide. *Hepatology* **48**(3)**:** 889-897.

Marzec JM, Christie JD, Reddy SP, Jedlicka AE, Vuong H, Lanken PN*, et al.* (2007). Functional polymorphisms in the transcription factor NRF2 in humans increase the risk of acute lung injury. *FASEB J* **21**(9)**:** 2237-2246.

McMahon M, Itoh K, Yamamoto M, Chanas SA, Henderson CJ, McLellan LI*, et al.* (2001). The Cap'n'Collar basic leucine zipper transcription factor Nrf2 (NF-E2 p45-related factor 2) controls both constitutive and inducible expression of intestinal detoxification and glutathione biosynthetic enzymes. *Cancer Res* **61**(8)**:** 3299-3307.

McMahon M, Itoh K, Yamamoto M, Hayes JD (2003). Keap1-dependent proteasomal degradation of transcription factor Nrf2 contributes to the negative regulation of antioxidant response element-driven gene expression. *J Biol Chem* **278**(24)**:** 21592-21600.

Menzel HJ, Sarmanova J, Soucek P, Berberich R, Grunewald K, Haun M*, et al.* (2004). Association of NQO1 polymorphism with spontaneous breast cancer in two independent populations. *Br J Cancer* **90**(10)**:** 1989-1994.

Miller JA (1970). Carcinogenesis by chemicals: an overview--G. H. A. Clowes memorial lecture. *Cancer Res* **30**(3)**:** 559-576.

Moi P, Chan K, Asunis I, Cao A, Kan YW (1994). Isolation of NF-E2-related factor 2 (Nrf2), a NF-E2-like basic leucine zipper transcriptional activator that binds to the tandem NF-E2/AP1 repeat of the beta-globin locus control region. *Proc Natl Acad Sci U S A* **91**(21)**:** 9926-9930.

Moinova HR, Mulcahy RT (1999). Up-regulation of the human gamma-glutamylcysteine synthetase regulatory subunit gene involves binding of Nrf-2 to an electrophile responsive element. *Biochem Biophys Res Commun* **261**(3)**:** 661-668.

Nair S, Xu C, Shen G, Hebbar V, Gopalakrishnan A, Hu R*, et al.* (2007). Toxicogenomics of endoplasmic reticulum stress inducer tunicamycin in the small intestine and liver of Nrf2 knockout and C57BL/6J mice. *Toxicol Lett* **168**(1)**:** 21-39.

Nair S, Xu C, Shen G, Hebbar V, Gopalakrishnan A, Hu R*, et al.* (2006). Pharmacogenomics of phenolic antioxidant butylated hydroxyanisole (BHA) in the small intestine and liver of Nrf2 knockout and C57BL/6J mice. *Pharm Res* **23**(11)**:** 2621-2637.

Nelson SD (1995). Mechanisms of the formation and disposition of reactive metabolites that can cause acute liver injury. *Drug Metab Rev* **27**(1-2)**:** 147-177.

Nioi P, McMahon M, Itoh K, Yamamoto M, Hayes JD (2003). Identification of a novel Nrf2-regulated antioxidant response element (ARE) in the mouse NAD(P)H:quinone oxidoreductase 1 gene: reassessment of the ARE consensus sequence. *Biochem J* **374**(Pt 2)**:** 337-348.

Nishino H, Nishino A, Takayasu J, Hasegawa T, Iwashima A, Hirabayashi K*, et al.* (1988). Inhibition of the tumor-promoting action of 12-O-tetradecanoylphorbol-13-acetate by some oleanane-type triterpenoid compounds. *Cancer Res* **48**(18)**:** 5210-5215.

Nurfadhlina M, Foong K, Teh LK, Tan SC, Mohd Zaki S, Ismail R (2006). CYP2A6 polymorphisms in Malays, Chinese and Indians. *Xenobiotica* **36**(8)**:** 684-692.

O'Brien PJ, Slaughter MR, Swain A, Birmingham JM, Greenhill RW, Elcock F*, et al.* (2000). Repeated acetaminophen dosing in rats: adaptation of hepatic antioxidant system. *Hum Exp Toxicol* **19**(5)**:** 277-283.

Okawa H, Motohashi H, Kobayashi A, Aburatani H, Kensler TW, Yamamoto M (2006). Hepatocyte-specific deletion of the keap1 gene activates Nrf2 and confers potent resistance against acute drug toxicity. *Biochem Biophys Res Commun* **339**(1)**:** 79-88.

Osburn WO, Yates MS, Dolan PD, Chen S, Liby KT, Sporn MB*, et al.* (2008). Genetic or pharmacologic amplification of nrf2 signaling inhibits acute inflammatory liver injury in mice. *Toxicol Sci* **104**(1)**:** 218-227.

Ozer J, Ratner M, Shaw M, Bailey W, Schomaker S (2008). The current state of serum biomarkers of hepatotoxicity. *Toxicology* **245**(3)**:** 194-205.

Park BK, Kitteringham NR, Maggs JL, Pirmohamed M, Williams DP (2005a). The role of metabolic activation in drug-induced hepatotoxicity. *Annu Rev Pharmacol Toxicol* **45:** 177-202.

Park BK, Kitteringham NR, Maggs JL, Pirmohamed M, Williams DP (2005b). The role of metabolic activation in drug-induced hepatotoxicity. *Annu Rev Pharmacol* **45:** 177-202.

Park BK, Pirmohamed M, Kitteringham NR (1995). The role of cytochrome P450 enzymes in hepatic and extrahepatic human drug toxicity. *Pharmacol Ther* **68**(3)**:** 385-424.

Park HJ, Lee YW, Lee SK (2004). Baicalin induces NAD(P)H:quinone reductase through the transactivation of AP-1 and NF-kappaB in Hepa 1c1c7 cells. *European journal of cancer prevention : the official journal of the European Cancer Prevention Organisation* **13**(6)**:** 521-528.

Park HM, Cho JM, Lee HR, Shim GS, Kwak MK (2008). Renal protection by 3H-1,2-dithiole-3-thione against cisplatin through the Nrf2-antioxidant pathway. *Biochem Pharmacol* **76**(5)**:** 597-607.

Pearson KJ, Lewis KN, Price NL, Chang JW, Perez E, Cascajo MV*, et al.* (2008). Nrf2 mediates cancer protection but not prolongevity induced by caloric restriction. *Proc Natl Acad Sci U S A* **105**(7)**:** 2325-2330.

Pergola PE, Raskin P, Toto RD, Meyer CJ, Huff JW, Grossman EB*, et al.* (2011). Bardoxolone methyl and kidney function in CKD with type 2 diabetes. *N Engl J Med* **365**(4)**:** 327-336.

Pi J, Leung L, Xue P, Wang W, Hou Y, Liu D*, et al.* (2010). Deficiency in the nuclear factor E2-related factor-2 transcription factor results in impaired adipogenesis and protects against diet-induced obesity. *J Biol Chem* **285**(12)**:** 9292-9300.

Place AE, Suh N, Williams CR, Risingsong R, Honda T, Honda Y*, et al.* (2003). The novel synthetic triterpenoid, CDDO-imidazolide, inhibits inflammatory response and tumor growth in vivo. *Clin Cancer Res* **9**(7)**:** 2798-2806.

Potter WZ, Thorgeirsson SS, Jollow DJ, Mitchell JR (1974). Acetaminophen-induced hepatic necrosis. V. Correlation of hepatic necrosis, covalent binding and glutathione depletion in hamsters. *Pharmacology* **12**(3)**:** 129-143.

Primiano T, Sutter TR, Kensler TW (1997). Antioxidant-inducible genes. *Adv Pharmacol* **38:** 293-328.

R_Development_Core_Team (2009). R: A language and environment for statistical computing. . *R Foundation for Statistical Computing, Vienna, Austria.*

Rahman I, Kode A, Biswas SK (2006). Assay for quantitative determination of glutathione and glutathione disulfide levels using enzymatic recycling method. *Nature protocols* **1**(6)**:** 3159-3165.

Ramos-Gomez M, Kwak MK, Dolan PM, Itoh K, Yamamoto M, Talalay P*, et al.* (2001). Sensitivity to carcinogenesis is increased and chemoprotective efficacy of enzyme inducers is lost in nrf2 transcription factor-deficient mice. *Proc Natl Acad Sci U S A* **98**(6)**:** 3410-3415.

Randle LE, Goldring CE, Benson CA, Metcalfe PN, Kitteringham NR, Park BK*, et al.* (2008). Investigation of the effect of a panel of model hepatotoxins on the Nrf2-Keap1 defence response pathway in CD-1 mice. *Toxicology* **243**(3)**:** 249-260.

Ray SD, Jena N (2000). A hepatotoxic dose of acetaminophen modulates expression of BCL-2, BCL-X(L), and BCL-X(S) during apoptotic and necrotic death of mouse liver cells in vivo. *Arch Toxicol* **73**(10-11)**:** 594-606.

Ray SD, Kumar MA, Bagchi D (1999). A novel proanthocyanidin IH636 grape seed extract increases in vivo Bcl-XL expression and prevents acetaminophen-induced programmed and unprogrammed cell death in mouse liver. *Arch Biochem Biophys* **369**(1)**:** 42-58.

Ray SD, Mumaw VR, Raje RR, Fariss MW (1996). Protection of acetaminophen-induced hepatocellular apoptosis and necrosis by cholesteryl hemisuccinate pretreatment. *J Pharmacol Exp Ther* **279**(3)**:** 1470-1483.

Reddy NM, Kleeberger SR, Bream JH, Fallon PG, Kensler TW, Yamamoto M*, et al.* (2008). Genetic disruption of the Nrf2 compromises cell-cycle progression by impairing GSH-induced redox signaling. *Oncogene* **27**(44)**:** 5821-5832.

Reglinski J, Smith WE, Brzeski M, Marabani M, Sturrock RD (1992). Clinical analysis by 1H spin-echo NMR. 2. Oxidation of intracellular glutathione as a consequence of penicillamine therapy in rheumatoid arthritis. *J Med Chem* **35**(11)**:** 2134-2137.

Rehman I, Evans CA, Glen A, Cross SS, Eaton CL, Down J*, et al.* (2012). iTRAQ identification of candidate serum biomarkers associated with metastatic progression of human prostate cancer. *PLoS One* **7**(2)**:** e30885.

Reisman SA, Buckley DB, Tanaka Y, Klaassen CD (2009a). CDDO-Im protects from acetaminophen hepatotoxicity through induction of Nrf2-dependent genes. *Toxicol Appl Pharmacol* **236**(1)**:** 109-114.

Reisman SA, Aleksunes LM, Klaassen CD (2009b). Oleanolic acid activates Nrf2 and protects from acetaminophen hepatotoxicity via Nrf2-dependent and Nrf2-independent processes. *Biochem Pharmacol* **77**(7)**:** 1273-1282.

Robertson DG (2005). Metabonomics in toxicology: a review. *Toxicol Sci* **85**(2)**:** 809-822.

Rojas C, Cadenas S, Perez-Campo R, Lopez-Torres M, Pamplona R, Prat J*, et al.* (1993). Relationship between lipid peroxidation, fatty acid composition, and ascorbic acid in the liver during carbohydrate and caloric restriction in mice. *Arch Biochem Biophys* **306**(1)**:** 59-64.

Ross PL, Huang YN, Marchese JN, Williamson B, Parker K, Hattan S*, et al.* (2004). Multiplexed protein quantitation in Saccharomyces cerevisiae using amine-reactive isobaric tagging reagents. *Molecular & cellular proteomics : MCP* **3**(12)**:** 1154-1169.

Rossi R, Milzani A, Dalle-Donne I, Giustarini D, Lusini L, Colombo R*, et al.* (2002). Blood glutathione disulfide: in vivo factor or in vitro artifact? *Clin Chem* **48**(5)**:** 742-753.

Ryder SD, Beckingham IJ (2001). ABC of diseases of liver, pancreas, and biliary system. Other causes of parenchymal liver disease. *BMJ* **322**(7281)**:** 290-292.

Saha PK, Reddy VT, Konopleva M, Andreeff M, Chan L (2010). The triterpenoid 2-cyano-3,12-dioxooleana-1,9-dien-28-oic-acid methyl ester has potent anti-diabetic effects in diet-induced diabetic mice and Lepr(db/db) mice. *J Biol Chem* **285**(52)**:** 40581-40592.

Santori G, Domenicotti C, Bellocchio A, Pronzato MA, Marinari UM, Cottalasso D (1997). Different efficacy of iodoacetic acid and N-ethylmaleimide in high-performance liquid chromatographic measurement of liver glutathione. *Journal of chromatography. B, Biomedical sciences and applications* **695**(2)**:** 427-433.

Satarug S, Nishijo M, Ujjin P, Vanavanitkun Y, Baker JR, Moore MR (2004). Evidence for concurrent effects of exposure to environmental cadmium and lead on hepatic CYP2A6 phenotype and renal function biomarkers in nonsmokers. *Environmental health perspectives* **112**(15)**:** 1512-1518.

Sato K, Ueda Y, Ueno K, Okamoto K, Iizuka H, Katsuda S (2005). Hepatocellular carcinoma and nonalcoholic steatohepatitis developing during long-term administration of valproic acid. *Virchows Archiv : an international journal of pathology* **447**(6)**:** 996-999.

Satoh K, Itoh K, Yamamoto M, Tanaka M, Hayakari M, Ookawa K*, et al.* (2002). Nrf2 transactivator-independent GSTP1-1 expression in 'GSTP1-1 positive' single cells inducible in female mouse liver by DEN: a preneoplastic character of possible initiated cells. *Carcinogenesis* **23**(3)**:** 457-462.

Shi Q, Hong H, Senior J, Tong W (2010). Biomarkers for drug-induced liver injury. *Expert review of gastroenterology & hepatology* **4**(2)**:** 225-234.

Shibata T, Ohta T, Tong KI, Kokubu A, Odogawa R, Tsuta K*, et al.* (2008). Cancer related mutations in NRF2 impair its recognition by Keap1-Cul3 E3 ligase and promote malignancy. *Proc Natl Acad Sci U S A* **105**(36)**:** 13568-13573.

Shimada T, Yamazaki H, Guengerich FP (1996). Ethnic-related differences in coumarin 7-hydroxylation activities catalyzed by cytochrome P4502A6 in liver microsomes of Japanese and Caucasian populations. *Xenobiotica* **26**(4)**:** 395-403.

Shin S, Wakabayashi J, Yates MS, Wakabayashi N, Dolan PM, Aja S*, et al.* (2009). Role of Nrf2 in prevention of high-fat diet-induced obesity by synthetic triterpenoid CDDO-imidazolide. *Eur J Pharmacol* **620**(1-3)**:** 138-144.

Shin S, Wakabayashi N, Misra V, Biswal S, Lee GH, Agoston ES*, et al.* (2007). NRF2 modulates aryl hydrocarbon receptor signaling: influence on adipogenesis. *Mol Cell Biol* **27**(20)**:** 7188-7197.

Shishodia S, Sethi G, Konopleva M, Andreeff M, Aggarwal BB (2006). A synthetic triterpenoid, CDDO-Me, inhibits IkappaBalpha kinase and enhances apoptosis induced by TNF and chemotherapeutic agents through down-regulation of expression of nuclear factor kappaB-regulated gene products in human leukemic cells. *Clin Cancer Res* **12**(6)**:** 1828-1838.

Siegel D, Bolton EM, Burr JA, Liebler DC, Ross D (1997). The reduction of alpha-tocopherolquinone by human NAD(P)H: quinone oxidoreductase: the role of alpha-tocopherolhydroquinone as a cellular antioxidant. *Mol Pharmacol* **52**(2)**:** 300-305.

Singh BK, Tripathi M, Pandey PK, Kakkar P (2010). Nimesulide aggravates redox imbalance and calcium dependent mitochondrial permeability transition leading to dysfunction in vitro. *Toxicology* **275**(1-3)**:** 1-9.

Soga T, Baran R, Suematsu M, Ueno Y, Ikeda S, Sakurakawa T*, et al.* (2006). Differential metabolomics reveals ophthalmic acid as an oxidative stress biomarker indicating hepatic glutathione consumption. *J Biol Chem* **281**(24)**:** 16768-16776.

Speranza G, Gutierrez ME, Kummar S, Strong JM, Parker RJ, Collins J*, et al.* (2012). Phase I study of the synthetic triterpenoid, 2-cyano-3, 12-dioxoolean-1, 9-dien-28-oic acid (CDDO), in advanced solid tumors. *Cancer Chemother Pharmacol* **69**(2)**:** 431-438.

Sriram N, Kalayarasan S, Sudhandiran G (2009). Epigallocatechin-3-gallate augments antioxidant activities and inhibits inflammation during bleomycin-induced experimental pulmonary fibrosis through Nrf2-Keap1 signaling. *Pulm Pharmacol Ther* **22**(3)**:** 221-236.

Stack C, Ho D, Wille E, Calingasan NY, Williams C, Liby K*, et al.* (2010). Triterpenoids CDDO-ethyl amide and CDDO-trifluoroethyl amide improve the behavioral phenotype and brain pathology in a transgenic mouse model of Huntington's disease. *Free Radic Biol Med* **49**(2)**:** 147-158.

Stacy DR, Ely K, Massion PP, Yarbrough WG, Hallahan DE, Sekhar KR*, et al.* (2006). Increased expression of nuclear factor E2 p45-related factor 2 (NRF2) in head and neck squamous cell carcinomas. *Head & neck* **28**(9)**:** 813-818.

Starkey Lewis PJ, Dear J, Platt V, Simpson KJ, Craig DG, Antoine DJ*, et al.* (2011). Circulating microRNAs as potential markers of human drug-induced liver injury. *Hepatology* **54**(5)**:** 1767-1776.

Steghens JP, Flourie F, Arab K, Collombel C (2003). Fast liquid chromatography-mass spectrometry glutathione measurement in whole blood: micromolar GSSG is a sample preparation artifact. *Journal of chromatography. B, Analytical technologies in the biomedical and life sciences* **798**(2)**:** 343-349.

Stewart D, Killeen E, Naquin R, Alam S, Alam J (2003). Degradation of transcription factor Nrf2 via the ubiquitin-proteasome pathway and stabilization by cadmium. *J Biol Chem* **278**(4)**:** 2396-2402.

Subramanian A, Tamayo P, Mootha VK, Mukherjee S, Ebert BL, Gillette MA*, et al.* (2005). Gene set enrichment analysis: a knowledge-based approach for interpreting genome-wide expression profiles. *Proc Natl Acad Sci U S A* **102**(43)**:** 15545-15550.

Sugimoto H, Okada K, Shoda J, Warabi E, Ishige K, Ueda T*, et al.* (2010). Deletion of nuclear factor-E2-related factor-2 leads to rapid onset and progression of nutritional steatohepatitis in mice. *American journal of physiology. Gastrointestinal and liver physiology* **298**(2)**:** G283-294.

Suh N, Honda T, Finlay HJ, Barchowsky A, Williams C, Benoit NE*, et al.* (1998). Novel triterpenoids suppress inducible nitric oxide synthase (iNOS) and inducible cyclooxygenase (COX-2) in mouse macrophages. *Cancer Res* **58**(4)**:** 717-723.

Suh N, Roberts AB, Birkey Reffey S, Miyazono K, Itoh S, ten Dijke P*, et al.* (2003). Synthetic triterpenoids enhance transforming growth factor beta/Smad signaling. *Cancer Res* **63**(6)**:** 1371-1376.

Suh N, Wang Y, Honda T, Gribble GW, Dmitrovsky E, Hickey WF*, et al.* (1999). A novel synthetic oleanane triterpenoid, 2-cyano-3,12-dioxoolean-1,9-dien-28-oic acid, with potent differentiating, antiproliferative, and anti-inflammatory activity. *Cancer Res* **59**(2)**:** 336-341.

Sun Z, Huang Z, Zhang DD (2009). Phosphorylation of Nrf2 at multiple sites by MAP kinases has a limited contribution in modulating the Nrf2-dependent antioxidant response. *PLoS One* **4**(8)**:** e6588.

Sussan TE, Rangasamy T, Blake DJ, Malhotra D, El-Haddad H, Bedja D*, et al.* (2009). Targeting Nrf2 with the triterpenoid CDDO-imidazolide attenuates cigarette smoke-induced emphysema and cardiac dysfunction in mice. *Proc Natl Acad Sci U S A* **106**(1)**:** 250-255.

Suzuki M, Betsuyaku T, Ito Y, Nagai K, Nasuhara Y, Kaga K*, et al.* (2008). Down-regulated NF-E2-related factor 2 in pulmonary macrophages of aged smokers and patients with chronic obstructive pulmonary disease. *Am J Respir Cell Mol Biol* **39**(6)**:** 673-682.

Tanaka Y, Aleksunes LM, Goedken MJ, Chen C, Reisman SA, Manautou JE*, et al.* (2008a). Coordinated induction of Nrf2 target genes protects against iron nitrilotriacetate (FeNTA)-induced nephrotoxicity. *Toxicology and applied pharmacology* **231**(3)**:** 364-373.

Tanaka Y, Aleksunes LM, Yeager RL, Gyamfi MA, Esterly N, Guo GL*, et al.* (2008b). NF-E2-related factor 2 inhibits lipid accumulation and oxidative stress in mice fed a high-fat diet. *J Pharmacol Exp Ther* **325**(2)**:** 655-664.

Team RDC (2005). R: A language and environment for statistical computing. Vienna, Austria: R Foundation for Statistical Computing.

Thimmulappa RK, Mai KH, Srisuma S, Kensler TW, Yamamoto M, Biswal S (2002). Identification of Nrf2-regulated genes induced by the chemopreventive agent sulforaphane by oligonucleotide microarray. *Cancer Res* **62**(18)**:** 5196-5203.

Tietze F (1969). Enzymic method for quantitative determination of nanogram amounts of total and oxidized glutathione: applications to mammalian blood and other tissues. *Analytical biochemistry* **27**(3)**:** 502-522.

Tipnis SR, Blake DG, Shepherd AG, McLellan LI (1999). Overexpression of the regulatory subunit of gamma-glutamylcysteine synthetase in HeLa cells increases gamma-glutamylcysteine synthetase activity and confers drug resistance. *Biochem J* **337 (Pt 3):** 559-566.

Tong KI, Kobayashi A, Katsuoka F, Yamamoto M (2006). Two-site substrate recognition model for the Keap1-Nrf2 system: a hinge and latch mechanism. *Biological chemistry* **387**(10-11)**:** 1311-1320.

Tonge RP, Kelly EJ, Bruschi SA, Kalhorn T, Eaton DL, Nebert DW*, et al.* (1998). Role of CYP1A2 in the hepatotoxicity of acetaminophen: investigations using Cyp1a2 null mice. *Toxicol Appl Pharmacol* **153**(1)**:** 102-108.

Tsao T, Kornblau S, Safe S, Watt JC, Ruvolo V, Chen W*, et al.* (2010). Role of peroxisome proliferator-activated receptor-gamma and its coactivator DRIP205 in cellular responses to CDDO (RTA-401) in acute myelogenous leukemia. *Cancer Res* **70**(12)**:** 4949-4960.

Valko M, Leibfritz D, Moncol J, Cronin MT, Mazur M, Telser J (2007). Free radicals and antioxidants in normal physiological functions and human disease. *Int J Biochem Cell Biol* **39**(1)**:** 44-84.

Vannini N, Lorusso G, Cammarota R, Barberis M, Noonan DM, Sporn MB*, et al.* (2007). The synthetic oleanane triterpenoid, CDDO-methyl ester, is a potent antiangiogenic agent. *Mol Cancer Ther* **6**(12 Pt 1)**:** 3139-3146.

Verrotti A, Di Marco G, la Torre R, Pelliccia P, Chiarelli F (2009). Nonalcoholic fatty liver disease during valproate therapy. *European journal of pediatrics* **168**(11)**:** 1391-1394.

Wakabayashi N, Itoh K, Wakabayashi J, Motohashi H, Noda S, Takahashi S*, et al.* (2003). Keap1-null mutation leads to postnatal lethality due to constitutive Nrf2 activation. *Nat Genet* **35**(3)**:** 238-245.

Walgren JL, Mitchell MD, Thompson DC (2005). Role of metabolism in drug-induced idiosyncratic hepatotoxicity. *Crit Rev Toxicol* **35**(4)**:** 325-361.

Wang K, Zhang S, Marzolf B, Troisch P, Brightman A, Hu Z*, et al.* (2009). Circulating microRNAs, potential biomarkers for drug-induced liver injury. *Proc Natl Acad Sci U S A* **106**(11)**:** 4402-4407.

Wang L, Chen S, Zhang M, Li N, Chen Y, Su W*, et al.* (2012). Legumain: A biomarker for diagnosis and prognosis of human ovarian cancer. *J Cell Biochem* **113**(8)**:** 2679-2686.

Wang Y, Porter WW, Suh N, Honda T, Gribble GW, Leesnitzer LM*, et al.* (2000). A synthetic triterpenoid, 2-cyano-3,12-dioxooleana-1,9-dien-28-oic acid (CDDO), is a ligand for the peroxisome proliferator-activated receptor gamma. *Mol Endocrinol* **14**(10)**:** 1550-1556.

Weber LW, Boll M, Stampfl A (2003). Hepatotoxicity and mechanism of action of haloalkanes: carbon tetrachloride as a toxicological model. *Crit Rev Toxicol* **33**(2)**:** 105-136.

Wei Y, Gong J, Yoshida T, Eberhart CG, Xu Z, Kombairaju P*, et al.* (2011). Nrf2 has a protective role against neuronal and capillary degeneration in retinal ischemia-reperfusion injury. *Free Radic Biol Med* **51**(1)**:** 216-224.

Wellen KE, Hatzivassiliou G, Sachdeva UM, Bui TV, Cross JR, Thompson CB (2009). ATP-citrate lyase links cellular metabolism to histone acetylation. *Science* **324**(5930)**:** 1076-1080.

Wilkins MR, Pasquali C, Appel RD, Ou K, Golaz O, Sanchez JC*, et al.* (1996). From proteins to proteomes: large scale protein identification by two-dimensional electrophoresis and amino acid analysis. *Bio/technology* **14**(1)**:** 61-65.

Wu GY, Fang YZ, Yang S, Lupton JR, Turner ND (2004). Glutathione metabolism and its implications for health. *J Nutr* **134**(3)**:** 489-492.

Wu KC, Cui JY, Klaassen CD (2011). Beneficial role of nrf2 in regulating NADPH generation and consumption. *Toxicol Sci* **123**(2)**:** 590-600.

Xu JJ, Henstock PV, Dunn MC, Smith AR, Chabot JR, de Graaf D (2008a). Cellular imaging predictions of clinical drug-induced liver injury. *Toxicol Sci* **105**(1)**:** 97-105.

Xu W, Hellerbrand C, Kohler UA, Bugnon P, Kan YW, Werner S*, et al.* (2008b). The Nrf2 transcription factor protects from toxin-induced liver injury and fibrosis. *Lab Invest* **88**(10)**:** 1068-1078.

Yamamoto T, Yoh K, Kobayashi A, Ishii Y, Kure S, Koyama A*, et al.* (2004). Identification of polymorphisms in the promoter region of the human NRF2 gene. *Biochem Biophys Res Commun* **321**(1)**:** 72-79.

Yang H, Wang J, Huang ZZ, Ou X, Lu SC (2001). Cloning and characterization of the 5'-flanking region of the rat glutamate-cysteine ligase catalytic subunit. *Biochem J* **357**(Pt 2)**:** 447-455.

Yang RZ, Park S, Reagan WJ, Goldstein R, Zhong S, Lawton M*, et al.* (2009). Alanine aminotransferase isoenzymes: molecular cloning and quantitative analysis of tissue expression in rats and serum elevation in liver toxicity. *Hepatology* **49**(2)**:** 598-607.

Yao KS, O'Dwyer PJ (1995). Involvement of NF-kappa B in the induction of NAD(P)H:quinone oxidoreductase (DT-diaphorase) by hypoxia, oltipraz and mitomycin C. *Biochem Pharmacol* **49**(3)**:** 275-282.

Yates MS, Tran QT, Dolan PM, Osburn WO, Shin S, McCulloch CC*, et al.* (2009). Genetic versus chemoprotective activation of Nrf2 signaling: overlapping yet distinct gene expression profiles between Keap1 knockout and triterpenoid-treated mice. *Carcinogenesis* **30**(6)**:** 1024-1031.

Yates MS, Tauchi M, Katsuoka F, Flanders KC, Liby KT, Honda T*, et al.* (2007). Pharmacodynamic characterization of chemopreventive triterpenoids as exceptionally potent inducers of Nrf2-regulated genes. *Mol Cancer Ther* **6**(1)**:** 154-162.

Yokota S, Higashi E, Fukami T, Yokoi T, Nakajima M (2011). Human CYP2A6 is regulated by nuclear factor-erythroid 2 related factor 2. *Biochem Pharmacol* **81**(2)**:** 289-294.

Yore MM, Liby KT, Honda T, Gribble GW, Sporn MB (2006). The synthetic triterpenoid 1-[2-cyano-3,12-dioxooleana-1,9(11)-dien-28-oyl]imidazole blocks nuclear factor-kappaB activation through direct inhibition of IkappaB kinase beta. *Mol Cancer Ther* **5**(12)**:** 3232-3239.

Yu R, Lei W, Mandlekar S, Weber MJ, Der CJ, Wu J*, et al.* (1999). Role of a mitogen-activated protein kinase pathway in the induction of phase II detoxifying enzymes by chemicals. *J Biol Chem* **274**(39)**:** 27545-27552.

Zhang DD, Lo SC, Cross JV, Templeton DJ, Hannink M (2004). Keap1 is a redox-regulated substrate adaptor protein for a Cul3-dependent ubiquitin ligase complex. *Mol Cell Biol* **24**(24)**:** 10941-10953.

Zhang YK, Yeager RL, Tanaka Y, Klaassen CD (2010). Enhanced expression of Nrf2 in mice attenuates the fatty liver produced by a methionine- and choline-deficient diet. *Toxicol Appl Pharmacol* **245**(3)**:** 326-334.

Zhou S, Chan E, Duan W, Huang M, Chen YZ (2005). Drug bioactivation, covalent binding to target proteins and toxicity relevance. *Drug Metab Rev* **37**(1)**:** 41-213.

Zhu P, Oe T, Blair IA (2008). Determination of cellular redox status by stable isotope dilution liquid chromatography/mass spectrometry analysis of glutathione and glutathione disulfide. *Rapid communications in mass spectrometry : RCM* **22**(4)**:** 432-440.

Zou W, Liu X, Yue P, Zhou Z, Sporn MB, Lotan R*, et al.* (2004). c-Jun NH2-terminal kinase-mediated up-regulation of death receptor 5 contributes to induction of apoptosis by the novel synthetic triterpenoid methyl-2-cyano-3,12-dioxooleana-1, 9-dien-28-oate in human lung cancer cells. *Cancer Res* **64**(20)**:** 7570-7578.